Heat-sensitive immunoliposomes for targeted drug delivery in prostate cancer

Dissertation submitted in fulfillment of the requirements for the Degree

MASTER OF HEALTH SCIENCES IN BIOMEDICAL TECHNOLOGY

in the

Faculty of Health and Environmental Sciences

Department of Health Sciences

at the

Central University of Technology, Free State

South Africa

By

KEAMOGETSWE NICOLE RIET

Supervisor: Prof Mamello Patience Sekhoacha
Co-Supervisor: Prof Samuel Samson Mashele
Co-Supervisor: Prof Martin Munene Nyaga

2023

STATEMENT REGARDING INDEPENDENT WORK

I, KEAMOGETSWE NICOLE RIET, identity number _____ and student number _____, hereby declare that this research thesis being submitted to the Central University of Technology, Free State, for the Degree of MASTER OF HEALTH SCIENCES IN BIOMEDICAL TECHNOLOGY, is my original and independently conducted research work; and it adheres to the code of academic integrity, amongst the other requirements, rules, operations, and policies, outlined by the Central University of Technology. Prior to this, it has not been submitted by me or anybody else to another institution to fulfil (or in partial fulfilment) any requirement for any qualification whatsoever.

DATE

02 OCTOBER 2023

STUDENT's SIGNATURE

_____

Acknowledgments

I wish to express my unreserved appreciation to the Department of Biomedical Science, Central University of Technology, and the Department of Pharmacology, at the University of the Free State for their support and the platform given to me to achieve this.

A special thank you to my Maker and source of strength, GOD, for the opportunity granted me to run this postgraduate programme from beginning to the end, and for His grace that saw me through this journey. May His Name Be Praised Forevermore, Amen.

My main supervisor and mentor, Prof Mamello Patience Sekhoacha, I appreciate you for your continual guidance, encouragement, and valuable advice throughout my studies. Your patience and belief in me is appreciated. Thank you for allowing me to grow as a scientist and for all the lessons that extended beyond the laboratory.

My co-supervisor, Prof Samuel Samson Mashele; your guidance and support is well appreciated.

My co-supervisor, Prof Martin Munene Nyaga, for your support and for providing me with the opportunity to complete the Next Generation Sequencing laboratory training at your research unit in 2019.

A special thank you to Dr Ayodeji Adegoke for your valuable assistance, insightful suggestions, guidance, and support throughout this study.

Dr Joshua C. Nwabuife for your assistance and guidance throughout this journey.

I am grateful to my colleagues Maholomola Mokhatla, Paballo Motlong and Ipeleng Kgosiemang for their support and kindness. Without your support, this dissertation would not have been possible.

My friends and family, and more especially my mother Gaebusisiwe Riet, for always praying for me, supporting, and granting me the opportunity to pursue my education.

The **National Research Foundation (NRF),** for offering financial support to conduct this study. The results and conclusions noted in this manuscript, are those of the author and are not the NRF. **Funding:** Reference: TTK160607168752, UID 107835.

The support of the **Central University of Technology and the University of the Free state** in this research is hereby acknowledged. The results and conclusions arrived at, are those of the author and not the universities.

Health and Welfare Sector Education and Training Authority (HWSETA) for financial support to conduct this research. The results and conclusions arrived at are those of the author and not HWSETA.

Table of Contents

List of figures

List of tables

List of abbreviations

DCM	Dichloromethane
MeOH	Methanol
PSMA	Prostate-specific membrane antigen
TSL	Thermo-sensitive liposomes
DPPC	Dipalmitoylphosphatidylcholine
$DMSO_4$	Dimethyl sulfoxide
SCID	Severe combined immunodeficiency
DMEM	Dulbecco's Modified Eagle's medium
MTT	3-(4,5-dimethylthiazol-2-yl)-2,5-diphenyltetrazolium bromide
FBS	Fetal bovine serum
TC	Transition temperature
HSCP	L-α-phosphatidylcholine, hydrogenated (Soybean)
SEM	Scanning electron microscope
TEM	Transmission electron microscopy
FTIR	Fourier transform infrared spectroscopy

Chapter 1

1.1 Introduction

One-in-fifteen men in South Africa has a high chance of developing prostate cancer in their lifetimes. Globally, prostate cancer occurrence rates differ geographically, in regions and race groups. Prostate cancer is projected to grow exponentially to 1.7 million new cases, with approximately 499,000 fatalities, by 2030, owing to the rapidly increasing population of aged men who are above 65 years of age (Rawla, 2019).

Prostate cancer ensues when cells of the prostate gland grow uncontrollably. It can arise from epithelial cells in the secretory glands that line the prostatic ducts (Sekhoacha et al., 2022). Treatments such as chemotherapy, surgery, hormone therapy, and radiation therapy have been successful over the years in treating different cancers, including prostate cancer. The significant challenge facing various prostate cancer treatments is the side-effects on prostate cancer patients, which include the killing of normal cells and causing erectile dysfunction (Abbas et al., 2020). The use of nanotechnology in the treatment of cancer appears to be a promising alternative, with reduced subsequent side-effects (García-Pinel et al., 2019). Much interest in the use of nanotechnology has been in drug delivery, where its unique properties lead to increased drug efficacy, selectivity, drug retention time, and reduction of cytotoxicity (ALMOTAIRY et al., 2023). Various types of nanoparticles are designed to improve the efficiency and specificity of chemo-delivery nanosystems. Liposomal nanoparticles have added advantages as drug delivery systems, as they are known to increase drug delivery; protect the drug from degradation; stabilize therapeutic compounds; and improve drug performance in solid tumours (Guimarães et al., 2021).

Liposomes can be sensitive and responsive to stimuli such as pH, light, redox, matrix metalloproteinase, and temperature (Kansız and Elçin, 2023). The current study has explored the use of liposomes that are sensitive to temperature. Lipids have a specific temperature range at which their phases change from the gel phase to the liquid phase. This temperature range is commonly known as the transition temperature (TC) (Okotrub et al., 2018). The transition temperature has an impact on the encapsulation efficiency and the stability of the liposomes. Phosphatidylcholine (PC) is the most crucial phospholipid

in L-α-phosphatidylcholine, hydrogenated (soybean) (HSPC). The PC acyl chain degree of saturation and chain length primarily affect the phase of the liposomal membrane. When hyperthermia is applied above the TC, PCs change from a solid gel to a liquid phase, as the number of gauche conformations in the acyl chains increases from the trans-state of the solid gel phase. This change in the membrane from gel to liquid allows drugs which were encapsulated to be released from the liposomes. When 10% of DSPE-PEG2000 is added to the liposomal formulation, thermosensitive liposomes with steric stability can be obtained (Fahmy et al., 2022). Thermo-sensitive liposomes release the encapsulated drug when exposed to hyperthermia at 39-40°C (Mazzotta et al., 2018). DSPE-PEG (2000)-amine is used with different functional molecules, such as the DSPE-2000-maleimide, to prepare target-specific antibody-conjugated nanoparticles for improved cellular and receptor targeting (Bi et al., 2019). In this study, an anti-PSMA antibody was conjugated onto heat-sensitive liposomes to achieve specific binding to prostate cancer cells. Prostate-specific membrane antigen (PSMA) is highly expressed in prostate cells. The expression of PSMA is stimulated in malignant tissue with the highest level detected in metastatic androgen-independent prostate cancer (Czerwińska et al., 2020). PSMA targeting and binding to PSMA antigen increases the therapeutic specificity of nanoparticles charges with anti-PSMA antibody (Hyväkkä et al., 2021).

Chemotherapeutic drugs are limited by the fact that they are unable to reach the cancerous site in sufficient quantity to be effective (Sekhoacha et al., 2022). They must be administered in high doses, ultimately leading to adverse side-effects such as targeting normal cells (Alqosaibi, 2022). The experiments in this study were initiated with doxorubicin and continued with docetaxel, as docetaxel is the first-line chemotherapeutic standard drug used for prostate cancer in South Africa (Liu et al., 2023). The study hypothesizes that the targeting and binding of nanoparticles charged with anti-PSMA antibody to PSMA on the prostate cells increases specificity, delivery and the therapeutic potential of encapsulated anti-prostate cancer agents.

Medicinal plants were explored as sources of potential, new anti-cancer agents. Previous studies reported on the therapeutic uses of *Euphorbia milii*, and indicated that the plant has anticancer, antidiabetic and antimicrobial properties (Amtaghri et al., 2022). These properties are attributed to the different phytochemicals present in the plant (Salehi et al., 2019).

The current study aimed to overcome the challenges of non-specific and uncontrolled drug delivery facing chemotherapy by exploring the cancer cell growth inhibitory effect of a selected medicinal plant and the development of a controlled, target-specific nano-delivery system for prostate cancer. The study was conducted with liposomes encapsulating *Euphorbia milii* plant extract and two prostate cancer standard drugs, doxorubicin and docetaxel, for delivery into selected prostate cancer cell lines.

1.2 Problem statement

Prostate cancer is one of the most prevalent types of cancer among men in more than half of the countries globally (112 of 185 countries/territories) (Bergengren et al., 2023). Chemotherapeutic drugs, surgery, hormonal therapy, and radiation therapy have been used to treat cancers, but have unbearable negative side-effects on cancer patients. Chemotherapy in particular, is further limited by low bioavailability, uncontrolled drug release, degradation of drugs, and non-specificity, which are the main challenges the current study aims to address.

To overcome these challenges, the development of a target-specific and controlled drug-release nano-delivery system is explored. In this research, the heat-sensitive liposomes were conjugated with anti-PSMA antibodies through the reaction of sulfhydryl residues to ensure liposome specificity to prostate membrane antigen. This drug delivery system is designed to release only the encapsulated drug upon heat stimulus when the nanoparticles are attached to the prostate gland. In this way, both specificity and controlled release of the drug are addressed, ultimately limiting toxicity to normal cells. The encapsulation of chemo drugs or agents in liposomes serves as protection from possible degradation as well as a way to increase bioavailability. The current research is an *in vitro* study that explores a concept that, when applied in a clinical setting, could reduce mortality and poor treatment outcomes in patients, as well as the side-effects of toxicity associated with the treatment of prostate cancer.

1.3 Aim

This study aimed to discover potential chemotherapeutic agents from a medicinal plant, *Euphorbia milii*, and to incorporate its active constituents into thermosensitive immuno-liposomes for selective, targeted, and controlled release in prostate cancer cells.

1.4 The general objective of the study

Develop a drug delivery system that is specific to prostate cancer and has a drug-controlled release feature that is responsive to heat.

1.4.1 The objectives of the study:

1) Select highly cytotoxic plants with records of anti-cancer properties. Prepare extracts, and screen extracts for their cell growth inhibitory effects against prostate cancer DU145 and LNCap cell lines.

2) Synthesize heat-responsive liposomes and conjugate them with prostate-specific antibody.

3) Encapsulate active constituents from plant/ standard anti-cancer drugs (used as a positive control) into the synthesized liposomes.

4) Verify and calculate the drug encapsulation and release.

5) Evaluate the efficacy of the thermos-sensitive immunoliposome drug delivery system on prostate cancer cells, compared to free standard drug/plant extracts.

Chapter 2

2. Literature review

2. 1 Cancer

Cancer is the uncontrolled division of cells in the body, eventually forming a tissue mass known as a tumour (Brown et al., 2023). Tumours can either be benign and remain in their original location, or become malignant and move from one place to another (Patel, 2020). In normal cell division, there is a balance in the genes that promote cell proliferation and suppression. This balance, however, is distorted in cancerous cells. Several factors, such as damage to DNA and resultant mutations in genes, contribute to this imbalance. Genetic mutations, for example, can accelerate the rate of cell division via the dysregulation of growth signals that promote cell division or inhibit cell cycle control or programmed cell death. DNA repair mechanisms in the body can repair damaged DNA. Damaged DNA is not repaired in cancer cells as genetic mutations often lead to non-functional DNA repair mechanisms and consequently uncontrollable cell division (Alhmoud et al., 2021). Cancer can start anywhere in the body: uncontrollable cell division in the prostate gland can lead to prostate cancer.

2.2 The prostate gland

The anatomy of the prostate gland can be explained as a compound tubular walnut-sized gland situated in front of the rectum, right between the bladder and the penis. The prostate gland produces semen that nourishes and transports the sperm cells (Obukohwo et al., 2021). The prostate gland is the source of three well-known prostate conditions: benign prostatic hyperplasia (BPH), prostatitis, and prostate cancer (Shah et al., 2021). This study focuses on prostate cancer.

2.3 Prostate cancer

2.3.1 Epidemiology

Prostate cancer develops mainly in older men, aged 65 or older. Age-specific incidence rates (ASIRs) vary by 189-fold globally, with an ASIR of 68.0 per 100,000 in 2018 in SA. About 1,2 million new cases of prostate cancer were registered globally, showing as 7.1% of all cancers in men (Cassim et al., 2021). Prostate cancer is often seen in western countries, with one-in-six men diagnosed with the disease in the United States and 1-in-13 men in England (Lee, 2019). The incident rates of prostate cancer in Africa are lower than those in western countries (GLOBOCAN-WHO, 2018). Prostate tumours usually grow slowly and with no visible symptoms for years. About 95% of prostate cancers are adenocarcinomas (cancers that form and develop in the gland and spread to other parts of the body). By 2023, it is predicted that approximately 28,830 new prostate cancer cases will be diagnosed, and 34,700 men are likely to die from the disease (Oseni et al., 2023). Delayed detection of the disease until the mature stages is one of the factors resulting to the increased mortality rate. The detection and diagnosis of prostate cancer comprises digital rectal examination, prostate-specific antigen (PSA) analysis, and ultrasound biopsies.

2.3.2 Prostate cancer screening and detection

Most men undergo prostate cancer screening when they experience signs of erectile dysfunction, blood in their urine or semen, or inflammation. Most prostate cancer detections start with a digital rectal examination (DRE). During a DRE, a medical practitioner evaluates a patient’s lower rectum, assessing the prostate gland size (Christie et al., 2019). If abnormalities of shape, texture and size are detected, the patient's blood is collected for PSA screening. PSA is a glycoprotein formed by the prostate. It is located mainly in semen. However, can be detected in the bloodstream. PSA is a sensitive marker to detect and monitor prostate cancer progression. Men diagnosed with prostate diseases and adenocarcinoma of the prostate have higher serum PSA protein levels (Filella et al., 2018). The PSA cut-off point is 4 ng/ml. Levels higher than 4ng/ml indicate that the patient requires additional tests (Sekhoacha et al., 2022).

After detecting high PSA levels, tests such as transrectal ultrasound (TRUS) and magnetic resonance imaging (MRI) are conducted to diagnose patients.

2.3.3 Prostate cancer diagnosis

The prostate gland is viewed with an imaging test such as a TRUS or MRI. During transrectal ultrasound, a probe is inserted into the rectum, and an ultrasound image of the prostate gland is created by sound waves. An MRI scan is used to generate clearer images. To verify the presence of cancer cells, an ultrasound biopsy is performed by collecting tissue samples from the prostate. During a biopsy, small prostate samples are removed with a thin hallow needle and then examined under a microscope. After a biopsy report that indicates that the patient is positive for prostate cancer, the cancer will be assigned a grade using the Gleason grading system to indicate how differentiated the cancer is (Tagai et al., 2019). The Gleason grading system is the histologic pattern of cancer cells in H&E-stained sections obtained from a biopsy sample. The grade can range from 2 to 10. An increasing Gleason grade is directly related to tumour size and pathologic stage. A low Gleason grade indicates a non-aggressive, slow-growing prostate cancer. For lower Gleason grades, active surveillance is done, where the progression of the cancer is monitored with rectal examinations and biopsies. If tests indicate that the prostate cancer is progressing, treatment of the disease will be initiated. The Gleason grade assists with predicting patients' response to specific therapies, such as surgery and radiotherapy (Wulczyn et al., 2021).

2.4 Treatment

There are four treatment methods that are primarily used for prostate therapy. These are surgery, radiation, hormonal therapy, and chemotherapy (Debela et al., 2021). The treatment options, their advantages, and setbacks are discussed below in detail.

2.4.1 Surgery

Surgery is suggested for localized tumours that pose a high risk to the patients (Hofman et al., 2020). Radical prostatectomy and pelvic lymphadenectomy are known to be the most applicable surgery methods used for prostate cancer. Although surgery is known to significantly reduce mortality and the risk of metastasis, it has side-effects that include substantial sexual and urinary dysfunction (Guillaumier et al., 2018).

2.4.2 Hormonal Therapy

Hormonal therapy, which is also called hormone manipulation, endocrine therapy, or hormone withdrawal therapy, includes the use of drugs that affect the hormone secretion to inhibit, stop or slow down the growth of cancer cells that need specific hormones to grow. Recently developed drugs (aromatase inhibitors, LHRH analogues) are being used to treat prostate and breast cancer (Aggarwal et al., 2021). Hormonal therapy may be used to shrink a tumour and make it easier to remove. However, the use of androgen suppression therapy hormones has numerous side-effects, affecting insulin resistance fatigue; hypercholesterolemia; anaemia and bone mineral density leading to an increased risk of cardiac disorders (Edmunds et al., 2020).

2.4.3 Radiation therapy

Many radiation therapies, such as conformal proton beam therapy, stereotactic surgery, and intra-operative radiation, are being used for cancer treatment. Radiation energy, however, usually damages the DNA of any cells it comes into contact with, affecting cell division and causing cell death. The main challenge with radiation therapy is that it does the same damage to healthy cells as it does to cancerous cells (Gnutzmann et al., 2018).

2.4.4 Chemotherapy

Chemotherapy is a method to treat cancer in the form of drugs taken intravenously, orally, or injected into a muscle (Anand et al., 2022) . Chemotherapeutic drugs are limited by the fact that they are unable to reach the cancerous site in sufficient quantity to be effective. They must be administered in high doses, ultimately leading to adverse side-effects, such as targeting healthy fast-dividing cells (Mustapha et al., 2022) . Other disadvantages are the adverse side-effects on the body's immune system; cells becoming resistant to chemotherapeutic drugs; the suppression of blood cells and platelets by the bone marrow; neuropathy; and cardiotoxicity (Liu et al., 2021, Ugwunnaji and Berinyuy). The most commonly used chemotherapeutic drug for prostate cancer is docetaxel. Other FDA-approved chemotherapy drugs, such as sipuleucel-T; enzalutamide; cabazitaxel; doxorubicin; and abirateroneand have shown positive results in prostate cancer clinical trials (Oseni et al., 2023). Doxorubicin and docetaxel are discussed further, as these were used in the current study as the standard drugs that served as positive controls.

2.4.4.1 Doxorubicin

Doxorubicin is a drug called cytotoxic anthracycline antibiotic, extracted from streptomyces peucetius var. caesius in the 1970s. Doxorubicin is often used in soft tissue sarcomas, hematological malignancies, and carcinoma. Doxorubicin has been proven to stop the progression of cancer cells by blocking an enzyme known as topo isomerase 2 and inducing DNA breaks (Rawat et al., 2021) . The conventional composition of doxorubicin can be obtained as a solution or freeze-dried product. Even though doxorubicin is administered to treat prostate cancer, there are increased risks of chemotherapeutic failure due to drug resistance. To hinder resistance, doxorubicin is usually used with other therapies to resensitize cancer cells to the drug (Shu et al., 2018). The FDA-approved doxorubicin, encapsulated as doxil in PEG liposomes in the early 90s, is the first FDA-approved nanodrug. The synergy between doxorubicin and anthracyclines was seen previously in *in vitro* studies. Doxorubicin was synergistic when combined with docetaxel at dose levels equal to their IC50 values in PC3, DU145, and LNCap cells (Dyshlovoy et al., 2024).

2.4.4.2 Docetaxel

Docetaxel is an effective drug approved to treat different cancers, such as prostate cancer. The drug is also used to treat various malignancies. Docetaxel kills cells by interrupting the function of microtubules vital for cell survival. Docetaxel prevents the formation of new cells, causing existing cells to undergo apoptosis, stopping cells from maturing and replicating. As with all cytotoxic agents, docetaxel is not specific to cancerous cells and leads to various acute and long-term side-effects (Singh et al., 2019). Docetaxel is usually administered 3 - 4 times with lower concentrations. It is reported that 0.5mg/kg is the lowest effective dose resulting in 87% tumour reduction in mice (Grohmann et al., 2021).

Recently, new approaches such as target-specific nanoscale therapy and new drug combinations using medicinal plants are being explored to overcome multidrug resistance and side-effects caused by chemotherapy (More et al., 2021).

2.5 Medicinal plants

Medicinal plants are seen as an alternative to chemotherapeutic drugs as they contain a wide variety of bioactive compounds that possess anticancer, antibacterial, and antimicrobial properties. Secondary metabolites derived from medicinal plants have been the primary source of medical drug discoveries. Drugs such as vinblastine, paclitaxel, vincristine, etoposide, and taxel are examples of anticancer drugs derived from plants (Shaik et al., 2022).

2.5.1. Euphorbia species

The different species of euphorbia are used in folk medicine (Amtaghri et al., 2022). The plant genus is characterized by having milky latex which can be highly toxic in some species. According to the Planetary Biodiversity Inventory (2019: online), euphorbia has about 2000 plant members, ranging from small plants to huge trees. In this study, the euphorbia species used is the *Euphorbia milii* plant .

2.5.1.1 Euphorbia milii

Figure 1: *Euphorbia milii* plant species

Euphoria milii is commonly known as 'Christ of Thorns'. It belongs to the euphorbia genus. *E. milii* is a woody, spiny succulent plant that can grow up to 1.8m high; the spines can grow up to 3cm. The plant has green leaves and flowers ranging through colours like red, pink, white, and yellow. *E. milii* is well-known for cancer therapy (Kaur and Kumar, 2023).

Distribution:

The euphorbia genus is found in Pakistan, China, and Madagascar. *Euphorbia milii*, grows in bush and forest habitats, but usually in rocky areas. The plant is native to southern and western Madagascar and is found at an elevation of between 20 and 1609m above sea level. The plant is also found in other countries, like Brazil and Pakistan (Razanajatovo, 2020).

Historical Medicinal uses

Euphorbia milii is used to treat warts, hay fever, digestive problems, and breathing disorders like asthma and bronchitis (Rahman and Akter, 2013). In Brazil, *E. milii's* latex is used to treat warts. In other countries, it is commonly used in cancer treatment (Chohan et al., 2020). The bulbs are widely used to treat many illnesses, such as indigestion, stomach aches, constipation, diarrhea, and nausea.

Pharmacological activity and phytochemical composition

Euphorbia milii is known to have anticancer, antidiabetic, and antimicrobial properties. These properties are attributed to different phytochemicals present in the plant (Salehi et al., 2019). Phytochemical studies of *Euphorbia milii* show that flavonoids, triterpenes, saponins, phenols and tannins can be found in various parts of the plant (Kaur and Kumar, 2023). The leaves possess good cytotoxic activity due to the flavonoid-rich compounds. Flavonoids inhibit oxidative cell damage, indicating anti-inflammatory, anticancer, and antiseptic properties. The latex contains alkaloids such as β-sitosterol, euphol, euphorbol, and euphorbol hexacosanoa. The crude alcoholic extracts and ethyl acetate fractions have also shown high cytotoxic activity, suggesting that the potent cytotoxic molecules of the plant are more polar (Hassan et al., 2023). Medicinal plants' anticancer activity and efficacy are tested *in vitro* against cell lines to discover new drug formulations before being tested in pre-clinical and clinical trials. This study tested *E. milii* against prostate cancer cell lines *in vitro.*

2.6 Cell lines

2.6.1 Prostate cancer cell lines

Cell culture models are developed to test the cytotoxic activity of potential therapeutic agents, as well as to study different stages of various cancers. To be classified as a prostatic cell line, the cells have to express specific proteins, such as intermediate filament proteins IF, cytokeratins CKs 8 and 18. There are three prostate cell lines commonly used in *in vitro* research. These are LNCap, PC3, and DU145 cell lines. Together with the PC3 cells, DU145 cells are androgen receptor-negative and express AR mRNA. (Kaur and Kumar, 2023). Only the DU145 and LNCap prostate cancer cell lines were used in this study.

2.6.2 The DU145 cell line

DU145 cell line was the first prostate cancer cell line produced from a brain metastatic tumour in 1975. DU145 cells are haplotriploid human cells that do not secrete PSA and are hormone insensitive. In xenografts mice models, DU145 cells have a moderate potential to metastasize, especially to bone (Namekawa et al., 2019). The DU145 cell line is androgen-independent and can express mutated forms of androgen receptors and cytokeratins (Capone et al., 2020).

2.6.3 The LNCap cell line

LNCaP (lymph node carcinoma of the prostate) are androgen-sensitive prostate cancer cells, derived from the left supraclavicular lymph node metastasis of a 50-year-old Caucasian male (Saranyutanon et al., 2020). The malignant properties of LNCaP cells are sustained in nude mice which grow tumours at the inoculation site. Different cell lines have been derived from LNCaP cells to investigate various aspects of prostate cancer progression. When inoculated subcutaneously into male athymic nude mice, LNCaP cells do not metastasize (Abate-Shen and Nunes de Almeida, 2022). Prostate-specific antigen (PSA) is expressed by the LNCaP cell line. This is a clinically useful human prostate serum that can be used as a prostate cancer marker. The LNCaP cell line was used as the primary cell line for this study because it is the only prostate cancer cell line that is androgen-sensitive and secretes prostate-specific

antigen (PSA). Studies have indicated that the LNCaP cell line progression model is similar to human prostate cancer (Saranyutanon et al., 2020).

2.7 Nanotechnology

Nanomedicine uses nanotechnology and knowledge of the human body for medical diagnosis and treatment. In cancer treatment, nanomedicine is being explored for possible new targeted drug delivery systems to improve the pharmacodynamic and pharmacokinetic profiles of conventional therapeutics, therefore optimizing the efficacy of existing anti-cancer compounds and reducing their toxicity (Hafeez et al., 2021). With current cancer treatment, it is challenging to reach therapeutic levels of drugs at the tumour site without damaging and killing healthy cells. Nanotechnology offers a wide variety of solutions, including improved specificity and targeted delivery of chemo drugs to cancer sites (Alrushaid et al., 2023). Target-specific drug therapy is a priority research area in which nanotechnology plays a vital part in advancing cancer therapy. However, most efforts to improve cancer treatment through nanotechnology are still in the research or development stage.

2.7.1 Nanotechnology in drug delivery

Nanotechnology has attracted much interest in drug delivery over the years because of its unique properties that increase drug efficacy, selectivity, and retention time. Nanoparticles are drug-delivery vehicles ranging from 1 - 100nm in size. The size of the nanoparticles allows easy penetration into the tumour and enhances the therapeutic potential of the administered drug (Sahu et al., 2021). Nanoparticles composed of different biological compounds have been thoroughly studied for drug and gene delivery in nanomedicine. Nanoparticles used in nanotechnology include ceramic, metal, polymeric, lipid-based and semiconductor nanoparticles (Khan et al., 2019). The application of nanotechnology in drug delivery includes binding nanoparticles to the targeted cancer cells, allowing effective targeted drug delivery, and thereby reducing the destruction of healthy cells.

2.7.1.1 Advantages of nano particles

- Nanoparticles that are surface modified by hydrophilic polymers, such as polyethylene glycol (PEG), can avoid renal clearance and rapid uptake by cells of the reticuloendothelial system (RES); thereby maximizing blood circulation time.
- Nanoparticles have improved bioavailability by enhancing aqueous solubility.
- Nanoparticles can be modified to increase specificity for targeted receptors.
- Nanoparticles have controlled release of entrapped active substances when exposed to stimuli.
- Minimal doses of chemotherapeutic agents are administered during the targeted therapy (doses are smaller than those in standard chemotherapy).
- Nanoparticles reduce toxicity and increase efficacy.

The current study explores the use of lipid-based nanoparticles, known as liposomes. Between various gene and drug delivery systems, liposomes provide some advantages, such as low toxicity, biocompatibility, and the ability to change the pharmacokinetic outline of therapeutic agents (Rommasi and Esfandiari, 2021).

2.7.2 liposomes

Liposomes are small, closed lipid vesicles comprising a phospholipid bilayer containing the aqueous centre (Pande, 2023) . The stability and integrity of liposomes rely on their chemical composition. The ability of liposomes to entrap hydrophilic and lipophilic elements allows the encapsulation of a wide range of drugs. The hydrophilic molecules are entrapped in the aqueous centre, and hydrophobic molecules are in the lipid bilayer. Liposomes are delivery vehicles that can transport drugs to the

cancerous site. Liposomes have many advantages as drug carriers, mainly since they are noncovalent aggregates. Their electric charge, lipid composition and sized can easily be modulated. The concentration of the drugs encapsulated in liposomes can be determined by using various techniques, such as UV–vis detection and HPLC, depending on the active compound inside liposomes (Giordani et

al., 2023). Liposomes are easily metabolized and biodegradable *in vivo*. They can entrap various solutes with different characteristics and molecular weights (Sheikholeslami et al., 2022)

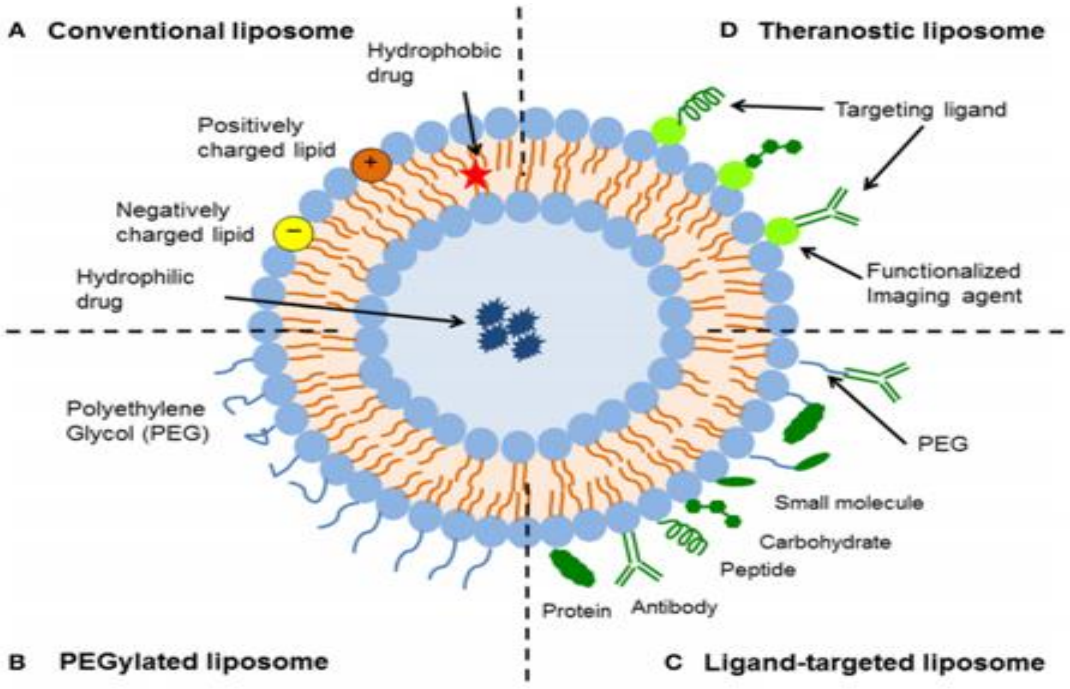

Figure 2: Different types of liposomal drug delivery systems (conventional, Theranostic, PEGylated and Ligand-targeted liposomes)

https://www.researchgate.net/figure/Schematic-representation-of-the-different-types-of-lip2014

In Figure 2 (A) shows the conventional liposome. Liposomes consist of a lipid bilayer and an aqueous core. Both the aqueous space and the lipid bilayer can incorporate hydrophilic and hydrophobic compounds respectively. Figure 2 (B) shows the PEGylated liposome. This is a hydrophilic polymer coating that modifies the behaviour and characteristics of the liposome surface *in vivo* to grant steric stabilization, Figure 2 (C) shows the ligand-targeted liposome that are utilized for specific targeting by attaching ligands such a antibodies and peptides to the surface or terminal end of the PEG chains. Figure

2 (D) shows the theranostic liposome. A single system of theranostic liposomes consists of a targeting element, a therapeutic component , and a functionalized imaging agent (Mundargi et al., 2022).

2.7.3 Classification of liposomes

The morphology of a liposome can be classified according to the compartments of the aqueous regions between bilayer shells. The size of vesicles is a crucial aspect in determining the circulation half-life of liposomes, and the total number of bilayers and the size affect the amount of drug encapsulation in the liposomes (Guimarães et al., 2021). Three groups of liposomes exist, classified by their structural morphology, using conventional classification: Multilamellar vesicle (MLV) liposomes have more than one bilayer around every aqueous compartment. If the aqueous regions are each separated by one bilayer, the liposomes are called unilamellar vesicles. There are large unilamellar vesicles (LUV) and small unilamellar vesicles (SUV) with sizes ranging from 25nm to 100nm. These various vesicular morphologies can be achieved through the self-assembly of a specific amphiphilic. Effective liposomes used for bioconjugates are the small spherical unilamellar vesicles with layers of hydrophilic head on their inner and outer surface. The membrane structure is essential for drug encapsulation to protect the drug from degradation (Sathe and Bangar, 2021).

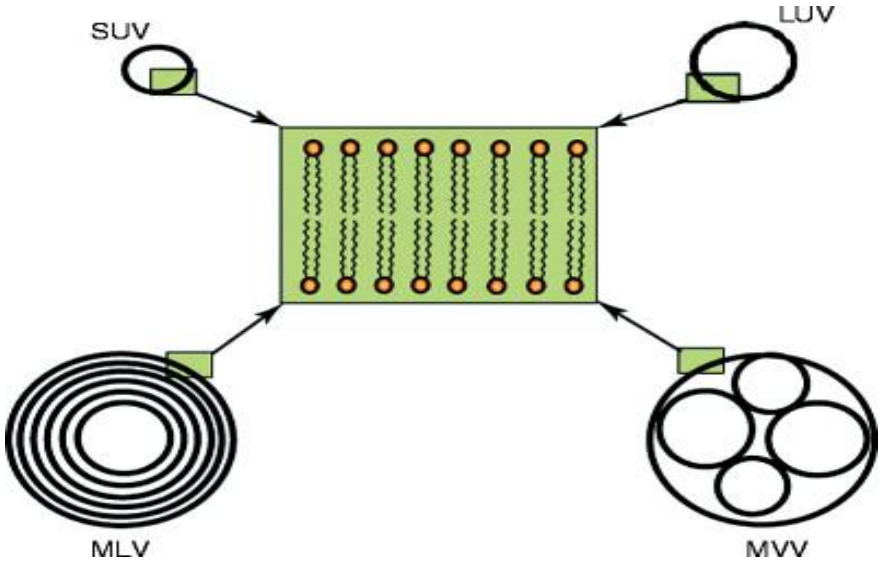

Figure 3: A schematic illustration of liposomes of different sizes and with different numbers of lamellae

https://www.researchgate.net/figure/02-Schematic-illustration-of-liposomes-of-different-size-and-number-of-lamellae-Small_fig8_278654572

Figure 3 is a schematic illustration of liposomes of different sizes and with different numbers of lamellae. SUV: small unilamellar vesicles; LUV: large unilamellar vesicles; MLV: multilamellar vesicles; and multivesicular vesicles (Nsairat et al., 2022).

There have been numerous attempts to develop liposomes that can regulate the release of drugs in response to stimuli, such as light, temperature and pH. Temperature-sensitive liposomes are the subject of this research. Conventional liposomes can enhance the effectiveness of drugs and treatment outcomes through temperature-controlled drug release at the cancer site. To achieve this, the carrier/drug relationship must be changed from a stable phase to gross instability at the target site (Chaudhry et al., 2022)

2.7.4 Temperature-sensitive liposomes

All lipids have a temperature at which their fluidity changes. This temperature is called the transition temperature (TC). The transition temperature can affect the stability of the liposome, the encapsulation efficiency, and the interaction between the liposomes and other lipids (Maritim et al., 2021). When the environmental temperature is higher than the phospholipid transition temperature, phospholipids present in a liquid state. The leaky lipid bilayer will then result in early drug release. It is thus, always safe to use phospholipids with a transition temperature higher than the body temperature when preparing liposomes (Bi et al., 2019). Thermo-sensitive liposomes can release drugs when exposed to heat at 39-to-42℃, due to thermosensitive polymers added to their formulation (Hossen et al., 2019, Maritim et al., 2021, Bi et al., 2019).

Heat-sensitive liposomes enable effective drug delivery to a targeted site because hyperthermia increases vascular permeability, interstitial transport, and the precision of the time the drug is released from the liposome into the tumour. Temperature-sensitive liposomes have an extended circulation time, enabling them to passively release the drug to accumulate at the desired site (Amin et al., 2020). Tumour cells usually have highly compact and disorganized vascular structures. Heat dissipation in these cells is often more complex than in normal cells, which provides a possible avenue for selectively targeting cells that contain heat (Raj et al., 2021). Temperature-sensitive liposomes have been triggered with different heating techniques, but there is no specification for ideal timing or duration when applying heat. A water bath can be used as a heat source in preclinical studies, such as animal studies.

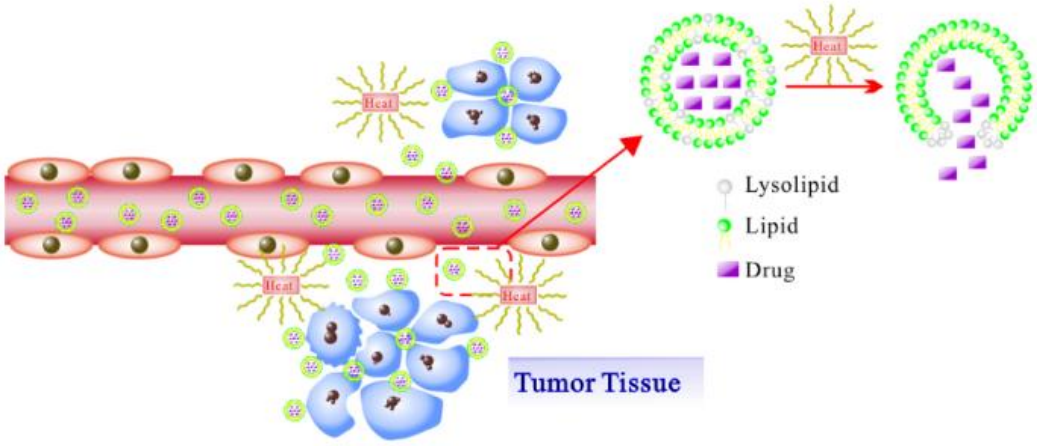

Figure 4: Thermosensitive liposomes passed through the tumour via enhanced permeability and retention where the external heating locates promoting drug release.

https://www.sciencedirect.com/science/article/pii/S1818087617307419

Temperature-sensitive liposomes are more dependent on the preparation method. Preparation includes using thermos-sensitive polymers such as poly (N_ isopropylacrylamide) PNIPA with a critical solution temperature near 31℃ for coating liposomes (Yang et al., 2020). Adding either hydrogenated soy phosphocholine (HSPC) or distearoyl phosphocholine (DSPC) to the temperature-sensitive liposomes increases load incompatibility, bilayer permeability, and the amount and rate of drug released (Heidarli et al., 2017). DSPE-PEG2000 1,2-distearoyl-sn-glycero-3-phosphoethnolamine-N-[amino(polyethyleneglycol)-2000] (ammonium salt) chloroform is a compound lipid with a PEG chain in the terminal end on the hydrophobic tail. Pegylated liposomes, also known as stealth liposomes, have an extended circulation half-life that can last days because of the PEG-lipid technology which enhances circulation at the tumour site. DSPE-PEG2000 is used as a PEGylated preparation for polymer micelles, liposomes, and microemulsions (Takayama et al., 2020). DSPE-PEG (2000)-amine has been used to synthesize solid lipid and thermosensitive liposomes, mainly for the delivery of anticancer drugs and the synthesis of fluorescein isothiocyanate-loaded mesoporous silica nanoparticles for imaging applications. DSPE-PEG (2000)-amine is used with different functional molecules, such as the DSPE-2000-maleimide, to prepare target-specific, antibody-conjugated nanoparticles for improved cellular and receptor targeting (Bi et al., 2019).

2.8 Targeted therapy

2.8.1 Enhanced permeability and retention effect

The inter-endothelial gap enhances the tumour's permeability, enabling nanoparticles to leak passively into the tumours (Duan et al., 2020). The use of targeted nanoparticles can improve the enhanced permeability and retention effect (EPR) for better delivery of anticancer drugs to the tumour site. Adding a polyethylene glycol (PEG) coating on the outer layer of liposomes aids localization of the liposomes at the desired target tissue through the EPR and increases blood circulation (Gawali et al., 2023).

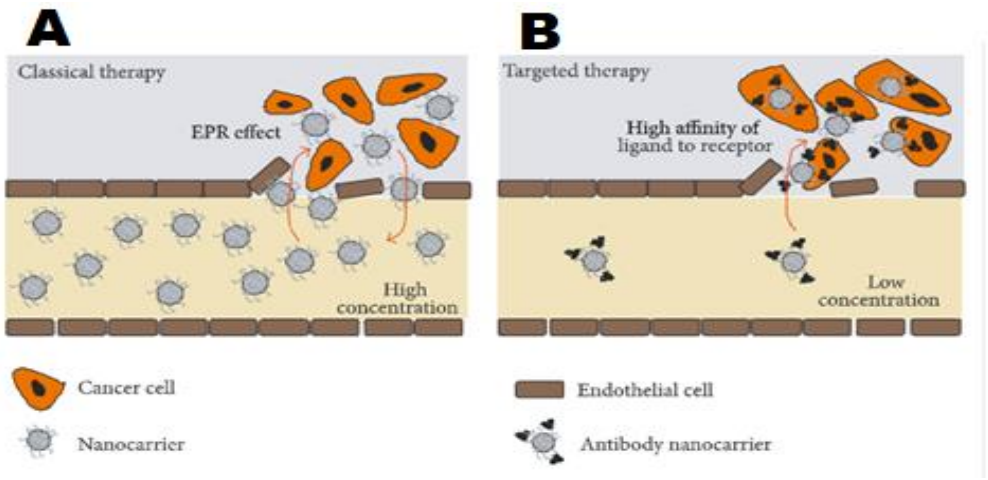

Figure 5: The chemistry of bioconjugation in a nanoparticles-based drug delivery system.

https://www.hindawi.com/journals/acmp/2015/198175/

Figure 5 illustrates the chemistry of bioconjugation in a nanoparticles-based drug delivery system: (A), passive drug targeting by EPR effect; (B), active drug targeting. Long-circulating liposomes that rely passively on the EPR effect have poor clinical efficacy. Active targeting relies on modifying the surface of liposomes with targeting ligands that bind to specific receptors at their target site (Sharifi et al., 2022).

2.8.2 Targeted thermosensitive liposomes

The overexpression of cell receptors on the outer surface of cancer cells in tumours facilitates cancer cell recognition by targeting moieties conjugated on drug delivery systems. Anticancer therapy targeting ligands can recognize tumours, such as antibody nucleic acids; peptides; oligosaccharides; carbohydrates; and vitamins, which can be conjugated on the surface of liposomes (Tiwari et al., 2023). After targeted liposomes off-load into the tumour interstitial space, ligand-receptor interactions increase cellular internalization (For example, interaction between antigens and antibodies). Compared to other ligands, antibody-conjugated liposomes, also termed immunoliposomes, have attracted considerable attention as a targeted therapy (Eroğlu and İbrahim, 2020).

2.8.3 Immunoliposomes

Immunoliposomes aim to increase the accumulation of the drugs in the diseased tissue using antibodies on the surface of liposomes. Scientific research conducted on antibody-conjugated liposomes was first reported by Sullivan and Huang in 1985. They used antiH2KK antibodies to make heat-sensitive immunoliposomes (Motamarry et al., 2017). Antibodies targeting specific receptors found on cancer cells are usually conjugated onto liposomes for targeted drug delivery. Once these antibodies are attached to antigens on tumour cells, temperature sensitive liposomes can then release their content upon heat stimulus. Conjugating antibodies to the liposome outer surfaces mainly involves covalent antibody bonding to the liposome surface. Temperature-sensitive immunoliposomes combine the advantages of triggered and controlled release. A study by Al-Ahmady et al. indicated that heat-sensitive liposomes conjugated with an IgG antibody resulted in a higher liposome accumulation on the tumour, compared to heat-sensitive liposomes not conjugated with an antibody. Successful targeting and long blood circulation times of immunoliposomes *in vivo* were demonstrated with PEG-coated liposomes. Liposome conjugation can be achieved through the N or C terminus. DSPE-PEG-Maleimide (DSPE-PEG-MAL) is a PEGylation reagent containing DSPE hydrophobic saturated phospholipids as well as maleimide, which has good reactivity to sulfhydryl (thiol, -SH) groups. DSPE-PEG(2000) maleimide is used to prepare conjugated polymer nanoparticles. DSPE-PEG(2000) maleimide provides a self-

assembling reagent to prepare PEGylated nanoparticles while supplying a thiol maleimide group. Maleimide PEG DSPE can bind antibodies and other ligands to the surface of lipid PEG nanoparticles (Zhang and Zhang, 2020).

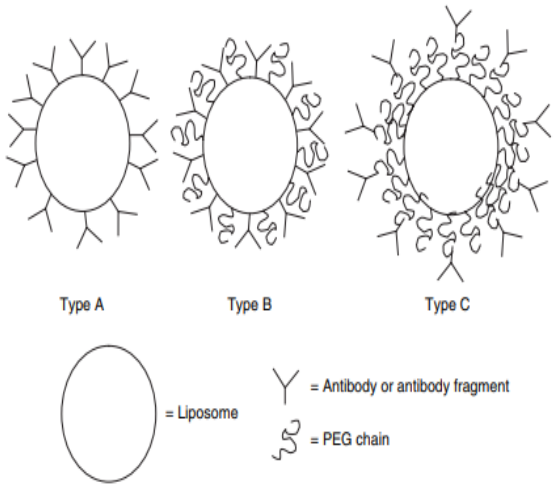

Figure 6: Different types of immunoliposomes

Figure 6 provides a diagrammatical representation of different kinds of immunoliposome: Type A: liposomes show the direct conjugation of antibodies to the head group of the lipid, to generate immunoliposomes with binding specificity, but having reduced blood circulation time; Type B: liposomes with constituents that consist of antibodies and PEGylated lipids (lipids conjugated to polyethylene glycol [PEG]); Type C: liposomes containing cell-targeting antibodies attached to the PEGylated lipids free termini.

Chapter 3

3. Research techniques

3.1 Plant extraction

Generally, plant extraction is the process of obtaining the constituents of the plant materials. In preparation for the plant material extraction, the plant materials are usually washed to remove debris, cut into small pieces, and dried. It is crucial to ensure that the grinder used is not too hot, to avoid the degradation of compounds. The powdered plant material measurement, depending on the amount needed for the extraction, is then weighed and the process of extraction is carried out using organic solvents (such as ethyl acetate, hexane, DCM, and methanol), or water, depending on the compounds of interest, in relation to polarity. Before filtering using filter paper, the plant-solvent mixtures are usually placed on a shaker or a stirrer for about 48 hours, for the purpose of extracting the pharmacological content of the plant material. The filtrates of organic extracts are concentrated under decreased pressure at a temperature of 45 °C, with 150 rotations per minute, using a rotatory evaporator, while the water extracts are concentrated with the help of a freeze dryer. Finally, the extracts are transferred into a pre-weighed vial and dried in a dark room at room temperature (Direko et al., 2019).

3.2 Phytochemistry screening

Phytochemicals are secondary metabolites detected in plants. Phytochemical screening is an easy, inexpensive experiment that provides answers to the phytochemical constituents in any phytochemical-containing mixture, and it remains a vital tool in the analysis of bioactive compounds. Some of these bioactive substances obtained from parts of a plant include flavonoids; alkaloids; carotenoids; tannins; antioxidants; proteins; amino acids and phenolic compounds. Usually, the powdered material of the plant is subjected to diverse phytochemical evaluation methods, to establish the presence of these bioactive compounds, such as saponins; flavonoids; pentose; glycosides; triterpenoids; tannins; anthraquinones; alkaloids, and phytosterols (Inayat et al., 2020).

3.3 Cell viability test

A cell viability test is conducted, based on the ratio of dead and live cells. This assay is based on analysing the viability of cells in a cell culture when testing *in vitro* drug effects in cell-mediated cytotoxicity assays to monitor cell proliferation. Cell viability and assays relies on different cell functions, such as cell adherence; enzyme activity; cell membrane permeability; nucleotide uptake activity; ATP production; and co-enzyme production (Zhang et al., 2023). Various assay methods can be utilized to assess the number of viable cells, such as the MTT assay.

The MTT (3-(4,5-dimethylthiazol-2-yl)-2,5-diphenyltetrazolium bromide) assay is a quantitative colorimetric assay commonly used for the measurement of metabolic activity and the cytotoxicity of cells tested in various culture conditions. The MTT substrate is developed in a physiologically balanced mixture which is added to cells. The viable cells then reduce the yellow colored water-soluble tetrazolium salt to purple water-insoluble formazan (Nwabuife et al., 2023). The absorbance at 540 nm using a plate reading spectrophotometer is used to detect the amount of formazan.

3.4 Thin film method

The thin film method is based on mixing the liposome formulation with a solvent, such as chloroform, to make a thin lipid film at the bottom of a round flask by removing an organic solvent, usually through a rotary evaporator at 60°C for ~20 minutes to form a solid film. After evaporation, the flask is placed in a vacuum desiccator overnight to remove organic solvent residue. It is vital to cover the flask's opening with stretched parafilm with small holes to prevent the entry of contaminants. When the solvent is successfully evaporated, PBS is added to hydrate the dry lipid (Nwabuife et al., 2023).

3.5 Characterization techniques

3.5.1 Transmission electron microscopy (TEM)

Transmission electron microscopy is a technique in which a beam of electrons in a microscope is transmitted through a specimen to create an image. The image is created when the sample interacts with electrons as the beam is transmitted through the specimen. The imaging system comprises the specimen

stage; the projector; intermediate lenses; the objective lens, and the image recorder mainly responsible for converting the electron image to one visible to the human eye (Dhale, 2023).

Transmission electron microscopes can produce images at higher resolution than light microscopes. This allows the microscope to capture detail as small as nanoparticles and a single column of atoms (Lin et al., 2021).

3.5.2 Scanning electron microscopy (SEM)

A scanning electron microscopy generates images by scanning the surface with a focused beam of electrons interacting with atoms in the sample. This produces a variety of signals with details of the sample's surface composition and topography. The microscope has an electron column; detectors; a scanning system; a vacuum system; and electronic controls. The electron column has electromagnetic lenses running in a vacuum as well as an electron gun. This electron gun produces electrons that accelerate to energies in the range 1-40 KeV in the SEM. Images are created when the electron beam is focused into a thin probe. When the accelerated electrons strike areas of the specimen, electromagnetic radiation signals are emitted. The detector collects a specific portion of radiation, and the image produced is easy to analyse (usually topographic imaging of objects at low modifications) (Chen et al., 2020).

3.5.3 Fourier transform infrared (FTIR) spectroscopy.

Fourier transform infrared spectroscopy is a common form of infrared spectroscopy. This technique is used to detect various functional groups and chemical bonds by generating an infrared range absorption spectrum. FTIR works on the vibrations of the atoms in molecules. It can be used to virtually analyse organic, inorganic, and polymeric samples in all states (liquids; gases; powders; solutions; pastes; powders; fibres; gases). The spectrometer comprises of a laser; mirrors; a source; a beam splitter; and a detector. The instrument transmits infrared radiation ranging from approximately 10,000 to 100cm-1(Eid, 2022).

3.5.4 High-performance liquid chromatography (HPLC)

High-performance liquid chromatography (or pressure) liquid chromatography (HPLC) is a chromatographic technique in analytical chemistry, utilized for the separation of compounds in a solution, as well as to quantify, purify, and detect different compositions within a chemical mixture (Reuhs, 2017). HPLC depends on pumps to drive pressurized liquid solvent containing the sample mixture through a column packed with stationary phase. The mobile phase moves the sample through the column to the detector. Compounds then separate due to different degrees of interaction with the stationary phase or absorbent material (Malhotra, 2023).

3.5.5 Liquid chromatography–mass spectrometry (LCMS)

Liquid chromatography–mass spectrometry is a technique that merges the physical separation capabilities of HPLC, or liquid chromatography with the mass analysis abilities of mass spectrometry (MS). Coupled chromatography-mass spectrometry is often used in chemical analysis because the individual abilities of each technique to work synergistically. While HPLC separates mixtures with various components, mass spectrometry gives detailed spectral information identifying or confirming the separated component's composition. LCMS has an interface responsible for transferring the maximum amount of the separated analyte from the LC column into the MS ion source. MS is sensitive and provides selective detection. MS analysers perform in a high vacuum, making it impossible to directly pump the eluate from the LC column into the MS source (Beccaria and Cabooter, 2020)

Chapter 4

4. Methodology

4.1 Study location

Plant extraction was carried out at the Central University of Technology, the Faculty of Health Sciences, in the Department of Biomedical Sciences. All cell culture experiments, synthesis of heat-responsive liposomes, preparation and conjugation of *Euphorbia milii* encapsulated heat-sensitive liposomes, were conducted by the researcher at the University of the Free State's Pharmacology Department, Health Sciences. Scientific ethics clearance was obtained from the University of the Free State, ethics number UFS-AED2020/0065/191.

4.2 Plant collection and extraction

The plant was collected from the Gariep nursery, situated at 309 Cliffendale Drive, Faerie Glen, Pretoria, South Africa, on 11 November 2020, at 11:00 (SAST), and identifiedby a taxonomist, Dr. Pienaar, of the Department of Botany, the University of the Free State, in Bloemfontein, South Africa. As the plant was obtained from a nursery, and not from the wild, the co-ordinates were deemed sufficient, and no specimen number was issued.

The plant was washed to remove debris, cut into pieces, and left to dry at room temperature; then ground to a fine powder. Nine grams (9 g) of the powder was suspended in 150 mL of hexane, dichloromethane, and methanol sequentially. The mixtures were placed in a rotary shaker for 48 h at 25°C at the solid:solvent ratio of 1:16. Each mixture was filtered using filter paper (whatman® Maidstone). Filtrates were concentrated under decreased pressure at 45°C and 150 rpm using a rotary vacuum evaporator; transferred into a pre-weighed, clean vial; shade dried (without direct exposure to sunlight) at room temperature; and stored at 4°C until required for use.

4.3 Phytochemical analysis

Standard qualitative screening of the *E. milii* plant specimen was conducted to detect the presence of secondary metabolites. The plant materials were ground and subjected to various phytochemical analysis methods to evaluate the presence of phytosterols, saponins, flavonoids, pentose, tannins, glycosides, alkaloids triterpenoids, and anthraquinones, based on previously published protocols (Inayat et al., 2020).

Determination of phytosterols

Chloroform (10 mL) was added to the powdered material (0.05 g), followed by the careful addition of concentrated H_2SO_4 (1 mL), down the walls of the test tube. The presence of a reddish-brown colour in the layer of the chloroform was taken to be an indication that phytosterols were present.

Determination of pentose

Distilled water (40 mL) was added to the powdered plant material (2 g), after which the filtration of the mixture was carried out. To a portion of 2 mL of the filtrate, 2 mL of a mixture of hydrochloric acid and phloroglucinol was added. Thereafter, the solution was warmed for a period of five minutes. The formation of red coloration indicated the presence of pentose.

Determination of tannins

Distilled water (20 mL) was added to the powdered plant material (0.5 g). Thereafter, the mixture was subjected to a high temperature by boiling, and the mixture was filtered before cooling. The treatment of the filtrate was carried out by the addition of three drops of ferric chloride (0.1%). The presence of tannins was confirmed by the formation of blue-black precipitates.

Determination of glycosides

Acetic acid (2 mL) was added to the powdered plant material (0.5 g). This was followed by the treatment of the mixture with one drop of ferric chloride (0.1%), and the gentle addition of concentrated sulphuric acid (1 mL). The observation of a brown ring indicated that deoxy sugars were present.

Determination of triterpenoids

To 2 mg of powdered plant material, 1mL of chloroform was added, then 3 mL of concentrated sulphuric acid was added to the solution. A reddish-brown coloration interface indicated that triterpenoids were present.

Determination of anthraquinones

A solution of 10% HCl (12 mL) was added to the powdered plant material (1 g). Thereafter, the solution was boiled for a period of five minutes. It was filtered, and allowed to cool down, before the addition of chloroform (10 mL) to the filtrate. A clean test tube was used to collect the chloroform layer and, thereafter, a solution of 10% ammonia (10 mL) was added to the chloroform mixture. The formation of a top layered rose-pink coloration while shaking the mixture was taken to be an indication of the presence of anthraquinones.

Determination of saponins

Distilled water (5 mL) was added to the powdered plant material (0.5 g), boiled, and then filtered. Distilled water (3 mL) was then poured into the resulting filtrate, and the solution was vortexed for a period of five minutes. An indication of frosting confirmed the detection of saponins.

Determination of flavonoids

Ethyl acetate (10 mL) was added to the powdered plant material (0.5 g) and heat was applied to the resultant mixture for about three minutes; and was thereafter cooled. The cooled mixture was filtered; and to the filtrate (5 mL), a diluted solution of ammonia (1 mL) was added. The presence of flavonoids was confirmed by the observation of a yellow precipitate when the mixture was shaken.

Determination of alkaloids

A solution of 1% HCl (2 mL) was added to the powdered plant material (0.2 g), and this was followed by the addition of 1 mL to both the Meyer's reagent and the Drangendorff's reagent. The greenish/creamy precipitate (for Meyer's reagent) and reddish-brown appearance (for Drangendorff's reagent) observed were taken as indications of alkaloids being present.

4.4 Cell culture

4.4.1 Cell culture conditions

The humidified culture environment was kept constant at 37°C, with 5% atmospheric CO_2. DMEM media was used to grow the cells, and was supplemented using 10% serum (FBS), and incubated in the culture environment until 90% confluence was reached.

4.4.2. Cell sub-culturing

When the cells attained an approximately 90% confluence, as confirmed with the use of microscope analysis equipment, trypsinization was performed. Aliquots of 2ml of 37°C warmed trypsin-EDTA solution were added for about 2 minutes to detach the cells. Then trypsin-EDTA was neutralized by adding equal amounts of the complete medium (Direko et al., 2019).

The cell suspensions were then centrifuged for 5 minutes at 700 rpm to obtain the cell pellets. The cell pellets were then re-suspended in a fresh growing medium (5 mL). A 20 µl aliquot was then removed and counted with the help of cell-counting equipment to evaluate the viability of the cells. The volume of suspended cell solution required to obtain cell suspension of 1×10^5 per mL was calculated, and 10 ml of complete medium was added to it. Thereafter, cell plating was carried out using a 96-well plate, followed by an incubation in a humidified atmospheric CO_2 (5%), at 37°C.

4.4.3 Cell viability count

The viability of the cells was evaluated with the use of a dye-stating solution called trypan blue. Aliquots of cell suspension and the staining solution of trypan (20 µl each) were mixed inside an Eppendorf tube. Thereafter, a portion of the suspended cell (20 µl) was measured using a pipette and transferred into a sealed hemocytometer to obtain the concentrations of both dead and viable cells.

4.4.4 Cell plating

From the above cell concentrations, dilutions to obtain the desired cell concentrations ($1x10^5$ cells/ml) were made using supplemented media. A 100 µl aliquot of cell suspensions with concentrations of 1 x 10^5 cells per ml was then plated in different wells of a 96-well plate, and 100µl of the growth media was also added to each well. Thereafter, the plate was incubated to allow attachment of the cells, in an incubator, for a period of 24 hours.

4.4.5 Culturing of the assay

After the 24-hour incubation, the medium was removed. The cells were exposed to the drugs at different concentrations (1 µg/ml, 10 µg/ml, 100 µg/ml) for 72 hours. Complete medium (100 µl) was added up to a volume of 200 µl. These plates were incubated for a period of 48 hours. The first column of the 96-well plate only contained 200ul of complete media, without cells, and served as a blank; while the second column contained cells not exposed to any test sample, which served as the positive control.

4.4.6 Measuring cell viability

The cell growth measurement was carried out using the MTT assay method. On completion of the 48-hour incubation, the addition of 25 µL of sterile MTT (5 mg/ml in PBS) to the individual wells was carried out; and thereafter the plates were incubated at 37°C for 4 hours. Thereafter, supernatant aspiration from the wells was carried out, and 100 µL of dimethylsulphoxide (DMSO) was pipetted into the individual wells to help in the dissolution of the formazan crystals. This was followed by gently shaking the plates for 2 minutes, using a microtitre plate shaker. Then the plates were read immediately, with the help of a microtitre plate reader, at a wavelength of 540 nm. To calculate the values for cell viability, a dose-response curve was plotted using nonlinear dose-response curve fitting analyses from Microsoft excel (Ghasemi et al., 2021).

4.5 Cytotoxic activity of docetaxel-loaded liposomes and *Euphorbia milii* liposomes.

To evaluate the cytotoxic activity of temperature-sensitive immunoliposomes encapsulation, the *E. milii* DCM root extracts, as well as the prostate cancer standard drug's (docetaxel), cytotoxicity was evaluated using the MTT assay in the LNCap cell line. This was done with, and without, exposure to hyperthermia. To ensure that the drugs were intracellularly bioavailable, mild hyperthermia was used to induce the release from liposomes, following cellular uptake. A specific heating strategy was followed to evaluate the effect of the drug release on cell viability above the liposomal transition temperature. The incubation of cells along with liposomal formulations at 39 - 40°C was carried out for about 15 minutes, followed by a 48-hour incubation period at 37°C. The control experiment included no application of hyperthermia. Thereafter, the cells were treated for 4 hours using MTT solution. The formazan crystals that were formed were then solubilized with DMSO, and their absorbance were measured using a multimode plate reader at 540 nm (Ghasemi et al., 2021).

4.6 Synthesis of heat-responsive liposomes

Liposomes were prepared and modified using the thin film method. Briefly, in a round-bottom flask, liposomes consisting of HSPC: DSPE-PEG-2000: DSPE-PEG2000-maleimide in the molar ratio of 4:1:0.2 (2mg:0.5mg:0.1mg) were dissolved in 5 ml chloroform, and 2 mg of *E milii* extract/docetaxel dissolution in methanol (concentration of 1 mg/mL) was prepared. The solution was mixed out and the organic solvents were evaporated at 60°C for ~20 minutes with the help of a rotary evaporator to form the liposome film, which was then covered with a parafilm, and left overnight. This process encapsulated the drugs inside the liposomes. The dry heat-sensitive nanoparticles were hydrated with 2 mL of PBS and vortexed three times for 10 seconds at a maximum speed to suspend the lipid materials in the solution. The solution was left to stand at 4°C overnight to efficiently hydrate the lipid formulation (Ghasemi et al., 2021).

Figure 7: Weighed HSPC, DSPE-PEG-2000, and doxorubicin liposomes

4.7 Liposome conjugation

Heat-sensitive liposomes, consisting of HSPC: DSPE-PEG2000 and DSPE- PEG2000-maleimide (DSPEPEG2000-Mal), 4:1:0.2 ratio, were prepared. The combination of the anti-PSMA antibody and liposomes through stirring constantly for 4 hours at a temperature of 4°C, with a 1:10 molar ratio (antibody/DSPE-PEG2000-Mal liposomes), was carried out, and the anti-PSMA antibody conjugation to liposomes was carried out by sulfhydryl residues reacting on the antibodies with the PEG chains C-terminal maleimide groups (Mofolo et al., 2020). The removal of the unconjugated antibody from the solution was carried out using an ultracentrifuge for 2h at a temperature of 4°C and 30,000 rpm. The amount of residual anti-PSMA antibody in the collected supernatant was determined with the use of a BCA protein assay kit.

Figure 8: Antibody-conjugated heat-sensitive liposomes

4.8 Weighing of liposomes

Heat-sensitive liposomes encapsulating *E. milii* extract and liposomes encapsulating docetaxel were measured after they were successfully synthesized and conjugated by centrifuging the PBS-hydrated liposomes for 30 min at 90,000 g using an ultracentrifuge at 4°C. Following centrifugation, the supernatant and pellets were separated. The pellets were weighed in milligrams.

4.9 Protein analysis

The BCA protein assay (Pierce) was used to quantify the amount of anti-PSMA antibody conjugation on the liposomes. The unconjugated antibody removal from the liposomes was made possible by using an ultracentrifuge for 1 hour. After removing the unconjugated antibody, the supernatant was collected to evaluate the quantity of anti-PSMA. The dilution scheme for the microplate procedure of the BCA kit was used. One ampule of 2 mg/mL albumin standard was used to produce a set of diluted standards. BSA standards were diluted to concentrations of 2000, 1500, 1000, 750, 500, 250, 125, and 25 µg/mL. The protein content of the samples was thereafter determined using a standard curve obtained at 562 nm (Zhao et al., 2023).

4.10 Characterization of liposomes.

4.10.1 Transmission electron microscopy (TEM)

Liposomes were analyzed using negative stain electron microscopy using a JEM 1200 EXII electron microscope. A drop of liposome suspension was applied to carbon-coated grids, after 2 minutes, the surplus was drawn off with filter paper. A saturated uranyl acetate aqueous solution was utilized as a staining agent. The surplus was removed with distilled water. The morphology of the sample was analyzed by TEM at 80 kV(Mofolo et al., 2020).

4.10.2 Scanning electron microscopy (SEM)

The SEM was used to analyse the uniformity of particle shape and size and the morphology of the liposomes. The shape of the heat-sensitive immunoliposomes was analyzed using a scanning electron microscopy, JEOL JEM 2010 UHR, equipped with a Gatan Imaging Filter, with a 15-eV window and a 794 slow-scan CCD camera, operating at 2.00 kV (Mofolo et al., 2020).

4.10.3 Fourier transform infrared spectroscopy (FTIR)

The FTIR spectra of *E. milii,* doxorubicin, and docetaxel-loaded thermosensitive immunoliposomes, were studied to gain an insight into the occurrence of interaction between drugs and phospholipids (Marasini et al., 2020). A Perkin Elmer spectrum FTIR spectrophotometer was used to determine the chemical composition of the samples. FTIR spectra were reported in the wavelength range of 4000 - 400 cm^{-1}, at a spectral resolution of 4 cm^{-1}. Data were analyzed using the software FTIR Spectrum (Perkin Elmer) (Asemani and Rabbani, 2020).

4.10.4 Determination of encapsulation efficiency

The amount of drugs in temperature-sensitive liposomes was determined as follows: Liposomes were centrifuged for 30 min at 90,000 g, using an ultracentrifuge at 4°C. Following centrifugation, the

supernatant and vesicles were separated. The pellets were washed 4 times with 0.9% NaCI solution. Thereafter, 2.75 mL of alcohol was added to 0.25 mL liposome solution, and at 42°C it was incubated for 10 min to break down the heat-sensitive liposomes. When the incubation was completed, temperature-sensitive liposomes were left to cool down. The free drugs were separated from heat-sensitive nanoparticles using centrifugation, and the supernatant-containing free drugs were collected and adjusted with methanol for further analysis. The amount of drug released in the supernatant was determined using HPLC. For doxorubicin, the HPLC analysis was conducted using a C18 column with a mobile phase containing acetonitrile and water (32:68, *v/v*) at a flow rate of 1.0 mL/min. The column temperature was kept at 25 °C, and 10 µL of the sample was injected. Fluorescence detection was used to monitor the peaks at 480 nm excitation wavelength, and 550 nm emission wavelength, using a fluorescence detector. For the *E. milii* extract, a C18 column was used for the HPLC analysis, with a mobile phase consisting of acetonitrile and water (32:68, *v/v*) at a 0.8 mL/min flow rate. The column temperature was kept at 25 °C, and 10 µL of the ample was injected. Peaks were monitored.

4.11 Statistics Analysis of data

Results are expressed as means ± standard deviation. Data was analyzed using one-way analysis of variance (ANOVA) to compare experimental groups. GraphPad prism version 8 software, a post hoc test (Bonferroni) was used to calculate the IC50 values and confirm the level of significance between means (P values of less than 0.05 were considered significant.

An inhibition percentage of $\geq$50% at concentrations of $\leq$10ug/mL was considered active. This was the point of reference determining for activity. Excel software was used for calculating and plotting graphs (Bar charts) and % inhibition.

Chapter 5

5. Results

5.1 Phytochemical analysis

Table 1, below, shows the colour changes observed during the phytochemical analysis of *E. milii* leaves, stems and roots.

Table 1:Phytochemical analysis of leaves, stems and roots of *Euphorbia milii*

Phytochemicals	Observation	Leaves	Stems	Roots
Phyosterols	Reddish brown layer	 (+)	 (+)	 (+)
Pentose	Red colour formation	 (+)	 (+)	 (+)
Tannins	Formation of a black precipitate	 (+)	 (+)	 (+)
Glycosides	Brown ring formation	 (+)	 (+)	 (+)

Triterpenoids	Reddish brown colour formation	 (-)	 (+)	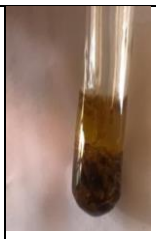 (-)
Anthraquinones	Rose pink colour	 (+)	 (+)	 (+)
Saponins	Frosting formation	 (-)	 (-)	 (+)
Flavonoids	Yellow precipitate	 (-)	 (+)	 (+)
Alkaloids	Formation of an organic precipitate	 (-)	 (-)	 (+)

The appearance of a reddish-brown colour indicated the presence of phytosterols. The formation of a red colour indicated the presence of pentose. A blue-black precipitate indicated the presence of tannins.

The appearance of a brown ring indicated the presence of glycosides. A rose-pink colour in the upper layer showed the presence of anthraquinones. Frosting indicated the presence of saponins, and a yellow precipitate indicated the presence of flavonoids. A greenish/creamy precipitate (for Meyer's reagent) and a reddish-brown appearance (for Drangendorff's reagent) indicated the presence of alkaloids. The formation of an interface with reddish brown coloration indicated the presence of triterpenoids. All phytochemicals were detected in the plant, except saponins, which were absent in the leaves and stems; and flavonoids, which were absent in the leaves.

Table 2: Summary of phytochemical screening results. Legend: '+' = present, '-' = not detected.

Phytochemicals	**Leaves**	**Stems**	**Roots**
Glycosides	+	+	+
Phytosterols	+	+	+
Saponins	-	-	+
Anthraquinones	+	+	+
Pentose	+	+	+
Alkaloids	-	-	+
Tannins	+	+	+
Triterpenoids	-	+	-
Flavonoids	-	+	+

5.2 Growth inhibition of DU145 cells anti-proliferation assay

The screening of the *E. milii* root, stem, and leaf extracts for cytotoxic activity against the prostate cancer DU-145 cell line was carried out. Extracts were tested in three replicates (n=3) at different concentrations of 100 µg/mL, 10 µg/mL, and 1 µg/mL. An inhibition percentage of ≥50% at concentrations of ≤10ug/mL is considered active.

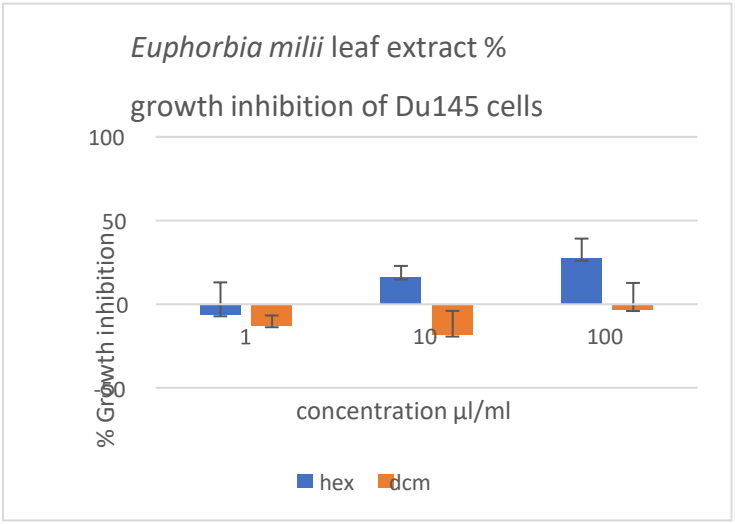

(a)

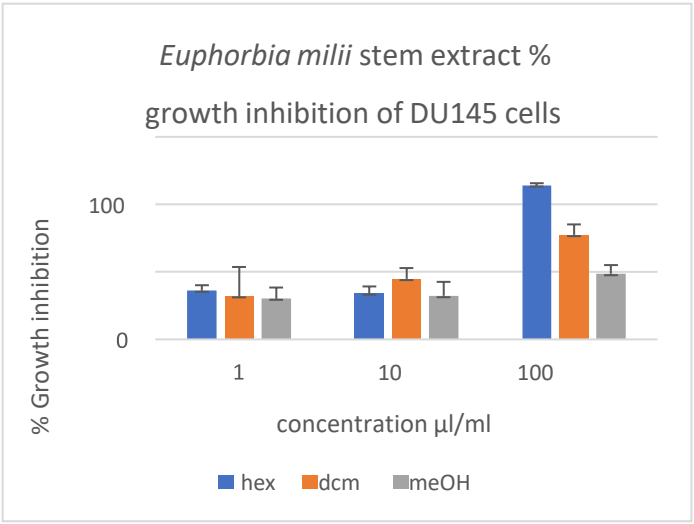

(b)

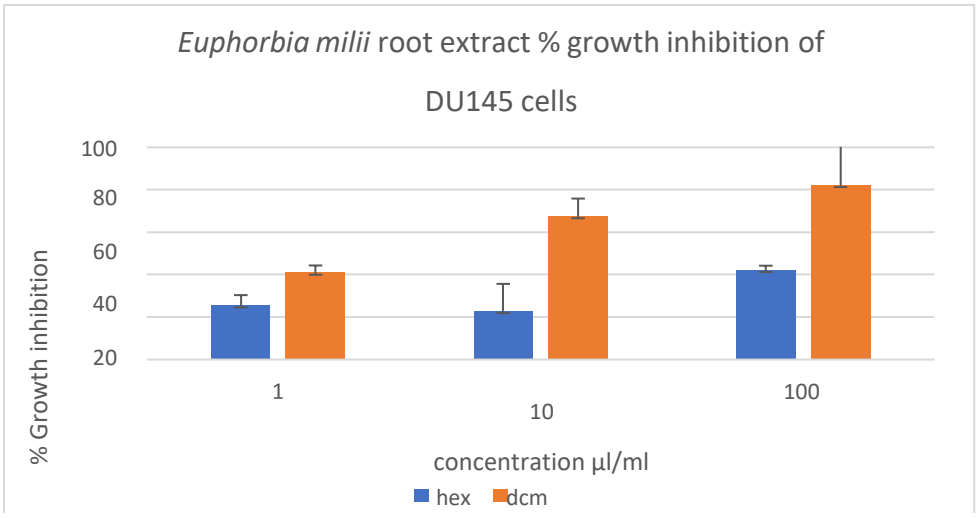

(C)

Figure 9: Cell growth inhibition of DU145 cells by different extracts

Figure 9 shows growth inhibition of DU145 cells by leaf extracts of *E. milii*. In figure 9 (a), hexane leaves showed less than 30% growth inhibition at all three concentrations. The DCM leaves showed no growth inhibition at all three concentrations. A significant difference of (*P-value* <0.05) was observed for hexane leaves compared to DCM leaves. In Figure 9 (b), growth inhibition of DU145 cells by stem extracts of *E. milii* hexane stem extract showed 114.2 ± 1.5% activity at 100µg/ml, but less than 50% activity at 1µg/ml and 10µg/ml. The DCM stem extract showed 37.4 ± 21.5% activity at 1µg/ml and 49.7 ± 7.9% 10µg/ml, and 78 ± 1.8% activity at 100µg/ml. No significant difference was observed for hexane stems compared to DCM stems (*P-value* <0.36). Methanol was only tested on stems and not on leaves and roots, hence the results for methanol are only reported for stems. The Euphorbia *milii* methanol extract showed no significant activity at all three concentrations. No significant difference was observed for methanol stems when compared to both hexane stems (*P-value* <0.35) and DCM stems (*P-value* <0.2). In Figure 9 (c), growth inhibition of DU145 cells by root extracts of *E. milii*. DCM root extract showed more than 50% activity at 1µg/ml, 10µg/m and 100µg/ml concentrations, inhibiting 67.51 ± 8.3% of the cells (IC50). This is the only extract that showed desirable activity when screened against the DU145 prostate cancer cells. A significant difference of (*P- value* <0.030) was observed for Hexane roots compared to DCM roots. The DCM root extract was further screened against the LNCap cell line. Results are presented as mean ± SD.

5.3 Growth inhibition of LNCap cells anti-proliferation assay

The *E. milii* DCM root extract was tested in three replicates (n=3) at different concentrations of 100 µg/mL, 10 µg/mL, and 1 µg/mL against the LNCap cell line.

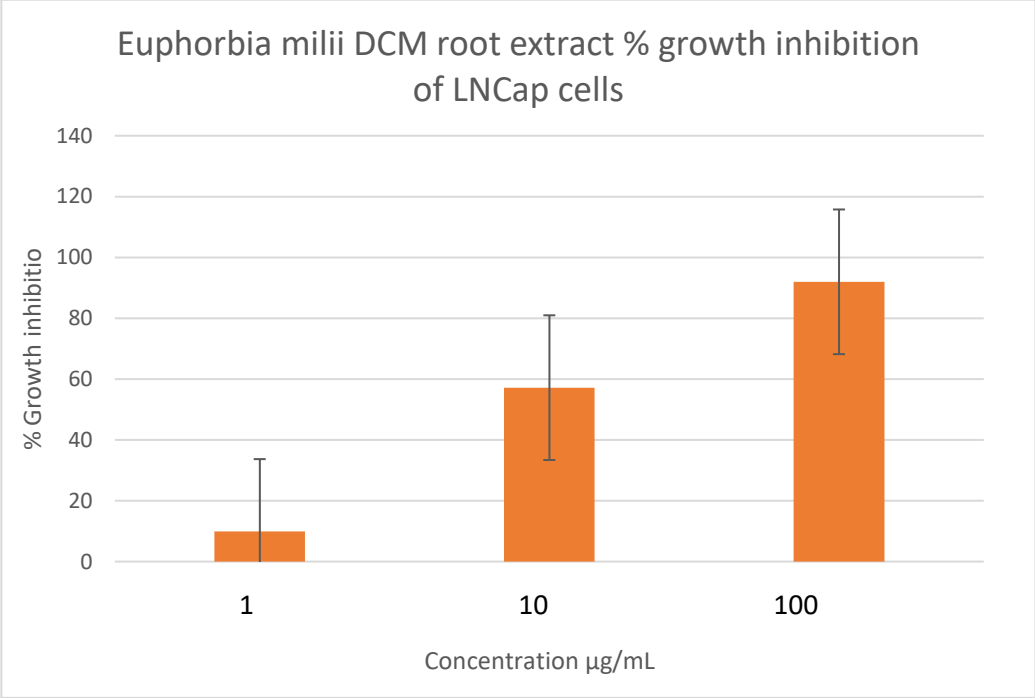

Figure 10: Growth inhibition of LNCap cells by root extracts of *E. Milii.*

Figure 10 shows the cell growth inhibition of LNCap cells when treated with different concentrations (100, 10, and 1 µg/mL) of DCM root extract of *E. milii.* The extract showed activity 91.98 ± 10.17% of growth inhibition at concentrations of 100 µg/mL, and 51.7 ± 6.13% inhibition at 10 µg/mL. More dilutions of the extract were performed and screened for activity in order to obtain more accurate IC50 values. The results are shown in Figure 11, below. The extract's activity was further investigated in cells when encapsulated into heat-sensitive liposomes. Results are presented as mean ± SD.

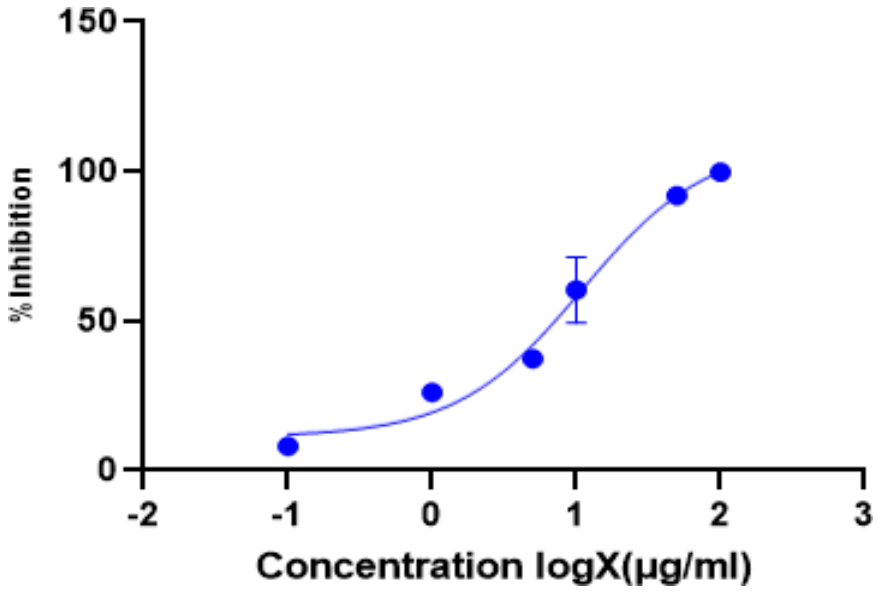

Figure 11: Cytotoxic activity of the *E. milii* DCM root extract on LNCap cells with a IC50 value of 11.34 µg/mL

5.4 Percentage inhibition of doxorubicin, docetaxel.

Doxorubicin and docetaxel were added as positive controls and screened against the DU145 and LNCap prostate cancer cell lines. The results are indicated in Figure, 12 below.

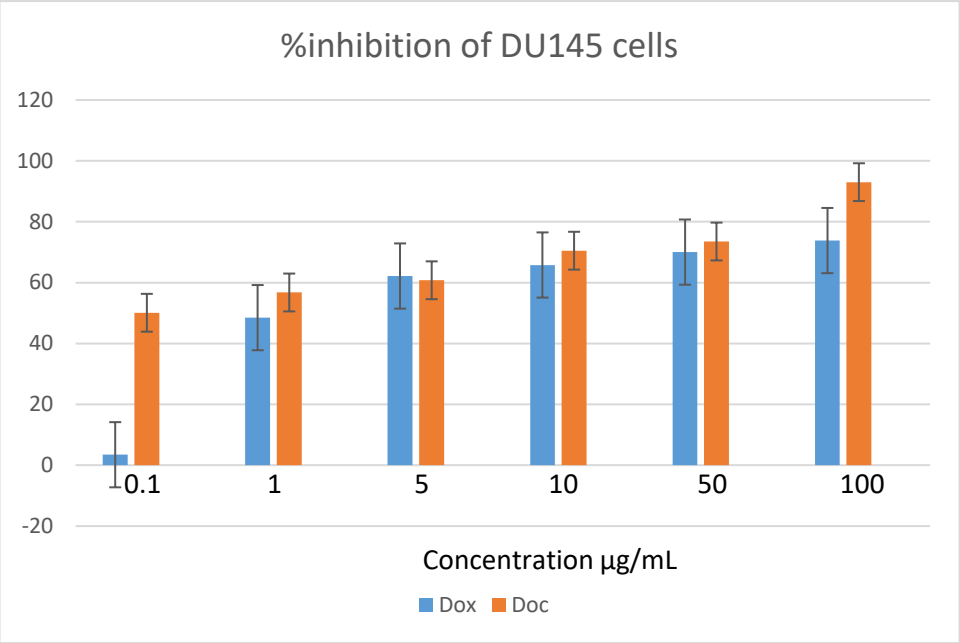

Figure 12: The cytotoxic activity of doxorubicin and docetaxel against the DU145 cell line

Doxorubicin (Dox) achieved $\geq$ 62.16 ± 2.5%, at concentrations of 5µg/mL and above, with a maximum of more than 70% inhibition at 100µg/ml. Docetaxel (Doc) was active, showing above 50% activity at all concentrations. No significant difference was observed for Dox when compared to Doc (*P-value* <0.12). Results are presented as mean ± SD.

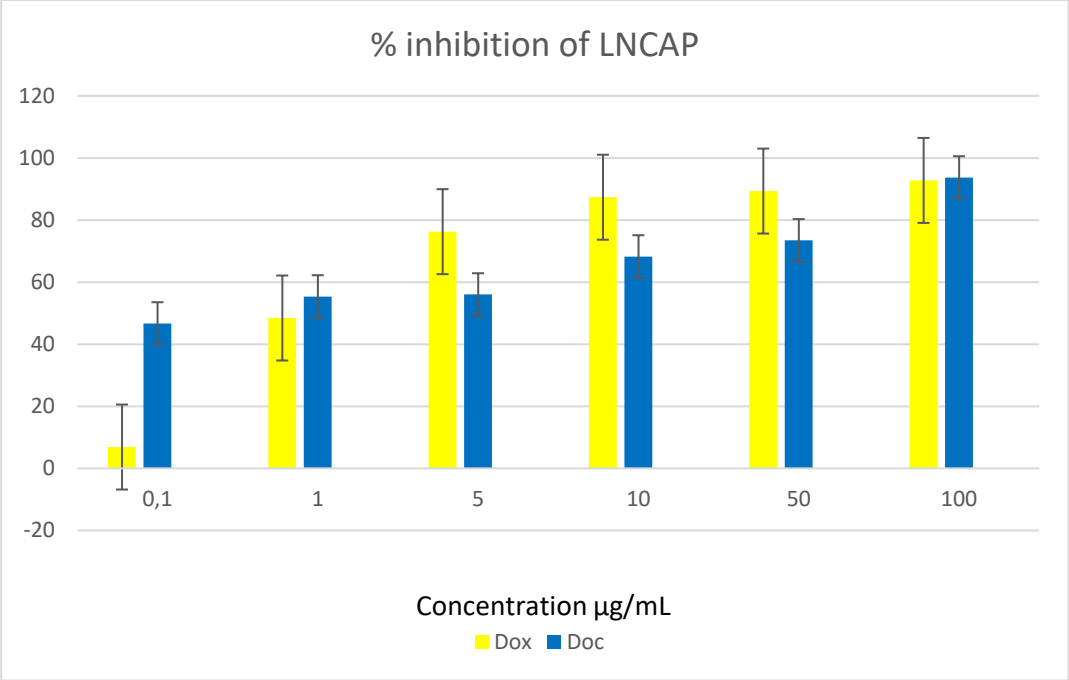

Figure 13: The cytotoxic activity of doxorubicin and docetaxel.

Figure 13 shows the cytotoxic activity of doxorubicin and docetaxel against the LNCap cell line. Doxorubicin showed activity of 76.25 ± 7.05% at 5 µg/ml, 87.34 ± 6.45 at 10 µg/ml, 89.32 ± 3.42% at 50 µg/ml, and 92.76 ± 3.2% inhibition at 100 µg/ml. Docetaxel showed activity of 55.3 ± 3.66% inhibition at 1µg/mL and more activity at higher concentrations, with 93.69 ± 2.41% at 100 µg/ml. No significant difference was observed for Dox when compared to Doc (*P-value* <0.89). Results are presented as mean ± SD.

5.5 Characterization of heat-sensitive immunoliposomes

The heat-sensitive immunoliposomes were characterized using FTIR, TEM, and SEM. The results are shown in Figure 14, 15 and 16, below.

5.5.1 FTIR results

FTIR spectrometry was used to examine the interaction between drugs and temperature-sensitive immunoliposomes.

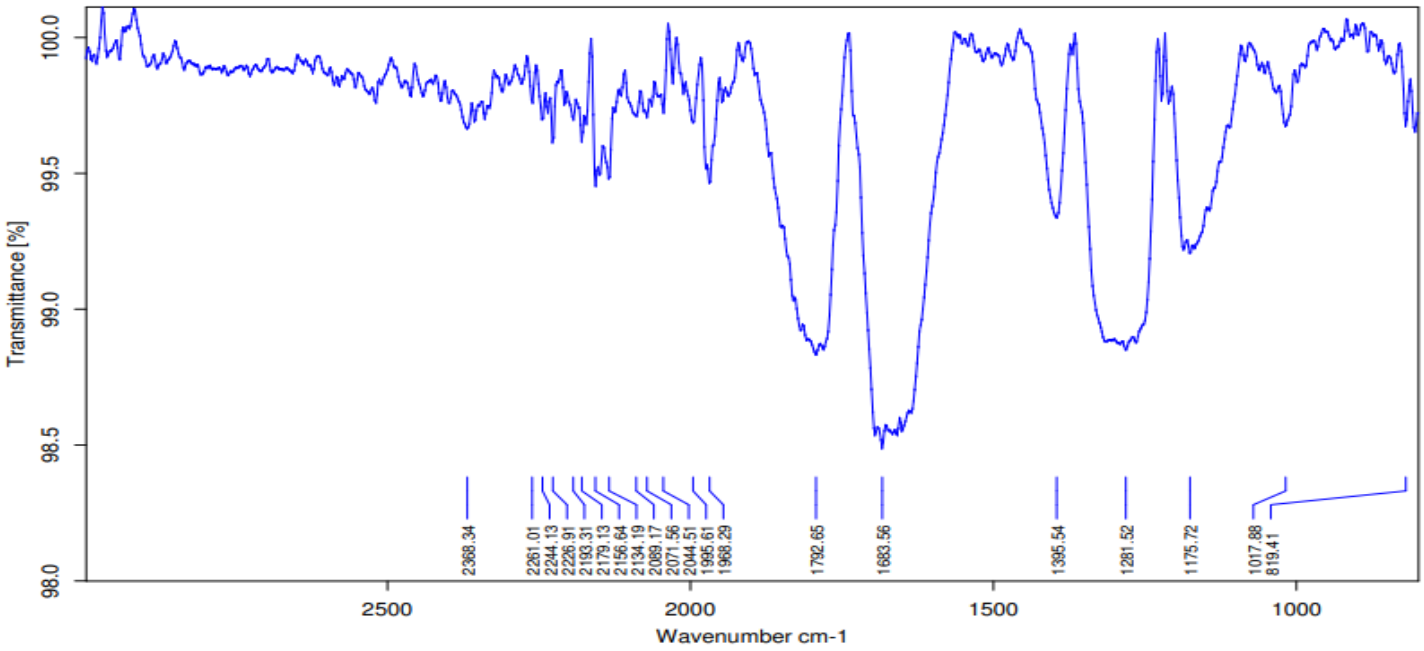

Figure 14: FTIR spectra of *E. milii* -loaded heat-sensitive immunoliposomes

Figure 14 is the FTIR spectra of *E. milii*-loaded heat-sensitive immunoliposomes have shown a C-O peak at 179265; a C-O stretching peak at 1683.56; a C-H bending peak at 1395.54; CH is usually found in aromatic compounds of plant extracts. The peak at 1281.52 confirmed the presence of carboxylic acid group and aromatic amine, CO stretching peak at 1017.88. The peak between 1150–1000 is the C-F stretch showing aliphatic fluoro compounds. The peak range between 2100 and 2250 can be attributed to the C-C functional group, which possibly indicates the presence of alkynes. Furthermore, the observed peak at 819.41 of the peak range between 1040 and 732 can be attributed to aromatic compounds.

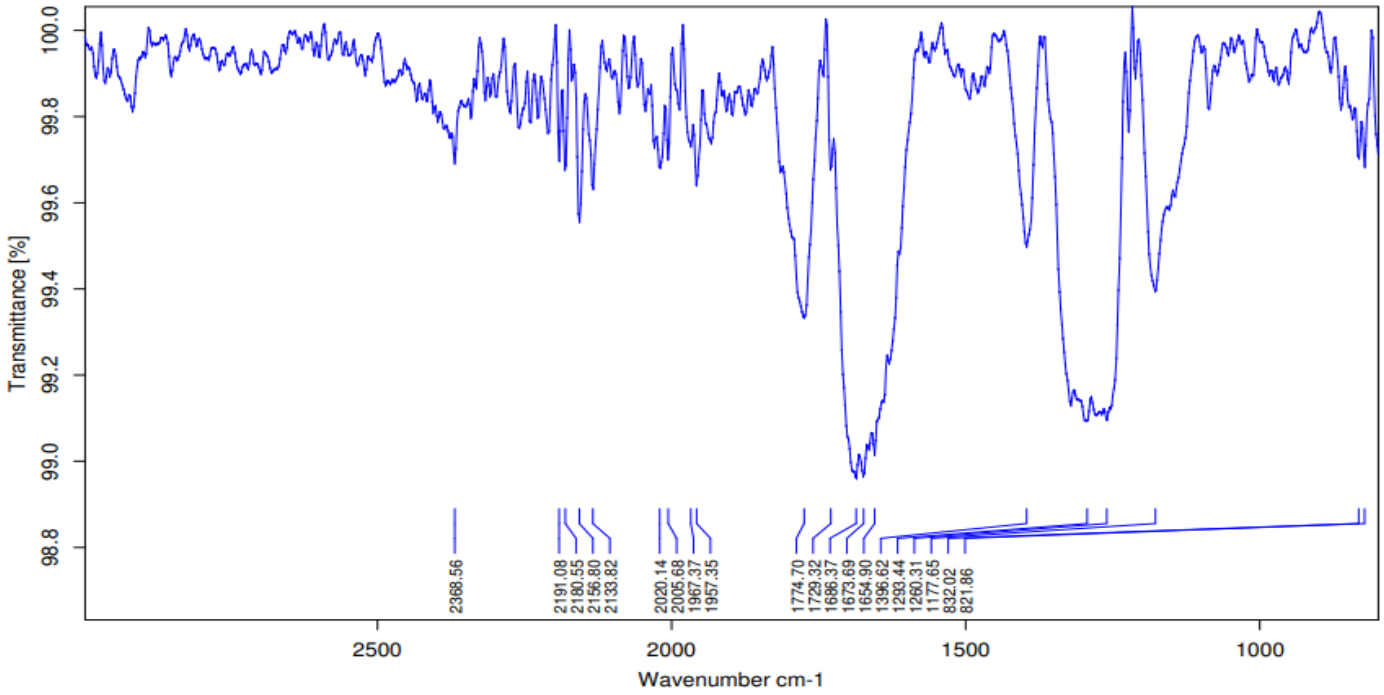

Figure 15: FTIR spectrum of doxorubicin-encapsulated heat-sensitive immunoliposomes.

Figure 15 is the FTIR spectrum of doxorubicin heat-sensitive immunoliposomes showing similar peak ranges to those contained in *E. milii*-loaded heat-sensitive liposomes. Doxorubicin-loaded heat-sensitive immunoliposomes have shown a C-O peak at 1774.70. C-O stretching peak at 1686.37, 1673,69 and 1654.90 found in aromatic compounds of plant extracts. C-H stretching peak at 1396.62. The peak at 1293.44 and 1260.31 confirmed the presence of carboxylic acid group and aromatic amine. The peak at 1177.65 was attributed to the OH stretching. The peak range at 2191.08 and 2180.55 can be attributed to the C-C functional group, which possibly indicates the presence of alkynes. The observed CH and Si-C stretching peak at 832.02 and 821.86 these peaks are in the peak rage attributed to aromatic compounds.

.

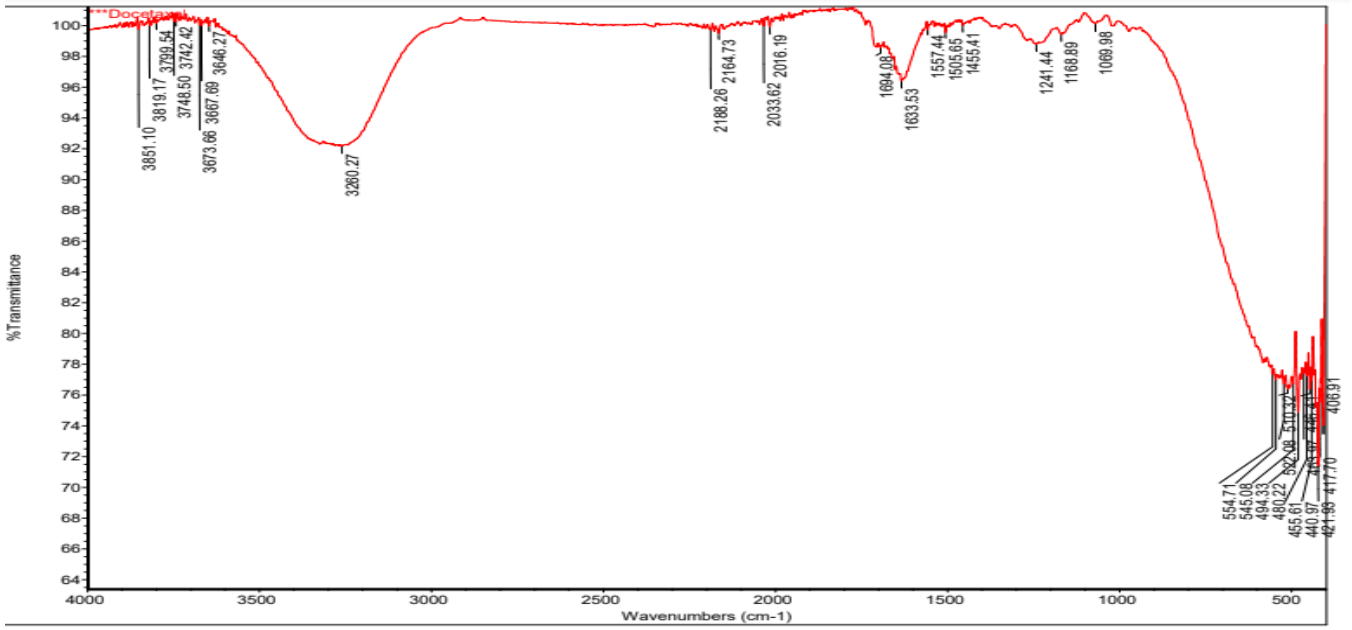

Figure 16: FTIR spectrum of docetaxel-encapsulated heat-sensitive immunoliposomes.

Figure 16 is the Docetaxel-loaded heat-sensitive liposomes have shown carboxyl acid peak at 3260.27, which is part of the 2500 - 3300 frequency range. The peaks in this range appear in FTIR analysis of the lipid DSPE-PEG when conjugated. In the study conducted by (Marasini et al., 2020), the peak range of 3169-3334 was attributed to the presence of methyl and methylene groups in the molecules of the PEG and amide. (C-O) peak at 1633.53. The alkyl ketone peak at 1241.44; the alkyl amine peak at 1168.89; and the peak at 1069.98 indicate the presence of polysaccharides, which are part of the 1035–1149 frequency range found the absorption pattern between 1282 and 1020 useful for determining a phospholipid calibration curve. This peak range is seen in *E. milli* extract, doxorubicin, and docetaxel liposomes.

5.5.2 TEM and SEM results

The transmission electron microscope (TEM) and scanning electron microscope (SEM) images, below, show the morphological structure of the prepared heat-sensitive immunoliposomes observed at 50nm,100 nm, 500 nm, and 1 micrometer. From the TEM analysis, the shape of the immunoliposomes appear opaque and spherical at various parts of the grid, showing the nanoparticles' stability. From the SEM analysis, the shape of the immunoliposomes appears to be a uniform spherical shape, which correlates with the observed morphology under the TEM.

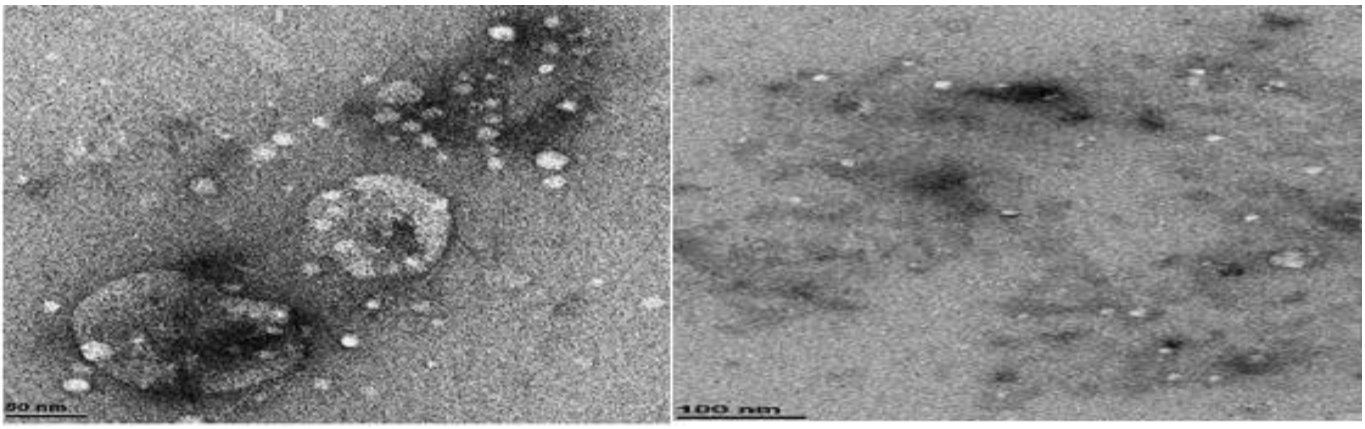

Figure 17: TEM images of empty liposomes at 50 nm and 100 nm

Figure 17 shows TEM images of empty liposomes at 50 nm and 100 nm. TEM was used to show the morphology of the immunoliposomes observed at 100 and 50 nm. The TEM analysis of empty liposomes was done to confirm the formation of liposomes under experimental conditions.

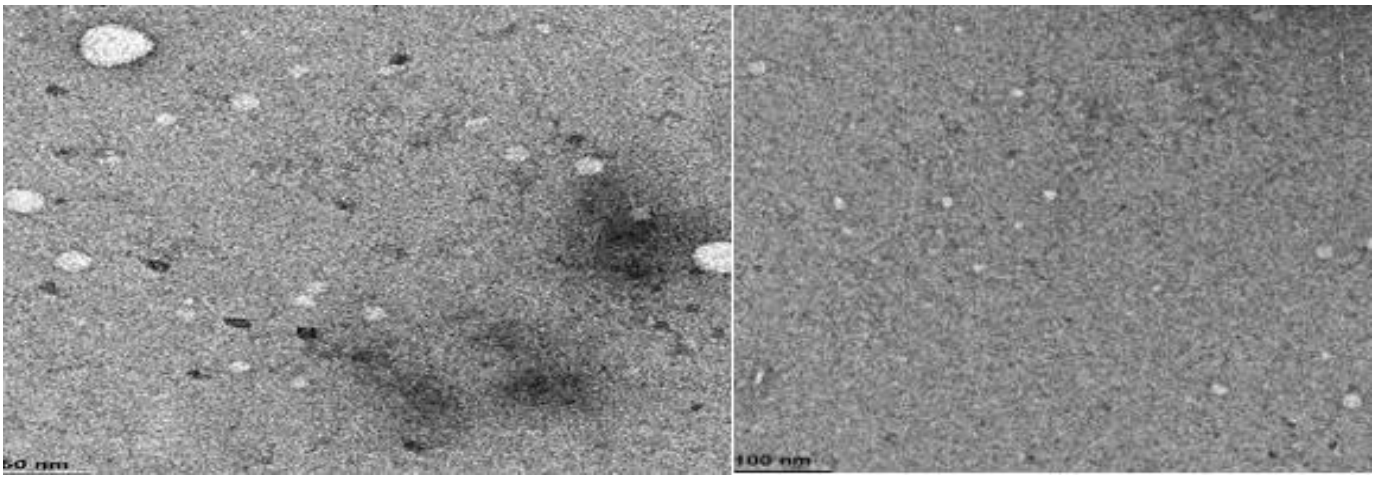

Figure 18: TEM images of *E. milii*-loaded immunoliposomes at 50 nm and 100 nm

At 50, nm the TEM images show that the *E. milii* loaded immunoliposomes are slightly bigger than the empty immunoliposomes. In both the empty immunoliposomes and *E. milii* extract-loaded immunoliposomes, the TEM images indicate that the shape of the immunoliposomes appear to be spherical and opaque. This indicates that the liposomes are stable and uniform in size at 100 nm and 50 nm. However, the empty liposomes seen in Figure 15 appear bigger, and are therefore more visible.

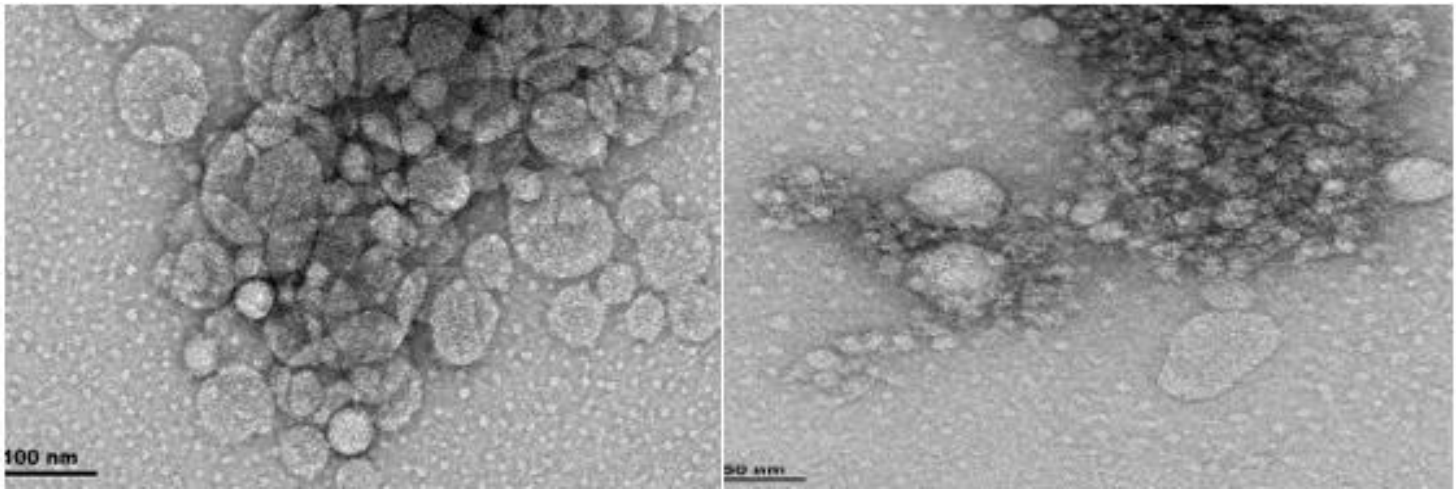

Figure 19: TEM images of doxorubicin-loaded liposomes at 100 nm and 50 nm

In the TEM images of doxorubicin-loaded liposomes at 100 nm and 50 nm (Figure 19), the larger circles that appear to be transparent are marks caused by air-dried PBS.

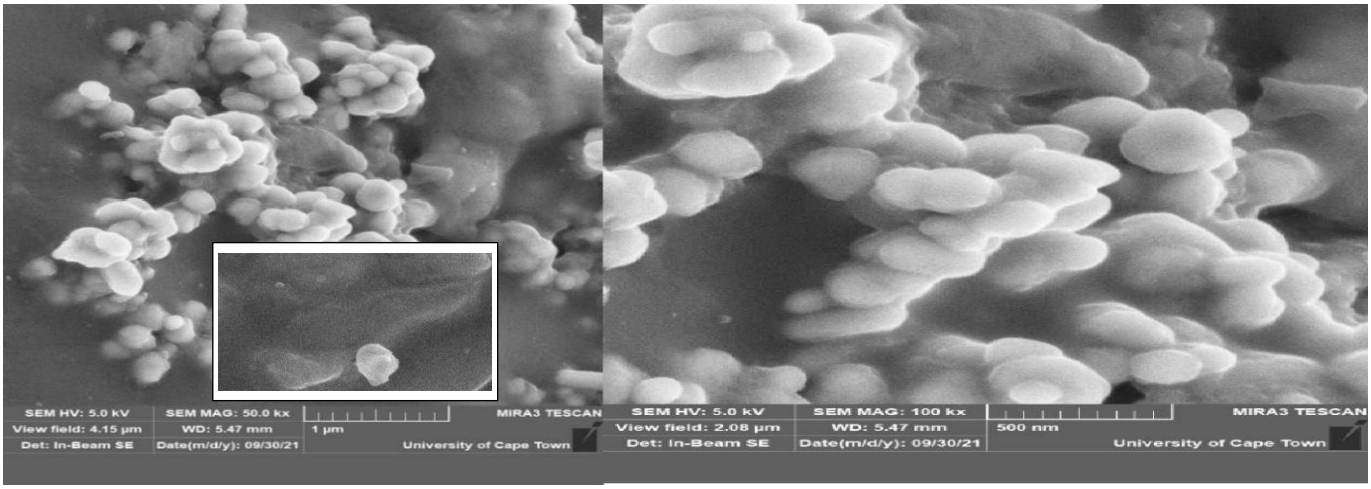

Figure 20: SEM images of empty liposomes at 1 micrometer and 500 nm

Figure 20 shows SEM images of empty liposomes at 1 micrometer and 500 nm. Scanning electron microscope (SEM) photographs of liposomes show the morphology of the synthesized heat-sensitive immunoliposomes. The highlighted insert shows a clear distinguishable morphology of the liposome. The impact the spherical morphology shows that the liposomes are properly formed and are stable as the phospholipids assembled into bilayer membranes which encloses an aqueous space successfully allowing encapsulation of drugs. This morphology confirms that the liposomes can be used to successfully deliver chemotherapeutic agents in the desired concentration and retain their controlled release property.

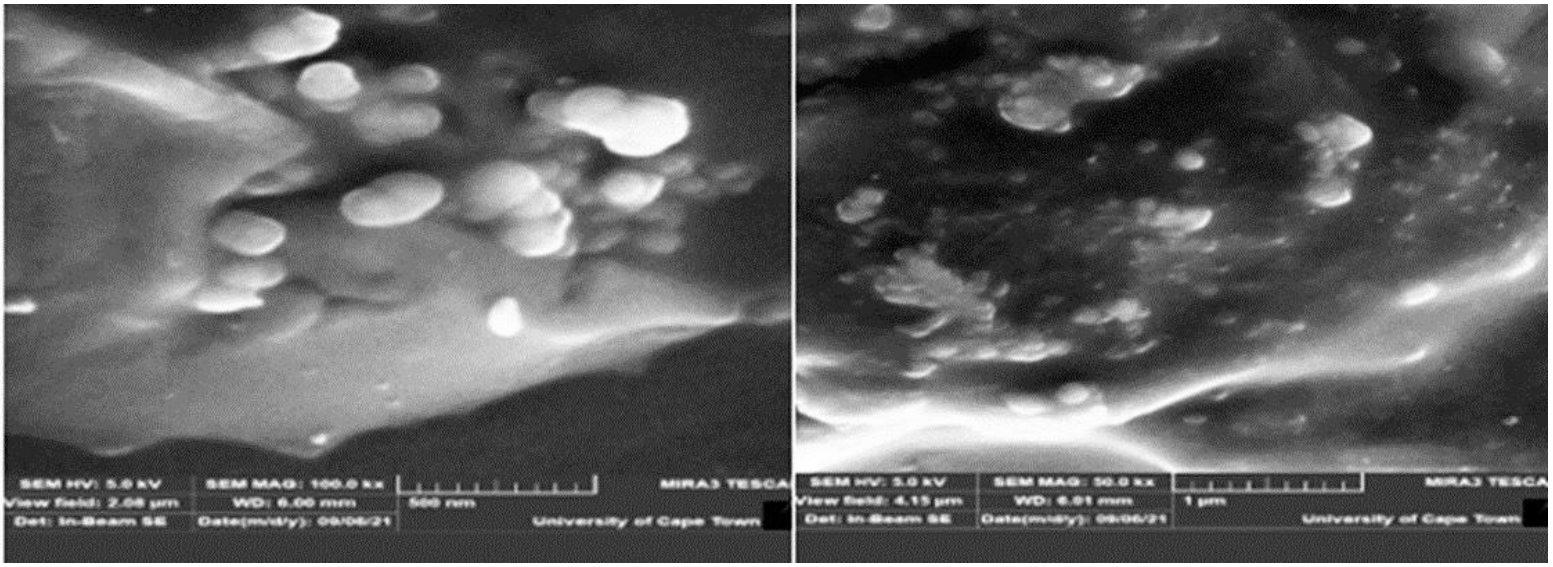

Figure 21: SEM images of *E. milii*-loaded liposomes at 500 nm and 1µ

As seen in Figure 21, the morphology of the liposomes appears to be spherical at different parts of the grid. The liposomes were air-dried, and the 'cloud' is background noise from the sampling grid. The empty liposomes appear bigger and more visible. This correlates with the results seen in the TEM samples. This indicates that the encapsulation of the drugs reduced the size of the liposomes.

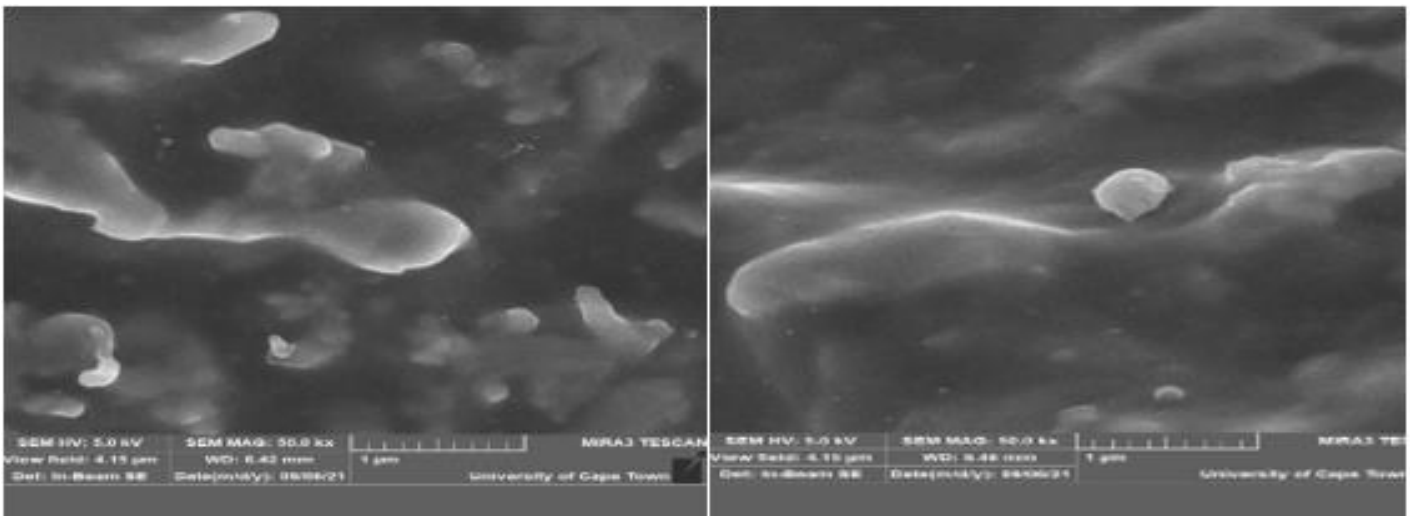

Figure 22: SEM images of doxorubicin-loaded liposomes 1 µm.

Figure 22 shows the SEM images of doxorubicin-loaded liposomes the morphology of the liposomes appears spherical. The air-dried cloud like appearance is background noise from the sampling grid.

5.5.3 Protein analysis results

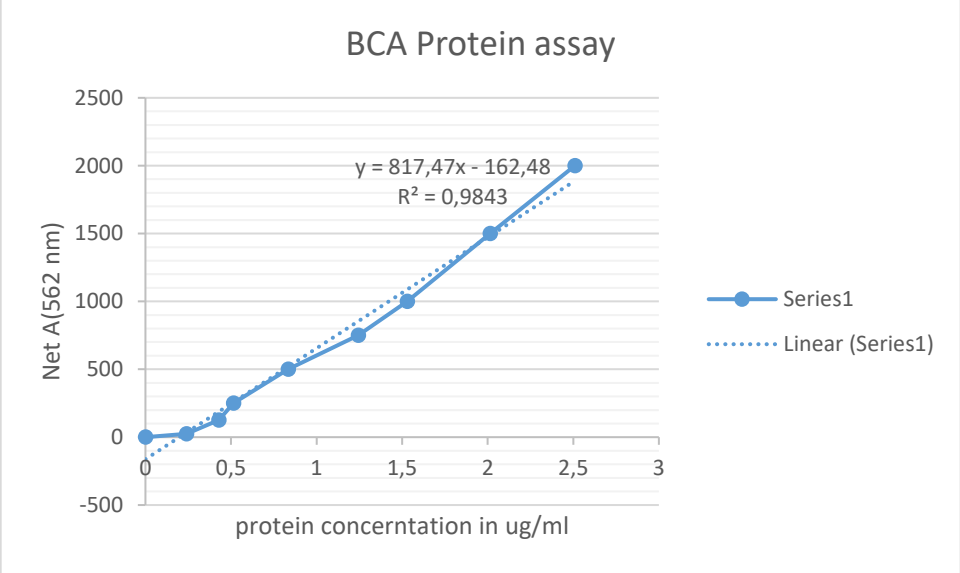

Figure 23: A calibration curve of the protein content

In the calibration curve of the docetaxel-loaded immunoliposomes and *E. milii*-loaded immunoliposomes, a linear relationship was observed as R^2 values > 0.984.

Table 3: The total protein content of the *E. milii* extract and the standard drug-encapsulated heat-sensitive immunoliposomes.

Samples	µg/ml	µg/ml
EM 1.41	Y = 817.47(1.41) − 162.48 = 990.1527	990.1527
Standard drug 1.774	Y = 817.47(1.774) − 162.48 = 1287.712	12877.12

A BCA protein assay (Pierce) was utilized to quantify the amount of anti-PSMA antibody conjugation onto the liposomes. The absorbance of the *E. milii* and the standard drug samples at 526 nm is 1.14 and 1.774 respectively. The BCA assay utilizes peptide bonds in proteins, decreasing Cu^{2+} to Cu^{+}, at a rate corresponding to the total protein. The bicinchoninic acid reagent forms a complex by binding

with the Cu^{+}. This complex then absorbs light at 562 nm wavelength, which allows a link between the sample's protein concentration and absorbance. R^2 of the standard curve is 0.984 (The R^2 value is calculated using the y = mx + c equation to describe the best fit of the standard curve and should be above 0.96) The amount of protein found in the *E. milii* and the standard drug sample was calculated to be 990.1527 µg/ml and 1287.712 µg/ml, respectively, indicating successful conjugation in both samples.

5.5.4 HPLC/LCMS for drug encapsulation

Table 4: The chromatogram's integrated peak area and peak height values for the selected masses in the *E. milii*-extract sample (Sample 1) and the concentration of doxorubicin (Sample 2).

Sample Name	Analyte Peak Name	Analyte Peak Area (counts)	Analyte Peak Height (cps)	Calculated Concentration (ppm)
EME	mass 271	1,98E + 07	1,23E + 06	0
EME	mass 301	1,66E + 07	6,54E + 05	0
EME	mass 318	2,62E + 07	1,44E + 06	0
EME	mass 352	4,73E + 06	2,12E + 05	0
EME	mass 637	5,39E + 05	1,57E + 04	0
EME	mass 678	1,28E + 05	2,89E + 03	0
EME	mass 754	2,17E + 06	1,74E + 05	0
EME	mass 796	9,67E + 06	6,87E + 05	0
Doxorubicin	Dox	6,78E + 06	6,66E + 05	0,607

The *E. milii* extract is not a pure drug. Therefore, the concentration is seen as 0 ppm in the table above. The concentration of doxorubicin was calculated as 0.607 ppm and was consequently used as a reference to calculate the concentration of *E. milii*. Taking into account the area and height of the peak of most of the *E. milii*-extract mass in relation to the area of the peak of the doxorubicin pure drug, there is more *E. milii* extract than doxorubicin encapsulated in the liposomes. This confirms the conjugation of both the extract and the standard drug.

Table 5: The integrated peak area and peak height values of the chromatograms for the mass 796 in the *E. milii*-extract sample and the concentration of docetaxel in the docetaxel-encapsulated liposomes when the drugs are released, and not released, from the liposomes.

TABLE SAMPLE NAME	*Analyte PeakName*	*Analyte Peak Area (counts)*	*Analyte Peak Height (cps)*	*Calculated Concentration*
EM RELEASED	mass796	4.33E+07	2.24E+06	0
EM ENCAPSULATED	mass796	1.69E+07	1.10E+06	0
DOC RELEASED	Doc	1.75E+006	1.12E+005	9
OC ENCAPSULATED	Doc	1.1E+006	7.70E+004	5.6

This table shows the thermosensitive liposomes encapsulating drugs when run through LCMS, and temperature liposomes when drugs were released by exposing the liposomes to hyperthermia at 40°C. The mass 796 of the *E. milii* plant was investigated to quantify the amount of drug detected in the liposomes. The area and height of the *E. milii* mass 796 peak was more significant than when the *E. milii* extract was released. The concentration of docetaxel detected when the drug was released was found to be 9 ug/ml; and when liposomes were not exposed to 40°C hyperthermia, the concentration was found to be 5.6 ug/ml.

The weight of liposomes was found to be:

E. milii extract encapsulating liposome sample was 4.3 mg (0.5mg drug added).

The liposome pellet was divided into two (*E. milii* released and *E. milii* encapsulated); 2.15mg was weighed for each pellet.

The doxorubicin encapsulated liposome sample was 4.5 mg (0.5mg drug added).

The liposome pellet was divided into two (Dox released and Dox encapsulated); 2.25mg was weighed for each pellet.

Table 6: The concentration of Docetaxel.

Sample name	Calculated concentration
Docetaxel	839 µg/ml

mg/L =1 ppm.

The concentration was found to be 839 µg/mL. in a sample of 2 mg of added drug.

5.5.5 Cytotoxic activity of *E. milii* extract and docetaxel-loaded immunoliposomes.

The results obtained, and shown, in Figures 9 and 10 led to further investigation of the plant extract. The cytotoxic activity of temperature-sensitive immunoliposomes encapsulating the *E. milii* extract and docetaxel was studied by measuring the cellular viability, using the MTT assay in the LNCap cells with, and without, exposure to hyperthermia. To ensure that the *E. milii* extract and docetaxel became bioavailable intracellularly, mild hyperthermia was applied to trigger release from liposomes in one experiment; and another experiment was conducted without hyperthermia. Figures 22 and 23 show the IC50 values of the *E. milii* extract and docetaxel-encapsulated immunoliposomes on LNCap cells when exposed to hyperthermia. Figures 24 and 25 show the IC50 value of the *E. milii* extract and docetaxel-encapsulated immunoliposomes on LNCap cells without hyperthermia.

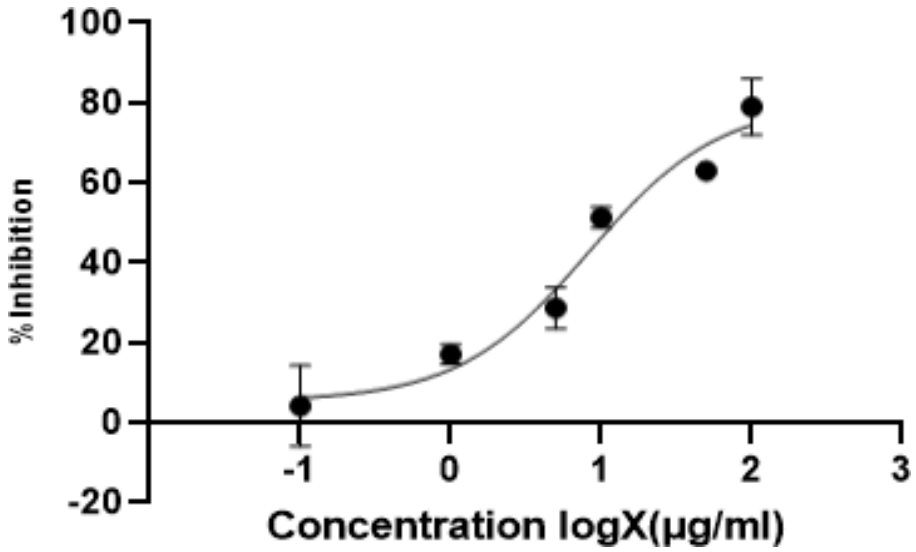

Figure 24: Growth inhibition of LNCap cell line by the *E. milii* extract-encapsulated heat-sensitive immunoliposomes when exposed to heat.

Inhibition of 51.34 ± 13.0% was recorded at 10 µg/mL. The IC50 was calculated to be 8.44 µg/mL.

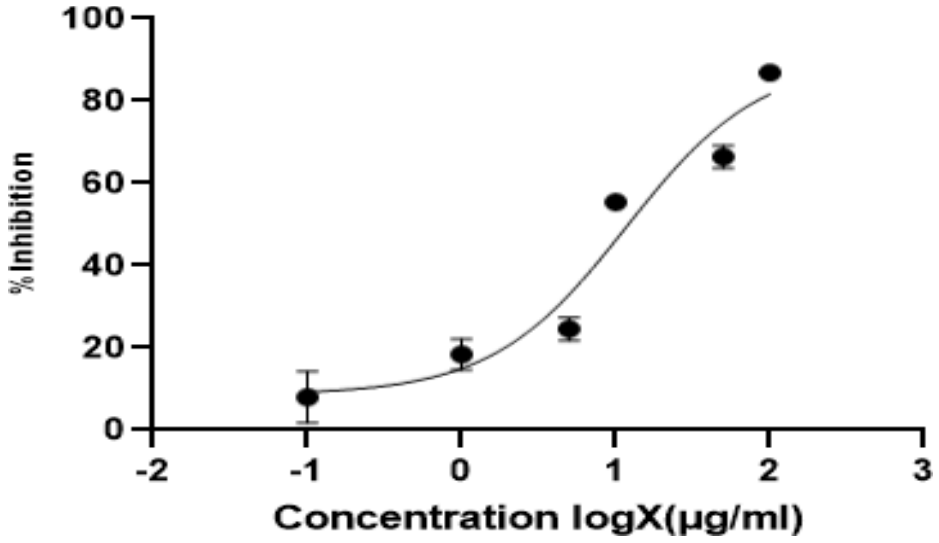

Figure 25: Growth inhibition of LNCap cells by docetaxel-encapsulated immunoliposomes when exposed to heat.

An inhibition of 55.4 ± 4.8% was recorded at a concentration of 10 µg/mL. The IC50 was calculated to be 11.74 µg/mL.

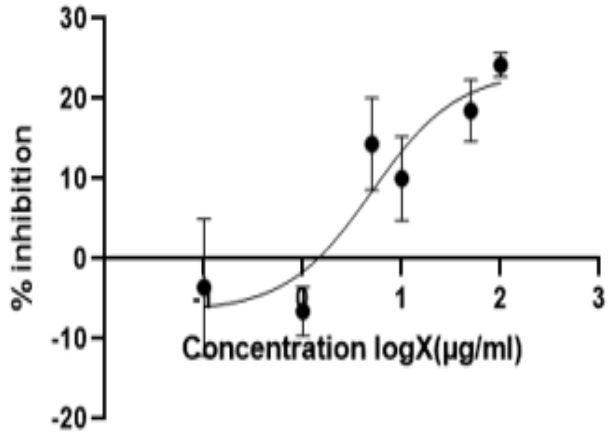

Figure 26: Growth inhibition of LNCap by *E. milii* extract-encapsulated immunoliposomes without exposure to heat

As shown in Figure 24, no significant activity was recorded at concentrations of 10, 50, and 100

µg/mL. The test sample did not achieve an IC50 value, as less than 50% inhibition was observed, even at the highest concentration of 100 µg/mL.

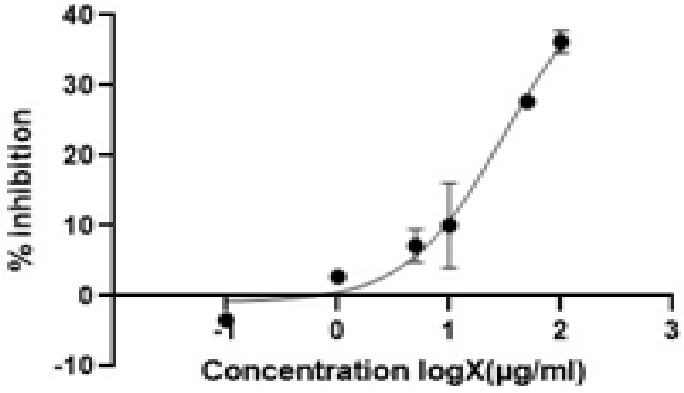

Figure 27: Growth inhibition of LNCap cells by docetaxel-encapsulated heat-sensitive immunoliposomes without exposure to heat.

As shown in Figure 25, no significant activity was recorded at concentrations of 10, 50, and 100 µg/mL. As shown in Figure 11, the significant cytotoxic activity of the *E. milii* DCM root extract on LNCap cells was recorded with an IC50 value of 11.34 µg/mL. When immunoliposomes were exposed to heat (Figures 22 and 23) cytotoxic activity was recorded at a concentration of 10 µg/mL, with IC50 values of 8.44 µg/mL. and 11.74 µg/mL for *E. milii* and docetaxel, respectively, indicating the effect of hyperthermia on heat-sensitive liposomes. A significant difference of (*P-value* <0.0008) was observed for *E.Milii*-extract encapsulated heat sensitive immunoliposomes when exposed to heat compared to *E.Milii*-extract encapsulated heat sensitive immunoliposomes without heat exposure. A significant difference of (*P-value* <0.00013) was observed for Docetaxel encapsulated heat sensitive immunoliposomes when exposed to heat compared to Docetaxel encapsulated heat sensitive immunoliposomes without heat exposure.

Chapter 6

6. Discussion

This research, although still at preliminary *in vitro* stage, is a significant effort to reduce mortality, poor treatment outcomes in prostate cancer patients, and the toxic side-effects caused by currently used treatment options. Due to the side-effects and poor therapeutic outcomes of chemotherapy, targeted and controlled drug delivery has become a relevant technique for more effective and specific cancer treatment, with reduced toxicity. To address these challenges, the study explored the use of heat-sensitive immunoliposomes encapsulating either *E. milii* extract or the standard prostate cancer drugs, doxorubicin and docetaxel, and assessed their cell growth inhibitory activities on selected prostate cancer cells.

A phytochemical screening experiment was conducted to identify the various types of phytochemicals present in *E. milii*. Bioactive constituents obtainable from parts of plants are flavonoids; alkaloids; carotenoids; tannins; antioxidants; proteins; amino acids; and phenolic compounds (Tyagi and Agarwal, 2017). As reported in Table 4, glycosides; triterpenoids; phytosterols; flavonoids; pentose; tannins; anthraquinones; saponins; and alkaloid phytochemicals were detected in the various parts of the plant examined, with exception of the presence of saponins and flavonoids in the leaves and stems, respectively. The cytotoxic activity results in this study also showed inactivity of leaves and stems which are in accordance with the findings of the absence in saponins and flavonoids which were present in the roots of this plant. Saponins are glycosides which poses pharmacological properties , the structural diversity of saponins have also been linked to anticancer activities (Elekofehinti et al., 2021). Flavonoids play a role in various anticancer mechanisms such triggering apoptosis (Nugraha et al., 2021). The cytotoxic activity of the *E. milii* roots may be attributed to the presence of flavonoids and saponins. The findings from our study are in agreement with those that were previously reported for the various parts of the plants analyzed (Saleem et al., 2019, Kaur and Kumar, 2023). Previously conducted research details that phytochemicals such as tannins, flavonoids, and others, can be biologically active (Shaker et al., 2022, Chohan et al., 2020). Flavonoids, saponins, and glycosides are known to have cytotoxicity, anti-inflammatory and antioxidant properties, and thus are responsible for the anticancer activities in most plant extracts (Direko et al., 2019)The *Euphorbia Milii* roots, stems, and leave extracts were initially screened for cytotoxic

activity against the prostate cancer DU145 cell line. The results obtained from the initial screening showed the DCM root extract to have a more significant cytotoxic effect against the tested cell line. A further analysis was performed against LNCap cells and IC50 of 11.34 µg/mL was obtained. The results of our study were comparable to the results obtained by another group of researchers who examined *E. milii* against cervical cancer cells, when IC50 of 22.1 ± 0.8 µg/ml was recorded (Chohan et al., 2020). A study, conducted by Radi et al., indicated an IC50 of 10.41 µg/mL when *E. milii* was screened against a breast cancer cell line (Radi et al., 2023). The results obtained are significantly different from the results obtained by Ebrahim et al. (2020) against liver cancer cells, which showed IC50 of 87.1 ± 9.4 µg/mL (Ebrahim et al., 2020). The anticancer activity obtained in our study could be owing to the flavonoids and saponins detected in the root extract of the plant. The root of *E. milii* has been reported to contain more flavonoid and saponins than other parts of the plant (Saleem et al., 2019), and this correlates with the results obtained from the phytochemical analysis performed in the study (Table 2), where saponins were only present in the root extract of the plant. Doxorubicin and docetaxel were used as positive controls and screened against the DU145 and LNCap prostate cancer cell lines. Docetaxel was observed to show above 50% cytotoxic activity against both LNcap and DU145 cell lines at concentrations as low as 1 µg/mL; while doxorubicin only achieved more than 50% cytotoxicity at a concentration of 5 µg/mL for both cell lines (Figures 12 and 13). The growth inhibition activities observed for the positive controls were higher than the ones obtained by Zhang et al. (2019), which showed docetaxel to have less than 50% cytotoxicity at a much higher concentration of 10 µg/mL.

Nano delivery systems, such as liposomes, have been proven to improve the bioactivity of pharmacologically active compounds, and this informed the basis of this study, which was to prepare a liposomal delivery system encapsulating the plant extract as well as the standard prostate cancer drugs. Liposomes were prepared using HSPC: DSPE-PEG-2000: DSPE-PEG2000- maleimide in the molar ratio of 4:1:0.2 and were conjugated with a PSA antibody. DSPE- PEG (2000)-amine has been used previously for the synthesis of thermosensitive liposomal nanoparticles, mainly for the delivery of anticancer drugs and the synthesis of fluorescein isothiocyanate-loaded mesoporous silica nanoparticles for imaging applications (Lu et al., 2018). It can be used with different functional molecules, such as the DSPE- 2000-malmide to prepare antibody-conjugated nanoparticles for improved cellular and receptor targeting (Bi et

al., 2019). After the preparation of the liposomes, the bicinchoninic acid (BCA) protein assay (Pierce) was used to quantify the amount of anti-PSMA antibody conjugated onto the liposomes. The BCA assay utilizes peptide bonds in proteins, decreasing Cu^{2+} to Cu^{+}, at a rate corresponding to the total protein in the sample. The bicinchoninic acid reagent forms a complex by binding with the Cu^{+}. This complex then absorbs light at 562 nm wavelength, which allows a link between the sample's protein concentration and absorbance (Hussain et al., 2019). The absorbance of the *E. milii* and the docetaxel samples at 526 nm was 1.14 and 1.774, respectively. Following the equation y = mx + c, the protein concentration of the liposomes encapsulating *E. milii,* and the standard drug sample, were calculated to be 990.1527 µg/ml and 1287.712 µg/ml, respectively. This indicates successful conjugation of anti-PSMA to the heat-sensitive liposomes for both samples.

To confirm the encapsulation percentage of plant extract and docetaxel drug, HPLC and LCMS techniques were employed. Different masses of the *E. milii* extract were identified, as seen in Table 4. Mass796 eluded as one prominent peak and was therefore used in refence to the standard drug. Other masses were badly resolved and eluted as multiple peaks. Two 0.5 mg samples were analyzed through LCMS: sample 1, the *E. milii* extract, and sample 2, the doxorubicin (used as a control). A calibration curve was constructed with the doxorubicin standard and was 0.6 × 100 = 60 ppm, taking into account the area of the peak of the *E. milii* extract in relation to the doxorubicin pure drug. The *E. milii* mass at 796 had a peak area of 9,67E + 06 and doxorubicin had an area of 6,78E + 06. Therefore, the area of the *E. milii* extract was 2.89 larger than that of the doxorubicin. The height of the *E. milii* extract peak was 6,87E + 05 and the height of the doxorubicin peak was 6,66E + 05. The height of the *E. milii* extract peak was 0.21 higher than that of doxorubicin. This indicates that more *E. milii* extract than doxorubicin was encapsulated in the liposomes. A chromatogram was constructed with the docetaxel standard drug and the concentration of docetaxel (100 × fold diluted) was determined. The concentration was found to be 839 µg/mL in a sample of 2 mg. The concentration of a plant extract within a sample cannot be quantified because extracts are not pure compounds. Therefore, in this experiment, it was crucial to compare the chromatographic peaks of the plant extract to that obtained from a sample of a known drug.

Figure 14,15 and 16 shows that the FTIR results of both *E. milii* and doxorubicin-loaded heat-sensitive

immunoliposomes were similar, indicating that the liposomal encapsulation of drugs did not result in the formation of new linkages. However, this was different for docetaxel, as different peaks were observed for the docetaxel-loaded heat-sensitive immunoliposomes. The transmission electron microscopy and the scanning electron microscope were then used to further investigate the stability and morphology of the synthesized immunoliposomes. Both TEM and SEM images indicated that the morphology of the immunoliposomes appeared spherical and opaque, indicating that stable liposomal delivery systems were formed with uniformity. Also, it is clear from the SEM and TEM images that the empty liposomes (Figures 17 and 20 for TEM and SEM, respectively) appear bigger in shape compared to the *E.milii* extract-(Figures 18 and 21 for TEM and SEM, respectively) and drug-loaded liposomes (Figures 19 and 22 for TEM and SEM, respectively). The encapsulation of the bioactive compounds in the bilayers of the lipids led to the liposomes' size reduction as result of osmotic pressure on the liposomes, which led to the loss of aqueous molecules from the liposomal core (Wolfram et al., 2014). This reduction in size is beneficial, for the enhancement of bioavailability as well as improved drug delivery (Ong et al., 2016, Wolfram et al., 2014).

After successful characterization of the liposomes, cell viability studies were performed. No significant cytotoxic inhibitory activity was recorded for the liposomes encapsulating both the extract and docetaxel, individually, without the presence of heat for all concentrations evaluated (activity less than 50% was termed insignificant). However, upon the addition of heat at a temperature ranging from 39 – 40°C, 51.34 ± 13.0% and 55.40 ± 4.8% cell inhibition was recorded at 10 μg/mL for the liposomes encapsulating the plant extract (Figure 24), and docetaxel drug (Figure 25), respectively. The IC50 were calculated to be 8.44 μg/mL and 11.74 μg/mL for liposomes encapsulating the plant extract and docetaxel drug, respectively.

We believe that the presence of HSPC in the constituents of the liposomal delivery systems may have been responsible for the significant activity recorded upon heat exposure. According to previous studies, HSPC has been used to give temperature-sensitive liposomes their stability without the presence of heat; and on heating to a temperature of 40°C, the structure of the liposomes is denatured. This then leads to the release of the bioactive compounds encapsulated in the liposomes, thus exhibiting their cytotoxic activity (Du et al., 2024).

Chapter 7

7. Conclusion

7.1 General Conclusion

Conventional forms of chemotherapeutic agents continue to experience drawbacks in the treatment of prostate cancer. There are various alternatives considered to remedy the present situation, among which is the use of alternative sources of pharmacologically active agents of plant origin, as well as the use of nanoparticles for the delivery of these chemotherapeutic agents. Liposomes are the most widely studied nano delivery systems, which have been shown to be a promising treatment alternative to the conventional delivery systems against cancer. This study focused on the development of a heat-sensitive immunoliposome nano drug delivery system, for the effective delivery of chemotherapeutic agents and *E. milii* plant extract against prostate cancer cells. *E. milii* DCM root extract showed to have a more significant cytotoxic effect against the tested prostate cancer cell lines (DU145 and LNCap). The results obtained in this study confirmed that the developed heat-sensitive immunoliposomes, used for the delivery of both *E. milii* plant extract and chemotherapeutic agents was able to successfully release the entrapped contents upon heat exposure above the phase transition temperature of the liposome membrane. The prepared, heat-sensitive immunoliposomes conjugated the active extract and showed better anticancer efficacy against the prostate cancer cell lines in the presence of heat, than in the absence of heat *in vitro*. This heat-sensitive delivery system has controlled and targeted release properties that addresses the challenges faced by current prostate cancer treatment and has the potential for further analysis which could potentiate it's use as a delivery system for anticancer drugs against prostate cancer. The challenges faced during the *in vivo* pilot study could be due to the number of cells inoculated in the mice (1x10^6) and the low viability of cells inoculated. The strain used was the NU/J nude mice strain, despite these mice being immunodeficient due to the absence of a thymus and T lymphocytes, B lymphocytes are present in these mice even though their development is partially defective. The presence of B lymphocytes can affect tumour growth. Using an immunodeficient mice strain which lacks both T and B lymphocytes could result in successful tumour growth. Various other ways of increasing the chances of tumour growth can be investigated such as designing a pre pilot study to test various concentrations to initiate tumour growth, inoculating

cells with viability of more than 98% and inoculating the cells with Matrigel instead of PBS. The exploitation of hyperthermia as an external trigger of thermosensitive liposomes demonstrated superior efficacy in various conducted preclinical studies. The use of heat sensitive immune liposomes in the clinical setting will ensure that a greater population of prostate cancer patients can benefit from controlled and target specific nano therapy. Prostate cancer is often treated with a combination of androgen deprivation therapy and docetaxel-based chemotherapy. However, many patients eventually develop resistance to these treatments. Application of this delivery system could also help overcome this resistance by delivering chemotherapeutic drugs directly to the tumour site. This delivery system has the potential for further development for application as a safe and efficient drug delivery system for prostate cancer. It also provides revolutionary research alternatives for treatment of various cancers as well as the possible use in other disciplines such as gene therapy which has the potential to develop specific and controlled personalized treatment of cancer. The use target specific nano delivery systems in personalized medicine will enable personalized treatment tailored to the unique cancer addressing currently faced treatment challenges such as low bioavailability, uncontrolled drug release, degradation of drugs, and non-specificity.

The major conclusions that were generated from this research project are summarized below:

1) A highly cytotoxic plant with proven records of anti-cancer properties was selected. The extracts were prepared and screened for cell growth inhibitory efficacy against prostate cancer DU145 and LNCap cell lines *in vitro*; and good anticancer efficacy was obtained.
2) The synthesis of the heat-responsive prostate-specific antibody-conjugated liposomes was successfully carried out and was used to encapsulate the active constituents of the plant extracts as well as of standard anti-cancer drugs.
3) The verification of the plant extract and drug encapsulation was successful through the use of HPLC and LCMS.
4) The evaluation of the anti-cancer efficacy of the prepared thermo-sensitive immunoliposome delivery system on prostate cancer cells, compared to the free standard conventional drug and the

plant extract, was successfully conducted with the use of an MTT assay and good results were obtained.

7.2 Limitations of the study

The study was intended to proceed to the *in vivo* stage, employing a male balb/c immunocompromised mice model for the evaluation of the prepared liposomes. However, despite our efforts to accomplish this, we were unsuccessful, owing to the inability to grow the tumors in the mice. Balb/c nude mice were inoculated with 100ul consisting of 1x10^6 prostate cancer cells with no tumor growth observed, despite this same concentration being reported to cause the growth of tumors in previous studies by (Liu et al., 2022, Zhang et al., 2021) increasing the number of cells can increase the possibility of tumor growth. Trouble shooting this increase in number of cells will reduce various factors which previously contributed to tumour growth failure, this may thus translate to reduced chances of *in-vivo* studies repetition, and ultimately saving costs.

- As a result of several unsuccessful trials for the *in vivo* studies, it was financially challenging to explore other research techniques, such as 3D cell culture or microfluidics, to compare with the results obtained from the 2D cell culture, due to financial constraints and study timelines. To mitigate the financial issues, I propose a continuation of this research at PhD level. Usually, the funding of PhD research is more than that of a Masters degree, and thus I recommend that a bigger portion of the PhD research funds be allocated to animal studies to further test the efficacy of the drug delivery system *in vivo.* A collaboration has been established with the North West University and thus, the animal studies will be conducted at North West University Animal facility, this facility also specializes in breeding animals which will eliminate the animal transportation costs, breading cost, and costs for labour. A collaboration and co-supervision of students is another way to reduce cost of research.

7.3 Future studies

- The *in vitro* results obtained in this study provide motivation for further studies. Therefore, I would recommend that more in-depth studies, such as the development of an *in vivo* prostate cancer mice

model using male balb/c immunodeficient nude mice (with absent T and B lymphocytes) between the ages of 6-8 weeks to be used for future animal studies , 3D cell culture, or microfluidics, be carried out in order to confirm the potential of the prepared liposomes as an alternative delivery system to conventional delivery systems for pharmacologically active agents against prostate cancer. Results from these studies could then be compared to the results obtained from the 2D cell culture.

- The plant root extract has exhibited considerable cell growth inhibition of both the DU145 and LNCap prostate cancer cells. This provides a rationale to fractionate the extract, and to isolate and purify the active constituents through bio-guided fractionation. Thin-layer chromatography (TLC), and Liquid chromatography–mass spectrometry (LC–MS) will be used in the isolation and characterization of the active constituents. Bio-guided fractionation and isolation of the active extract are important as they determine the quantity and quality of bioactive compounds. These isolated compounds are then used for the determination of structure of the active compound. The chemical structure can provide vital information for further studies including bioactivities, structural modifications, and synthesis of active compounds which are then further developed for chemotherapeutic testing and possible application in clinical trials. The information on active constituent is also useful for standardization of herbal products.

Chapter 8

8. References

ABATE-SHEN, C. & NUNES DE ALMEIDA, F. 2022. Establishment of the LNCaP cell line–the dawn of an era for prostate cancer research. *Cancer research,* 82**,** 1689-1691.

ABBAS, M., MASON, T., IBAD, A., KHRAIWESH, M., APPREY, V., KANAAN, Y., WILSON, B., DUNSTON, G., RICKS-SANTI, L. & BRIM, H. 2020. Genetic polymorphisms in IL-10 promoter are associated with smoking and prostate cancer risk in African Americans. *Anticancer research,* 40**,** 27-34.

AGGARWAL, S., VERMA, S. S., AGGARWAL, S. & GUPTA, S. C. Drug repurposing for breast cancer therapy: Old weapon for new battle. Seminars in cancer biology, 2021. Elsevier, 8-20.

AL-AHMADY, Z. S., CHALOIN, O. & KOSTARELOS, K. 2014. Monoclonal antibody-targeted, temperature-sensitive liposomes: in vivo tumor chemotherapeutics in combination with mild hyperthermia. *Journal of Controlled Release,* 196**,** 332-343.

ALAVIZADEH, S. H., GHEYBI, F., NIKPOOR, A. R., BADIEE, A., GOLMOHAMMADZADEH, S. & JAAFARI, M. R. 2017. Therapeutic efficacy of cisplatin thermosensitive liposomes upon mild hyperthermia in C26 tumor bearing BALB/c mice. *Molecular pharmaceutics,* 14**,** 712-721.

ALHMOUD, J. F., WOOLLEY, J. F., AL MOUSTAFA, A.-E. & MALLEI, M. I. 2021. DNA damage/repair management in cancers. *Advances in Medical Biochemistry, Genomics, Physiology, and Pathology***,** 309-339.

ALMOTAIRY, A., YUSUF, A., HENIDI, H., ALSHEHRI, O. & ALDUGHAIM, M. 2023. Nanoparticles as Drug Delivery Systems: A Review of the Implication of Nanoparticles' Physicochemical Properties on Responses in Biological Systems.

ALQOSAIBI, A. I. 2022. Nanocarriers for anticancer drugs: Challenges and perspectives. *Saudi Journal of Biological Sciences,* 29**,** 103298.

ALRUSHAID, N., KHAN, F. A., AL-SUHAIMI, E. A. & ELAISSARI, A. 2023. Nanotechnology in cancer diagnosis and treatment. *Pharmaceutics,* 15**,** 1025.

AMIN, M., HUANG, W., SEYNHAEVE, A. L. & TEN HAGEN, T. L. 2020. Hyperthermia and temperature-sensitive nanomaterials for spatiotemporal drug delivery to solid tumors. *Pharmaceutics,* 12**,** 1007.

AMTAGHRI, S., AKDAD, M., SLAOUI, M. & EDDOUKS, M. 2022. Traditional uses, pharmacological, and phytochemical studies of euphorbia: a review. *Current Topics in Medicinal Chemistry,* 22**,** 1553-1570.

ANAND, U., DEY, A., CHANDEL, A. K. S., SANYAL, R., MISHRA, A., PANDEY, D. K., DE FALCO, V., UPADHYAY, A., KANDIMALLA, R. & CHAUDHARY, A. 2022. Cancer chemotherapy and beyond: Current status, drug candidates, associated risks and progress in targeted therapeutics. *Genes & Diseases*.

ASEMANI, M. & RABBANI, A. R. 2020. Detailed FTIR spectroscopy characterization of crude oil extracted asphaltenes: Curve resolve of overlapping bands. *Journal of Petroleum Science and Engineering,* 185**,** 106618.

ASLANTÜRK, Ö. S. 2018. In vitro cytotoxicity and cell viability assays: principles, advantages, and disadvantages. *Genotoxicity-A predictable risk to our actual world,* 2**,** 64-80.

BAHRAMI, B., HOJJAT-FARSANGI, M., MOHAMMADI, H., ANVARI, E., GHALAMFARSA, G., YOUSEFI, M. & JADIDI-NIARAGH, F. 2017. Nanoparticles and targeted drug delivery in cancer therapy. *Immunology letters,* 190**,** 64-83.

BECCARIA, M. & CABOOTER, D. 2020. Current developments in LC-MS for pharmaceutical analysis. *Analyst,* 145**,** 1129-1157.

BERGENGREN, O., PEKALA, K. R., MATSOUKAS, K., FAINBERG, J., MUNGOVAN, S. F., BRATT, O., BRAY, F., BRAWLEY, O., LUCKENBAUGH, A. N. & MUCCI, L. 2023. 2022 Update on Prostate Cancer Epidemiology and Risk Factors—A Systematic Review. *European Urology*.

BHANDARY, S. K., BHAT, V. S., SHARMILA, K. & BEKAL, M. P. 2012. Preliminary phytochemical screening of various extracts of Punica granatum peel, whole fruit and seeds. *Journal of Health and Allied Sciences NU,* 2**,** 34-38.

BI, H., XUE, J., JIANG, H., GAO, S., YANG, D., FANG, Y. & SHI, K. 2019. Current developments in drug delivery with thermosensitive liposomes. *Asian journal of pharmaceutical sciences,* 14**,** 365-379.

BROWN, J. S., AMEND, S. R., AUSTIN, R. H., GATENBY, R. A., HAMMARLUND, E. U. & PIENTA, K. J. 2023. Updating the definition of cancer. *Molecular Cancer Research,* 21**,** 1142-1147.

CAPONE, F., POLO, A., SORICE, A., BUDILLON, A. & COSTANTINI, S. 2020. Integrated analysis to study the relationship between tumor-associated selenoproteins: focus on prostate cancer. *International Journal of Molecular Sciences,* 21**,** 6694.

CASSIM, N., AHMAD, A., WADEE, R., REBBECK, T., GLENCROSS, D. & GEORGE, J. 2021. Prostate cancer age-standardised incidence increase between 2006 and 2016 in Gauteng Province, South Africa: A laboratory data-based analysis. *South African Medical Journal,* 111**,** 26-32.

CASTANARES, M. A., COPELAND, B. T., CHOWDHURY, W. H., LIU, M. M., RODRIGUEZ, R., POMPER, M. G., LUPOLD, S. E. & FOSS, C. A. 2016. Characterization of a novel metastatic prostate cancer cell line of LNCaP origin. *The Prostate,* 76**,** 215-225.

CHAUDHRY, M., LYON, P., COUSSIOS, C. & CARLISLE, R. 2022. Thermosensitive liposomes: a promising step toward localised chemotherapy. *Expert Opinion on Drug Delivery,* 19**,** 899-912.

CHEN, J., CHENG, D., LI, J., WANG, Y., GUO, J.-X., CHEN, Z.-P., CAI, B.-C. & YANG, T. 2013. Influence of lipid composition on the phase transition temperature of liposomes composed of both DPPC and HSPC. *Drug development and industrial pharmacy,* 39**,** 197-204.

CHEN, Q., DWYER, C., SHENG, G., ZHU, C., LI, X., ZHENG, C. & ZHU, Y. 2020. Imaging beam-sensitive materials by electron microscopy. *Advanced Materials,* 32**,** 1907619.

CHOHAN, T. A., SARFRAZ, M., REHMAN, K., MUHAMMAD, T., GHORI, M. U., KHAN, K. M., AFZAL, I., AKASH, M. S. H., MALIK, A. & CHOHAN, T. A. 2020. Phytochemical profiling, antioxidant and antiproliferation potential of Euphorbia milii var.: Experimental analysis and in-silico validation. *Saudi Journal of Biological Sciences,* 27**,** 3025-3034.

CHRISTIE, D. R., WINDSOR, J. & SHARPLEY, C. F. 2019. A systematic review of the accuracy of the digital rectal examination as a method of measuring prostate gland volume. *Journal of Clinical Urology,* 12**,** 361-370.

CZERWIŃSKA, M., BILEWICZ, A., KRUSZEWSKI, M., WEGIEREK-CIUK, A. & LANKOFF, A. 2020. Targeted radionuclide therapy of prostate cancer—from basic research to clinical perspectives. *Molecules,* 25**,** 1743.

DASS, K., AHMAD, A., AZMI, A. S., SARKAR, S. H. & SARKAR, F. H. 2008. Evolving role of uPA/uPAR system in human cancers. *Cancer treatment reviews,* 34**,** 122-136.

DEBELA, D. T., MUZAZU, S. G., HERARO, K. D., NDALAMA, M. T., MESELE, B. W., HAILE, D. C., KITUI, S. K. & MANYAZEWAL, T. 2021. New approaches and procedures for cancer treatment: Current perspectives. *SAGE open medicine,* 9**,** 20503121211034366.

DHALE, D. 2023. *Advanced Techniques in Plant Sciences*, Book Saga Publications.

DIREKO, P., MFENGWANA, H., MASHELE, S. & SEKHOACHA, M. 2019. Investigating the angiogenic modulating properties of Spirostachys africana in MCF-7 breast cancer cell line. *International Journal of Pharmacology,* 15**,** 970-977.

DU, Q., DING, X.-Q., GAO, F., CUI, B., WANG, T.-Y., CHEN, F.-Y., CHEN, L., CHEN, H.-Y., CUI, H.-X. & WANG, Y. 2024. Thermo-responsive liposome nano-vesicles for co-delivery of emamectin benzoate and nitenpyram with synergistic pest control. *Chemical Engineering Journal*, 479**,** 147548.

DUAN, L., YANG, L., JIN, J., YANG, F., LIU, D., HU, K., WANG, Q., YUE, Y. & GU, N. 2020. Micro/nano-bubble-assisted ultrasound to enhance the EPR effect and potential theranostic applications. *Theranostics,* 10**,** 462.

DYSHLOVOY, S. A., MANSOUR, W. Y., RAMM, N. A., HAUSCHILD, J., ZHIDKOV, M. E., KRIEGS, M., ZIELINSKI, A., HOFFER, K., BUSENBENDER, T. & GLUMAKOVA, K. A. 2024. Synthesis and new DNA targeting activity of 6-and 7-tert-butylfascaplysins.

EBRAHIM, H. Y., OSMAN, S. A., HAFFEZ, H. R. & HASSAN, Z. A. 2020. In-vitro screening of some plant extracts for their potential anticancer activity. *African Journal of Traditional, Complementary and Alternative Medicines,* 17**,** 1-8.

EDMUNDS, K., TUFFAHA, H., SCUFFHAM, P., GALVÃO, D. A. & NEWTON, R. U. 2020. The role of exercise in the management of adverse effects of androgen deprivation therapy for prostate cancer: a rapid review. *Supportive Care in Cancer,* 28**,** 5661-5671.

EID, M. M. 2022. Characterization of Nanoparticles by FTIR and FTIR-Microscopy. *Handbook of Consumer Nanoproducts.* Springer.

ELEKOFEHINTI, O. O., IWALOYE, O., OLAWALE, F. & ARIYO, E. O. 2021. Saponins in cancer treatment: Current progress and future prospects. *Pathophysiology,* 28**,** 250-272.

EROĞLU, İ. & İBRAHIM, M. 2020. Liposome–ligand conjugates: a review on the current state of art. *Journal of drug targeting,* 28**,** 225-244.

FAHMY, S. A., PREIS, E., DAYYIH, A. A., ALAWAK, M., EL-SAID AZZAZY, H. M., BAKOWSKY, U. & SHOEIB, T. 2022. Thermosensitive Liposomes Encapsulating Nedaplatin and Picoplatin Demonstrate Enhanced Cytotoxicity against Breast Cancer Cells. *ACS omega,* 7**,** 42115-42125.

FILELLA, X., FERNÁNDEZ-GALAN, E., FERNANDEZ BONIFACIO, R. & FOJ, L. 2018. Emerging biomarkers in the diagnosis of prostate cancer. *Pharmacogenomics and personalized medicine***,** 83-94.

FREIMOSER, F. M., JAKOB, C. A., AEBI, M. & TUOR, U. 1999. The MTT [3-(4, 5-dimethylthiazol-2-yl)-2, 5-diphenyltetrazolium bromide] assay is a fast and reliable method for colorimetric determination of fungal cell densities. *Applied and environmental microbiology,* 65**,** 3727-3729.

GARCÍA-PINEL, B., PORRAS-ALCALÁ, C., ORTEGA-RODRÍGUEZ, A., SARABIA, F., PRADOS, J., MELGUIZO, C. & LÓPEZ-ROMERO, J. M. 2019. Lipid-based nanoparticles: application and recent advances in cancer treatment. *Nanomaterials,* 9**,** 638.

GAWALI, P., SARASWAT, A., BHIDE, S., GUPTA, S. & PATEL, K. 2023. Human solid tumors and clinical relevance of the enhanced permeation and retention effect: a 'golden gate'for nanomedicine in preclinical studies? *Nanomedicine,* 18**,** 169-190.

GHASEMI, M., TURNBULL, T., SEBASTIAN, S. & KEMPSON, I. 2021. The MTT assay: utility, limitations, pitfalls, and interpretation in bulk and single-cell analysis. *International journal of molecular sciences,* 22**,** 12827.

GIORDANI, S., MARASSI, V., ZATTONI, A., RODA, B. & RESCHIGLIAN, P. 2023. Liposomes characterization for market approval as pharmaceutical products: analytical methods, guidelines and standardized protocols. *Journal of Pharmaceutical and Biomedical Analysis***,** 115751.

GNUTZMANN, D., KORTES, N., SUMKAUSKAITE, M., SCHMITZ, A., WEISS, K.-H. & RADELEFF, B. 2018. Transvascular therapy of hepatocellular carcinoma (HCC), status and developments. *Minimally Invasive Therapy & Allied Technologies,* 27**,** 69-80.

GROHMANN, C., WALKER, F., DEVLIN, M., LUO, M.-X., CHÜEH, A. C., DOHERTY, J., VAILLANT, F., HO, G.-Y., WAKEFIELD, M. J. & WEEDEN, C. E. 2021. Preclinical small molecule WEHI-7326 overcomes drug resistance and elicits response in patient-derived xenograft models of human treatment-refractory tumors. *Cell Death & Disease,* 12**,** 268.

GUILLAUMIER, S., PETERS, M., ARYA, M., AFZAL, N., CHARMAN, S., DUDDERIDGE, T., HOSKING-JERVIS, F., HINDLEY, R. G., LEWI, H. & MCCARTAN, N. 2018. A multicentre

study of 5-year outcomes following focal therapy in treating clinically significant nonmetastatic prostate cancer. *European urology*, 74**,** 422-429.

GUIMARÃES, D., CAVACO-PAULO, A. & NOGUEIRA, E. 2021. Design of liposomes as drug delivery system for therapeutic applications. *International journal of pharmaceutics*, 601**,** 120571.

HAFEEZ, M. N., CELIA, C. & PETRIKAITE, V. 2021. Challenges towards targeted drug delivery in cancer nanomedicines. *Processes*, 9**,** 1527.

HASSAN, A. Z., SWEELAM, H.-T. M., SHAKER, K. H., ZOHAIR, M. M., ASHOUR, W. E. & ABD-ALLA, H. I. 2023. Phytochemical Analysis and Antimicrobial Activity of Euphorbia milii. *Egyptian Journal of Chemistry*, 66**,** 461-473.

HEIDARLI, E., DADASHZADEH, S. & HAERI, A. 2017. State of the art of stimuli-responsive liposomes for cancer therapy. *Iranian journal of pharmaceutical research: IJPR*, 16**,** 1273.

HOFMAN, M. S., LAWRENTSCHUK, N., FRANCIS, R. J., TANG, C., VELA, I., THOMAS, P., RUTHERFORD, N., MARTIN, J. M., FRYDENBERG, M. & SHAKHER, R. 2020. Prostate-specific membrane antigen PET-CT in patients with high-risk prostate cancer before curative-intent surgery or radiotherapy (proPSMA): a prospective, randomised, multicentre study. *The Lancet*, 395**,** 1208-1216.

HOSSEN, S., HOSSAIN, M. K., BASHER, M., MIA, M., RAHMAN, M. & UDDIN, M. J. 2019. Smart nanocarrier-based drug delivery systems for cancer therapy and toxicity studies: A review. *Journal of advanced research*, 15**,** 1-18.

HUSSAIN, M. T., FORBES, N. & PERRIE, Y. 2019. Comparative analysis of protein quantification methods for the rapid determination of protein loading in liposomal formulations. *Pharmaceutics*, 11**,** 39.

HYVÄKKÄ, A., VIRTANEN, V., KEMPPAINEN, J., GRÖNROOS, T. J., MINN, H. & SUNDVALL, M. 2021. More than meets the eye: scientific rationale behind molecular imaging and therapeutic targeting of prostate-specific membrane antigen (PSMA) in metastatic prostate cancer and beyond. *Cancers*, 13**,** 2244.

INAYAT, N., ZAHIR MUHAMMAD, R. & MAJEED, A. 2020. 90. Phytochemical screening and allelopathic evaluation of aqueous and methanolic leaf extracts of Populus nigra L. *Pure and Applied Biology (PAB)*, 9**,** 956-962.

KAMAT, A. A., KIM, T. J., LANDEN JR, C. N., LU, C., HAN, L. Y., LIN, Y. G., MERRITT, W. M., THAKER, P. H., GERSHENSON, D. M. & BISCHOFF, F. Z. 2007. Metronomic chemotherapy enhances the efficacy of antivascular therapy in ovarian cancer. *Cancer research,* 67**,** 281-288.

KANNAN, M. 2018. Transmission electron microscope—Principle, components and applications. *A textbook on fundamentals and applications of nanotechnology***,** 93-102.

KANSıZ, S. & ELÇIN, Y. M. 2023. Advanced liposome and polymersome-based drug delivery systems: Considerations for physicochemical properties, targeting strategies and stimuli-sensitive approaches. *Advances in Colloid and Interface Science***,** 102930.

KAUR, R. & KUMAR, J. 2023. Phytochemical screening, antioxidant activity and metal binding studies on floral extracts of Euphorbia milii. *Materials Today: Proceedings*.

KHAN, I., SAEED, K. & KHAN, I. 2019. Nanoparticles: Properties, applications and toxicities. *Arabian journal of chemistry,* 12**,** 908-931.

KNEIDL, B., PELLER, M., WINTER, G., LINDNER, L. H. & HOSSANN, M. 2014. Thermosensitive liposomal drug delivery systems: state of the art review. *International journal of nanomedicine***,** 4387-4398.

LEE, D. 2019. *Analysis and Assessment on Effects of Different Therapies in Cancer Treatment Based on Fuzzy Cognitive Maps.* Victoria University.

LIN, Y., ZHOU, M., TAI, X., LI, H., HAN, X. & YU, J. 2021. Analytical transmission electron microscopy for emerging advanced materials. *Matter,* 4**,** 2309-2339.

LIU, L., LI, M., ZHANG, J., XU, D., GUO, Y., ZHANG, H. & CANG, S. 2023. KIF14 mediates cabazitaxel-docetaxel cross-resistance in advanced prostate cancer by promoting AKT phosphorylation. *Archives of Biochemistry and Biophysics,* 737**,** 109551.

LIU, W., ZHU, Y., YE, L., ZHU, Y. & WANG, Y. 2022. Establishment of an orthotopic prostate cancer xenograft mouse model using microscope-guided orthotopic injection of LNCaP cells into the dorsal lobe of the mouse prostate. *BMC cancer,* 22**,** 173.

LIU, Y.-Q., WANG, X.-L., HE, D.-H. & CHENG, Y.-X. 2021. Protection against chemotherapy-and radiotherapy-induced side effects: A review based on the mechanisms and therapeutic opportunities of phytochemicals. *Phytomedicine,* 80**,** 153402.

LIU, Y., YOO, S. D., LI, L., FANG, L., WEN, Z. & LI, T. 2012. Formulation and characterization of boanmycin-loaded liposomes prepared by pH gradient experimental design. *Drug delivery,* 19**,** 90-101.

LU, L., DING, Y., ZHANG, Y., HO, R. J., ZHAO, Y., ZHANG, T. & GUO, C. 2018. Antibody-modified liposomes for tumor-targeting delivery of timosaponin AIII. *International journal of nanomedicine***,** 1927-1944.

MALHOTRA, P. 2023. High Performance Liquid Chromatography. *Analytical Chemistry: Basic Techniques and Methods*. Springer.

MARASINI, R., NGUYEN, T. D. T., RAYAMAJHI, S. & ARYAL, S. 2020. Synthesis and characterization of a tumor-seeking LyP-1 peptide integrated lipid–polymer composite nanoparticle. *Materials Advances,* 1**,** 469-480.

MARITIM, S., BOULAS, P. & LIN, Y. 2021. Comprehensive analysis of liposome formulation parameters and their influence on encapsulation, stability and drug release in glibenclamide liposomes. *International journal of pharmaceutics,* 592**,** 120051.

MAZZOTTA, E., TAVANO, L. & MUZZALUPO, R. 2018. Thermo-sensitive vesicles in controlled drug delivery for chemotherapy. *Pharmaceutics,* 10**,** 150.

MOFOLO, M. J., KADHILA, P., CHINSEMBU, K. C., MASHELE, S. & SEKHOACHA, M. 2020. Green synthesis of silver nanoparticles from extracts of Pechuel-loeschea leubnitziae: their anti-proliferative activity against the U87 cell line. *Inorganic and Nano-Metal Chemistry,* 50**,** 949-955.

MORE, M. P., PARDESHI, S. R., PARDESHI, C. V., SONAWANE, G. A., SHINDE, M. N., DESHMUKH, P. K., NAIK, J. B. & KULKARNI, A. D. 2021. Recent advances in phytochemical-based Nano-formulation for drug-resistant Cancer. *Medicine in Drug Discovery,* 10**,** 100082.

MOTAMARRY, A., ASEMANI, D. & HAEMMERICH, D. 2017. Thermosensitive liposomes. *Liposome. Rijeka InTech***,** 187-212.

MUNDARGI, R. C., TANEJA, N., HADIA, J. J. & KHOPADE, A. J. 2022. Liposomes as Targeted Drug-Delivery Systems. *Targeted Drug Delivery***,** 69-125.

MUSTAPHA, A., ISMAIL, A., ABDULLAHI, S. U., HASSAN, O. N., UGWUNNAJI, P. I. & BERINYUY, E. B. 2022. Cancer chemotherapy: a review update of the mechanisms of actions, prospects and associated problems. *J Biomed,* 1**,** 001-16.

NAMEKAWA, T., IKEDA, K., HORIE-INOUE, K. & INOUE, S. 2019. Application of prostate cancer models for preclinical study: advantages and limitations of cell lines, patient-derived xenografts, and three-dimensional culture of patient-derived cells. *Cells,* 8**,** 74.

NSAIRAT, H., KHATER, D., SAYED, U., ODEH, F., AL BAWAB, A. & ALSHAER, W. 2022. Liposomes: Structure, composition, types, and clinical applications. *Heliyon.*

NUGRAHA, A. T., RAMADANI, A. P., WERDYANI, S., PRATIWI, I. A., JUNIARDY, T., ARFADILA, S. & MAHARDHIKA, M. R. P. 2021. Cytotoxic activity of flavonoid from local plant Eriocaulon cinereum RB against MCF-7 breast cancer cells. *Journal of Advanced Pharmaceutical Technology & Research,* 12**,** 425.

NWABUIFE, J. C., HASSAN, D., PANT, A. M., DEVNARAIN, N., GAFAR, M. A., OSMAN, N., RAMBHAROSE, S. & GOVENDER, T. 2023. Novel vancomycin free base–Sterosomes for combating diseases caused by Staphylococcus aureus and Methicillin-resistant Staphylococcus aureus infections (S. Aureus and MRSA). *Journal of Drug Delivery Science and Technology,* 79**,** 104089.

OBUKOHWO, O. M., KINGSLEY, N. E., RUME, R. A. & VICTOR, E. 2021. The concept of Male reproductive anatomy. *Male Reproductive anatomy*.

OKOTRUB, K. A., MOKROUSOVA, V. I., AMSTISLAVSKY, S. Y. & SUROVTSEV, N. V. 2018. Lipid droplet phase transition in freezing cat embryos and oocytes probed by Raman spectroscopy. *Biophysical Journal,* 115**,** 577-587.

ONG, S. G. M., MING, L. C., LEE, K. S. & YUEN, K. H. 2016. Influence of the encapsulation efficiency and size of liposome on the oral bioavailability of griseofulvin-loaded liposomes. *Pharmaceutics,* 8**,** 25.

OSENI, S. O., NAAR, C., PAVLOVIĆ, M., ASGHAR, W., HARTMANN, J. X., FIELDS, G. B., ESIOBU, N. & KUMI-DIAKA, J. 2023. The Molecular Basis and Clinical Consequences of Chronic Inflammation in Prostatic Diseases: Prostatitis, Benign Prostatic Hyperplasia, and Prostate Cancer. *Cancers,* 15**,** 3110.

PANDE, S. 2023. Liposomes for drug delivery: review of vesicular composition, factors affecting drug release and drug loading in liposomes. *Artificial Cells, Nanomedicine, and Biotechnology,* 51**,** 428-440.

PATEL, A. 2020. Benign vs malignant tumors. *JAMA oncology,* 6**,** 1488-1488.

RADI, M. H., EL-SHIEKH, R. A., EL-HALAWANY, A. M., AL-ABD, A. M. & ABDEL-SATTAR, E. 2023. In Vitro Cytotoxic Study of Euphorbia grantii Oliv. Aerial Parts against MCF-7 and MCF-7ADR Breast Cancer Cell Lines: A Bioactivity-Guided Isolation. *ACS omega*.

RAHMAN, A. & AKTER, M. 2013. Taxonomy and medicinal uses of Euphorbiaceae (Spurge) family of Rajshahi, Bangladesh. *Research in Plant Sciences,* 1**,** 74-80.

RAJ, S., KHURANA, S., CHOUDHARI, R., KESARI, K. K., KAMAL, M. A., GARG, N., RUOKOLAINEN, J., DAS, B. C. & KUMAR, D. Specific targeting cancer cells with nanoparticles and drug delivery in cancer therapy. Seminars in cancer biology, 2021. Elsevier, 166-177.

RAWAT, P. S., JAISWAL, A., KHURANA, A., BHATTI, J. S. & NAVIK, U. 2021. Doxorubicin-induced cardiotoxicity: An update on the molecular mechanism and novel therapeutic strategies for effective management. *Biomedicine & Pharmacotherapy,* 139**,** 111708.

RAWLA, P. 2019. Epidemiology of prostate cancer. *World journal of oncology,* 10**,** 63.

RAZANAJATOVO, H. 2020. Euphorbia milii. *IUCN Red List of Threatened Species*.

REUHS, B. L. 2017. *High-performance liquid chromatography*, Springer.

RICH, G. T., BUCHWEITZ, M., WINTERBONE, M. S., KROON, P. A. & WILDE, P. J. 2017. Towards an understanding of the low bioavailability of quercetin: a study of its interaction with intestinal lipids. *Nutrients,* 9**,** 111.

ROMMASI, F. & ESFANDIARI, N. 2021. Liposomal nanomedicine: applications for drug delivery in cancer therapy. *Nanoscale Research Letters,* 16**,** 95.

SAHU, T., RATRE, Y. K., CHAUHAN, S., BHASKAR, L., NAIR, M. P. & VERMA, H. K. 2021. Nanotechnology based drug delivery system: Current strategies and emerging therapeutic potential for medical science. *Journal of Drug Delivery Science and Technology*, 63**,** 102487.

SALEEM, H., ZENGIN, G., LOCATELLI, M., MOLLICA, A., AHMAD, I., MAHOMOODALLY, F. M., ABIDIN, S. A. Z. & AHEMAD, N. 2019. In vitro biological propensities and chemical profiling of Euphorbia milii Des Moul (Euphorbiaceae): A novel source for bioactive agents. *Industrial Crops and Products,* 130**,** 9-15.

SALEHI, B., IRITI, M., VITALINI, S., ANTOLAK, H., PAWLIKOWSKA, E., KRĘGIEL, D., SHARIFI-RAD, J., OYELEYE, S. I., ADEMILUYI, A. O. & CZOPEK, K. 2019. Euphorbia-derived natural products with potential for use in health maintenance. *Biomolecules,* 9**,** 337.

SARANYUTANON, S., DESHMUKH, S. K., DASGUPTA, S., PAI, S., SINGH, S. & SINGH, A. P. 2020. Cellular and molecular progression of prostate cancer: models for basic and preclinical research. *Cancers,* 12**,** 2651.

SATHE, K. P. & BANGAR, V. B. 2021. LIPOSOMES: AN OVERVIEW.

SEKHOACHA, M., RIET, K., MOTLOUNG, P., GUMENKU, L., ADEGOKE, A. & MASHELE, S. 2022. Prostate Cancer Review: Genetics, Diagnosis, Treatment Options, and Alternative Approaches. *Molecules,* 27**,** 5730.

SERCOMBE, L., VEERATI, T., MOHEIMANI, F., WU, S. Y., SOOD, A. K. & HUA, S. 2015. Advances and challenges of liposome assisted drug delivery. *Frontiers in pharmacology,* 6**,** 286.

SHAH, A., SHAH, A. A., K, N. & LOBO, R. 2021. Mechanistic targets for BPH and prostate cancer–a review. *Reviews on Environmental Health,* 36**,** 261-270.

SHAIK, B. B., KATARI, N. K. & JONNALAGADDA, S. B. 2022. Role of natural products in developing novel anticancer agents: a perspective. *Chemistry & Biodiversity,* 19**,** e202200535.

SHAKER, K. H., ZOHAIR, M. M., HASSAN, A. Z., SWEELAM, H.-T. M. & ASHOUR, W. E. 2022. LC–MS/MS and GC–MS based phytochemical perspectives and antimicrobial effects of endophytic fungus Chaetomium ovatoascomatis isolated from Euphorbia milii. *Archives of Microbiology,* 204**,** 661.

SHARIFI, M., CHO, W. C., ANSARIESFAHANI, A., TARHAROUDI, R., MALEKISARVAR, H., SARI, S., BLOUKH, S. H., EDIS, Z., AMIN, M. & GLEGHORN, J. P. 2022. An updated review on EPR-based solid tumor targeting nanocarriers for cancer treatment. *Cancers,* 14**,** 2868.

SHEIKHOLESLAMI, B., LAM, N. W., DUA, K. & HAGHI, M. 2022. Exploring the impact of physicochemical properties of liposomal formulations on their in vivo fate. *Life Sciences,* 300**,** 120574.

SHU, Y., XIE, B., LIANG, Z. & CHEN, J. 2018. Quercetin reverses the doxorubicin resistance of prostate cancer cells by downregulating the expression of c-met. *Oncology letters,* 15**,** 2252-2258.

SHUKLA, S. & MEHTA, A. 2015. Anticancer potential of medicinal plants and their phytochemicals: a review. *Brazilian Journal of Botany,* 38**,** 199-210.

SINGH, S. K., APATA, T., GORDETSKY, J. B. & SINGH, R. 2019. Docetaxel combined with thymoquinone induces apoptosis in prostate cancer cells via inhibition of the PI3K/AKT signaling pathway. *Cancers,* 11**,** 1390.

TAGAI, E. K., MILLER, S. M., KUTIKOV, A., DIEFENBACH, M. A., GOR, R. A., AL-SALEEM, T., CHEN, D. Y., FLESZAR, S. & ROY, G. 2019. Prostate cancer patients' understanding of the Gleason scoring system: implications for shared decision-making. *Journal of Cancer Education,* 34**,** 441-445.

TAKAYAMA, R., INOUE, Y., MURATA, I. & KANAMOTO, I. 2020. Characterization of nanoparticles using DSPE-PEG2000 and soluplus. *Colloids and Interfaces,* 4**,** 28.

TIWARI, P., YADAV, K., SHUKLA, R. P., GAUTAM, S., MARWAHA, D., SHARMA, M. & MISHRA, P. R. 2023. Surface modification strategies in translocating nano-vesicles across different barriers and the role of bio-vesicles in improving anticancer therapy. *Journal of Controlled Release,* 363**,** 290-348.

TSAKALOZOU, E., ECKMAN, A. M. & BAE, Y. 2012. Combination effects of docetaxel and doxorubicin in hormone-refractory prostate cancer cells. *Biochemistry Research International,* 2012.

TYAGI, T. & AGARWAL, M. 2017. Phytochemical screening and GC-MS analysis of bioactive constituents in the ethanolic extract of Pistia stratiotes L. and Eichhornia crassipes (Mart.) solms. *Journal of Pharmacognosy and phytochemistry,* 6**,** 195-206.

UDDIN, G. & QAISAR, M. 2014. Abdur Rauf, Ajmal Khan 2, Nizam Uddin 3, 5, Muhammad Akram, Mohammad Arfan. *Pak. J. Pharm. Sci,* 27**,** 947-951.

UGWUNNAJI, P. I. & BERINYUY, E. B. Cancer Chemotherapy: A Review Update of the Mechanisms of Actions, Prospects, and Associated Problems Aishatu Mustapha1, Abdulfatai Ismail2, Shehu U. Abdullahi3, Opeyemi N. Hassan4.

VAN ELK, M., MURPHY, B. P., EUFRÁSIO-DA-SILVA, T., O'REILLY, D. P., VERMONDEN, T., HENNINK, W. E., DUFFY, G. P. & RUIZ-HERNÁNDEZ, E. 2016. Nanomedicines for advanced cancer treatments: Transitioning towards responsive systems. *International journal of pharmaceutics,* 515**,** 132-164.

WANG, Z. L. 2003. New developments in transmission electron microscopy for nanotechnology. *Advanced Materials,* 15**,** 1497-1514.

WERENGOWSKA-CIEĆWIERZ, K., WIŚNIEWSKI, M., TERZYK, A. P. & FURMANIAK, S. 2015. The chemistry of bioconjugation in nanoparticles-based drug delivery system. *Advances in Condensed Matter Physics,* 2015.

WOLFRAM, J., SURI, K., YANG, Y., SHEN, J., CELIA, C., FRESTA, M., ZHAO, Y., SHEN, H. & FERRARI, M. 2014. Shrinkage of pegylated and non-pegylated liposomes in serum. *Colloids and surfaces B: biointerfaces,* 114**,** 294-300.

WU, T. T., SIKES, R. A., CUI, Q., THALMANN, G. N., KAO, C., MURPHY, C. F., YANG, H., ZHAU, H. E., BALIAN, G. & CHUNG, L. W. 1998. Establishing human prostate cancer cell xenografts in bone: Induction of osteoblastic reaction by prostate-specific antigen-producing tumors in athymic and SCID/bg mice using LNCaP and lineage-derived metastatic sublines. *International journal of cancer,* 77**,** 887-894.

WULCZYN, E., NAGPAL, K., SYMONDS, M., MORAN, M., PLASS, M., REIHS, R., NADER, F., TAN, F., CAI, Y. & BROWN, T. 2021. Predicting prostate cancer specific-mortality with artificial intelligence-based Gleason grading. *Communications Medicine,* 1**,** 10.

YANG, L., FAN, X., ZHANG, J. & JU, J. 2020. Preparation and characterization of thermoresponsive poly (N-isopropylacrylamide) for cell culture applications. *Polymers,* 12**,** 389.

YUSUF, A., ZAKIR, A., SHEMAU, Z., ABDULLAHI, M. & HALIMA, S. 2014. Phytochemical analysis of the methanol leaves extract of Paullinia pinnata linn. *Journal of pharmacognosy and phytotherapy,* 6**,** 10-16.

ZHANG, D. & ZHANG, J. 2020. Surface engineering of nanomaterials with phospholipid-polyethylene glycol-derived functional conjugates for molecular imaging and targeted therapy. *Biomaterials,* 230**,** 119646.

ZHANG, L., LU, S.-Y., GUO, R., MA, J.-X., TANG, L.-Y., WANG, J.-J., SHEN, C.-L., LU, L.-M., LIU, J. & WANG, Z.-G. 2021. STK10 knockout inhibits cell migration and promotes cell proliferation via modulating the activity of ERM and p38 MAPK in prostate cancer cells. *Experimental and Therapeutic Medicine,* 22**,** 1-8.

ZHANG, W., ZHAO, Y. & DONG, J. Impact of blue light irradiation on the viability of four types of human cells. 2022 19th China International Forum on Solid State Lighting & 2022 8th International Forum on Wide Bandgap Semiconductors (SSLCHINA: IFWS), 2023. IEEE, 259-262.

ZHAO, Y., CULMAN, J., CASCORBI, I., NITHACK, N., MARX, M., ZUHAYRA, M. & LÜTZEN, U. 2023. PSMA-617 inhibits proliferation and potentiates the 177Lu-PSMA-617-induced death of human prostate cancer cells. *Naunyn-Schmiedeberg's Archives of Pharmacology***,** 1-12.

Chapter 9

9.1 Appendix A HPLC and LCMS chromatograms

The determination of the NP's entrapment efficiency of the drug was done using LCMS.

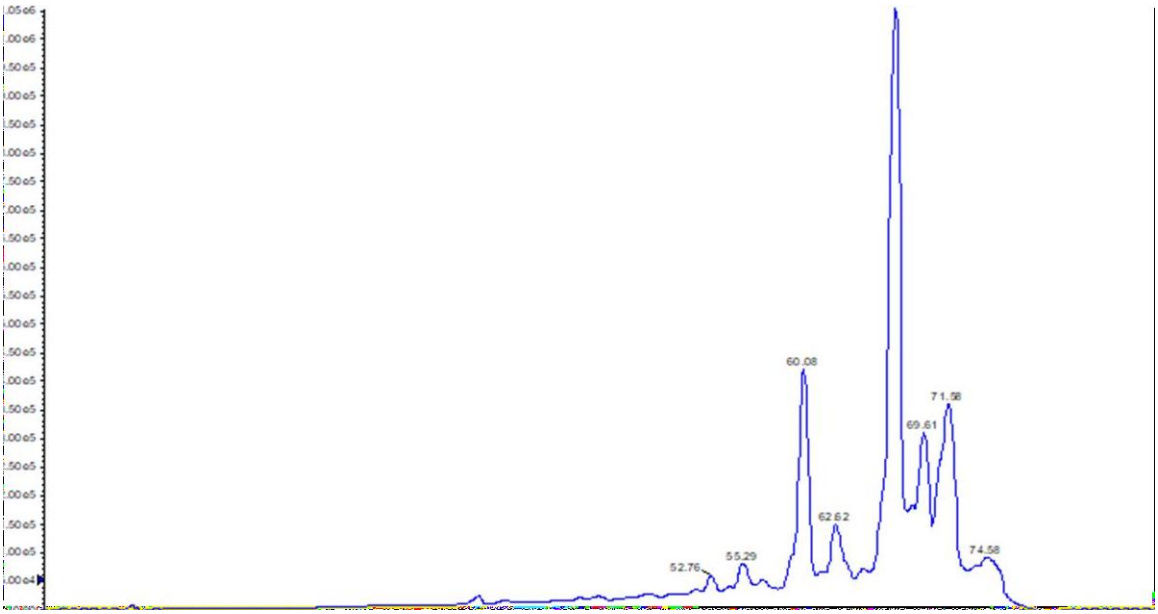

Figure 28: LCMS run on the *E. milii* sample.

The most intense peak of the EM extract was observed at 67 min and this shows the spectrum of all the masses in that peak (at 67 min) between 200–1000 Da (in positive ionization mode).

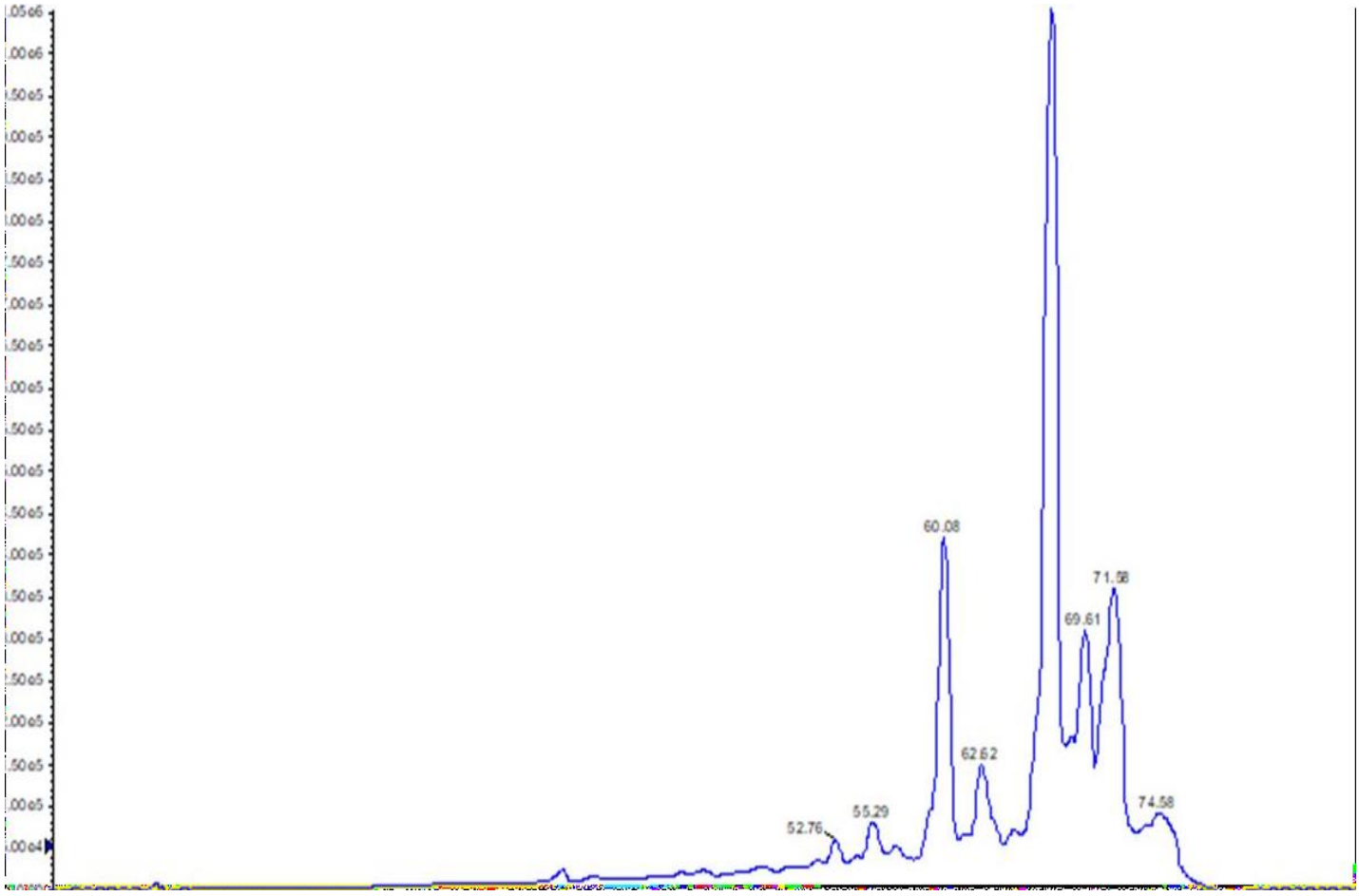

Figure 29: LCMS run on the *E.milii* sample showing the most intense peak.

The most intense peak of the *E milii* extract was observed at 67 min and this shows the spectrum of all the masses in that peak (at 67 min) between 200–1000 Da (in positive ionization mode).

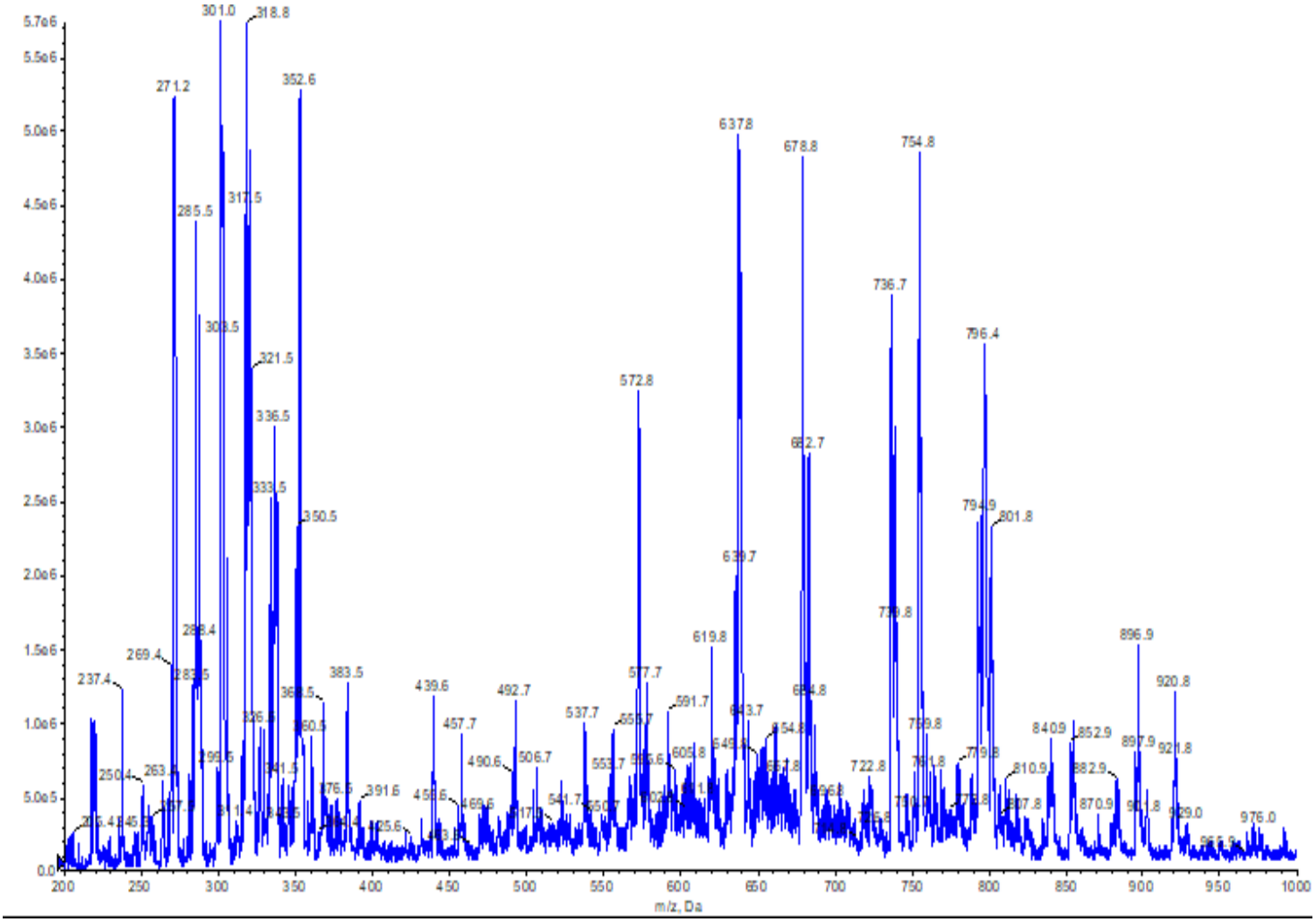

Figure 30: Several masses that were identified in the *E. milii* plant extract

The masses, and the peak at 67 min were chosen as a marker for HPLC. Several masses were identified in the most intense (peak at 67 min) chromatographic peaks. The masses selected were 271, 301, 318, 352, 637, 678, 754, and 796 and were used as marker masses. There are only two masses that are separated as well-structured peaks: 754 and796. The other masses were badly resolved and eluted as multiple peaks and were then integrated as one to give the values above 111.

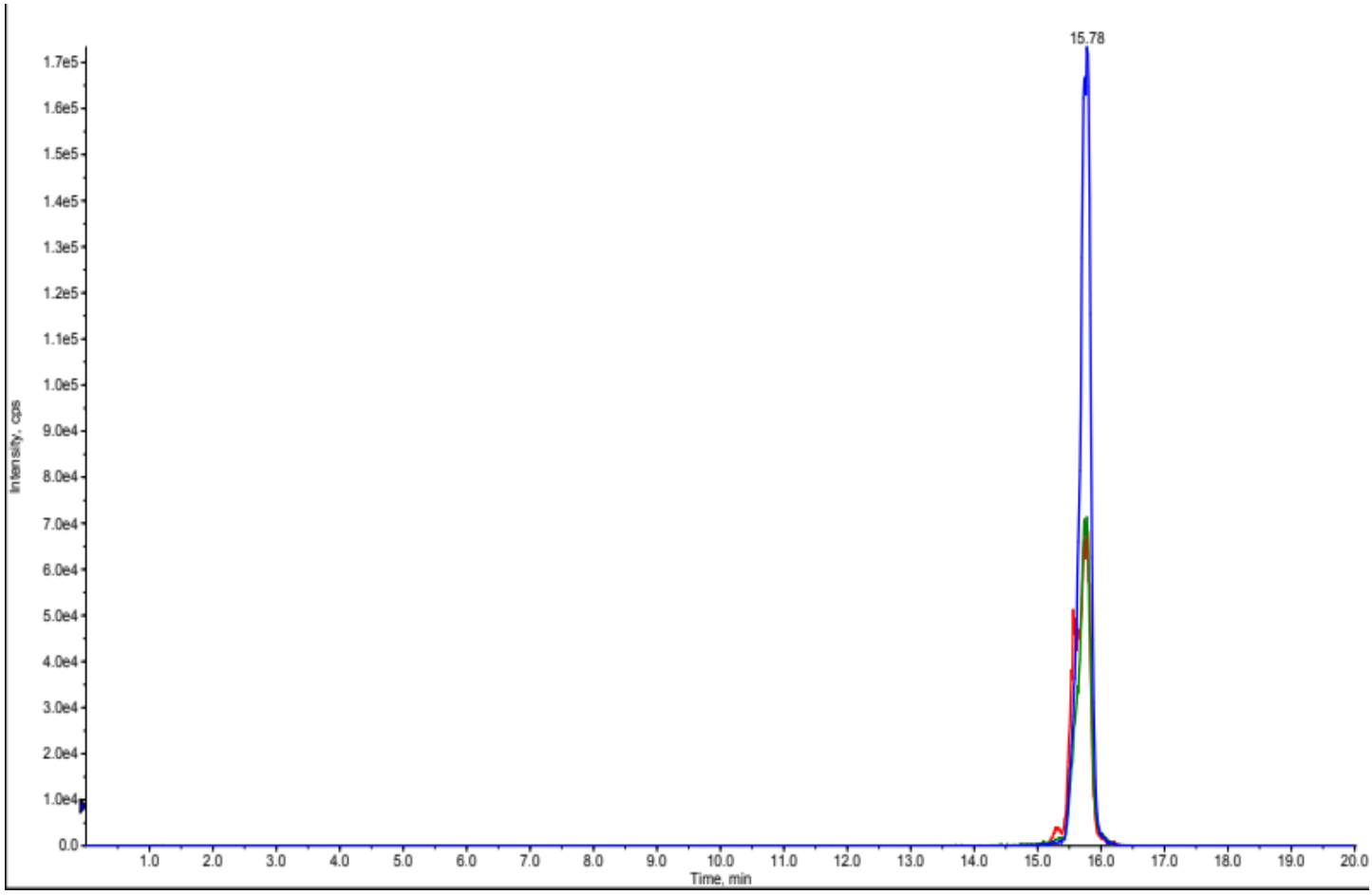

Figure 31: The chromatogram of Mass 754 of the *E. milii* extract

.

.

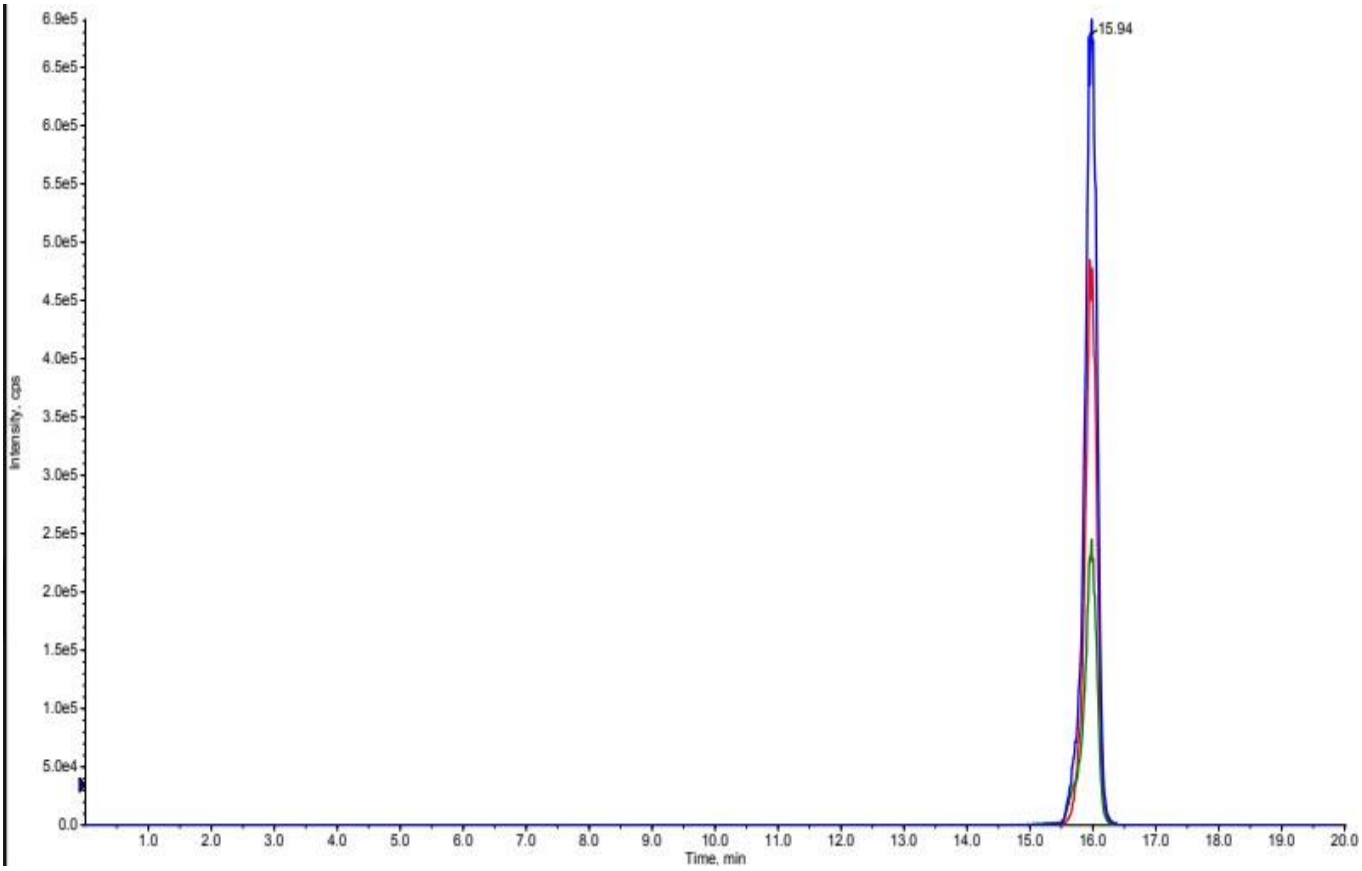

Figure 32: The chromatogram of Mass 769 of the *E. milii* extract.

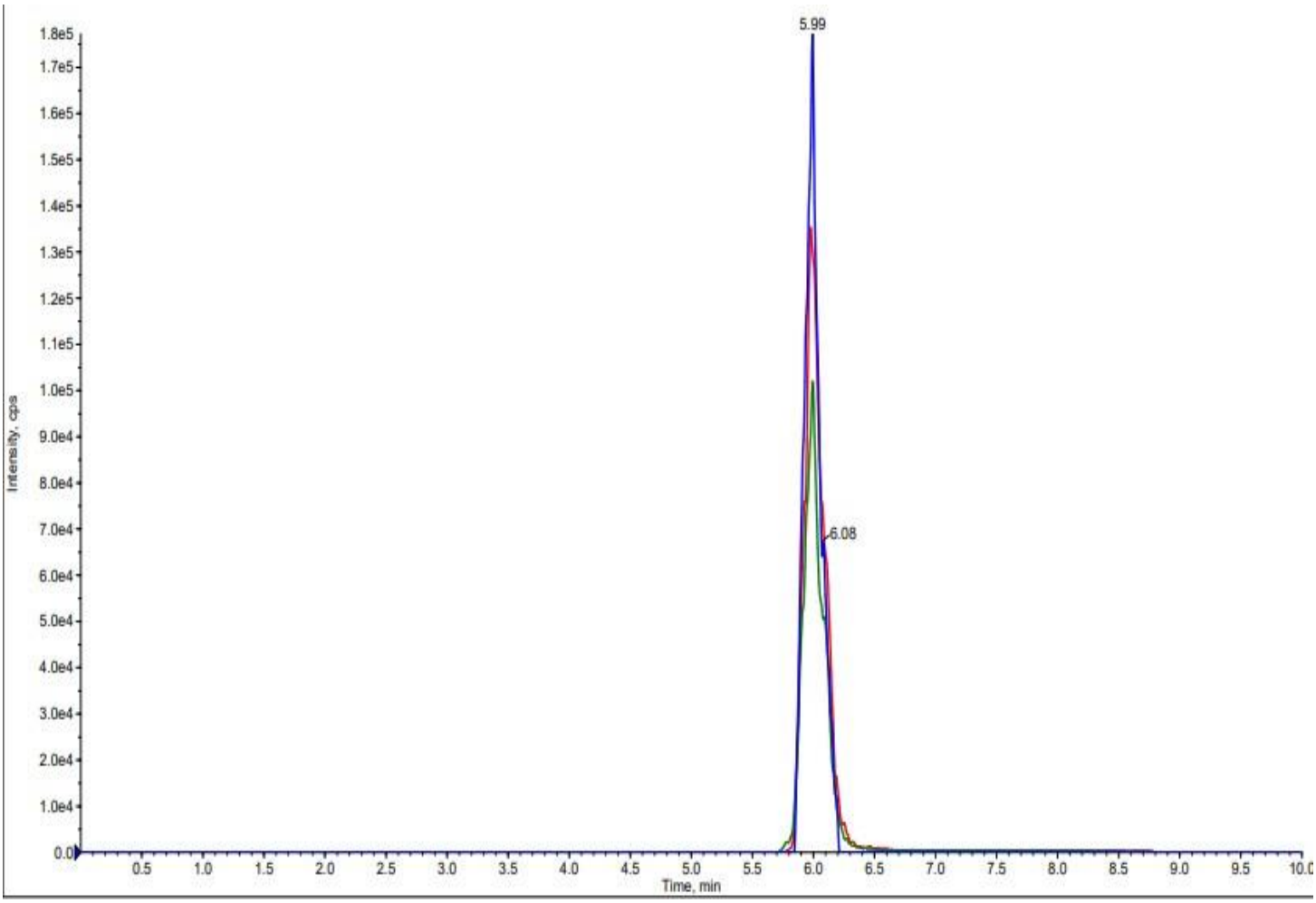

Figure 33: The chromatogram of docetaxel.

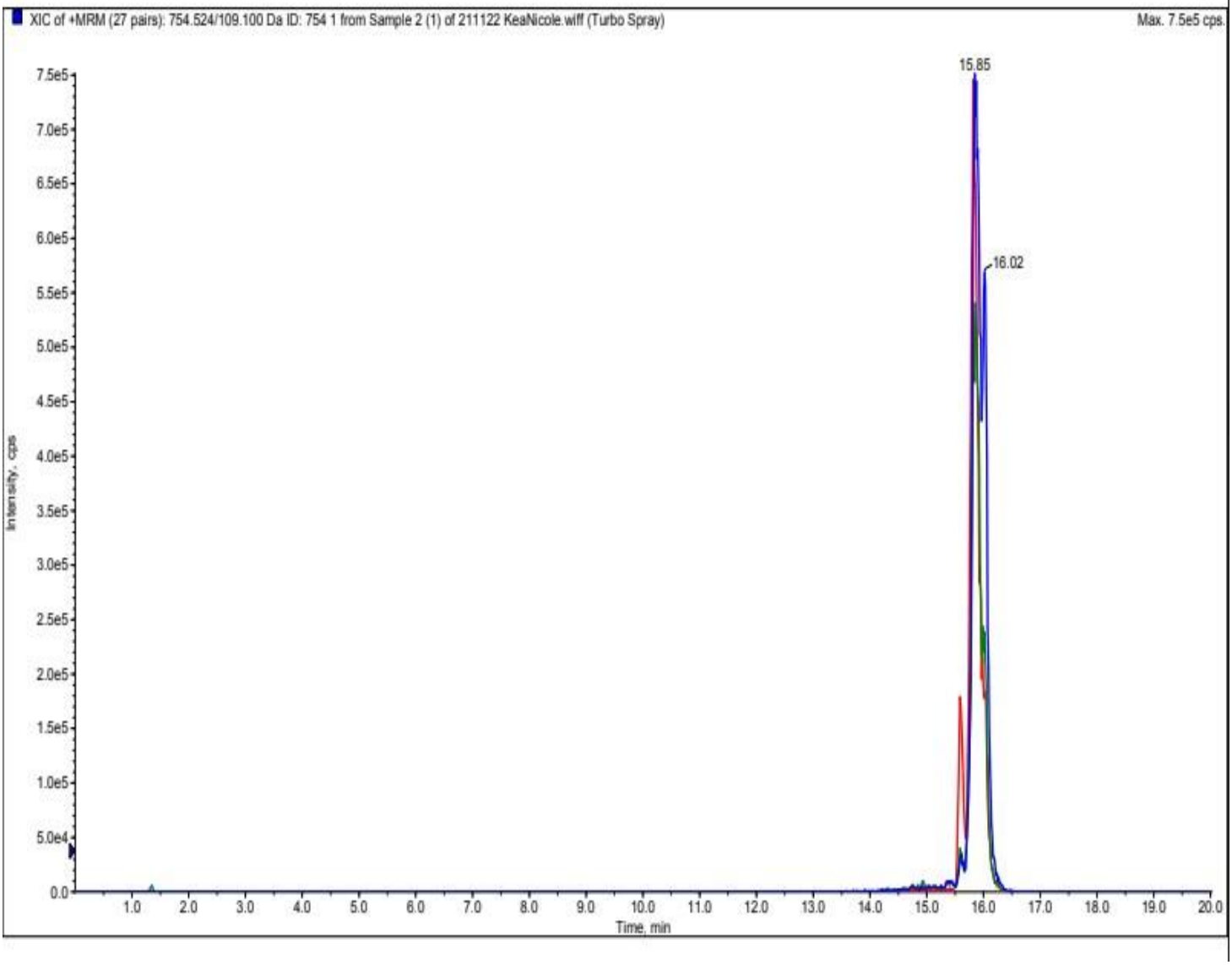

Figure 34: The chromatogram of mass 754 of the euphorbia released.

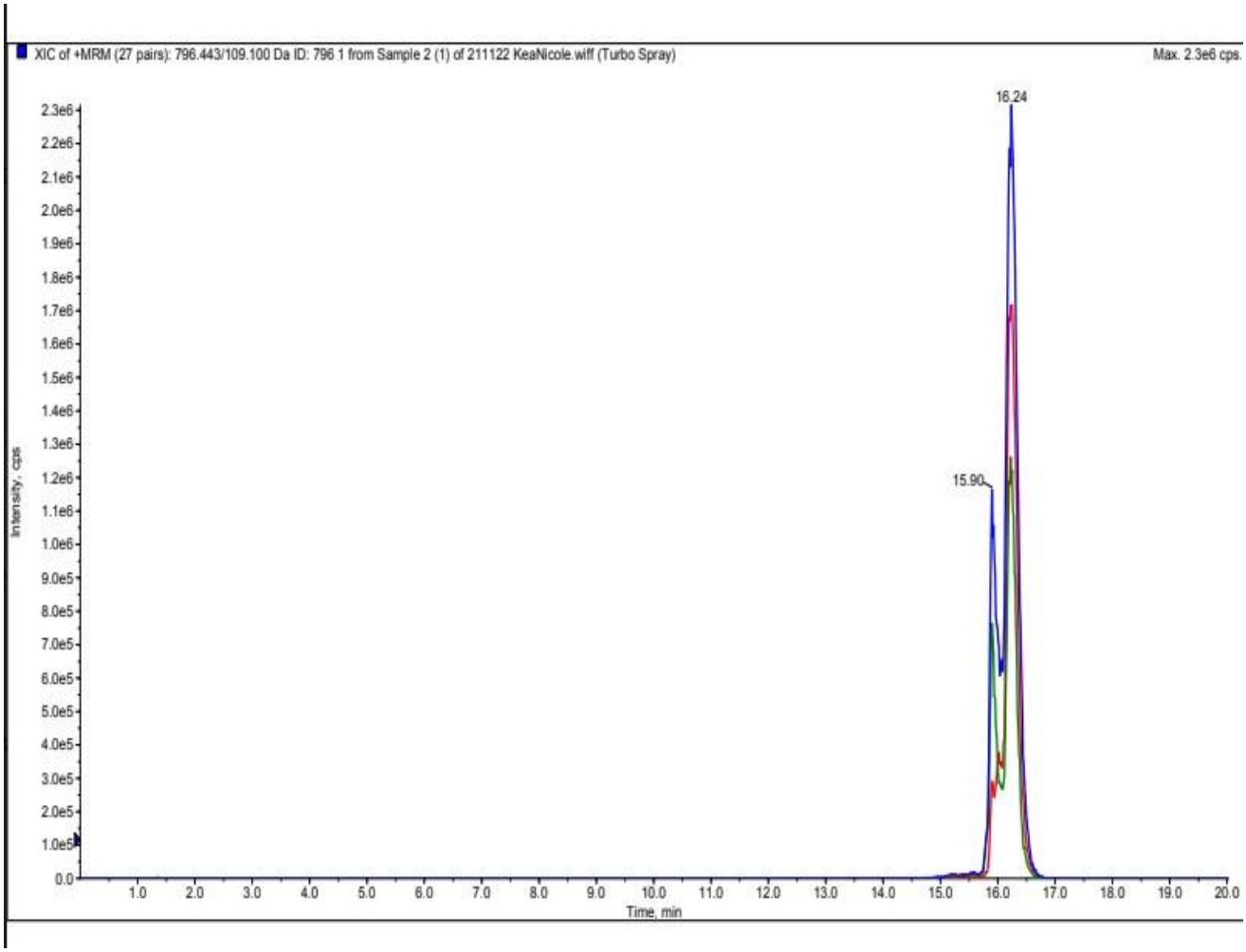

Figure 35: The chromatogram of mass 796 of the *E. milii* released.

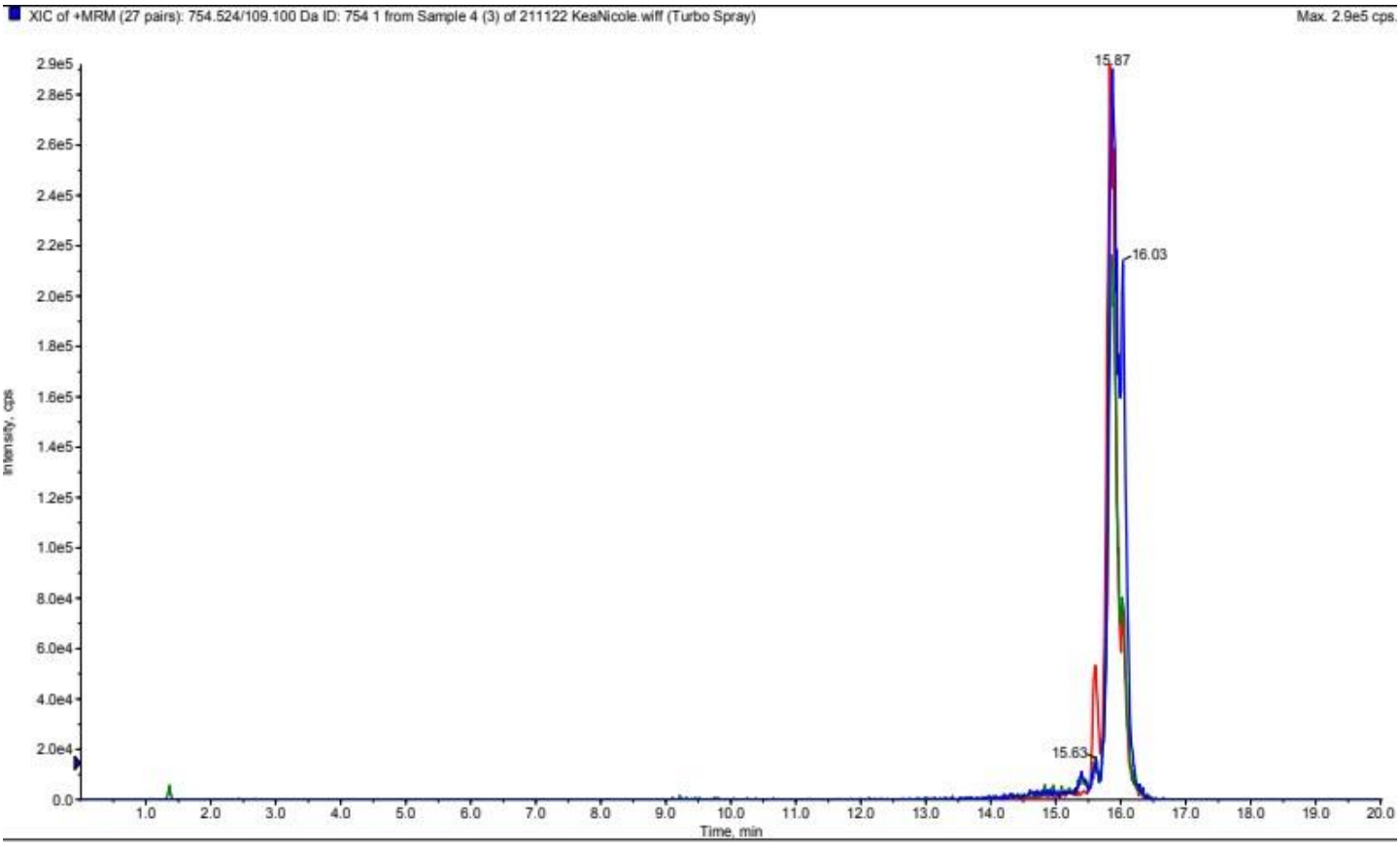

Figure 36: The chromatogram of mass 754 of the euphorbia unreleased

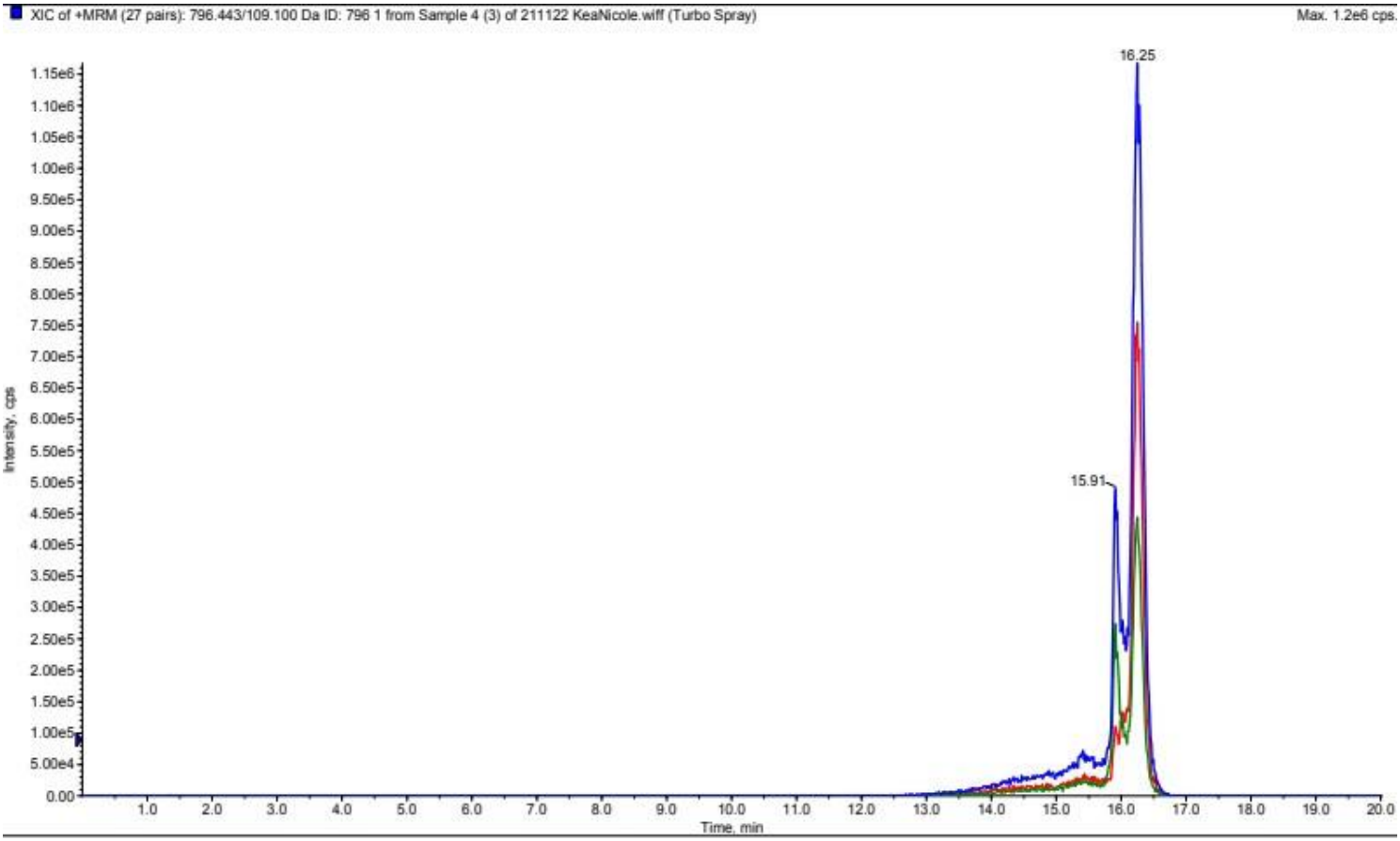

Figure 37: The chromatogram of mass 796 of unreleased euphorbia

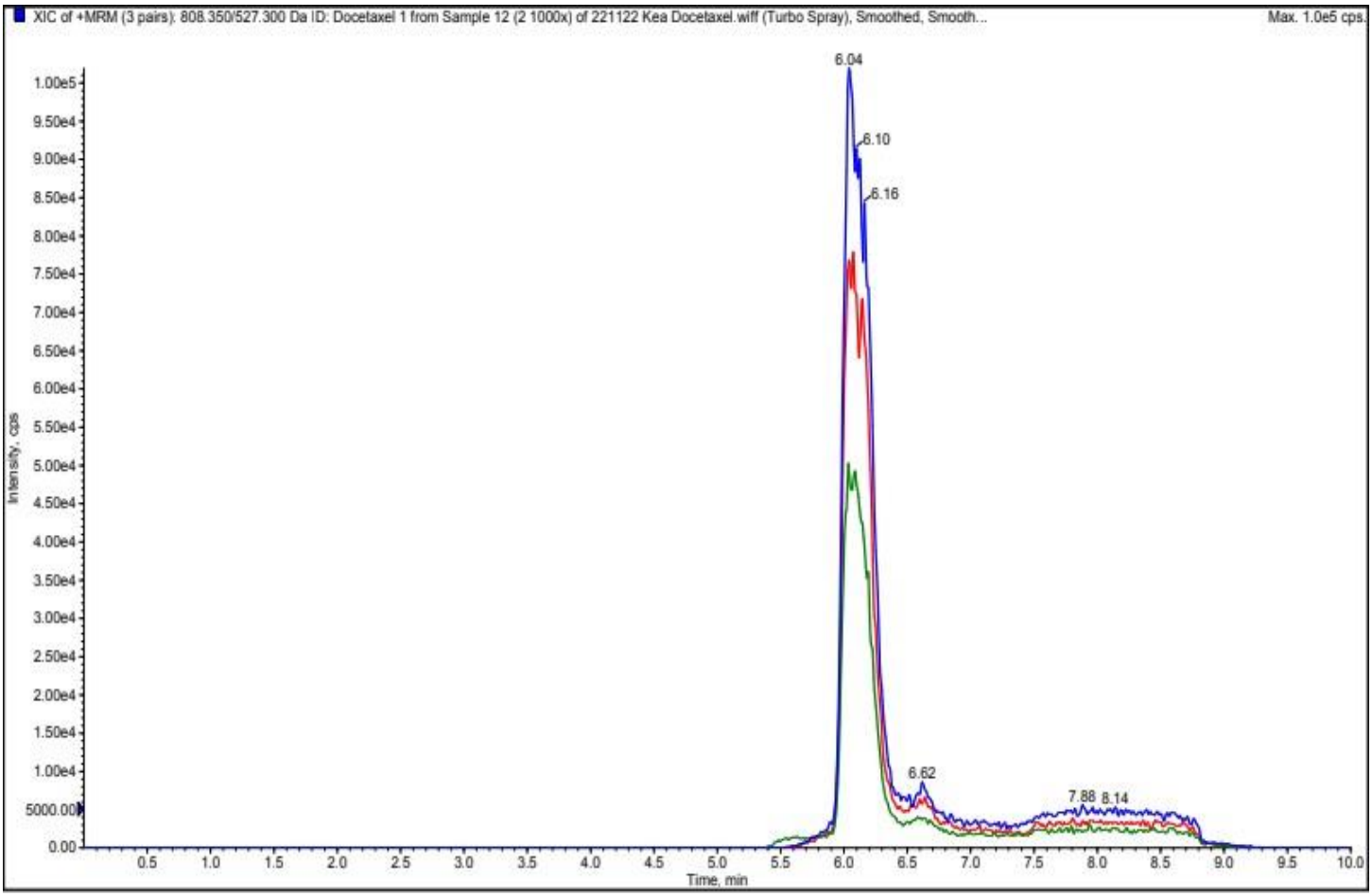

Figure 38: The chromatogram of released docetaxel.

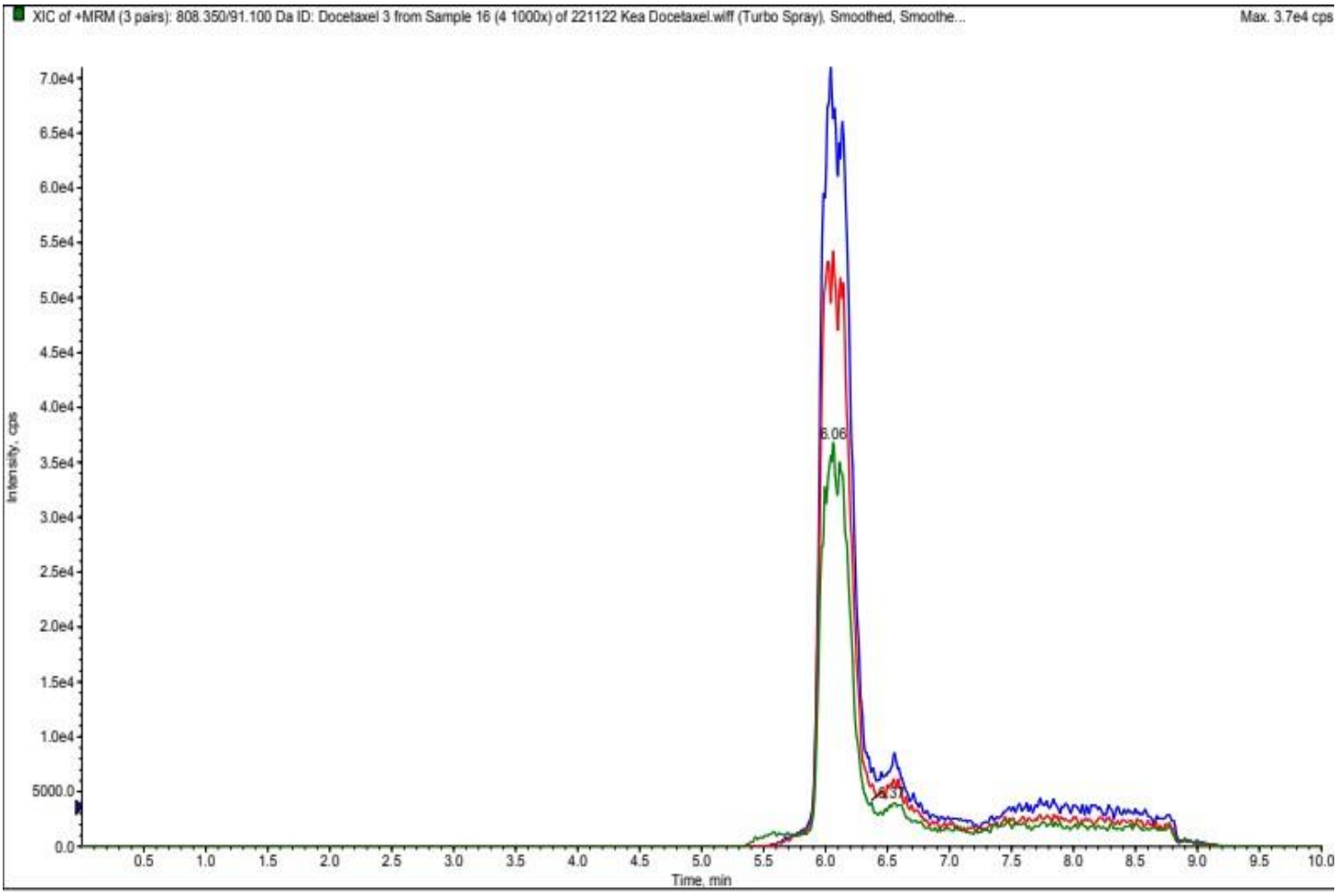

Figure 39: The Chromatogram of unreleased docetaxel

Appendix 2 Articles

Review article submitted to Molecules Journal: Article successfully published.

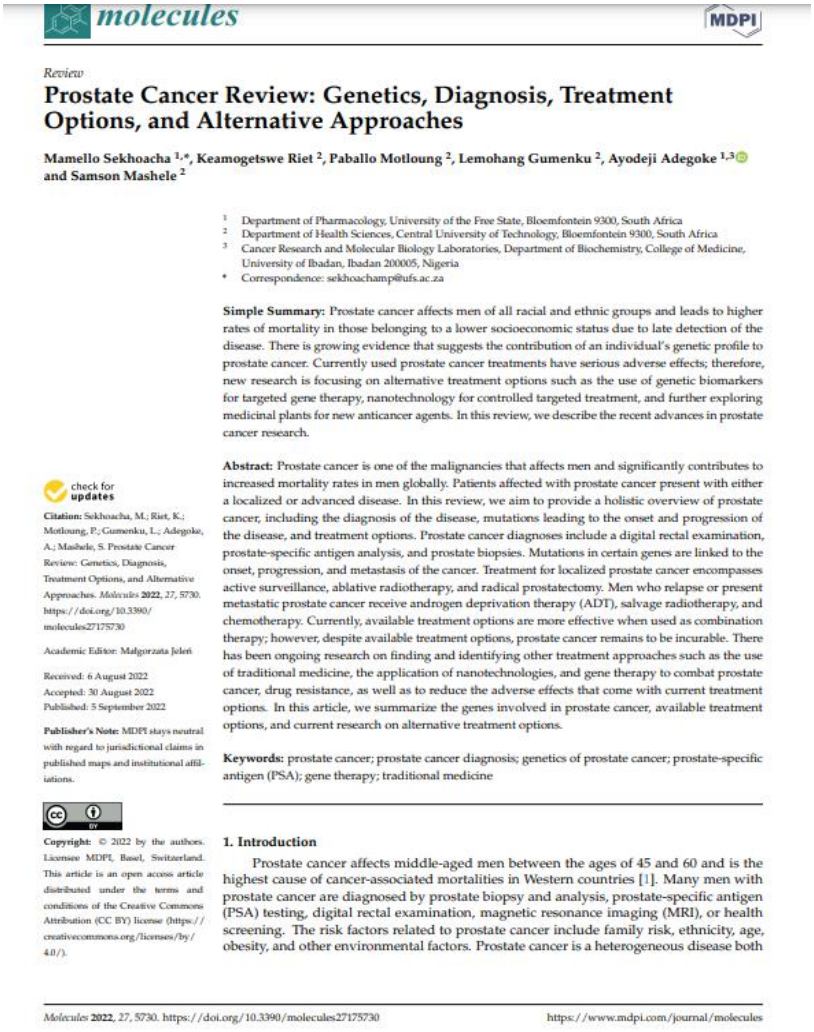

molecules

MDPI

Review

Prostate Cancer Review: Genetics, Diagnosis, Treatment Options, and Alternative Approaches

Mamello Sekhoacha [1,*], Keamogetswe Riet [2], Paballo Motloung [2], Lemohang Gumenku [2], Ayodeji Adegoke [1,3] and Samson Mashele [2]

[1] Department of Pharmacology, University of the Free State, Bloemfontein 9300, South Africa
[2] Department of Health Sciences, Central University of Technology, Bloemfontein 9300, South Africa
[3] Cancer Research and Molecular Biology Laboratories, Department of Biochemistry, College of Medicine, University of Ibadan, Ibadan 200005, Nigeria
* Correspondence: sekhoachamp@ufs.ac.za

Simple Summary: Prostate cancer affects men of all racial and ethnic groups and leads to higher rates of mortality in those belonging to a lower socioeconomic status due to late detection of the disease. There is growing evidence that suggests the contribution of an individual's genetic profile to prostate cancer. Currently used prostate cancer treatments have serious adverse effects; therefore, new research is focusing on alternative treatment options such as the use of genetic biomarkers for targeted gene therapy, nanotechnology for controlled targeted treatment, and further exploring medicinal plants for new anticancer agents. In this review, we describe the recent advances in prostate cancer research.

Abstract: Prostate cancer is one of the malignancies that affects men and significantly contributes to increased mortality rates in men globally. Patients affected with prostate cancer present with either a localized or advanced disease. In this review, we aim to provide a holistic overview of prostate cancer, including the diagnosis of the disease, mutations leading to the onset and progression of the disease, and treatment options. Prostate cancer diagnoses include a digital rectal examination, prostate-specific antigen analysis, and prostate biopsies. Mutations in certain genes are linked to the onset, progression, and metastasis of the cancer. Treatment for localized prostate cancer encompasses active surveillance, ablative radiotherapy, and radical prostatectomy. Men who relapse or present metastatic prostate cancer receive androgen deprivation therapy (ADT), salvage radiotherapy, and chemotherapy. Currently, available treatment options are more effective when used as combination therapy; however, despite available treatment options, prostate cancer remains to be incurable. There has been ongoing research on finding and identifying other treatment approaches such as the use of traditional medicine, the application of nanotechnologies, and gene therapy to combat prostate cancer, drug resistance, as well as to reduce the adverse effects that come with current treatment options. In this article, we summarize the genes involved in prostate cancer, available treatment options, and current research on alternative treatment options.

Keywords: prostate cancer; prostate cancer diagnosis; genetics of prostate cancer; prostate-specific antigen (PSA); gene therapy; traditional medicine

check for updates

Citation: Sekhoacha, M.; Riet, K.; Motloung, P.; Gumenku, L.; Adegoke, A.; Mashele, S. Prostate Cancer Review: Genetics, Diagnosis, Treatment Options, and Alternative Approaches. *Molecules* **2022**, *27*, 5730. https://doi.org/10.3390/molecules27175730

Academic Editor: Małgorzata Jeleń

Received: 6 August 2022
Accepted: 30 August 2022
Published: 5 September 2022

Publisher's Note: MDPI stays neutral with regard to jurisdictional claims in published maps and institutional affiliations.

1. Introduction

Prostate cancer affects middle-aged men between the ages of 45 and 60 and is the highest cause of cancer-associated mortalities in Western countries [1]. Many men with prostate cancer are diagnosed by prostate biopsy and analysis, prostate-specific antigen (PSA) testing, digital rectal examination, magnetic resonance imaging (MRI), or health screening. The risk factors related to prostate cancer include family risk, ethnicity, age, obesity, and other environmental factors. Prostate cancer is a heterogeneous disease both

on the basis of epidemiology and genetics. The interplay among genetics, environmental influences, and social influences causes race-specific prostate cancer survival rate estimates to decrease, and thus, results in differences observed in the epidemiology of prostate cancer in different countries [2]. There is documented proof of a genetic contribution to prostate cancer. Hereditary prostate cancer and a genetic component predisposition to prostate cancer have been studied for years. One of the most predisposing genetic risk factors for prostate cancer is family inheritance. Twin studies and epidemiological studies have both proven the role of hereditary prostate cancer [3]. Many researchers have looked into the possible role of genetic variation in androgen biosynthesis and metabolism, as well as the role of androgens [4,5]. Genomics research has identified molecular processes that result in certain cancer developments, such as chromosomal rearrangements [2].

In general, gene mutations are a prevalent cause of cancer. Candidate genes for prostate cancer predisposition are genes that partake in the androgen pathway and metabolism of testosterone. The development of prostate epithelium and prostate cancer cells relies on the androgen receptor signaling pathway and testosterone [6]. The identification of cancer biomarkers and targeting of specific genetic mutations can be used for targeted treatment of prostate cancer. Biomarkers that can be used for targeted treatment are DNA tumor biomarkers, DNA biomarkers, and general biomarkers [7].

Prostate cancer can either be classified as androgen sensitive or androgen insensitive, which is an indicator of testosterone stimulation and the possible treatment option [8]. Treatment options available for prostate cancer are active surveillance, chemotherapy, radiation therapy, hormonal therapy, surgery, and cryotherapy. Treatment options delivered to a patient depend on the nature of the tumor, PSA level, grade and stage, and possible recurrence. For example, radical prostatectomy, a surgical option that involves the removal of the prostate and nearby tissues, is used in conjunction with radiation therapy for the treatment of low-risk prostate cancer [9]. For treating cancers that have spread beyond the prostate and have reoccurred, androgen-deprivation therapy, also called hormonal therapy, is recommended [1]. Each treatment is associated with severe side effects such as toxicity and reduced white and red blood cell counts, which lead to fatigue, hair loss, peripheral neuropathy, erectile incontinence and dysfunction, metastasis, and lastly, developing resistance to the initial treatment. Available treatment options are expensive and pose severe side effects. The discovery of new cost-effective chemotherapeutic agents with little or no side effects and higher efficacy is necessary [3]. In this review, we provide a holistic overview of prostate cancer, including the diagnosis of the disease, genes and mutations leading to the onset and progression of the disease, treatment options, and alternative treatment options.

2. Materials and Methods

In order to carry out the current review, in 2020, our team began to collect information and carry out a comprehensive search from different databases, i.e., Google Scholar, Pubmed, Springer, Elsevier ScienceDirect, and Web of Science, for studies published from 2010 to 2022, and older studies published as early as 2000 were included in this paper due to relevancy. The articles selected only utilized English texts, and searches were carried out for the following keywords and headings: "prostate cancer", "prostate cancer genetics", "prostate cancer diagnosis and treatment", ' cancer statistics", "the prostate", "medicinal plants in prostate cancer treatment", "traditional medicine", "alternative therapy for prostate cancer", "nanomedicine in prostate cancer", "next generation sequencing", "bioactive compounds in prostate cancer", and "drug repurposing in cancer". Duplicate papers were eliminated, the data were screened, irrelevant works were factored out, and then full-text documents were screened. The inclusion criteria included several factors which involved original articles or review papers. The criteria for exclusion included articles with inadequate and irrelevant information and those without access to full text articles.

2.1. Epidemiology of Prostate Cancer

2.1.1. Global Scale

Prostate cancer is one of the most common malignancies in men worldwide [10]. In 2018, GLOBOCAN reported approximately 1,276,106 new cases of prostate cancer resulting in about 358,989 deaths worldwide, with a higher prevalence in developed countries. On average, 190,000 new prostate cancer cases arise each year, with about 80,000 deaths occurring annually around the world [11]. The worldwide incidence of prostate cancer differs among various geographical regions and ethnic groups. Black men have the most reported incidence rates of prostate cancer in the world [12]. The incidence rates of Black Americans are approximately 60% higher than those of white men in America. The highest recorded incidence rates of prostate cancer are seen in developed countries where there is prostate cancer awareness and where prostate-specific antigen (PSA) testing is a prevalent screening practice [13]. The GLOBOCAN reports of PSA tests indicated high incidence rates in Australasia (111.6 per 100,000) and the USA (97.2 per 100,000) in the year 2012 [14]. Globally, prostate cancer is predicted to increase to approximately 1.7 million new cases and 499,000 deaths by the year 2030 because of the exponentially growing population and the large population of men who will be 65 years and older [15].

2.1.2. Local Scale

Little is known about prostate cancer in African countries. Prostate cancer screening using the PSA test or digital rectal examination is not a well-established practice in Africa. There is a higher incidence rate of prostate cancer among men in Southern Africa as compared with Northern Africa [16]. In South Africa, prostate cancer is one of the most diagnosed cancers in men across the country. As recorded by the South African National Cancer Registry, the incidence rate of prostate cancer in 2007 was 29.4 per 100,000 men. In 2012, the incidence increased to 67.9 per 100,000 men [15].

2.2. Screening and Diagnosis of Prostate Cancer

Prostate cancer diagnoses at mature stages of the disease and failure of therapy are the main factors leading to an increased mortality rate. There is no single, specific test for prostate cancer; however, it has conventionally been diagnosed by a digital rectal examination (DRE), where a gloved finger is inserted into the patient's rectum to assess the size of the prostate gland and any abnormalities. However, the prostate-specific antigen (PSA) test remains to be the keystone for prostate cancer screening [17]. PSA is a glycoprotein secreted by the epithelial cells of the prostate gland. It is usually found in semen, but can also be found in the bloodstream [18]. During PSA testing, blood samples are taken to test the level of PSA. Then, the blood samples are analyzed at a PSA cut-off point of 4 ng/mL. PSA levels above 4 ng/mL suggest that the patient needs further testing [19]. Patients with PSA levels between 4 ng/mL and 10 ng/mL have an approximately one in four chance of having prostate cancer. If the PSA is more than 10 ng/mL the possibility of having prostate cancer is over 50% [20]. PSA is prostate gland specific and not prostate cancer specific; therefore, prostate-specific antigen levels can indicate benign pathologies such as benign prostatic hyperplasia (BPH) and prostatitis and not prostate cancer, and men who do not have prostate cancer have also been reported to have elevated PSA levels. A prostate tissue biopsy is usually performed to confirm the presence of cancer [21].

A biopsy is a medical procedure in which a thin hollow needle is used to collect small tissue samples from the prostate gland to be observed under a microscope. The biopsy can be performed through the skin between the anus and scrotum or through the rectal wall (known as a transrectal biopsy) [22]. During a biopsy, the prostate gland is usually located with devices such as magnetic resonance imaging (MRI) and transrectal ultrasound (TRUS). An MRI scanner creates detailed images of body tissue using a strong magnetic field and radio waves [23]. MRI positive results can be used for specifically targeting abnormal areas of the prostate gland during a biopsy [24]. A multiparametric MRI can also be a triage test performed without a biopsy if the results were negative for DRE, PSA test, and MRI. A

TRUS is a small probe that is deposited into the rectum of a patient. The probe emits sound waves that go through the prostate gland and produce echoes. The probe then recognizes and reads the echoes, and a computer system turns them into a black and white image of the organ [25].

Biopsy analysis is one of the most reliable methods of prostate cancer diagnosis. Tissue samples of a biopsy are studied and analyzed in the laboratory using a microscope. The cells can also be analyzed to determine how quickly cancer will spread. The biopsy results are usually reported as follows:

1. Negative for prostate cancer, there were no cancer cells detected in the biopsy samples.
2. Positive for prostate cancer, there were cancer cells detected in the biopsy samples.
3. Suspicious, abnormal cells present, but may not be cancer cells [26].

However, artificial intelligence (AI) and machine learning algorithms have recently advanced, resulting in new classifications for prostate cancer. In recent years, the availability of novel molecular markers, as well as the introduction of advanced imaging techniques such as multiparametric magnetic resonance imaging (mpMRI) and prostate-specific membrane antigen positron emission tomography (PSMA-PET) scans have shifted the paradigm of prostate cancer screening, diagnosis, and treatment to a more individualized approach [27]. According to the most recent guidelines, any man at risk of prostate cancer should have an MRI of the prostate performed before obtaining a prostate biopsy [28]. This serves to minimize complications such as lower urinary tract symptoms, hematuria, and temporary erectile dysfunction. Furthermore, the number of biopsy cores obtained is linked to a higher risk of complications such as rectal bleeding, hematospermia, bleeding problems, and acute urine retention [29]. Therefore, radiomics can help with prostate volume selection and segmentation; prostate cancer (PCa) screening, detection, and classification; and risk stratification, treatment, and prognosis (Table 1).

Table 1. Benefits and drawbacks of radiogenomics as compared with actual prostate cancer peril stratification management [30].

Radiogenomics	Advantages	Limitations
	Could provide precise imaging indicators that are less expensive than genetic testing.	Lack of prospective studies
	AI and deep learning are used to produce computer-aided tools for clinical practice translation, employing large public databases containing genomes and imaging information.	Image acquisition for defining and contouring the regions of interests need expert radiologists
	Computer-designed software, both automatic and semiautomatic, is utilized to eliminate downsides (lack of standardization, imaging, and reporting protocols which differ significantly among institutions).	Significant time used for proper manual delineation
	Radiomics/radiogenomics biomarkers may be utilized to tailor treatment options and predict risk and outcomes.	Reading and segmenting regions of interest have a lot of inter-observer variability
	Biopsies are required to provide insight into the tumor genome, which is an intrusive technique that may increase patient morbidity. Tumor genetic changes can be predicted using radiogenomics.	Different acquisition techniques, scanners, and radiomic investigations, as well as a lack of repeatability and reproducibility due to a lack of standardization
	Whole-tumor data are available with a radiomics-based approach that can provide predictive and prognostic information.	Because of the differences in patient characteristics and imaging techniques, matching whole-genome sequencing data with imaging data is problematic

2.3. Prostate Cancer and Genetics

Genetic Inheritance

Close family lineage is the primary risk factor for prostate cancer. Men with close relatives diagnosed with prostate cancer are at a 50% risk of developing cancer as compared with men with no family history of prostate cancer [26]. First-degree relatives with successive generations of diagnosed prostate cancer usually have early onset prostate cancer [31]. Epidemiologic studies have shown the inheritance of prostate cancer susceptibility genes. Analyses of case-control, twin, and family studies have concluded that prostate cancer risk may be a result of heritable factors. Research has shown specific gene mutations in hereditary prostate cancer and has reported that patients with these mutations have an increased risk of the disease [4]. In the genetic evaluation of inheritance, scientists use multigene sequencing of men diagnosed with prostate cancer, as well as men at high risk of developing cancer. About 5.5% of these men had detectable mutations in DNA repair genes such as *ATM*, *BRCA1*, and *BRCA2* genes. African men have certain genetic mutations that predispose them to prostate cancer; therefore, race and environmental conditions such as migration and food diets are considered to be contributing factors [21].

Cancer occurs because of changes in the DNA sequence due to mutations such as point mutations, single nucleotide polymorphisms (SNPs), and somatic copy number alterations (SCNAs) [31]. Mutations can cause prostate cells to become cancerous by turning off tumor suppressor genes and turning on oncogenes [32]. This often leads to uncontrolled cell division. Mutations in genes can be passed on from generation to generation or be acquired by an individual. Acquired mutations usually occur during DNA replication in the nucleus [33]. The common genes used as biomarkers for prostate cancer are BRCA genes, HOX genes, the ATM gene, RNase L (HPC1, lq22), MSR1 (8p), and ELAC2/HPC2 (17p11). Table 2 shows most of the genes used as biomarkers for prostate cancer.

Table 2. Prostate cancer genes used as biomarkers for the disease.

Gene	Gene Description	Diagnostic/Prognostic or Predictive
BRCA genes	The comparative risk of prostate cancer at 65 years is 1.8–4.5-fold for *BRCA1* carriers and 2.5–8.6-fold for *BRCA2* gene carriers [31,34]. Mutations in BRCA genes inhibit DNA repair leading to prostate cancer [35].	Diagnostic Predictive [36]
RNASEL	Mutations in the ribonuclease L (*RNase L*) gene have been associated with prostate cancer [37]. The mutations found can inactivate the *RNase L* gene and make unsusceptible to prostate cancer [38]. RNase L is an endoribonuclease that plays a role in interferon action pathways protecting against viral infections [35,39].	Predictive [40]
HOXB13	*HOXB13* reduces prostate cancer growth and hormone-mediated androgen receptor activity [41,42]. The (rs339331) polymorphism increases *HOXB13* binding to a transcriptional enhancer, resulting in upregulation. Most *HOXB13* mutations correlate to the risk of aggressive and earlier-onset prostate cancer [43].	Predictive [44]
ATM gene	The ATM protein controls cell division and growth. It also leads to the development of certain body systems and helps cells recognize damaged DNA. Germline ATM mutations are linked to early metastasis and a lower prostate cancer survival rate [45,46].	Prognostic [47]

Table 2. *Cont.*

Gene	Gene Description	Diagnostic/Prognostic or Predictive
HPC2 or *ELAC2* gene	*HPC2* (hereditary prostate cancer gene 2) and *ELAC2* (elaC homolog 2) are a candidate genes for hereditary prostate cancer. As with *HPC1*, mutations associated with prostate cancer are missense mutations [48].	Predictive [40]
MSR1 gene	*MSR1* (macrophage scavenger receptor 1) at 8p22–23 of the hereditary prostate cancer (HPC) locus, and mutations linked to this gene have been associated with prostate cancer [49,50].	Predictive [40]
ANXA7	ANXA7 is a prostate cancer prognosis factor that shows a bimodal correlation to tumor progression [51,52]. Analyses of the ANX7 protein in prostate tumor microarrays have shown increased rates of reductions in ANX7 expression in recurrence and metastasis of hormone-refractory prostate cancer as compared with primary tumors [53].	Prognosis [51]
(*ATBF1*)-*A*	The AT-motif binding factor 1 (*ATBF1*)-*A* is a candidate for prostate cancer tumor suppression due to its function in cell inhibition and high mutation rate. A decrease in *ATBF1*-*A* mRNA levels is associated with a poor diagnosis. *ATBF1* inhibits cell proliferation; therefore, the loss of ATBF1 leads to uncontrolled cell growth [54,55].	Predictive [41]
CDKN1B	The CDKN1B's main function is cell cycle gatekeeping. Research indicates that the CDKN1B gene is a vital tumor suppressor gene in prostate cancer. There is a correlation between the location of the CDKN1B gene (12p13) and susceptibility to prostate cancer in different populations [56,57].	Prognostic [58]
(*KLF6*) gene	Kruppel-like factor 6 (*KLF6*) is a tumor suppressor gene and a zinc finger transcription factor. In a study by Narla et al., 2008, an allele in the *KLF6* gene was deleted in 77% of prostate tumors, and the normal KLF6 gene upregulated p21 (WAF1/CIP1) and decreased cell proliferation. The KLF6-SV1 mutation overexpression elevated metastasis [59,60].	Predictive [60]
MYC gene	MYC proto-oncogene, BHLH transcription factor encodes transcription factors, promoting tumorigenesis in prostate cancer. Studies show that prostate cancer tumor foci show overexpression of MYC and protein, which is associated with the severity of the cancer. TMPRSS2-ERG gene fusion caused by a mutation of the MYC is linked to the aggressiveness of prostate cancer and seen in 60% patients [61–63].	Predictive [63]
NK3 21	NK3 homeobox 1 (Nkx3.1) gene expression is usually lost during the process of prostate cancer initiation and growth in humans and mouse models. It was found that the loss of Nkx3.1 expression intercedes at the transcriptional stage via the 11 kb region [64,65].	Diagnostic [64]
PON1	Paraoxonase 1 (PON1) is a protein coding gene. The gene reduces oxidative stress, which leads to cancer development [66]. A study by Stevens et al., 2008, investigated the relationship between SNPs (Q192R and L55M) and prostate cancer. The results showed that the presence of a variant allele found in the Q192R and L55M SNPs was linked to an increased risk of aggressive prostate cancer [67].	Prognostic [66]

Table 2. *Cont.*

Gene	Gene Description	Diagnostic/Prognostic or Predictive
PTEN	Loss of phosphatase and tensin homolog *PTEN* is common in androgen-independent prostate cancer [68,69]. The loss of function in the *PTEN* gene is linked to irregular cellular proliferation. Studies have shown that mutations in the *PTEN* gene play a role in prostate carcinogenesis [70]. The *PTEN* gene is mutated in the prostate cell lines LNCaP, PC3, and DU145, and prostate cancer xenografts [71].	Prognostic [70]
mtDNA	Mitochondrial DNA has 16,569 bases that encode 37 genes. Mutations found in mitochondrial DNA genes have been found to cause prostate cancer [72]. In a study on mtDNA genes, approximately 12% of patients had mutations in cytochrome oxidase subunit I (COI) [73].	Prognostic [73]
RAS	Rat sarcoma virus (RAS) is part of a family of genes consisting of the N-RAS H-RAS and K-RAS, which are important in cell signaling. Point mutations that happen at codons 12, 13, or 61 of the family genes allow the protooncogene to be translated to a RAS oncogene [74].	Diagnostic [75]

Biomarkers show the advantages of being used for diagnostic procedures, staging, assessing the aggressiveness of the disease, and evaluating the therapeutic process. Multiple advances have been achieved through profiling technologies, including novel biomarkers that guide diagnosis and precision medicine. Modern biological markers, such as the prostate health index (PHI), the TMPRSS2-ERG fusion gene, 4K tests, and PCA3, have proven to increase PSA specificity and sensitivity, resulting in patients avoiding biopsies and reducing over diagnosis [76]. Table 3 below shows different diagnostic biomarkers and their different tests and categories.

Table 3. Examples of other diagnostic biomarkers classified as serum-based, urine-based, and tissue-based biomarkers used for prostate cancer [77].

Biomarker	Test	Category
Prostate-specific antigen	A PSA count >4 ng/mL has a specificity of 94%, but only 20% sensitivity in PCa detection; only 1 in 4 men with elevated PSA will be diagnosed with PCa.	Serum-based biomarker Standard prostate cancer screening method
4K score kallikrein markers	The 4K test includes a PCa diagnostic algorithm that includes four kallikreins in blood plasma. The analysis includes a 4K panel = total PSA (tPSA), free PSA (fPSA), intact PSA, and human kallikrein 2 (hK2).	Serum-based biomarker Detection of high-grade PCa in previously unscreened men with elevated PSA
Prostate health index (PHI)	PHI result = (−2) (proPSA/fPSA) x $\sqrt{}$ tPSA). First, the PHI test was developed to predict the probability of PCa. The use of the PHI with a cut-off ≥25 could avoid 40% of biopsies.	Serum-based biomarker Detection of any PCa PHI test also makes it possible to examine the possibility of PCa progression during active surveillance
SelectMDx HOXC6, KLK3, DLX1 mRNA, and PSAd	SelectMDx test analyzes urine samples obtained after strokes of prostate during DRE. The presence of the HOXC6 and DLX1 genes is assessed to assess the risk of any PCa during biopsy, and the risk of high-grade PCa.	Urine-based biomarker mpMRI outcomes indicate that SelectMDx score is a promising tool in PCa detection

Table 3. *Cont.*

Biomarker	Test	Category
TMPRSS2-ERG Fusion	TMPRSS2-ERG levels are linked to castration-resistant PCa. Fusion trans-membrane serine protease 2 (TMPRSS2) and ERG gene can be detected in 50% of PCa patients.	Urine-based TMPRSS2-ERG low sensitivity
PCA3 Progensa Prostate Cancer Antigen 3	Prostate cancer gene 3 (PCA3 or DD3) is a specific non-coding mRNA which is overexpressed in more than 95% of primary prostate tumors.	Urine-based biomarker PCA3 score over PSA, in terms of predictive value and specificity, has lower sensitivity
ConfirmMDx Hypermethylation of GSTP1, APC and RASSF1 genes, PSA	Screening patients at risk of HG PCa after an initial negative biopsy. It is clinically validated for detection of PCa in tissue from PCa-negative biopsies.	Tissue-based biomarker Tissue from prostate biopsy

Figure 1 depicts the developmental stages of prostate cancer [78].

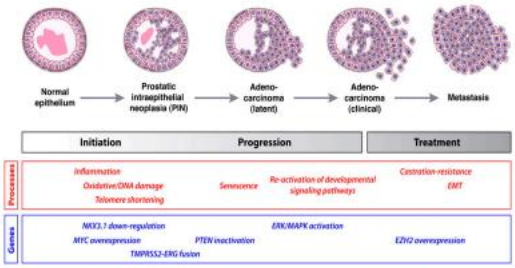

Figure 1. A schematic depicting the development of prostate cancer. The stages of the cancer onset and progression are indicated by the molecular processes, genes, and signaling pathways which are important in different stages of cancer. The first sign of prostate cancer is an inflammation of the prostate gland as a result of uncontrollable cell division. This uncontrollable cell division is caused by mutations that arise due to damaged DNA. At a chromosomal level, the initiation of prostate cancer begins with the shortening of telomerase at the end of the chromosome. Oxidative stress from prostate gland inflammation can shorten prostatic telomeres [78]. Research on the *Nkx3.1* homeobox gene has shown the impact of the gene on the prostate cancer initiation phase in mice. No tumor suppressor gene has been solely given a role in prostate cancer initiation or progression. However, several genes such as *MYC*, *PTEN*, *NKX3.1*., and TMPRSS2-ERG gene fusions are implicated in prostate cancer initiation. TMPRSS2-ERG gene fusions are responsible for the main molecular subtype of prostate cancer. The gene fusion activates the ERG oncogenic pathway, which contributes to the development of the disease. Metastasis of prostate cancer is conserved by the reactivation of pathways involved in cell division, which results in uncontrolled cell division and cell proliferation, leading to metastasis of the cancer [79]. Gene expression profiling results have indicated an overexpression in EZH2 mRNA and proteins present in metastatic prostate cancer. Due to the functions of EZH2 involving apoptosis and proliferation, EZH2 is a novel target for prostate cancer [80].

2.4. Precision Medicine for Prostate Cancer

Precision medicine is an emerging field that represents an alternative method, for some men with advanced cancer, to find gene-specific treatment for prostate cancer. It uses genetics as well as environmental biomarkers to determine diagnoses, prognosis therapeutic options for patients, and accurate dosing. Precision medicine classifies diseases using genome sequencing to identify patients who have tumors exhibiting actionable targets and promoting more informed and accurate treatment decisions [81]. Mutations in prostate cancer-related genes *BRCA1* and *BRCA2* render men with mCRPC suitable for treatment with either rucaparib or olaparib, and other prostate cancer genes that have responded well to olaparib treatment, which include *ATM*, *CDK12*, *CHECK2*, *CHECK1*, *PALB2*, *PP2R2A*, and *RAD54L* [82]. The influence of BRCA mutations on therapeutic outcomes in a study of 1302 patients with 67 BRCA mutation carriers was investigated. The results showed that patients who received prostatectomy or radiotherapy developed metastasis and had shorter survival as compared with patients who did not have mutations of the BRCA gene. This study also found that the BRCA1 gene was 12% more common than the BRCA2 gene, which was only 2% common. In a recent study, conducted in 2019, the mutation in the BRCA gene (c.4211C > G) was identified in a Chinese patient treated with radiotherapy and ADT for prostate cancer. The study indicated that prostate cancer patients with this specific mutation were sensitive to ADT as well as radiotherapy, making the treatment more effective [83]. Mutations that make it difficult to treat or design effective CRPC include the *F876L* mutation, which changes the binding ligand pocket in the AR. Similarly, the W741L/C mutation stimulates specific AR binding that is able to move AR into its active conformation. Such mutations create obstacles to designing effective treatment for CRPC [84].

2.5. Treatment and Management of Prostate Cancer

The prognostic factors consisting of initial PSA level, clinical TNM stage, and Gleason's score have been considered together with other factors such as baseline urinary function, comorbidities, and age as a choice of treatment for prostate cancer [85]. Advances in prostate cancer diagnosis and treatment have enhanced clinicians' capacities to classify patients by risk and propose therapy based on cancer prognosis and patient preference [86]. Surveillance, prostatectomy, and radiotherapy are recognized as the standard treatments for stage I–III prostate cancer patients. Androgen ablation by surgical or pharmacological castration can bring about lasting remission in all stage IV and high-risk stage III patients. In this case, first-generation antiandrogens such as flutamide and bicalutamide can aid. However, in stage IV, castration resistance, which is characterized by genomic mutations in the androgen receptor, invariably occurs, and the prognosis is poor [87]. Table 4 below summarizes prostate cancer treatment options and their adverse effects.

Table 4. Common prostate cancer treatment options and potential adverse effects [88].

Treatment Option	Disease Progression	Potential Adverse Effects
Active surveillance	Localized	Illness uncertainty
Radical prostatectomy	Localized	Erectile dysfunction Urinary incontinence
External beam radiation	Localized and advanced disease	Urinary urgency and frequency, dysuria, diarrhea, and proctitis Erectile dysfunction Urinary incontinence
Brachytherapy	Localized	Urinary urgency and frequency, dysuria, diarrhea, and proctitis Erectile dysfunction Urinary incontinence

Table 4. *Cont.*

Treatment Option	Disease Progression	Potential Adverse Effects
Cryotherapy	Localized	Erectile dysfunction Urinary incontinence and retention Rectal pain and fistula
Hormone therapy	Advanced	Fatigue Hot flashes and flare effect Hyperlipidemia Insulin resistance Cardiovascular disease Anemia Osteoporosis Erectile dysfunction Cognitive deficits
Chemotherapy	Advanced	Myelosuppression Hypersensitivity reaction Gastrointestinal upset Peripheral neuropathy

2.5.1. Active Surveillance

Active surveillance is a structured program that employs monitoring and expected intervention as the main techniques in the management of prostate cancer [89]. For patients who have low-risk cancers or those who have a short life expectancy, active surveillance has been recognized as the best option. The criteria for active surveillance have recommendations that are usually based on the following factors: disease characteristics, health conditions, life expectancy, side effects, and patient preference [90]. The PSA level, clinical progression, or histologic progression are used as prostate cancer trigger points [91].

The advantages of active surveillance are the preservation of erectile function, decreased costs of treatment, avoidance of needless treatment of inactive cancers, and sustaining life quality and normal activities. Its disadvantages include the likelihood of cancer metastasis before treatment, missed opportunity for a remedy, need for a complex therapy with side effects for larger and aggressive cancers, reduced chances of potency preservation mostly after surgery, chances of increased anxiety by patients, and frequent medical checks [92].

2.5.2. Radical Prostatectomy

Radical prostatectomy is the procedure of medically removing the prostate gland by open and/or laparoscopic surgery [93]. The procedure requires making small incisions on the abdomen or via the perineum.

Salvage radical prostatectomy is usually recommended to patients with local recurrence in the absence of metastases after undergoing external beam radiation therapy, brachytherapy, or cryotherapy. This may, however, lead to increased morbidity. Patients younger than age 70 with organ-confined prostate cancer, with a life expectancy higher than 10 years who have little to no comorbidities, are best suited for radical prostatectomy. However, there are a few complications associated with its use. These complications include incontinence and erectile dysfunction arising from surgical damage to the urinary sphincter and erectile nerves [94].

2.5.3. Cryotherapy

This method involves the use of surgical insertion of cryoprobes into the prostate under ultrasound guidance. It involves freezing of the prostate gland to a temperature from −100 °C to −200 °C for about 10 min. However, there are reports of complications associated with the use of this method, including urinary incontinence and urinary retention, erectile dysfunction, fistula, and rectal pain [95].

2.5.4. Radiation

Radiation therapy is regarded as one of the most effective therapies that kills prostate cancer cells using high radiations. Radiations are sent to cancerous cells through various techniques such as brachytherapy (the use of seeds placed in the body) and external beam (where the energy is projected through the skin) to the cancerous sites. Radiation therapy aims at specifically transferring high-energy rays or particle doses directly to the prostate without affecting the normal tissues. These doses are based on the level of prostate cancer. This treatment is considered to be an acceptable therapy for patients who are not suited for surgical procedures [96]. Various techniques of radiation therapy are discussed below.

Brachytherapy

Brachytherapy includes the direct placement of radioactive sources into the prostate gland with the aid of seeds, injections, or wires under the guidance of transrectal ultrasound. This often involves two techniques: low dose and high dose rates. The low dose rate refers to the permanent implantation of seeds in the prostate tissue, which loses radioactivity gradually [97], and the latter refers to the supply of a dose of radiation to the prostate tissues with significant risk of leakage to other surrounding organs. The advantage associated with brachytherapy is that it can be completed within a day or less. There is a minimal risk of incontinence in patients without a previous transurethral resection of the prostate (TURP). Erectile function is also not affected. Its disadvantages are usually a requirement for general anesthesia, acute urinary retention risks, and persistent irritative voiding symptoms [98].

External Beam Radiation Therapy

External beam radiation therapy (EBRT) is a commonly used treatment technique that involves emitting strong X-ray beams specifically targeting the prostate tissues. It radiates higher prostate radiation doses, with less emission to the surrounding tissues. Radiation therapy is considered to be an effective intermediate-risk and high-risk prostate cancer treatment when used together with androgen deprivation therapy (ADT) [80]. It is a suitable therapy for attenuating metastasizing cancer cells. This technique is more advantageous than surgical therapy. It can treat early stages of cancer, and it is associated with fewer risks such as bleeding, myocardial infarction, pulmonary embolus, urinary incontinence, and erectile dysfunction. It can also relieve symptoms such as bone and joint pain [93]. Side effects of radiation include urinary urgency and frequency, erectile dysfunction, dysuria, diarrhea, and proctitis [97].

2.5.5. Radium-223 Therapy

The radium-223 dichloride (Xofigo) technique makes use of a substance used for therapy in patients with metastatic prostate cancer that is resistant to hormone therapy. Its ability to mimic calcium makes radium-223 dichloride be selectively absorbed by the cancer cells in bone tissue. This technique has been reported to have a considerable impact on the survival and recovery of metastatic prostate cancer patients, leading to delayed onset of bone fracture and pain [85].

2.5.6. Hormonal Therapy

Hormonal therapy is also known as androgen deprivation therapy (ADT). This technique is applied in the treatment of advanced and/or metastasized prostate cancer. Its therapeutic mechanism is based on the blockage of testosterone production and other male hormones, preventing them from fueling prostate cancer cells. Therefore, significantly decreased male hormonal levels are responsible for inhibition of the action of androgen on the androgen receptor [99]. This is often achieved using bilateral orchiectomy or medical castration via administration of luteinizing hormone-releasing hormone (LHRH) analogs or antagonists. LHRH analog primarily elevates the luteinizing hormone (LH) and follicle-stimulating hormone (FSH) by stimulating hypophysis receptors, thus, enabling the drug to downregulate the hypophysis receptors with concomitant reduction of LH and FSH levels,

leading to suppressed testosterone production. Leuprolide, goserelin, triptorelin, and histrelin are among the common LHRH agonists. The antagonists cause action by blocking the hypophysis receptors, thereby triggering the immediate inhibition of testosterone synthesis [100]. ADT has, however, been associated with acute and long-term side effects, such as hyperlipidemia, fatigue, hot flashes, flare effect, osteoporosis, insulin resistance, cardiovascular disease, anemia, and sexual dysfunction [101].

Flutamide is a type of drugnthat is nonsteroidal and pure antiandrogenic lacking hormonal agonist activity. Flutamide is antiandrogen at the androgen-dependent accessory genitals. Its biological activity is based on 2-hydroxyflutamide. Treating prostate cancer with flutamide and an (LHRH) agonist has produced promising results. In vivo studies of flutamide have shown certain antagonist at the ventral prostate and androgen-dependent seminal vesicles [102,103]. Flutamide is known to result in hepatic dysfunction; however, a study on antiandrogen therapy (AAT) in combination with flutamide indicated that flutamide could be successful when performing regular hepatic function testing during treatment periods [104]. Maximum androgen blockade (MAB) using flutamide as a second-line hormonal therapy can give a prostate-specific antigen response without side effects, making this a possible treatment option for patients with HRPC with no bone metastases or whose cancer has progressed more than a year following first-line therapy [105].

Chlormadinone acetate (CMA) is an oral steroidal antiandrogen. Chlormadinone has proven to have anticancer activity. Similar to progesterone used in maximum androgen blockade (MAB) therapy as well as monotherapy for prostate cancer in Japan [106]. To determine the success of the antiandrogen chlormadinone acetate in treating stage A prostate cancer, a study of 111 patients who received chlormadinone acetate was conducted. The progression rates linked to antiandrogen therapy for stage A1 and A2 patients were lesser in non-treatment receiving groups, concluding that antiandrogen treatment with chlormadinone acetate inhibited the progression [107]. Chlormadinone is also used to treat benign prostatic hyperplasia, it decreases testosterone level, prostate-specific antigen (PSA) level, and prostate volume, in benign prostatic hyperplasia slowing the progression of Prostate cancer [108].

2.5.7. Abiraterone

Abiraterone is a second-generation therapy targeted at adrenal and tumor androgen production. It is associated with the irreversible inhibition of the hydroxylase and lyase activities of CYP17A, AR pathways, and 3β-hydroxysteroid dehydrogenase activity, and is used to treat prostate cancer that has metastasized to other parts of the body [109]. Abiraterone has also been proven to be a potent inhibitor of other microsomal drug-metabolizing enzymes, including CYP1A2 and CYP2D6 [109]. Clinical data of abiraterone have indicated remarkable results, but there are reports of variable responses and concomitant increasing PSA levels. Abiraterone is correlated with high CYP17A upstream mineralocorticoids, with concomitant side effects including edema, hypertension, fatigue, and hypokalemia [110].

Immunotherapy or biological therapy is based on stimulating or suppressing the immune system. The treatment uses vaccines designed to work with the patient's immune system to fight cancer cells. Sipuleucel-T (Provenge) is one of such vaccines, designed for advanced and metastatic prostate cancer cells that have developed resistance to hormone therapy. It is developed from the immune cells by collecting the white blood cells and activating them with prostatic acid phosphatase [109]. This is then associated with a protein that can trigger the immune system before infusing into the blood [99]. Sipuleucel-T (Provenge, Dendreon) is an autologous dendritic cell-based immunotherapy used in treating asymptomatic patients by assisting a patient's immune system in fighting back cancer cells. It is intravenously administered in three doses over one month. Its lesser side effects make it more favorable compared to other chemotherapies. Its side effects include fever, nausea, chills, and muscle aches [111].

2.5.8. Chemotherapy

Chemotherapy uses anticancer drugs to kill or inhibit the growth of cancerous cells. There has been progress in treatment of prostate cancer after decades of learning and understanding genetics, diagnosis, and treatment. The most common chemotherapy drug for prostate cancer is docetaxel (Taxotere) [112].

Docetaxel

Docetaxel is regarded as the first-line standard therapy for prostate cancer cells that are castration-resistant. It is an antimicrotubule agent which attaches to β-tubulin to inhibit microtubule depolymerization, thereby suppressing mitotic cell division and initiating apoptosis [113]. CYP3A is a major requirement for the activation of Docetaxel. The development of Docetaxel resistance has been associated with relapse. Docetaxel resistance has been attributed to increased upregulation of the multidrug resistance (MDR) 1 gene that encodes P-glycoprotein [114].

Cabazitaxel

Cabazitaxel is a novel antineoplastic semi-synthetic derived from the needles of various species of yew trees (Taxus). It is usually sold under the name Jevtana. Cabazitaxel is a second-generation therapy aimed at suppressing docetaxel resistance [99]. It has a low affinity for Pglycoprotein owing to its additional methyl groups. It is metabolized in the hepatic tissues by CYP3A4/5 and CYP2C8 (10–20%). Hypotension, bronchospasm, renal failure, neurotoxicity fatigue, alopecia, and generalized rash/erythema are among the common side effects associated with its use. There have also been reports of diarrheal deaths related to Cabazitaxel therapy resulting in electrolyte imbalances and dehydration [114].

Enzalutamide

Enzalutamide is a second-generation AR inhibitor that was recognized as one of the chemotherapeutic drugs for prostate cancer in 2012. This drug focuses on the androgen pathway and has functions such as (1) competitively inhibiting the binding of androgen to the androgen receptor, (2) inhibiting nuclear translocation and recruitment of cofactors, and (3) inhibiting the association of the activated androgen receptor. Enzalutamide targets androgens such as testosterone and dihydrotestosterone. Its therapeutic mechanism includes:

1. Competitive inhibition of androgen binding to the androgen receptor;
2. Inhibition of nuclear translocation and co-factor recruitment;
3. Inhibition of the binding of DNA with activated androgen receptor.

The side effects of enzalutamide include fatigue, asthenia, diarrhea, and vomiting [115].

2.6. Combination Therapy

Combination therapy has been demonstrated as an effective strategy for prostate cancer treatment. Combination therapy is a strategy that was developed to treat castration-resistant prostate cancer and other forms of prostate cancer. There are no drugs to date that treat castration-resistant prostate cancer (CRPC), and currently approved treatment options either used alone or in combination therapy are useful in extending a patient's lifespan by a few months [116]. Current treatment options used for the treatment of prostate cancer are not curative, and disease progresses to the castration-resistant phenotype over a period of time. Combination therapy with currently used treatment options for prostate cancer could successfully increase a patient's lifespan and suppress tumors. Amongst all the available treatment strategies available for metastatic prostate cancer, androgen deprivation therapy (ADT) has more potential combination treatment compared to other therapeutic strategies for prostate cancer, and approved and currently ongoing clinical trials with ADT treatment include ADT with radiation therapy, which often treats high-risk patients to delay or prevent the disease from progressing to CRPC; (ii) ADT and chemotherapy, which in several clinical studies has shown to increase patient survival but results in adverse side effects and sometimes death; and (iii) immunotherapy and

ADT, which has been reported to increase patient survival by 8.5 months [117]. Clinical trials are ongoing to analyze the effects of survival in ADT and the PSA-targeted poxviral vaccine, PROSTVAC-IF; a combination of radiation therapy with immunotherapy under ADT; a combination of chemotherapy with immunotherapy under ADT; and a combination of docetaxel under ADT [118]. There are a number of completed and ongoing clinical studies/trials for combination therapy of prostate cancer. Some of the clinical trials are listed in Tables 5 and 6.

Table 5. Combination therapies for prostate cancer—completed clinical trials [116].

Primary Anticancer Agent	Secondary Anticancer Agent	Clinical Trial
Sipuleucel-T	Docetaxel	
ADT	Radiation	
Docetaxel	Thalidomide and Bevacizumab	ISRCTN01534787
ADT	Radiation	NCT00091364
Docetaxel	Bevacizumab	NCT00002633/ISRCTN24991896
ADT	Docetaxel	
Ipilimumab	Radiation	NCT00110214
ADT	Docetaxel	GETUG-AFU 15 (NCT00104715)
ADT	Docetaxel	NCT00861614
ADT	Radiation	CHAARTED (NCT00309985)
Abiraterone	Olaparib	STAMPEDE (NCT00268476)
Abiraterone	Radium 223	NCT00002874
Abiraterone	Enzalutamide	NCT01972217
		ERA 223 (NCT02043678)

Table 6. Combination therapies for prostate cancer—ongoing clinical trials [116].

Primary Anticancer Agent	Secondary Anticancer Agent	Clinical Trial	Phase and Current Status
Abiraterone	Apalutamide	LACOG-0415 (NCT02867020)	Phase 2, recruiting
Abiraterone	ADT	LATITUDE	Phase 3, active and not recruiting
Abiraterone	Olaparib	NCT03732820	Phase 3, recruiting
ADT	PROSTVAC	NCT00450463	Phase 2, no compiled results but completed
Apalutamide	Docetaxel, Abiraterone	NCT02913196	Phase 1, recruiting
Cabazitaxel	ADT, radiation	NCT01420250	Phase 1, active and not recruiting
Docetaxel	PROSTVAC-IF	NCT02649855	Phase 2, active and not recruiting
Olaparib	Durvalumab	NCT03810105	Phase 2, recruiting
			Phase 2, recruiting

2.7. *Drug Repurposing*

Drug repurposing, also known as drug repositioning, reprofiling, or retasking, is a way of identifying new uses for approved drugs [119]. The advantage of drug repurposing over de novo drug development (developing new drugs) is that repurposed drug candidates have undergone extensive research in animal models and clinical trials, testing the

safety, optimization, and, in most cases, formulation development of the drug, as well as pharmacokinetic and pharmacodynamic properties. This advantage usually speeds up the research and development for new use of the drug and reduces the failure rate in later efficacy testing clinical trials [120]. These previously tested drugs can rapidly progress into phase II and phase III human clinical studies, which implies that the associated drug development cost could be drastically deceased. Researchers show great interest in this phenomenon because drug repurposing alleviates the dilemma of some challenges currently faced in clinical research for finding new cancer therapies, such as drug shortage. It can take a period of 10–17 years for a development of a new drug compared to 3–12 years for repurposed drugs. Technology advances play a major role in scanning large databases and detecting key molecular similarities in different diseases to identify drugs that can be repurposed. Androgen deprivation therapy (ADT) is used to treat advanced-stage prostate cancer patients. Metformin is a drug commonly used to treat type II diabetes, repurposed to treat prostate cancer. It can be utilized to sensitize prostate cancer to the currently used standard prostate cancer therapies and improve the efficacy of treatment. It is reported that Metformin is able to increase the effectiveness of ADT for the treatment of prostate cancer [121]. Here, we discuss three main categories of drug repurposing studies for PCa, classified by different discovery and validation categories, such as the knowledge and ability of the drug to be researched. For example, ormeloxifene, a selective estrogen receptor modulator, is known for its anticancer properties in several cancers such as breast and ovarian cancers, but ormeloxifene is reported to have mediated the inhibition of oncogenic β-catenin signaling and EMT progression in prostate cancer by significantly suppressing β-catenin/TCF-4 transcriptional activity, N-cadherin, MMPs, and triggering pGSK3β expression. The other category is drugs that have been tested in assays and classified in accordance with their activity. For example, Itraconazole, an antifungal drug responsible for preventing angiogenesis and the initiation of the Hedgehog signaling pathway, was experimented in phase II clinical trials and established to be effective in patients with metastatic CRPC [122]. Table 7 shows different drugs repositioning candidates in prostate cancer clinical trial studies.

Other anticancer drugs that are currently being researched in vitro and in vivo for treatment of prostate cancer include naftopidil, an alpha blocker; niclosamide, an anthelminthic agent; ormeloxifene, an estrogen receptor modulator; nelfinavir, an antiretroviral agent; glipizide, an antidiabetic agent; clofoctol, an antibacterial agent; and triclosan, an antibacterial agent [32]. Drug repurposing for prostate cancer presents an opportunity to address current treatment challenges. This strategy should be implemented using computational genomic and proteomic tools to assist and guide researchers in their decision making regarding patient treatment [122].

2.8. Treatment Challenges

Despite the various treatment options, mCRPC remains to be an incurable disease. Over time, the disease continues to develop resistance to different conventional treatment options [123]. This has led to continuous research on understanding the growth, metastasis, tumorigenesis, tumor microenvironment, and tumor environmental interactions that promote disease progression.

Table 7. Anticancer drug repositioning candidates under clinical investigation for the treatment of prostate cancer [32].

Drugs	Original Use	Proposed Anticancer Mechanisms	Phase	Identifier *	Recruitment Status
Zoledronic Acid	Bisphosphonate	Inhibition of mevalonate pathway Activity of metalloproteinases	Clinical trial Phase 4	NCT00219271	Completed
Dexamethasone	Anti-inflammatory agent	Modulator of ERG activity	Clinical trial Phase 3	NCT00316927	Completed
Aspirin	Anti-inflammatory agent	COX inhibitor suppression of the neoplastic prostaglandins Inhibition of NF-κB	Clinical trial Phase 3	NCT00316927	Completed
Minocycline	Antibacterial agent	Inhibition of proinflammatory cytokines Inhibition of matrix metalloproteinases	Clinical trial Phase 3	NCT02928692	Recruiting
Celecoxib	Anti-inflammatory agent	Selective Cox-2 inhibitor Inhibition of NF-κB activity Inhibition of PDPK1/Akt signaling pathway	Clinical trial Phase 2/3	NCT00136487	Completed
Leflunomide	Immunomodulatory agent	Potent inhibitor of tyrosine kinases	Clinical trial Phase 2/3	NCT00004071	Completed
Statins	HMG-CoA reductase inhibitors	Inhibition of mevalonate pathway	Clinical trial Phase 2	NCT01992042	Completed

2.8.1. Drug Resistance

Castration resistance has been reported in prostate cancer that has reached advanced stages. Castration resistance allows for androgen signaling via amplification of the androgen receptor's synthesis of the intra-tumoral hormone, while disrupting the androgen receptor's coexpressors and coactivators [124]. Resistance to enzalutamide and abiraterone acetate, as well as gene mutation in metastatic prostate cancer, has been attributed to the overexpression of the active androgen receptor (AR) in patients. Prostate cancer often develops owing to androgens; thus, most treatments are targeted at blocking androgen hormones. This is beneficial to anticancer drug-resistant patients.

Mutations have also been shown to contribute to drug resistance in cancer cells, allowing for bypassing of the targeted pathways. Alterations in intrinsic pathways such as the AR signaling pathways, MAPK/ERK pathway, endothelin A receptor (EAR), and Akt/PI3K pathways as well as exacerbated expression of the androgen receptor have been shown to contribute to ADT resistance [46].

2.8.2. ABC Transporters

These transporters are expressed in the plasma membrane, where they serve as efflux pumps and are well-known triggers of multidrug resistance. They transport drugs and xenobiotics in and out of the cells [125]. Multidrug resistance protein (MRP) transporters MRP2, MRP3, MRP4, and MDR-1 protein (P-glycoprotein) have been reported in prostate cancer [110]. The exacerbated expression of these transporters has been implicated in the increased efflux of drugs, thereby leading to multidrug resistance. Of these transporters, MRP2 has been reported to exhibit the highest potency of resistance to natural product agents, MRP3 exhibits the lowest resistance to etoposide, and MRP4 and MRP5 are responsible for resistance to nucleoside analogs and transport cyclic nucleotides. MRP4 also influences resistance to chemotherapeutic agents such as camptothecins, cyclophosphamide, topotecan, methotrexate, and nucleoside analogs [126].

2.8.3. Cytochrome P450

Cytochromes P450 are a well-known multigene superfamily of heme-containing monooxygenases that are both constitutive and inducible. They catalyze the metabolism of a variety of xenobiotics and endocrine disruptors [127]. The family including CYP2C19, CYP4B1, CYP3A5, CYP2D6, CYP1A2, and CYP1B1, has been reported in human prostate

cells [128]. CYP4B1's main functions are the metabolism and activation of arylamines via N-hydroxylation, an activity that results in bladder tumor [129]. Exacerbated expression of CYP1B1 has been implicated in the advances of drug resistance in prostate cancers. This is often achieved by 2-hydroxylation of flutamide [130]. CYP17A speeds up the process of sequential hydroxylase and the lyase steps in the androgen biosynthetic pathway in humans, thus, making it a critical therapeutic marker for prostate cancer treatment [131].

2.8.4. Mutations in Androgen Receptors

Mutations in androgen receptors occur owing to a disorder in androgen sensitivity. Androgen receptor (AR) signaling plays an important role in the development, activity, and homeostasis of the prostate gland. It regulates the process of gene transcription via attaching to the androgen response elements on specific genes, as well as allowing nuclear translocation of the androgen receptor [132]. Gene changes in the AR signaling pathway (Figure 2) have been reported in prostate cancers. AR mutations were first reported in an androgen-responsive cell line, LNCap. These mutations have been implicated in the development of AR resistance arising from AR-targeted therapy [133]. This has led to the use of androgen deprivation therapy (ADT) and antihormone therapy in the treatment of advanced prostate cancer. The majority of AR mutations result in single amino acid substitutions, which are mostly found in the AR androgen-binding domain. The mutation T877A, which has been found in roughly 30% of metastatic CRPC patients, is the most common [134]. Other mutations have resulted in enhanced AR binding to coregulators, resulting in higher AR transcriptional activity vis-à-vis H874Y and W435L mutations. These mutations have been implicated in the development of AR resistance arising from AR-targeted therapy [124]. Figure 3 illustrates the transcription activity of the androgen receptor gene [135].

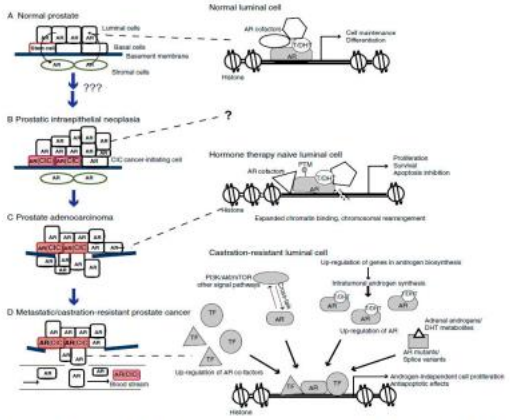

Figure 2. The function of AR signaling in prostate cancer and development: (**A**) Prostate homeostasis is maintained in a healthy prostate via reciprocal signaling between the stromal and epithelial layers;

(**B**) normal prostate cells are converted into cancer initiating cells by unknown mechanisms, histological evidence of prostatic intraepithelial neoplasia and early cancer lesions appears, cells at the basal layer express higher levels of AR in response to this event; (**C**) cellular and molecular alterations occur in prostate adenocarcinoma, resulting in luminal cells with the AR transcriptional pathway; (**D**) Prostate cancer cells in CRPC maintain AR activity through other mechanisms (including upregulation of AR and its splice variants, intra-tumoral androgen synthesis, cross communicate with other signal pathways, and increased/altered expression of AR cofactors) as the availability of androgen from the blood steam becomes limited [134].

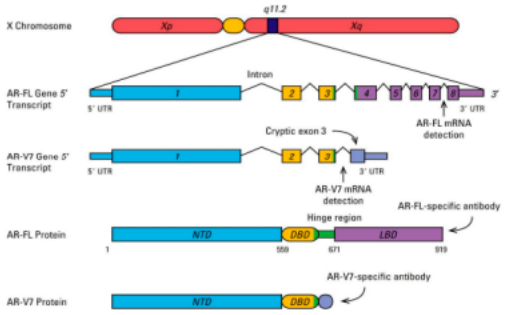

Figure 3. The androgen receptor gene encodes a 110 kD protein composed of 919 amino acids that are classified by an androgen-binding domain (ABD), a conserved DNA-binding domain (DBD), and an N-terminal transactivation domain, which has two polymorphic trinucleotide repeat segments. These repeated segments, consisting of variable numbers of polyglycine repeats and polyglutamine, highly influence the androgen receptor transcription activity. The gene transcript consists of eight exons in total: exon 1 codes for the N-terminal domain, exons 2–3 code for the DBD, and exons 4–8 code for the ABD [135].

2.8.5. Tumor Microenvironment

The tumor microenvironment has a crucial role in the development and progression of prostate cancer to the advanced stage, as per recent studies. According to experimental research, the milieu and malignant tumor cells have a mutually reinforcing relationship in which early changes in the microenvironment of normal tissue can foster carcinogenesis and tumor cells can foster more protumor modifications in the microenvironment [136]. A tumor microenvironment comprises a wide interlinked niche encompassing the extracellular matrix and specialized cells such as neural cells, blood vessels, immune cells, and mesenchymal/stromal stem cells, all of which secrete factors such as chemokines, cytokines, and matrix-degrading enzymes. They interact with cancer cells through paracrine and autocrine mechanisms [137,138].

According to a tumor stage-specific histological investigation, high-grade PC is linked to enhanced stromal immune cell infiltrates with a variety of cellular types [139]. Chronic stresses such as direct infection, urine reflux, a high-fat diet, and estrogens affect the prostate's ability to become inflamed on a long-term basis [140]. The stromal compartment experiences an inflow of several immune cells, including CD3+ T-cells, macrophages, and mast cells, amid ongoing inflammation [141]. High levels of cytokines and chemokines, primary tumor necrosis factor, nuclear factor kappa B, to mention a few, are produced by inflammatory cells. The regulation of angiogenesis, cellular proliferation, and inflamma-

tion involves these proteins among others. They control the PC's shift to the malignant phenotype [136].

The surrounding stromal agents go through complex modifications as a result of the interaction between prostatic epithelial cells and the tumor microenvironment, and these changes control the severity of the disease, its capacity to spread, and its susceptibility to traditional treatments [142,143].

2.9. Role of Estrogen Receptors (ERs) in Prostate Cancer Etiology and Progression

Prostate cancer is often regarded as hormone dependent, since steroid hormones direct its initiation and progression. Earlier reports have emphasized the significance of steroid levels in the etiology of PCa [144,145]. Estrogen plays an indispensable role in the secretion of male sex hormones, and it also plays cardinal roles in the growth, differentiation, and homeostasis of prostate tissues. Estrogens also contribute to the development of prostate cancer [146]. In a report from Ellem and Risbridger using aromatase knockout (KO) mice, the knockout mice could not metabolize androgens to estrogens, and it was observed that high levels of testosterone led to the development of prostate gland enlargement (prostatic hyperplasia). Meanwhile, increased estrogen and decreased testosterone levels gave rise to inflammatory events and lesions [147]. Epidemiological studies have also proposed that the serum level of estradiol and the serum estradiol/testosterone (E/T) ratio influence the initiation of PC and its progression [148]. Estrogen activities are carried out by two receptors, which are estrogen receptor α (ERα) or β (ERβ); ERα and Erβ are expressed in prostate tissue [125]. ERα is confined to the prostatic stroma, and has an indirect effect on the epithelial cells, while ERβ is found to be expressed within the epithelial domain and regulates epithelial proliferation and differentiation [149]. No less than five ERβ homologues (ERβ1, -2, -3, -4, and -5) exist in humans [145]. ERβ1 plays a functional role, while the other isoforms control its activity. The role of ERβ may consequently depend on the ratio of expression of ERβ1 and ERβ isoforms. It is known that ERα brings about the adverse effects induced by estrogens, while ERβ directs the protective and anti-apoptotic effects of estrogen in PCa [149]. On the one hand, the expression of estradiol receptor α has been found to be remarkably linked with a high Gleason's score and poor survival rate in patients with PCa [150]; on the other hand, ERβ expression was found to be decreased or lost in the examined PCa samples [151]. Furthermore, the expression of ERβ2 and ERβ5 together has been shown to constitute a marker for biochemical relapse, post-surgery spread/metastasis, and the period to spread after radical prostatectomy in PCa patients. Based on the aforementioned, the expression of ERβ1 decreased, and that of ERβ2 and ERβ5 increased with the progression of PCa. This expression pattern corresponded with the spreading and metastasis of PCa [152]. In PCa, on the one hand, ERα has an oncogenic role and directs the deleterious effects of estrogen, which include proliferation, inflammation, and prostate carcinogenesis. Erβ, on the other hand, may elicit antitumor activity (oncosuppressor) in PCa manipulation of ERβ by ligands. Novel drug candidates might be useful in the therapeutic strategies towards PCa, specifically during the earlier stages of the disease [145].

2.10. Experimental Work Exploring Alternative Treatments

Traditional Medicine in Prostate Cancer Medicine in Prostate Cancer Treatment

Traditional medicine plays a significant role in healthcare in developing countries, and such countries also have a long history of treating different diseases and ailments. The use of medicinal plants in cancer has gained substantial attention, and recently, research is ongoing, with the National Cancer Institute (NCI) playing a pivotal role in the research of traditional medicine to treat cancer [153]. Traditional medicine is used significantly by patients with cancer to minimize side effects or used entirely as a single treatment rather than conventional therapy. This is because plants are easily accessible, effective, and affordable. Plant-derived compounds and plant extracts have been widely used due to their anti-inflammatory, antioxidant, and antimicrobial properties [154]. Various anticancer

agents used in therapy today are derived from plants, for example, paclitaxel and taxol are derived from *Taxus brevifolia*, docetaxel (Taxotere) from *Taxus baccata*, and vincristine and vinblastine from *Catharanthus roseus* [155].

There is considerable proof supporting the utilization of a plant-based diet for the prohibition of acute disorders. Consumption of plant-based food provides necessary nutritional supplements and phytochemicals that aid in growth and shield against the occurrence of various acute illnesses [156]. They also offer protection against oxidative stress related to chronic disorders such as cancer. Phenolic compounds serve protective roles including antibacterial, anti-inflammatory, and anticancer roles [157]. Plants containing organosulfur compounds have chemoprotective activity. Carotenoids and polyphenols have anti-inflammatory and antioxidant activity [158]. Consequently, medicinal plants are commonly used for the treatment of cancers [159]. Several flavonoids have shown anticancer activity in the treatment of prostate cancer. Flavonoids are polyphenolic compounds characterized by a benzene ring condensed with a six-member phenyl ring attached to the carbon 2 and carbon 3 (C2 and C3) carbon positions. Among flavonoids, flavonols which can be identified by a distinctive hydroxyl group at the carbon 3 carbon position, have been reported in a number of studies, both preclinical and clinical, for their anticancer activity in prostate cancer cell lines. Flavonols, myricetin, fisetin, and kaempferol are commonly found in several fruits and vegetables and display anti-inflammatory, antiviral, antineoplastic, antibacterial, and antioxidant activity, among many others, in different cells [160].

Several specific plants have been analyzed for their activity as anticancer agents for cancer treatment. Plant anticancer activity is linked to phytochemical constituents present in extracts. Table 8 summarizes various medicinal plants used in cancer treatment [161].

Table 8. Summary of various medicinal plants used against different types of cancers [161].

Plant Name	Phytochemical/Anticancer Agent	Type of Cancer Suppressed, Clinical and Research
Moringa oliefera	Niazinine A	Blood cancer (in vitro)
Catharanthus roseus	Vincristine and vinblastine	Testis, breast, rectum, ovary, lung, and cervical cancer (in vitro), in clinical use
Panax ginseng	Panaxadiol, panaxatriol	Prostate, breast, colon, ovary, lung, and colon cancer (in vitro)
Solanum Lycopersicum	Lycopene	Colon cancer as well as prostate (in vivo)
Cannabis sativa	Cannabinoid	Colorectal cancer, lung, prostate, pancreas, and breast cancer (in vitro and in vivo)
Taxus brevifolia	nab-Paclitaxel	Ovarian cancer as well as breast cancer (in vitro and animal studies), in clinical use
Vitis vinifera	Cyanidin	Colon cancer (in vitro)
Pyrus malus	Procyanidin, quercetin	Colon cancer (in vivo, in vitro)
Curcuma longa	Curcumin	Stomach cancer, prostate cancer (in vitro)
Camellia sinensis	Epigallocatechin gallate	Brain, bladder cancer, prostate, cervical, and bladder cancer (in vivo)
Taxus baccata	Cabazitaxel	Prostate cancer (in vivo), in clinical use
Taxus baccata	Docetaxel	Prostate, breast, and stomach cancer, in clinical use
Taxus baccata	Larotaxel	Pancreatic, bladder, and breast cancer (in vivo)
Taxus brevifolia	Paclitaxel	Breast cancer and ovarian cancer (in vivo)

Table 8. *Cont.*

Plant Name	Phytochemical/Anticancer Agent	Type of Cancer Suppressed, Clinical and Research
Berberis vulgaris	Cannabisin, berberine	Liver, prostate, and breast cancer (in vivo)
Zingiber officinale	6-Shogaol Gingerol	Ovarian cancer (in vitro) Ovarian, colon, and breast cancer (both in animal experiments and in vitro experiments)
Aloe vera	Alexin B, emodin	Stomach cancer and leukemia (in vivo)
Vaccinium macrocarpon	Hydroxycinnamoyl ursolic acid	Prostate and cervical cancer (in vitro)
Hibiscus mutabilis	Lectin	Breast and liver cancer (in vitro)
Momordica charantia	Cucurbitane-triterpene, charantin	Breast and colon cancer (in vitro)
Podophyllum peltate	Etoposide Teniposide	Lung, testicular, leukemia, lymphoma Hodgkin's lymphoma
Curcuma longa	Curcumin	Stomach cancer (in vitro) Lung, prostate, skin, colon breast, lung, colon, prostate, liver esophagus (in vitro)
Cicer arietinum Crocus	Bowman–Birk-type protease	Prostate as well as breast cancer (in vitro)

2.11. Gene Therapy

The developments achieved in genetics, biotechnology, tumor biology, and immunology have facilitated new advancements in gene therapy. Gene therapy is a therapy that includes inserting or deleting a DNA sequence or base pair to rectify a genetic defect in a specific protein or to target a certain molecular pathway. A few gene editing technologies are currently being developed for gene therapy. Gene therapies usually involve the encapsulation of DNA nucleotides into viral and non-viral vectors that deliver the gene to a specific site, then, inserting the gene into the human genome to edit the DNA sequence and regulate cellular processes [162]. The main idea of gene therapy is to deliver exogenous nucleotides to specific DNA parts in the cells of various tissues. Viruses are well known for being efficient in transferring their genome into a host to infect it. The viral vector can be administered intravenously by injecting it directly into the targeted tissue. Non-viral vectors such as nanoparticles and polymers have also been studied for their use in gene therapy for the treatment of prostate cancer. These non-viral vectors usually condense DNA through electrostatic interactions, which also protects the genetic material from degrading. Gene therapies also explore the use of apoptosis. Failure of cells to undergo apoptosis can lead to uncontrolled cell division, which then leads to the development of cancer [163]. The suppression of apoptosis usually occurs as a result of the genetic mutations in cancerous cells. Gene therapy for prostate cancer targets apoptosis cellular pathways by introducing a gene that encodes a mediator or inducer of apoptosis in defective cells encoding an inducer, mediator, or executioner of apoptosis. Apoptosis-inducing genes, such as caspases, induce cell death in cancer cells [164]. Numerous challenges such as enhancing DNA transfer efficiency to cells, as well as immune responses that interfere with gene expression lie ahead for gene therapy. However, irrespective of the difficulties, it is definite that gene therapy will be the next up-and-coming medical technique used against prostate cancer in the future. Some clinical trial studies investigating prostate cancer therapy using gene therapy include various transgenes such as p53 and herpes simplex tk [165]. Recently used prostate cancer gene therapy procedures involve rectifying abnormal gene expression, utilizing programmed cell death mechanisms and biological pathways, specifically targeting important cell functions, initiating mutant or cell lytic suicide genes, strengthening the immune system anticancer response, and connecting treatment with radiation therapy or chemotherapy [166]. Animal studies in prostate cancer gene therapy have made use of intraprostatic administration of gene therapy delivery systems. This route of admin-

istration has been found to be more effective, as most of the dose was delivered directly to the prostate. This targeted delivery allowed the administered dose to reach prostate cancer metastasis. Lactoferrin and transferrin are multifunctional proteins that can bind to iron-binding proteins that are usually overexpressed on prostate cancer cells [167]. The proteins are responsible for regulating free iron levels. High iron levels have negative side effects such as increasing the risk of bacterial infections, as well generating free radicals and promoting the conversion of oxidation states ferrous ion (Fe2+) to ferric ion (Fe3+). Various studies in animals have used transferrin and lactoferrin for active targeting of prostate cancer cells. Prostate stem cell antigen (PSCA) is a cell surface antigen that is expressed in androgen-dependent and androgen-independent prostate cancer cells; therefore, it can be used as a marker for prostate cancer. Human epidermal growth factor receptor 2 (HER2) is another ligand that can be used as a marker for targeted treatment of prostate cancer due to mutations causing overexpression of tumor cells [168]. A study conducted on prostate cancer-induced xenograft mice models indicated that the inhibition of HER2 and epidermal growth factor receptor (EGFR) by specifically targeting tumor-initiating cells could highly improve the efficacy of the chemotherapy treatment for castration-resistant prostate cancer with activated STAT3, and could prevent metastasis EGF-induced STAT3 phosphorylation, which is responsible for enabling prostate cancer metastasis [169,170]. Various gene targeting systems have experimented on immune response treatment with a DAB-Lf dendriplex encoding IL12, which has demonstrated drastic tumor reduction in the PC3 and DU145 prostate tumors. MiRNA (miR)-205, miR-455-3p, miR-23b, miR-221, miR-222, miR-30c, miR-224, and miR-505 are downregulated in patients with prostate cancer and are known to be associated with tumor suppressors in prostate cancer cells, affecting proliferation, invasion, and aerobic glycolysis. MiR-663a and miR-1225-5p are linked to the development of prostate cancer, showing potential to be used as candidate markers. The specific functions of miR-663a and miR-1225-5p in stimulating prostate cancer growth and tumor progression are unclear [171–173].

2.12. CRISPR Cas9

The clustered regularly interspaced short palindromic repeats (CRISPR)/CRISPR-associated protein 9 (Cas9) is a natural defense mechanism found in archaea and bacteria. This system is currently being extensively researched because of its simplicity and effectiveness [145]. The ability to target intraprostatic inoculation of specific gene therapy vectors is an advantage of immunotherapy-based and cytotoxic gene therapy approaches. Because changes in DNA sequences result in mutations that cause cancer, scientists have been interested in new approaches to correct such changes by manipulating DNA [174]. The clustered regularly interspaced short palindromic repeats (CRISPR)/CRISPR-associated protein 9 (Cas9) system uses single-guide RNA (sgRNA) to identify and bind to certain DNA sequences through Watson–Crick base pairing [175]. CRISPR and the CRISPR–Cas9 (CRISPR-associated 9) system have been extensively studied and have changed the study of biological systems. CRISPR allows the precise altering, inserting, or deleting of DNA nucleotides in the target DNA sequence by initiating double-strand breaks. A guide RNA binds to Cas9, leading it to a complementary DNA target sequence, where a double-strand break is inserted to repair or edit DNA nucleotides. CRISPR can also be used for detecting DNA from RNA from cancerous cells and cancer-causing viruses. CRISPR/Cas9 delivery in nanoparticle lipid-based vectors is safer to use and effective [176]. Liposomal vectors offer a wide range of advantages and modifications, giving direct control over the physicochemical properties of the liposomal surface, and can accommodate the conjugation of targeting ligands. An antibody-targeted delivery system of lipid nanoparticles (LNPs) was initially developed and standardized for the targeted treatment with small interfering RNA (siRNA). Recently, LNPs were used in a proof-of-concept study to target disseminated ovarian cancer in mice with CRISPR/Cas9 [177]. A study by Ye et al., 2017, analyzed the function of GPRC6A in the progression of prostate cancer progression in vitro and in animal studies. The study indicated that GPRG6A was expressed in human prostate cancer

cell lines, and also showed polymorphism that improved mTOR signaling. Clustered regularly interspaced short palindromic repeats (CRISPR) and CRISPR-associated protein 9 nuclease (Cas9) (CRISPR/Cas9) were used to interrupt the GPRC6A gene in the PC-3 cell line. The results indicated that editing the GPRC6A gene using CRISPR/Cas9 stopped cell proliferation and migration in vitro, and also that osteocalcin activated the ERK, AKT, and mTOR signaling pathways. It was found that the GPRC6A gene mediated the progression of prostate cancer in animal studies mainly through assessing the response to osteocalcin in human prostate cancer xenograft models with cells expressing GPRC6A gene or the CRISPR/Cas9-mediated deletion of the gene. The findings of the study supported the use of CRISPR as a potential therapeutic target [178]. The first genome-scale CRISPRi screen in metastatic PCa models indicated that kinesin family member 4A (KIF4A) and WD repeat domain 62 (WDR62) initiate aggressive PCa. Novel targets for prostate cancer are also provided by CRISPR screen in prostate-specific cell lines, also suggesting the importance of assessing the results in other cancer cells, which may lead to the discovery of biomarkers for prostate cancer therapy [179].

2.13. Nanotechnology

Nanotechnology is an integrative field that combines pharmacology, biomedical science, and nanotechnology. Nanoparticles have characteristics that allow drug efficacy, can easily penetrate tumors, prevent drug degradation, and can be modified to target specific tissues [170]. Nanoparticles such as liposomes, polymers, metal nanomaterials, and porous silicon nanoparticles have been highly researched for application in prostate cancer treatment and prognosis. Active targeting nanoparticles have modified surfaces with attached antibodies, affibodies, peptides, or oligosaccharides. These targeting ligands target receptor cells on cancerous cells, such as the prostate-specific membrane antigen (PSMA) receptors on prostate cancer cells [180]. There is interest in developing nanoparticles for prostate cancer therapy due to challenges faced by currently used treatments. A study conducted at Mount Sinai New York on 16 patients used gold silica nanoparticles for localized prostate cancer. The gold silica nanoparticles absorbed infrared light at a wavelength that could penetrate biological tissues. The gold nanoparticles possessed plasmon resonance that could drastically decrease side effects related to the therapy. Patients were injected intravenously with gold nanoparticles with laser ablation. The growth of the tumor was analyzed using magnetic resonance imaging after 48 and 72 h of therapy. The results showed a decrease in tumor size with no side effects. While only a few studies have progressed to clinical trials, a study on targeted and controlled release for prostate cancer therapy has recently started clinical trials, which has led to the development of the BIND-014 docetaxel encapsulated nanoprototype [155]. The results of preclinical and clinical improvements linked to liposomal drug delivery in cancer treatment suggest that liposomal encapsulation signals a positive future for the treatment of prostate cancer. Nanocarriers have been demonstrated as useful in combination therapy, as they are able to overcome differences in pharmacokinetics in chemotherapeutic agents [173]. Combining nanotechnology and other therapeutic strategies can effectively enhance and improve the effectiveness of drugs. In prostate cancer, nanotechnology is used in diagnostics and therapeutic treatment. Not only are nanoparticles effective delivery systems, but they also improve the solubility of poorly soluble drugs, and multifunctional nanoparticles display adequate specificity toward urological cancers, bladder, renal, and prostate cancer. In a study conducted by Zhang et al., the encapsulation of docetaxel and doxorubicin in nanoparticles increased the observed cytotoxicity in prostate cancer cells [180]. Another study, conducted to assess the codelivery of doxorubicin (DOX) and docetaxel (DOC) by nanocarriers for synergistic activity, suggested that both anticancer agents DOX and DOC in the nanoparticles acted synergistically and promoted the curative effect of Dox and Doc in a xenograft mouse model, which acted on androgen-dependent and androgen-independent prostate cancer cell lines [181]. A multicenter phase II open-label clinical trial consisting of 42 patients with progressing mCRPC who received abiraterone acetate and/or enzalutamide treat-

ment studied the safety and efficacy of a docetaxel-containing nanoparticle (BIND-014) targeting prostate-specific membrane antigen (PSMA) in metastatic castration-resistant prostate cancer. Targeted delivery of docetaxel by prostate-specific membrane antigen (PSMA)-conjugated nanoparticles was found to be clinically effective, drastically reducing circulating tumor cells [182]. A modern method of heating tumors after inoculation of magnetic nanoparticles has been extensively researched in prostate cancer clinical trials. The feasibility and tolerability were evaluated with the first prototype of an alternating magnetic field applicator in a study experimenting with magnetic nanoparticle thermotherapy alone or in combination with permanent seed brachytherapy. The results reported that magnetic nanoparticle thermotherapy had been shown to be hyperthermic and effective to thermoablative temperatures and could be achieved in the prostate at low magnetic field strengths of 4–5 kA/m [183,184].

2.14. Next-Generation Sequencing

Recently, the development of next-generation sequencing (NGS) technologies has proven to be a substantial advancement in the documentation of unique genetic alterations that have improved our understanding of cancer cell biology [185]. Precision medicine, also known as personalized medicine, strives to produce individualized treatment plans and do away with "one-size-fits-all" approaches to therapy [186]. The development of personalized treatment was supported by NGS, which not only increased our understanding of cancer but also gave oncologists a strong tool for understanding each patient's disease and its distinct genetic characteristics and whole-genome mutational status [187,188]. NGS can identify tumor-specific alterations with single-nucleotide resolution [189]. The NGS technologies are whole-genome, whole-exome, RNA, reduced representation bisulfite, and chromatin immunoprecipitation sequencing. The three crucial phases in NGS are library preparation and amplification, sequencing, and data analysis [190]. Even though the Sanger sequencing and PCR methods have long been used to examine tumor biomarkers, the development of NGS has made it possible to screen more genes in a single test. Predictive biomarkers have subsequently been developed to assist in selecting the right patient populations for clinical investigations. Additionally, NGS enables researchers to identify the most prevalent known variants as well as the long tail of uncommon mutations that occur in less than 1% of patients and can offer helpful data on treatment sensitivity [187].

The application of NGS in PC genomics has significantly advanced the systematic cataloging of all DNA alterations occurring in cancer [188]. The identification and production of novel long non-coding RNAs and novel gene fusions in PC have been greatly aided by the use of RNA sequencing. This has resulted in the discovery of new recurrent alterations that have been identified, which are TMPRSS2-ERG translocation, SPOP and CHD1 mutations, and chromoplexy, and also the pathways that have been previously well-established have been validated (e.g., androgen receptor overexpression and mutations; PTEN, RB1, and TP53 loss/mutations) [189,190]. DNA sequencing is now far more sensitive and scaleable due to NGS [191]. PC continues to present a significant challenge in terms of diagnosis and prognosis due to its highly diverse nature [192]. To more accurately determine the cancer's aggressiveness, clinicopathological and radiological data should be combined with the knowledge gathered from NGS investigations [193,194]. Despite having great hopes for NGS benefits, there are a number of limitations to the method that should be taken into consideration [194]. Firstly, there are valid arguments against NGS replacing established and thoroughly supported histopathological diagnoses. Although NGS can often be utilized to identify and subtype various cancer entities, an accurate pathological examination should always come first [195]. Second, NGS from tumor biopsies only provides limited temporal and geographical resolution of the entire tumor since it can only evaluate DNA and RNA changes in a small group of tumor cells at a particular timepoint [196]. This issue can be approached from a variety of angles, including improving spatial resolution through novel techniques, single-cell sequencing, serial analysis of circulating cell-free nucleic acids or tumor cells, or pragmatically focusing on the actionability of specific targets via functional

studies [197]. Third, the creation of the software tools required for the analysis and clinical interpretation of the "big data" produced by NGS to support clinical decision making is still lagging behind the hardware infrastructure that is currently in place for its calculation, management, and storage [198]. Additionally, significant bioinformatical work is required to directly compare data obtained on various NGS platforms and evaluated by various bioinformatic pipelines and algorithms. Therefore, the success of NGS and precision oncology depends greatly on efficient communication and constructive teamwork among all parties [199].

3. Conclusions

Prostate cancer is one of the leading causes of death in men globally, after lung disease. Commonly mutated genes, proteins, and pathways associated with an increased risk of prostate cancer development can be used as biomarkers for the disease, which provide information on the stage and cause of cancer. Biomarkers can also give specifications on the type of treatment required for cancer. There is an urgent need for effective and targeted specific treatment for prostate cancer. The current treatments available for prostate cancer are beneficial to only a few patients, and present numerous side effects that eventually affect the quality of life of most patients. Chemotherapy, radiotherapy, and hormonal treatment have adverse side effects, including drug resistance, which remains a setback to anticancer treatment. Many medicinal plants, gene therapy, and the application of nanotechnology currently in research have proven to reduce side effects as well as restore chemosensitivity in resistant tumor cells. Medicinal plant fractions and compounds, genetic material encapsulated in target-specific nanocarriers with controlled release, and targeted therapies based on cellular pathways appear to be promising alternatives for prostate cancer treatment.

Author Contributions: M.S., supervision—oversight and leadership of the research, planning and execution, critical review and editing of the manuscript, funding acquisition; K.R., summary, introduction, abstract, genetics, diagnosis, treatment options, alternative approaches, conclusion and referencing, review and editing, project administration; P.M., summary, introduction, abstract, genetics, diagnosis, treatment options, alternative approaches, conclusion and referencing; L.G., summary, introduction, abstract, diagnosis, treatment options, alternative approaches, conclusion referencing; A.A., genetics, treatment options, critical review and editing of the manuscript; S.M., review and editing of the manuscript. All authors have read and agreed to the published version of the manuscript.

Funding: Reference: TTK200415513610, NRF grant no 129891.

Institutional Review Board Statement: Not applicable.

Informed Consent Statement: Not applicable.

Data Availability Statement: Information was available in the public domain. Databases have been provided in Section 2.

Conflicts of Interest: The authors declare that there are no conflicts of interest that could be perceived as prejudicing the impartiality of this review.

References

1. Chen, J.; Zhang, D.; Yan, W.; Yang, D.; Shen, B. Translational Bioinformatics for Diagnostic and Prognostic Prediction of Prostate Cancer in the Next-Generation Sequencing Era. *BioMed Res. Int.* **2013**, *2013*, 901578. [CrossRef]
2. Hjelmborg, J.B.; Scheike, T.; Holst, K.; Skytthe, A.; Penney, K.L.; Graff, R.E.; Pukkala, E.; Christensen, K.; Adami, H.-O.; Holm, N.V.; et al. The Heritability of Prostate Cancer in the Nordic Twin Study of Cancer. *Cancer Epidemiol. Biomark. Prev.* **2014**, *23*, 2303–2310. [CrossRef]
3. Termini, D.; Hartogh, D.J.D.; Jaglanian, A.; Tsiani, E. Curcumin against Prostate Cancer: Current Evidence. *Biomolecules* **2020**, *10*, 1536. [CrossRef]
4. Wen, S.; Chang, H.-C.; Tian, J.; Shang, Z.; Niu, Y.; Chang, C. Stromal Androgen Receptor Roles in the Development of Normal Prostate, Benign Prostate Hyperplasia, and Prostate Cancer. *Am. J. Pathol.* **2015**, *185*, 293–301. [CrossRef]
5. Cittadini, A.; Isidori, A.M.; Salzano, A. Testosterone therapy and cardiovascular diseases. *Cardiovasc. Res.* **2021**, *118*, 2039–2057. [CrossRef]

6. Bluemn, E.G.; Nelson, P.S. The androgen/androgen receptor axis in prostate cancer. *Curr. Opin. Oncol.* **2012**, *24*, 251–257. [CrossRef]
7. Ziaran, S.; Novakova, Z.V.; Böhmer, D.; Danišovič, L. Biomarkers for determination prostate cancer: Implication for diagnosis and prognosis. *Neoplasma* **2015**, *62*, 683–691. [CrossRef]
8. Takayama, K.-I. Splicing Factors Have an Essential Role in Prostate Cancer Progression and Androgen Receptor Signaling. *Biomolecules* **2019**, *9*, 131. [CrossRef]
9. Bach, C.; Pisipati, S.; Daneshwar, D.; Wright, M.; Rowe, E.; Gillatt, D.; Persad, R.; Koupparis, A. The status of surgery in the management of high-risk prostate cancer. *Nat. Rev. Urol.* **2014**, *11*, 342–351. [CrossRef]
10. Ziegler, A.; Koch, A.; Krockenberger, K.; Großhennig, A. Personalized medicine using DNA biomarkers: A review. *Qual. Life Res.* **2012**, *131*, 1627–1638. [CrossRef]
11. Rawla, P. Epidemiology of Prostate Cancer. *World J. Oncol.* **2019**, *10*, 63–89. [CrossRef] [PubMed]
12. Barbieri, C.; Bangma, C.H.; Bjartell, A.; Catto, J.; Culig, Z.; Grönberg, H.; Luo, J.; Visakorpi, T.; Rubin, M. The Mutational Landscape of Prostate Cancer. *Eur. Urol.* **2013**, *64*, 567–576. [CrossRef] [PubMed]
13. Haas, G.P.; Delongchamps, N.; Brawley, O.W.; Wang, C.Y.; De La Roza, G. The worldwide epidemiology of prostate cancer: Perspectives from autopsy studies. *Can. J. Urol.* **2008**, *15*, 3866–3871. [PubMed]
14. Sung, H.; Ferlay, J.; Siegel, R.L.; Laversanne, M.; Soerjomataram, I.; Jemal, A.; Bray, F. Global Cancer Statistics 2020: GLOBOCAN Estimates of Incidence and Mortality Worldwide for 36 Cancers in 185 Countries. *CA Cancer J. Clin.* **2021**, *71*, 209–249. [CrossRef]
15. Taitt, H.E. Global Trends and Prostate Cancer: A Review of Incidence, Detection, and Mortality as Influenced by Race, Ethnicity, and Geographic Location. *Am. J. Men's Health* **2018**, *12*, 1807–1823. [CrossRef]
16. Bashir, M.N. Epidemiology of Prostate Cancer. *Asian Pac. J. Cancer Prev.* **2015**, *16*, 5137–5141. [CrossRef]
17. Ferlay, J.; Parkin, D.; Steliarova-Foucher, E. Estimates of cancer incidence and mortality in Europe in 2008. *Eur. J. Cancer* **2010**, *46*, 765–781. [CrossRef]
18. Matshela, R.F.; Maree, L.; van Belkum, C. Prevention and Detection of Prostate Cancer. *Cancer Nurs.* **2014**, 37, 189–197. [CrossRef]
19. Babb, C.; Urban, M.; Kielkowski, D.; Kellett, P. Prostate Cancer in South Africa: Pathology Based National Cancer Registry Data (1986–2006) and Mortality Rates (1997–2009). *Prostate Cancer* **2014**, *2014*, 419801. [CrossRef]
20. Altwaijry, N.; Somani, S.; Parkinson, J.; Tate, R.; Keating, P.; Warzecha, M.; MacKenzie, G.R.; Leung, H.Y.; Dufès, C. Regression of prostate tumors after intravenous administration of lactoferrin-bearing polypropylenimine dendriplexes encoding TNF-α, TRAIL, and interleukin-12. *Drug Deliv.* **2018**, *25*, 679–689. [CrossRef]
21. Adhyam, M.; Gupta, A.K. A Review on the Clinical Utility of PSA in Cancer Prostate. *Indian J. Surg. Oncol.* **2012**, *3*, 120–129. [CrossRef] [PubMed]
22. Suzuki, K.; Kise, H.; Nishioka, J.; Hayashi, T. The Interaction among Protein C Inhibitor, Prostate-Specific Antigen, and the Semenogelin System. *Semin. Thromb. Hemost.* **2007**, *33*, 46–52. [CrossRef] [PubMed]
23. Lamy, P.-J.; Allory, Y.; Gauchez, A.-S.; Asselain, B.; Beuzeboc, P.; de Cremoux, P.; Fontugne, J.; Georges, A.; Hennequin, C.; Lehmann-Che, J.; et al. Prognostic Biomarkers Used for Localised Prostate Cancer Management: A Systematic Review. *Eur. Urol. Focus* **2018**, *4*, 790–803. [CrossRef]
24. Meyer, A.R.; Joice, G.A.; Schwen, Z.R.; Partin, A.W.; Allaf, M.E.; Gorin, M.A. Initial Experience Performing In-office Ultrasound-guided Transperineal Prostate Biopsy Under Local Anesthesia Using the PrecisionPoint Transperineal Access System. *Urology* **2018**, *115*, 8–13. [CrossRef] [PubMed]
25. Niraj, L.K. MRI in Dentistry—A Future Towards Radiation Free Imaging—Systematic Review. *J. Clin. Diagn. Res.* **2016**, *10*, ZE14–ZE19. [CrossRef] [PubMed]
26. Chopra, S.; Foltz, W.D.; Milosevic, M.F.; Toi, A.; Bristow, R.G.; Ménard, C.; Haider, M.A. Comparing oxygen-sensitive MRI (BOLD R2*) with oxygen electrode measurements: A pilot study in men with prostate cancer. *Int. J. Radiat. Biol.* **2009**, *85*, 805–813. [CrossRef]
27. Kasivisvanathan, V.; Rannikko, A.S.; Borghi, M.; Panebianco, V.; Mynderse, L.A.; Vaarala, M.H.; Briganti, A.; Budäus, L.; Hellawell, G.; Hindley, R.G.; et al. MRI-Targeted or Standard Biopsy for Prostate-Cancer Diagnosis. *N. Engl. J. Med.* **2018**, *378*, 1767–1777. [CrossRef]
28. Albright, F.; Stephenson, R.A.; Agarwal, N.; Teerlink, C.C.; Lowrance, W.T.; Farnham, J.M.; Albright, L.A.C. Prostate cancer risk prediction based on complete prostate cancer family history. *Prostate* **2015**, *75*, 390–398. [CrossRef]
29. Prando, A. Diffusion-weighted MRI of peripheral zone prostate cancer: Comparison of tumor apparent diffusion coefficient with Gleason score and percentage of tumor on core biopsy. *Int. Braz. J. Urol.* **2010**, *36*, 504–517. [CrossRef]
30. Ferro, M.; de Cobelli, O.; Vartolomei, M.D.; Lucarelli, G.; Crocetto, F.; Barone, B.; Sciarra, A.; Del Giudice, F.; Muto, M.; Maggi, M.; et al. Prostate Cancer Radiogenomics—From Imaging to Molecular Characterization. *Int. J. Mol. Sci.* **2021**, *22*, 9971. [CrossRef]
31. Moran, A.; O'Hara, C.; Khan, S.; Shack, L.; Woodward, E.R.; Maher, E.; Lalloo, F.; Evans, D.G.R. Risk of cancer other than breast or ovarian in individuals with BRCA1 and BRCA2 mutations. *Fam. Cancer* **2012**, *11*, 235–242. [CrossRef] [PubMed]
32. Turanli, B.; Grøtli, M.; Boren, J.; Nielsen, J.; Uhlen, M.; Arga, K.Y.; Mardinoglu, A. Drug Repositioning for Effective Prostate Cancer Treatment. *Front. Physiol.* **2018**, *9*, 500. [CrossRef]

33. Bardis, M.D.; Houshyar, R.; Chang, P.D.; Ushinsky, A.; Glavis-Bloom, J.; Chahine, C.; Bui, T.-L.; Rupasinghe, M.; Filippi, C.G.; Chow, D.S. Applications of Artificial Intelligence to Prostate Multiparametric MRI (mpMRI): Current and Emerging Trends. *Cancers* **2020**, *12*, 1204. [CrossRef] [PubMed]
34. Beroukhim, R.; Mermel, C.H.; Porter, D.; Wei, G.; Raychaudhuri, S.; Donovan, J.; Barretina, J.; Boehm, J.S.; Dobson, J.; Urashima, M.; et al. The landscape of somatic copy-number alteration across human cancers. *Nature* **2010**, *463*, 899–905. [CrossRef] [PubMed]
35. Berger, A.H.; Knudson, A.G.; Pandolfi, P.P. A continuum model for tumour suppression. *Nature* **2011**, *476*, 163–169. [CrossRef] [PubMed]
36. Castro, E.; Eeles, R. The role of BRCA1 and BRCA2 in prostate cancer. *Asian J. Androl.* **2012**, *14*, 409–414. [CrossRef]
37. Meyer, M.S.; Penney, K.L.; Stark, J.R.; Schumacher, F.R.; Sesso, H.D.; Loda, M.; Fiorentino, M.; Finn, S.; Flavin, R.J.; Kurth, T.; et al. Genetic variation in RNASEL associated with prostate cancer risk and progression. *Carcinogenesis* **2010**, *31*, 1597–1603. [CrossRef]
38. Silverman, R.H. Implications for RNase L in Prostate Cancer Biology. *Biochemistry* **2003**, *42*, 1805–1812. [CrossRef]
39. Wallis, C.J.; Nam, R.K. Prostate Cancer Genetics: A Review. *EJIFCC* **2015**, *26*, 79–91.
40. Alvarez-Cubero, M.J.; Martinez-Gonzalez, L.J.; Saiz, M.; Carmona-Saez, P.; Alvarez, J.C.; Pascual-Geler, M.; Lorente, J.A.; Cozar, J.M. Prognostic role of genetic biomarkers in clinical progression of prostate cancer. *Exp. Mol. Med.* **2015**, *47*, e176. [CrossRef]
41. Chandrasekaran, G.; Hwang, E.C.; Kang, T.W.; Kwon, D.D.; Park, K.; Lee, J.-J.; Lakshmanan, V.K. Computational Modeling of complete HOXB13 protein for predicting the functional effect of SNPs and the associated role in hereditary prostate cancer. *Sci. Rep.* **2017**, *7*, 43830. [CrossRef] [PubMed]
42. Marlin, R.; Créoff, M.; Merle, S.; Jean-Marie-Flore, M.; Rose, M.; Malsa, S.; Promeyrat, X.; Martin, F.; Comlan, G.; Rabia, N.; et al. Mutation *HOXB13* c.853delT in Martinican prostate cancer patients. *Prostate* **2020**, *80*, 463–470. [CrossRef] [PubMed]
43. Manzari, Z.; Mehrabani-Yeganeh, H.; Nejati-Javaremi, A.; Moradi, M.H.; Gholizadeh, M. Detecting selection signatures in three Iranian sheep breeds. *Anim. Genet.* **2019**, *50*, 298–302. [CrossRef] [PubMed]
44. Jeong, T.-O.; Oh, K.-J.; Nguyen, N.T.X.; Kim, Y.-R.; Kim, M.S.; Lee, S.D.; Ryu, S.B.; Jung, C. Evaluation of HOXB13 as a molecular marker of recurrent prostate cancer. *Mol. Med. Rep.* **2012**, *5*, 901–904. [CrossRef]
45. Guarini, A.; Marinelli, M.; Tavolaro, S.; Bellacchio, E.; Magliozzi, M.; Chiaretti, S.; De Propris, M.S.; Peragine, N.; Santangelo, S.; Paoloni, F.; et al. ATM gene alterations in chronic lymphocytic leukemia patients induce a distinct gene expression profile and predict disease progression. *Haematologica* **2012**, *97*, 47–55. [CrossRef]
46. Antonarakis, E.S.; Lu, C.; Wang, H.; Luber, B.; Nakazawa, M.; Roeser, J.C.; Chen, Y.; Mohammad, T.A.; Chen, Y.; Fedor, H.L.; et al. AR-V7 and Resistance to Enzalutamide and Abiraterone in Prostate Cancer. *N. Engl. J. Med.* **2014**, *371*, 1028–1038. [CrossRef]
47. Gallagher, D.J.; Gaudet, M.M.; Pal, P.; Kirchhoff, T.; Balistreri, L.; Vora, K.; Bhatia, J.; Stadler, Z.; Fine, S.W.; Reuter, V.; et al. Germline BRCA Mutations Denote a Clinicopathologic Subset of Prostate Cancer. *Clin. Cancer Res.* **2010**, *16*, 2115–2121. [CrossRef]
48. Xu, B.; Tong, N.; Li, J.-M.; Zhang, Z.-D.; Wu, H.-F. ELAC2 polymorphisms and prostate cancer risk: A meta-analysis based on 18 case–control studies. *Prostate Cancer Prostatic Dis.* **2010**, *13*, 270–277. [CrossRef]
49. Suzuki, T.; Li, W.; Zhang, Q.; Karim, A.; Novak, E.K.; Sviderskaya, E.V.; Hill, S.P.; Bennett, D.C.; Levin, A.V.; Nieuwenhuis, H.K.; et al. Hermansky-Pudlak syndrome is caused by mutations in HPS4, the human homolog of the mouse light-ear gene. *Nat. Genet.* **2002**, *30*, 321–324. [CrossRef]
50. Moore, K.J.; Freeman, M.W. Scavenger Receptors in Atherosclerosis. *Arter. Thromb. Vasc. Biol.* **2006**, *26*, 1702–1711. [CrossRef]
51. Leighton, X.; Bera, A.; Eidelman, O.; Eklund, M.; Puthillathu, N.; Pollard, H.B.; Srivastava, M. High ANXA7 Potentiates Eucalyptol Toxicity in Hormone-refractory Prostate Cancer. *Anticancer Res.* **2018**, *38*, 3831–3842. [CrossRef] [PubMed]
52. Srivastava, M.; Leighton, X.; Starr, J.; Eidelman, O.; Pollard, H.B. Diverse Effects of ANXA7 and p53 on LNCaP Prostate Cancer Cells Are Associated with Regulation of SGK1 Transcription and Phosphorylation of the SGK1 Target FOXO3A. *BioMed Res. Int.* **2014**, *2014*, 193635. [CrossRef] [PubMed]
53. Miura, Y.; Kataoka, H.; Joh, T.; Tada, T.; Asai, K.; Nakanishi, M.; Okada, N.; Okada, H. Susceptibility to killer T cells of gastric cancer cells enhanced by mitomycin-C involves induction of ATBF1 and activation of p21 (Waf1/Cip1) promoter. *Microbiol. Immunol.* **2004**, *48*, 137–145. [CrossRef] [PubMed]
54. Kai, K.; Zhang, Z.; Yamashita, H.; Yamamoto, Y.; Miura, Y.; Iwase, H. Loss of heterozygosity at the ATBF1-A locus located in the 16q22 minimal region in breast cancer. *BMC Cancer* **2008**, *8*, 262. [CrossRef] [PubMed]
55. Sun, X.; Frierson, H.F.; Chen, C.; Li, C.; Ran, Q.; Otto, K.B.; Cantarel, B.M.; Vessella, R.L.; Gao, A.C.; Petros, J.; et al. Frequent somatic mutations of the transcription factor ATBF1 in human prostate cancer. *Nat. Genet.* **2005**, *37*, 407–412. [CrossRef]
56. Chang, B.-L.; Zheng, S.L.; Isaacs, S.D.; Wiley, K.E.; Turner, A.; Li, G.; Walsh, P.C.; Meyers, D.A.; Isaacs, W.B.; Xu, J. A Polymorphism in the *CDKN1B* Gene Is Associated with Increased Risk of Hereditary Prostate Cancer. *Cancer Res.* **2004**, *64*, 1997–1999. [CrossRef]
57. Soyano, A.E.; Baldeo, C.; Kasi, P.M. BRCA Mutation and Its Association With Colorectal Cancer. *Clin. Color. Cancer* **2018**, *17*, e647–e650. [CrossRef]
58. Sirma, H.; Broemel, M.; Stumm, L.; Tsourlakis, T.; Steurer, S.; Tennstedt, P.; Salomon, G.; Michl, U.; Haese, A.; Simon, R.; et al. Loss of CDKN1B/p27Kip1 expression is associated with ERG fusion-negative prostate cancer, but is unrelated to patient prognosis. *Oncol. Lett.* **2013**, *6*, 1245–1252. [CrossRef]
59. Slavin, D.A.; Koritschoner, N.P.; Prieto, C.C.; López-Díaz, F.J.; Chatton, B.; Bocco, J.L. A new role for the Krüppel-like transcription factor KLF6 as an inhibitor of c-Jun proto-oncoprotein function. *Oncogene* **2004**, *23*, 8196–8205. [CrossRef]

60. Narla, G.; DiFeo, A.; Fernandez, Y.; Dhanasekaran, S.M.; Huang, F.; Sangodkar, J.; Hod, E.; Leake, D.; Friedman, S.L.; Hall, S.J.; et al. KLF6-SV1 overexpression accelerates human and mouse prostate cancer progression and metastasis. *J. Clin. Investig.* **2008**, *118*, 2711–2721. [CrossRef]
61. *Multiple Sclerosis. Cold Spring Harbor Perspectives in Medicine*; Cold Spring Harbor (New York): Cold Spring Harbor Laboratory Press. $135.00. viii + 362 p.; ill.; index. ISBN: 9781621820765. 2018. *Q. Rev. Biol.* **2019**, *94*, 450. Available online: https://www.journals.uchicago.edu/doi/10.1086/706427 (accessed on 25 May 2022). [CrossRef]
62. Rebello, R.J.; Pearson, R.B.; Hannan, R.D.; Furic, L. Therapeutic Approaches Targeting MYC-Driven Prostate Cancer. *Genes* **2017**, *8*, 71. [CrossRef] [PubMed]
63. Chen, H.; Liu, W.; Roberts, W.; Hooker, S.; Fedor, H.; DeMarzo, A.; Isaacs, W.; Kittles, R.A. 8q24 allelic imbalance and MYC gene copy number in primary prostate cancer. *Prostate Cancer Prostatic Dis.* **2010**, *13*, 238–243. [CrossRef] [PubMed]
64. Gurel, B.; Ali, T.Z.; Montgomery, E.A.; Begum, S.; Hicks, J.; Goggins, M.; Eberhart, C.G.; Clark, D.P.; Bieberich, C.J.; Epstein, J.I.; et al. NKX3.1 as a Marker of Prostatic Origin in Metastatic Tumors. *Am. J. Surg. Pathol.* **2010**, *34*, 1097–1105. [CrossRef]
65. Menini, T.; Gugliucci, A. Paraoxonase 1 in neurological disorders. *Redox Rep.* **2014**, *19*, 49–58. [CrossRef]
66. Stevens, V.L.; Rodriguez, C.; Talbot, J.T.; Pavluck, A.L.; Thun, M.J.; Calle, E.E. Paraoxonase 1 (PON1) polymorphisms and prostate cancer in the CPS-II Nutrition Cohort. *Prostate* **2008**, *68*, 1336–1340. [CrossRef]
67. Markowska, A.; Pawałowska, M.; Lubin, J.; Markowska, J. Signalling pathways in endometrial cancer. *Współczesna Onkol.* **2014**, *18*, 143–148. [CrossRef]
68. Steelman, L.S.; Chappell, W.H.; Abrams, S.L.; Kempf, C.R.; Long, J.; Laidler, P.; Mijatovic, S.; Maksimovic-Ivanic, D.; Stivala, F.; Mazzarino, M.C.; et al. Roles of the Raf/MEK/ERK and PI3K/PTEN/Akt/mTOR pathways in controlling growth and sensitivity to therapy-implications for cancer and aging. *Aging* **2011**, *3*, 192–222. [CrossRef]
69. Fraser, M.; Zhao, H.; Luoto, K.R.; Lundin, C.; Coackley, C.; Chan, N.; Joshua, A.M.; Bismar, T.A.; Evans, A.; Helleday, T.; et al. *PTEN* Deletion in Prostate Cancer Cells Does Not Associate with Loss of RAD51 Function: Implications for Radiotherapy and Chemotherapy. *Clin. Cancer Res.* **2012**, *18*, 1015–1027. [CrossRef]
70. Jamaspishvili, T.; Berman, D.M.; Ross, A.E.; Scher, H.I.; De Marzo, A.M.; Squire, J.A.; Lotan, T.L. Clinical implications of PTEN loss in prostate cancer. *Nat. Rev. Urol.* **2018**, *15*, 222–234. [CrossRef]
71. Penta, J.S.; Johnson, F.; Wachsman, J.T.; Copeland, W.C. Mitochondrial DNA in human malignancy. *Mutat. Res. Mutat. Res.* **2001**, *488*, 119–133. [CrossRef]
72. Petros, J.A.; Baumann, A.K.; Ruiz-Pesini, E.; Amin, M.B.; Sun, C.Q.; Hall, J.; Lim, S.; Issa, M.M.; Flanders, W.D.; Hosseini, S.H.; et al. mtDNA mutations increase tumorigenicity in prostate cancer. *Proc. Natl. Acad. Sci. USA* **2005**, *102*, 719–724. [CrossRef] [PubMed]
73. Sanchez-Vega, F.; Mina, M.; Armenia, J.; Chatila, W.K.; Luna, A.; La, K.; Dimitriadoy, S.; Liu, D.L.; Kantheti, H.S.; Heins, Z.; et al. Abstract 3302: The molecular landscape of oncogenic signaling pathways in The Cancer Genome Atlas. *Cancer Res.* **2018**, *78*, 3302. [CrossRef]
74. Cox, A.D.; Der, C.J. Ras history: The Saga Continues. *Small GTPases* **2010**, *1*, 2–27. [CrossRef]
75. Hessels, D.; Schalken, J.A. Urinary biomarkers for prostate cancer: A review. *Asian J. Androl.* **2013**, *15*, 333–339. [CrossRef] [PubMed]
76. Alford, A.V.; Brito, J.M.; Yadav, K.K.; Yadav, S.S.; Tewari, A.K.; Renzulli, J. The Use of Biomarkers in Prostate Cancer Screening and Treatment. *Rev. Urol.* **2017**, *19*, 221–234. [CrossRef]
77. Porzycki, P.; Ciszkowicz, E. Modern biomarkers in prostate cancer diagnosis. *Cent. Eur. J. Urol.* **2020**, *73*, 300–306. [CrossRef]
78. Shen, M.M.; Abate-Shen, C. Molecular genetics of prostate cancer: New prospects for old challenges. *Genes Dev.* **2010**, *24*, 1967–2000. [CrossRef]
79. Duan, R.; Du, W.; Guo, W. EZH2: A novel target for cancer treatment. *J. Hematol. Oncol.* **2020**, *13*, 104. [CrossRef]
80. Kipriyanov, E.A.; Karnaukh, P.A.; Vazhenin, I.A.; Vazhenin, A.V. Radical prostatectomy and robotic radiosurgery as treatment options for localized prostate cancer. *Sib. J. Oncol.* **2020**, *19*, 50–56. [CrossRef]
81. Mateo, L.; Duran-Frigola, M.; Gris-Oliver, A.; Palafox, M.; Scaltriti, M.; Razavi, P.; Chandarlapaty, S.; Arribas, J.; Bellet, M.; Serra, V.; et al. Personalized cancer therapy prioritization based on driver alteration co-occurrence patterns. *Genome Med.* **2020**, *12*, 78. [CrossRef] [PubMed]
82. Giri, V.N.; Morgan, T.M.; Morris, D.S.; Berchuck, J.E.; Hyatt, C.; Taplin, M.; Morris, F.D.S.; Ms, C.C.H. Genetic testing in prostate cancer management: Considerations informing primary care. *CA: A Cancer J. Clin.* **2022**, *72*, 360–371. [CrossRef] [PubMed]
83. Liu, Q.; Tong, D.; Liu, G.; Yi, Y.; Xu, J.; Yang, X.; Wang, L.; Zhang, J.; Ye, J.; Zhang, Y.; et al. A novel BRCA2 mutation in prostate cancer sensitive to combined radiotherapy and androgen deprivation therapy. *Cancer Biol. Ther.* **2018**, *19*, 669–675. [CrossRef] [PubMed]
84. McCrea, E.M.; Lee, D.K.; Sissung, T.M.; Figg, W.D. Precision Medicine Applications in Prostate Cancer. *Ther. Adv. Med. Oncol.* **2018**, *10*, 175883591877692. [CrossRef]
85. Trewartha, D.; Carter, K. Advances in prostate cancer treatment. *Nat. Rev. Drug Discov.* **2013**, *12*, 823–824. [CrossRef]
86. Dunn, M.W.; Kazer, M.W. Prostate Cancer Overview. *Semin. Oncol. Nurs.* **2011**, *27*, 241–250. [CrossRef]
87. Lima, Z.S.; Ghadamzadeh, M.; Arashloo, F.T.; Amjad, G.; Ebadi, M.R.; Younesi, L. Recent advances of therapeutic targets based on the molecular signature in breast cancer: Genetic mutations and implications for current treatment paradigms. *J. Hematol. Oncol.* **2019**, *12*, 39. [CrossRef]

88. Shah, S.; Young, H.N.; Cobran, E.K. Comparative Effectiveness of Conservative Management Compared to Cryotherapy in Localized Prostate Cancer Patients. *Am. J. Men's Health* **2018**, *12*, 1681–1691. [CrossRef]
89. Choo, R.; Klotz, L.; Danjoux, C.; Morton, G.C.; DeBoer, G.; Szumacher, E.; Fleshner, N.; Bunting, P.; Hruby, G. Feasibility Study: Watchful Waiting For Localized Low To Intermediate Grade Prostate Carcinoma With Selective Delayed Intervention Based On Prostate Specific Antigen, Histological And/Or Clinical Progression. *J. Urol.* **2002**, *167*, 1664–1669. [CrossRef]
90. Bergh, R.C.V.D.; Roemeling, S.; Roobol, M.J.; Aus, G.; Hugosson, J.; Rannikko, A.S.; Tammela, T.L.; Bangma, C.H.; Schröder, F.H. Outcomes of Men with Screen-Detected Prostate Cancer Eligible for Active Surveillance Who Were Managed Expectantly. *Eur. Urol.* **2009**, *55*, 1–8. [CrossRef]
91. Luzzago, S.; Suardi, N.; Dell'Oglio, P.; Cardone, G.; Gandaglia, G.; Esposito, A.; De Cobelli, F.; Cristel, G.; Kinzikeeva, E.; Freschi, M.; et al. Multiparametric MRI represents an added value but not a substitute of follow-up biopsies in patients on active surveillance for low-risk prostate cancer. *Eur. Urol. Suppl.* **2017**, *16*, e1395–e1396. [CrossRef]
92. Costello, A.J. Considering the role of radical prostatectomy in 21st century prostate cancer care. *Nat. Rev. Urol.* **2020**, *17*, 177–188. [CrossRef] [PubMed]
93. Mellman, I.; Coukos, G.; Dranoff, G. Cancer immunotherapy comes of age. *Nature* **2011**, *480*, 480–489. [CrossRef] [PubMed]
94. Mohan, R.; Schellhammer, P.F. Treatment options for localized prostate cancer. *Am. Fam. Physician* **2011**, *84*, 413–420. [PubMed]
95. Mouraviev, V.; Polascik, T.J. Update on cryotherapy for prostate cancer in 2006. *Curr. Opin. Urol.* **2006**, *16*, 152–156. [CrossRef]
96. Baskar, R.; Lee, K.A.; Yeo, R.; Yeoh, K.-W. Cancer and Radiation Therapy: Current Advances and Future Directions. *Int. J. Med. Sci.* **2012**, *9*, 193–199. [CrossRef]
97. Potosky, A.L.; Legler, J.; Albertsen, P.C.; Stanford, J.L.; Gilliland, F.D.; Hamilton, A.S.; Eley, J.W.; Stephenson, R.A.; Harlan, L.C. Health Outcomes after Prostatectomy or Radiotherapy for Prostate Cancer: Results From the Prostate Cancer Outcomes Study. *JNCI J. Natl. Cancer Inst.* **2000**, *92*, 1582–1592. [CrossRef]
98. Wallner, K.; Lee, H.; Wasserman, S.; Dattoli, M. Low risk of urinary incontinence following prostate brachytherapy in patients with a prior transurethral prostate resection. *Int. J. Radiat. Oncol.* **1997**, *37*, 565–569. [CrossRef]
99. Crawford, E.D.; Higano, C.S.; Shore, N.D.; Hussain, M.; Petrylak, D.P. Treating Patients with Metastatic Castration Resistant Prostate Cancer: A Comprehensive Review of Available Therapies. *J. Urol.* **2015**, *194*, 1537–1547. [CrossRef]
100. Heidenreich, A.; Aus, G.; Bolla, M.; Joniau, S.; Matveev, V.B.; Schmid, H.P.; Zattoni, F. EAU Guidelines on Prostate Cancer. *Eur. Urol.* **2008**, *53*, 68–80. [CrossRef]
101. Seidenfeld, J.; Samson, D.J.; Hasselblad, V.; Aronson, N.; Albertsen, P.C.; Bennett, C.L.; Wilt, T.J. Single-Therapy Androgen Suppression in Men with Advanced Prostate Cancer: A Systematic Review and Meta-Analysis. *Ann. Intern. Med.* **2000**, *132*, 566–577. [CrossRef] [PubMed]
102. Brogden, R.N.; Chrisp, P. Flutamide. *Drugs Aging* **1991**, *1*, 104–115. [CrossRef] [PubMed]
103. Goldspiel, B.R.; Kohler, D.R. Flutamide: An Antiandrogen for Advanced Prostate Cancer. *DICP* **1990**, *24*, 616–623. [CrossRef] [PubMed]
104. Iguchi, T.; Tamada, S.; Kato, M.; Yasuda, S.; Machida, Y.; Ohmachi, T.; Ishii, K.; Iwata, H.; Yamamoto, S.; Kanamaru, T.; et al. Enzalutamide versus flutamide for castration-resistant prostate cancer after combined androgen blockade therapy with bicalutamide: The OCUU-CRPC study. *Int. J. Clin. Oncol.* **2020**, *25*, 486–494. [CrossRef]
105. Miyake, H.; Hara, I.; Eto, H. Clinical outcome of maximum androgen blockade using flutamide as second-line hormonal therapy for hormone-refractory prostate cancer. *Br. J. Urol.* **2005**, *96*, 791–795. [CrossRef]
106. Koike, H.; Morikawa, Y.; Matsui, H.; Shibata, Y.; Ito, K.; Suzuki, K. Chlormadinone acetate is effective for hot flush during androgen deprivation therapy. *Prostate Int.* **2013**, *1*, 113–116. [CrossRef]
107. Kubota, Y.; Nakada, T.; Sasagawa, I.; Yanai, H.; Itoh, K.; Suzuki, H. The prognosis of stage A patients treated with the antiandrogen chlormadinone acetate. *Int. Urol. Nephrol.* **1999**, *31*, 229–235. [CrossRef]
108. Sugimoto, M.; Kakehi, Y.; Horie, S.; Hirao, Y.; Akaza, H. A randomized controlled trial evaluating the effect of low-dose chlormadinone in patients with low-risk prostate cancer: PROSAS study. *Jpn. J. Clin. Oncol.* **2022**, *52*, 187–196. [CrossRef]
109. Molina, A.; Belldegrun, A. Novel Therapeutic Strategies for Castration Resistant Prostate Cancer: Inhibition of Persistent Androgen Production and Androgen Receptor Mediated Signaling. *J. Urol.* **2011**, *185*, 787–794. [CrossRef]
110. Obligacion, R.; Ramzan, I.; Murray, M. Drug-Metabolizing Enzymes and Transporters: Expression in the Human Prostate and Roles in Prostate Drug Disposition. *J. Androl.* **2006**, *27*, 138–150. [CrossRef]
111. Stein, M.N.; Singer, E.A.; Patel, N.; Bershadskiy, A.; Sokoloff, A. Androgen synthesis inhibitors in the treatment of castration-resistant prostate cancer. *Asian J. Androl.* **2014**, *16*, 387–400. [CrossRef] [PubMed]
112. Jain, K.K. Personalised medicine for cancer: From drug development into clinical practice. *Expert Opin. Pharmacother.* **2005**, *6*, 1463–1476. [CrossRef] [PubMed]
113. Zhu, Y.; Liu, C.; Nadiminty, N.; Lou, W.; Tummala, R.; Evans, C.P.; Gao, A.C. Inhibition of ABCB1 Expression Overcomes Acquired Docetaxel Resistance in Prostate Cancer. *Mol. Cancer Ther.* **2013**, *12*, 1829–1836. [CrossRef] [PubMed]
114. Abidi, A. Cabazitaxel: A novel taxane for metastatic castration-resistant prostate cancer-current implications and future prospects. *J. Pharmacol. Pharmacother.* **2013**, *4*, 230–237. [CrossRef]
115. Cookson, M.S.; Roth, B.J.; Dahm, P.; Engstrom, C.; Freedland, S.J.; Hussain, M.; Lin, D.W.; Lowrance, W.T.; Murad, M.H.; Oh, W.; et al. Castration-Resistant Prostate Cancer: AUA Guideline. *J. Urol.* **2013**, *190*, 429–438. [CrossRef]

116. Gerritsen, W.R.; Sharma, P. Current and Emerging Treatment Options for Castration-Resistant Prostate Cancer: A Focus on Immunotherapy. *J. Clin. Immunol.* **2012**, *32*, 25–35. [CrossRef]
117. Nishiyama, T. Androgen deprivation therapy in combination with radiotherapy for high-risk clinically localized prostate cancer. *J. Steroid Biochem. Mol. Biol.* **2012**, *129*, 179–190. [CrossRef]
118. Singh, P.; Pal, S.K.; Alex, A.; Agarwal, N. Development of PROSTVAC immunotherapy in prostate cancer. *Future Oncol.* **2015**, *11*, 2137–2148. [CrossRef]
119. Pushpakom, S.; Iorio, F.; Eyers, P.A.; Escott, K.J.; Hopper, S.; Wells, A.; Doig, A.; Guilliams, T.; Latimer, J.; McNamee, C.; et al. Drug repurposing: Progress, challenges and recommendations. *Nat. Rev. Drug Discov.* **2019**, *18*, 41–58. [CrossRef]
120. Rudrapal, M.; Khairnar, S.J.; Jadhav, A.G. Drug Repurposing (DR): An emerging approach in drug discovery. In *Drug Repurposing: Hypothesis, Molecular Aspects and Therapeutic Applications*; Intechopen: London, UK, 2020. [CrossRef]
121. Gillessen, S.; Gilson, C.; James, N.; Adler, A.; Sydes, M.; Clarke, N. Repurposing Metformin as Therapy for Prostate Cancer within the STAMPEDE Trial Platform. *Eur. Urol.* **2016**, *70*, 906–908. [CrossRef]
122. Bahmad, H.F.; Demus, T.; Moubarak, M.M.; Daher, D.; Moreno, J.C.A.; Polit, F.; Lopez, O.; Merhe, A.; Abou-Kheir, W.; Nieder, A.M.; et al. Overcoming Drug Resistance in Advanced Prostate Cancer by Drug Repurposing. *Med. Sci.* **2022**, *10*, 15. [CrossRef] [PubMed]
123. Braga-Basaria, M.; Muller, D.C.; Carducci, M.A.; Dobs, A.S.; Basaria, S. Lipoprotein profile in men with prostate cancer undergoing androgen deprivation therapy. *Int. J. Impot. Res.* **2006**, *18*, 494–498. [CrossRef] [PubMed]
124. Watson, P.A.; Arora, V.K.; Sawyers, C.L. Emerging mechanisms of resistance to androgen receptor inhibitors in prostate cancer. *Nat. Cancer* **2015**, *15*, 701–711. [CrossRef] [PubMed]
125. Giacinti, S.; Poti, G.; Roberto, M.; Macrini, S.; Bassanelli, M.; Di Pietro, F.; Aschelter, A.M.; Ceribelli, A.; Ruggeri, E.M.; Marchetti, P. Molecular Basis of Drug Resistance and Insights for New Treatment Approaches in mCRPC. *Anticancer Res.* **2018**, *38*, 6029–6039. [CrossRef] [PubMed]
126. Hwang, C. Overcoming docetaxel resistance in prostate cancer: A perspective review. *Ther. Adv. Med. Oncol.* **2012**, *4*, 329–340. [CrossRef] [PubMed]
127. Zanger, U.M.; Schwab, M. Cytochrome P450 enzymes in drug metabolism: Regulation of gene expression, enzyme activities, and impact of genetic variation. *Pharmacol. Ther.* **2013**, *138*, 103–141. [CrossRef]
128. Kinoshita, Y.; Singh, A.; Rovito, P.M.; Wang, C.Y.; Haas, G.P. Double Primary Cancers of the Prostate and Bladder: A Literature Review. *Clin. Prostate Cancer* **2004**, *3*, 83–86. [CrossRef]
129. Tokizane, T.; Shiina, H.; Igawa, M.; Enokida, H.; Urakami, S.; Kawakami, T.; Ogishima, T.; Okino, S.T.; Li, L.-C.; Tanaka, Y.; et al. Cytochrome *P*450 1B1 Is Overexpressed and Regulated by Hypomethylation in Prostate Cancer. *Clin. Cancer Res.* **2005**, *11*, 5793–5801. [CrossRef]
130. Rochat, B.; Morsman, J.M.; Murray, G.I.; Figg, W.D.; McLeod, H.L. Human CYP1B1 and anticancer agent metabolism: Mechanism for tumor-specific drug inactivation? *J. Pharmacol. Exp. Ther.* **2001**, *296*, 537–541.
131. DeVore, N.M.; Scott, E.E. Structures of cytochrome P450 17A1 with prostate cancer drugs abiraterone and TOK-001. *Nature* **2012**, *482*, 116–119. [CrossRef]
132. Lam, T.; Birzniece, V.; McLean, M.; Gurney, H.; Hayden, A.; Cheema, B.S. The Adverse Effects of Androgen Deprivation Therapy in Prostate Cancer and the Benefits and Potential Anti-oncogenic Mechanisms of Progressive Resistance Training. *Sports Med.-Open* **2020**, *6*, 13–14. [CrossRef]
133. Yu, J.; Gritsina, G.; Gao, W.-Q. Transcriptional repression by androgen receptor: Roles in castration-resistant prostate cancer. *Asian J. Androl.* **2019**, *21*, 215–223. [CrossRef] [PubMed]
134. Zhou, Y.; Bolton, E.C.; Jones, J.O. Androgens and androgen receptor signaling in prostate tumorigenesis. *J. Mol. Endocrinol.* **2015**, *54*, R15–R29. [CrossRef] [PubMed]
135. Cimadamore, A.; Mazzucchelli, R.; Lopez-Beltran, A.; Massari, F.; Santoni, M.; Scarpelli, M.; Cheng, L.; Montironi, R. Prostate Cancer in 2021: Novelties in Prognostic and Therapeutic Biomarker Evaluation. *Cancers* **2021**, *13*, 3471. [CrossRef]
136. Shiao, S.L.; Chu, G.C.-Y.; Chung, L.W. Regulation of prostate cancer progression by the tumor microenvironment. *Cancer Lett.* **2016**, *380*, 340–348. [CrossRef] [PubMed]
137. Sejda, A.; Sigorski, D.; Gulczyński, J.; Wesołowski, W.; Kitlińska, J.; Izycka-Świeszewska, E. Complexity of Neural Component of Tumor Microenvironment in Prostate Cancer. *Pathobiology* **2020**, *87*, 87–99. [CrossRef]
138. Arora, H.; Panara, K.; Kuchakulla, M.; Kulandavelu, S.; Burnstein, K.L.; Schally, A.V.; Hare, J.M.; Ramasamy, R. Alterations of tumor microenvironment by nitric oxide impedes castration-resistant prostate cancer growth. *Proc. Natl. Acad. Sci. USA* **2018**, *115*, 11298–11303. [CrossRef]
139. Hussein, M.-R.A.; Al-Assiri, M.; Musalam, A.O. Phenotypic characterization of the infiltrating immune cells in normal prostate, benign nodular prostatic hyperplasia and prostatic adenocarcinoma. *Exp. Mol. Pathol.* **2009**, *86*, 108–113. [CrossRef]
140. Gurel, B.; Lucia, M.S.; Thompson, I.M.; Goodman, P.J.; Tangen, C.M.; Kristal, A.R.; Parnes, H.L.; Hoque, A.; Lippman, S.M.; Sutcliffe, S.; et al. Chronic Inflammation in Benign Prostate Tissue Is Associated with High-Grade Prostate Cancer in the Placebo Arm of the Prostate Cancer Prevention Trial. *Cancer Epidemiol. Biomark. Prev.* **2014**, *23*, 847–856. [CrossRef]
141. De Marzo, A.M.; Platz, E.A.; Sutcliffe, S.; Xu, J.; Grönberg, H.; Drake, C.G.; Nakai, Y.; Isaacs, W.B.; Nelson, W.G. Inflammation in prostate carcinogenesis. *Nat. Cancer* **2007**, *7*, 256–269. [CrossRef]

142. Worthington, J.J.; Fenton, T.M.; Czajkowska, B.I.; Klementowicz, J.E.; Travis, M.A. Regulation of TGFβ in the immune system: An emerging role for integrins and dendritic cells. *Immunobiology* **2012**, *217*, 1259–1265. [CrossRef] [PubMed]
143. Hägglöf, C.; Bergh, A. The Stroma—A Key Regulator in Prostate Function and Malignancy. *Cancers* **2012**, *4*, 531–548. [CrossRef] [PubMed]
144. Snaterse, G.; Visser, J.A.; Arlt, W.; Hofland, J. Circulating steroid hormone variations throughout different stages of prostate cancer. *Endocr.-Relat. Cancer* **2017**, *24*, R403–R420. [CrossRef]
145. Di Zazzo, E.; Galasso, G.; Giovannelli, P.; Di Donato, M.; Castoria, G. Estrogens and Their Receptors in Prostate Cancer: Therapeutic Implications. *Front. Oncol.* **2018**, *8*, 2. [CrossRef]
146. Rahman, H.P.; Hofland, J.; Foster, P.A. In touch with your feminine side: How oestrogen metabolism impacts prostate cancer. *Endocr.-Relat. Cancer* **2016**, *23*, R249–R266. [CrossRef]
147. Ellem, S.J.; Risbridger, G.P. Aromatase and regulating the estrogen:androgen ratio in the prostate gland. *J. Steroid Biochem. Mol. Biol.* **2010**, *118*, 246–251. [CrossRef] [PubMed]
148. Warner, M.; Huang, B.; Gustafsson, J.-A. Estrogen Receptor β as a Pharmaceutical Target. *Trends Pharmacol. Sci.* **2017**, *38*, 92–99. [CrossRef]
149. Bonkhoff, H. Estrogen receptor signaling in prostate cancer: Implications for carcinogenesis and tumor progression. *Prostate* **2018**, *78*, 2–10. [CrossRef]
150. Takizawa, I.; Lawrence, M.G.; Balanathan, P.; Rebello, R.; Pearson, H.B.; Garg, E.; Pedersen, J.; Pouliot, N.; Nadon, R.; Watt, M.J.; et al. Estrogen receptor alpha drives proliferation in PTEN-deficient prostate carcinoma by stimulating survival signaling, MYC expression and altering glucose sensitivity. *Oncotarget* **2015**, *6*, 604–616. [CrossRef]
151. Bardin, A.; Boulle, N.; Lazennec, G.; Vignon, F.; Pujol, P. Loss of ERβ expression as a common step in estrogen-dependent tumor progression. *Endocr.-Relat. Cancer* **2004**, *11*, 537–551. [CrossRef]
152. Christoforou, P.; Christopoulos, P.F.; Koutsilieris, M. The Role of Estrogen Receptor β in Prostate Cancer. *Mol. Med.* **2014**, *20*, 427–434. [CrossRef] [PubMed]
153. Okaiyeto, K.; Oguntibeju, O. African Herbal Medicines: Adverse Effects and Cytotoxic Potentials with Different Therapeutic Applications. *Int. J. Environ. Res. Public Health* **2021**, *18*, 5988. [CrossRef] [PubMed]
154. Kuruppu, A.I.; Paranagama, P.; Goonasekara, C.L. Medicinal plants commonly used against cancer in traditional medicine formulae in Sri Lanka. *Saudi Pharm. J.* **2019**, *27*, 565–573. [CrossRef]
155. Matowa, P.R.; Gundidza, M.; Gwanzura, L.; Nhachi, C.F.B. A survey of ethnomedicinal plants used to treat cancer by traditional medicine practitioners in Zimbabwe. *BMC Complement. Med. Ther.* **2020**, *20*, 278. [CrossRef] [PubMed]
156. Ahmadibeni, Y.; Karim, K.; Boadi, W. Abstract 2180: Triphenylmethanol conjugates of leuprorelin asanti-cancer prodrugs. *Cancer Res.* **2017**, *77*, 2180. [CrossRef]
157. Hashemi, S.R.; Davoodi, H. Herbal plants and their derivatives as growth and health promoters in animal nutrition. *Veter-Res. Commun.* **2011**, *35*, 169–180. [CrossRef] [PubMed]
158. Kumar, G.P.; Khanum, F. Neuroprotective potential of phytochemicals. *Pharmacogn. Rev.* **2012**, *6*, 81–90. [CrossRef] [PubMed]
159. Alara, J.A.; Alara, O.R. ETHNO-MEDICINAL POTENTIALS AND PHYTOCHEMICAL PROPERTIES OF Aloe vera: A REVIEW. *J. Chem. Eng. Ind. Biotechnol.* **2019**, *5*, 57–73. [CrossRef]
160. Crocetto, F.; di Zazzo, E.; Buonerba, C.; Aveta, A.; Pandolfo, S.D.; Barone, B.; Trama, F.; Caputo, V.F.; Scafuri, L.; Ferro, M.; et al. Kaempferol, Myricetin and Fisetin in Prostate and Bladder Cancer: A Systematic Review of the Literature. *Nutrients* **2021**, *13*, 3750. [CrossRef]
161. Iqbal, J.; Abbasi, B.H.; Mahmood, T.; Kanwal, S.; Ali, B.; Shah, S.A.; Khalil, A.T. Plant-derived anticancer agents: A green anticancer approach. *Asian Pac. J. Trop. Biomed.* **2017**, *7*, 1129–1150. [CrossRef]
162. Gori, J.L.; Hsu, P.; Maeder, M.L.; Shen, S.; Welstead, G.G.; Bumcrot, D. Delivery and Specificity of CRISPR/Cas9 Genome Editing Technologies for Human Gene Therapy. *Hum. Gene Ther.* **2015**, *26*, 443–451. [CrossRef] [PubMed]
163. Chen, Y.H.; Keiser, M.S.; Davidson, B.L. Viral Vectors for Gene Transfer. *Curr. Protoc. Mouse Biol.* **2018**, *8*, e58. [CrossRef] [PubMed]
164. Jan, R.; Chaudhry, G.-E. Understanding Apoptosis and Apoptotic Pathways Targeted Cancer Therapeutics. *Adv. Pharm. Bull.* **2019**, *9*, 205–218. [CrossRef] [PubMed]
165. Verma, A.K.; Mandal, S.; Tiwari, A.; Monachesi, C.; Catassi, G.N.; Srivastava, A.; Gatti, S.; Lionetti, E.; Catassi, C. Current Status and Perspectives on the Application of CRISPR/Cas9 Gene-Editing System to Develop a Low-Gluten, Non-Transgenic Wheat Variety. *Foods* **2021**, *10*, 2351. [CrossRef] [PubMed]
166. Singh, V.; Khurana, A.; Navik, U.; Allawadhi, P.; Bharani, K.K.; Weiskirchen, R. Apoptosis and Pharmacological Therapies for Targeting Thereof for Cancer Therapeutics. *Sci* **2022**, *4*, 15. [CrossRef]
167. Sharifi, N.; Salmaninejad, A.; Ferdosi, S.; Bajestani, A.N.; Khaleghiyan, M.; Estiar, M.A.; Jamali, M.; Nowroozi, M.R.; Shakoori, A. HER2 gene amplification in patients with prostate cancer: Evaluating a CISH-based method. *Oncol. Lett.* **2016**, *12*, 4651–4658. [CrossRef]
168. Rossini, A.; Giussani, M.; Ripamonti, F.; Aiello, P.; Regondi, V.; Balsari, A.; Triulzi, T.; Tagliabue, E. Combined targeting of EGFR and HER2 against prostate cancer stem cells. *Cancer Biol. Ther.* **2020**, *21*, 463–475. [CrossRef]
169. Jiang, F.; Liang, Y.; Wei, W.; Zou, C.; Chen, G.; Liu, Z.; Han, Z.; Zhu, J.; Zhong, W. Functional classification of prostate cancerassociated miRNAs through CRISPR/Cas9mediated gene knockout. *Mol. Med. Rep.* **2020**, *22*, 3777–3784. [CrossRef]

170. Yao, Y.; Zhou, Y.; Liu, L.; Xu, Y.; Chen, Q.; Wang, Y.; Wu, S.; Deng, Y.; Zhang, J.; Shao, A. Nanoparticle-Based Drug Delivery in Cancer Therapy and Its Role in Overcoming Drug Resistance. *Front. Mol. Biosci.* **2020**, *7*, 193. [CrossRef]
171. Desai, N.; Momin, M.; Khan, T.; Gharat, S.; Ningthoujam, R.S.; Omri, A. Metallic nanoparticles as drug delivery system for the treatment of cancer. *Expert Opin. Drug Deliv.* **2021**, *18*, 1261–1290. [CrossRef]
172. Mount Sinai School of Medicine. Gold Nanoparticles Shown to Be Safe and Effective Treatment for Prostate Cancer. 2019. Available online: https://www.sciencedaily.com/releases/2019/08/190827123513.htm (accessed on 21 July 2022).
173. Sechi, M.; Sanna, V.; Pala, N. Targeted therapy using nanotechnology: Focus on cancer. *Int. J. Nanomed.* **2014**, *9*, 467–483. [CrossRef] [PubMed]
174. Gregg, J.R.; Thompson, T.C. Considering the potential for gene-based therapy in prostate cancer. *Nat. Rev. Urol.* **2021**, *18*, 170–184. [CrossRef] [PubMed]
175. Balon, K.; Sheriff, A.; Jacków, J.; Łaczmański, Ł. Targeting Cancer with CRISPR/Cas9-Based Therapy. *Int. J. Mol. Sci.* **2022**, *23*, 573. [CrossRef] [PubMed]
176. Xu, H.; Kita, Y.; Bang, U.; Gee, P.; Hotta, A. Optimized electroporation of CRISPR-Cas9/gRNA ribonucleoprotein complex for selection-free homologous recombination in human pluripotent stem cells. *STAR Protoc.* **2021**, *2*, 100965. [CrossRef]
177. Rosenblum, D.; Gutkin, A.; Kedmi, R.; Ramishetti, S.; Veiga, N.; Jacobi, A.M.; Schubert, M.S.; Friedmann-Morvinski, D.; Cohen, Z.R.; Behlke, M.A.; et al. CRISPR-Cas9 genome editing using targeted lipid nanoparticles for cancer therapy. *Sci. Adv.* **2020**, *6*, eabc9450. [CrossRef]
178. Ye, R.; Pi, M.; Cox, J.V.; Nishimoto, S.K.; Quarles, L.D. CRISPR/Cas9 targeting of GPRC6A suppresses prostate cancer tumorigenesis in a human xenograft model. *J. Exp. Clin. Cancer Res.* **2017**, *36*, 90. [CrossRef]
179. Tsujino, T.; Komura, K.; Inamoto, T.; Azuma, H. CRISPR Screen Contributes to Novel Target Discovery in Prostate Cancer. *Int. J. Mol. Sci.* **2021**, *22*, 12777. [CrossRef]
180. Friedman, A.D.; Claypool, S.E.; Liu, R. The smart targeting of nanoparticles. *Curr. Pharm. Des.* **2013**, *19*, 6315–6329. [CrossRef]
181. Li, K.; Zhan, W.; Chen, Y.; Jha, R.K.; Chen, X. Docetaxel and Doxorubicin Codelivery by Nanocarriers for Synergistic Treatment of Prostate Cancer. *Front. Pharmacol.* **2019**, *10*, 1436. [CrossRef]
182. Autio, K.A.; Dreicer, R.; Anderson, J.; Garcia, J.A.; Alva, A.; Hart, L.L.; Milowsky, M.I.; Posadas, E.M.; Ryan, C.J.; Graf, R.P.; et al. Safety and Efficacy of BIND-014, a Docetaxel Nanoparticle Targeting Prostate-Specific Membrane Antigen for Patients With Metastatic Castration-Resistant Prostate Cancer: A Phase 2 Clinical Trial. *JAMA Oncol.* **2018**, *4*, 1344–1351. [CrossRef]
183. Johannsen, M.; Thiesen, B.; Wust, P.; Jordan, A. Magnetic nanoparticle hyperthermia for prostate cancer. *Int. J. Hyperth.* **2010**, *26*, 790–795. [CrossRef] [PubMed]
184. He, M.-H.; Chen, L.; Zheng, T.; Tu, Y.; He, Q.; Fu, H.-L.; Lin, J.-C.; Zhang, W.; Shu, G.; He, L.; et al. Potential Applications of Nanotechnology in Urological Cancer. *Front. Pharmacol.* **2018**, *9*, 745. [CrossRef] [PubMed]
185. Yap, T.A.; Smith, A.D.; Ferraldeschi, R.; Al-Lazikani, B.; Workman, P.; De Bono, J.S. Drug discovery in advanced prostate cancer: Translating biology into therapy. *Nat. Rev. Drug Discov.* **2016**, *15*, 699–718. [CrossRef] [PubMed]
186. Tüfekci, K.U.; Öner, M.G.; Meuwissen, R.L.J.; Genç, Ş. The Role of MicroRNAs in Human Diseases. In *miRNomics: MicroRNA Biology and Computational Analysis*; Humana Press: Totowa, NJ, USA, 2013; pp. 33–50. [CrossRef]
187. Palop, J.J.; Mucke, L.; Roberson, E.D. Quantifying Biomarkers of Cognitive Dysfunction and Neuronal Network Hyperexcitability in Mouse Models of Alzheimer's Disease: Depletion of Calcium-Dependent Proteins and Inhibitory Hippocampal Remodeling. In *Alzheimer's Disease and Frontotemporal Dementia*; Humana Press: Totowa, NJ, USA, 2010; Volume 670, pp. 245–262. [CrossRef]
188. Johnson, T.M. Perspective on Precision Medicine in Oncology. *Pharmacother. J. Hum. Pharmacol. Drug Ther.* **2017**, *37*, 988–989. [CrossRef]
189. Lancaster, E.M.; Jablons, D.; Kratz, J.R. Applications of Next-Generation Sequencing in Neoantigen Prediction and Cancer Vaccine Development. *Genet. Test. Mol. Biomark.* **2020**, *24*, 59–66. [CrossRef]
190. Kamps, R.; Brandão, R.D.; van den Bosch, B.J.; Paulussen, A.D.; Xanthoulea, S.; Blok, M.J.; Romano, A. Next-Generation Sequencing in Oncology: Genetic Diagnosis, Risk Prediction and Cancer Classification. *Int. J. Mol. Sci.* **2017**, *18*, 308. [CrossRef]
191. Wakai, T.; Prasoon, P.; Hirose, Y.; Shimada, Y.; Ichikawa, H.; Nagahashi, M. Next-generation sequencing-based clinical sequencing: Toward precision medicine in solid tumors. *Int. J. Clin. Oncol.* **2019**, *24*, 115–122. [CrossRef]
192. Thadani-Mulero, M.; Portella, L.; Sun, S.; Sung, M.; Matov, A.; Vessella, R.L.; Corey, E.; Nanus, D.M.; Plymate, S.R.; Giannakakou, P. Androgen Receptor Splice Variants Determine Taxane Sensitivity in Prostate Cancer. *Cancer Res.* **2014**, *74*, 2270–2282. [CrossRef]
193. Chen, Y.; Chi, P.; Rockowitz, S.; Iaquinta, P.J.; Shamu, T.; Shukla, S.; Gao, D.; Sirota, I.; Carver, B.S.; Wongvipat, J.; et al. ETS factors reprogram the androgen receptor cistrome and prime prostate tumorigenesis in response to PTEN loss. *Nat. Med.* **2013**, *19*, 1023–1029. [CrossRef]
194. Yadav, S.S.; Li, J.; Lavery, H.J.; Yadav, K.K.; Tewari, A.K. Next-generation sequencing technology in prostate cancer diagnosis, prognosis, and personalized treatment. *Urol. Oncol. Semin. Orig. Investig.* **2015**, *33*, 267.e1–267.e13. [CrossRef]
195. Friedman, A.A.; Letai, A.; Fisher, D.E.; Flaherty, K.T. Precision medicine for cancer with next-generation functional diagnostics. *Nat. Cancer* **2015**, *15*, 747–756. [CrossRef] [PubMed]
196. Meador, C.B.; Lovly, C. Liquid biopsies reveal the dynamic nature of resistance mechanisms in solid tumors. *Nat. Med.* **2015**, *21*, 663–665. [CrossRef] [PubMed]
197. Lianos, G.D.; Mangano, A.; Cho, W.C.; Dionigi, G.; Roukos, D.H. Circulating tumor DNA: New horizons for improving cancer treatment. *Future Oncol.* **2015**, *11*, 545–548. [CrossRef] [PubMed]

198. Pajares, M.J.; Ezponda, T.; Catena, R.; Calvo, A.; Pio, R.; Montuenga, L.M. Alternative splicing: An emerging topic in molecular and clinical oncology. *Lancet Oncol.* **2007**, *8*, 349–357. [CrossRef]
199. Yang, L.; Luquette, L.J.; Gehlenborg, N.; Xi, R.; Haseley, P.S.; Hsieh, C.H.; Zhang, C.; Ren, X.; Protopopov, A.; Chin, L.; et al. Diverse mechanisms of somatic structural variations in human cancer genomes. *Cell* **2013**, *153*, 919–929. [CrossRef]

Research article submitted to the journal Heliyon: Article still under review.

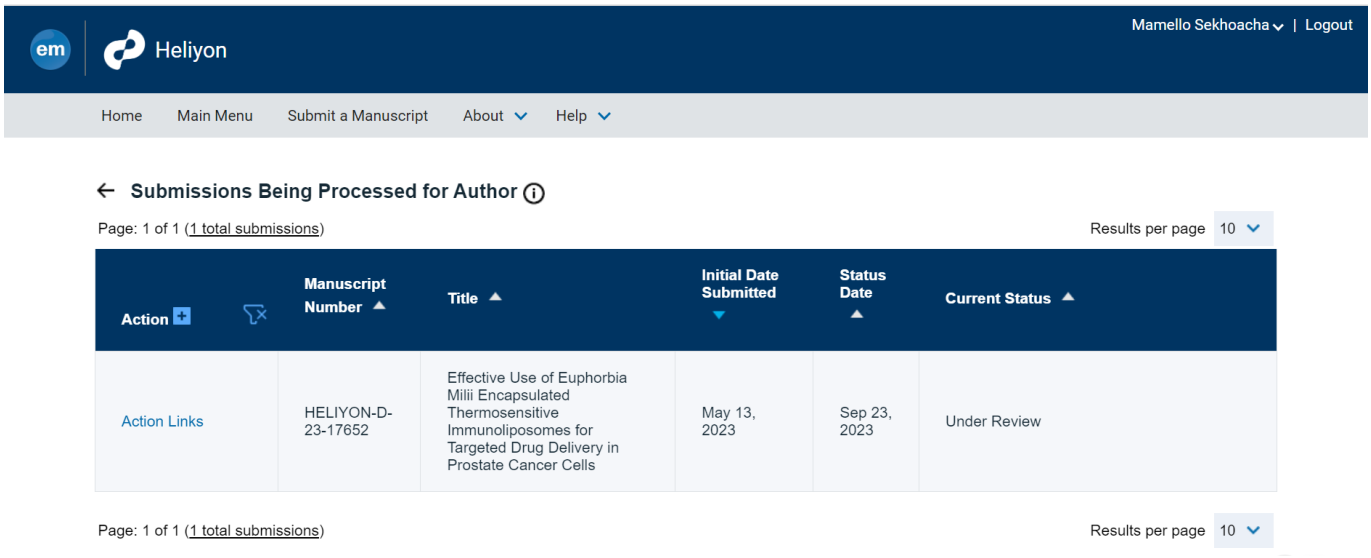

Article

Effective Use of *Euphorbia Milii* Encapsulated Thermosensitive Immunoliposomes for Targeted DrugDelivery in Prostate Cancer Cells

Keamogetswe Riet [1], Ayodeji Adegoke [2,3], Samson Mashele [1] and Mamello Sekhoacha [2,*]

1Department of Health Sciences, Central University of Technology, Bloemfontein 9300, Republic of South Africa.

[2] Department of Pharmacology, University of the Free State, P.O Box 339,Bloemfontein 9300, Republic of South Africa

[3] Cancer Research and Molecular Biology Laboratories, Department of Biochemistry,College of Medicine, University of Ibadan, Ibadan 200005, Nigeria.

*Correspondence: sekhoachamp@ufs.ac.za

Abstract: The delivery of anticancer drugs using nanotechnology is a promising approach aimed at improving therapeutic efficacy and reducing the toxicity of chemotherapeutic agents. Liposomes were prepared using HSPC: DSPE-PEG-2000: DSPE-PEG2000-maleimide in the ratio of 4:1:0.2 and conjugated with a PSA antibody. The *Euphorbia Milii* extract (EME) and Docetaxel encapsulated temperature-sensitive immunoliposomes were investigated for their activity against the prostate cancer LNCap and DU145 cell lines. *Euphorbia Milii* leaves, roots and stems were screened against the DU145 cells, *Euphorbia milii* Dichloromethane (DCM) root extract was found to be potent against the DU145 cells. This active extract was further screened against the LNCap cells inhibiting more than 50% of cells at 10 µg/mL. The EME and docetaxel incorporated immunoliposomes were active against the LNCap cells when exposed to hyperthermia at 39-40 °C. The liposomes not exposed to heat were inactive against the LNCap cells. The liposomes will further be investigated *in-vivo*.

Keywords: Docetaxel; Liposomes; Prostate-specific membrane;Targeted drug delivery; Thermosensitive; Immunosensitive

1. Introduction

One in fifteen men in South Africa has a high chance of developing prostate cancer in their lifetime. Globally prostate cancer rate of occurrence is different in a large number of geographical regions and races. African men have the most reported incidence rates of prostate cancer in the world [1]. Prostate cancer is projected to exponentially grow globally to 1.7 million new cases and approximately 499,000 lethalities by 2030 because of the rapidly increasing population and the large population of men who will be older than 65 years [2]. Prostate cancer ensues when cells of the prostate gland grow uncontrollably. Prostate cancer can arise from epithelial cells in the secretory glands which line the prostatic ducts [3]. The incidence of the disease has exponentially increased over the past 10 years [4]. Treatments such as chemotherapy, surgery, hormone therapy, and radiation therapy have been successful over the years for treatment of cancers, including prostate cancer. The big challenge is the side effects on prostate cancer patients, killing normal cells, and causing erectile dysfunction [5]. Nanotechnology has attracted much interest over the years in drug delivery, because of its unique properties that increase drug efficacy, selectivity, retention time, and reduction of cytotoxicity [6]. The use of nanotechnology in the treatment of cancer appears to be a promising alternative with reduced consequential side effects [7]. Immunoliposomes are phospholipid-based nanosized vehicles that have targeting molecules that help them bind to surface markers that are found on different types of tumors [8]. Liposomal nanoparticles have added advantages as drug delivery systems; they increase drug delivery, protect the drug from degradation, stabilize therapeutic compounds and increase drug performance in solid tumors [9]. Liposomes can be sensitive and responsive to stimuli such as pH, light; redox, matrixmetalloproteinase, and temperature [10]. Lipids have a certain temperature range at which their phases exchange commonly known as transition temperature (TC) [11]. The transition temperature has an impact on the encapsulation efficiency, and the stability of the liposomes. The Phosphatidylcholine (PC) is the most important phospholipid in Hydrosoy (HSPC). liposomal membranes consist of PC in a lamellar phase. The PC acyl chain degree of saturation as well as chain length largely affects the phase of the liposomal membrane. When hyperthermia is applied above the transition temperature (TC), PCs change from a solid gel to a liquid phase as the number of gauche conformations in the acyl chains increases from the trans-state of the solid gel phase. This results in a change in the membrane from gel to liquid phase allowing drugs to be released from the liposomes. When 10% of DSPE-PEG2000 is added to the liposomal formulation, thermosensitive, sterically stabilized liposomes can be obtained [12] Therefore temperature-sensitive liposomes can enhance the effectiveness of drugs and treatment outcomes, through the temperature-controlled release of the drug at the cancer site. This is achieved when the lipid is triggered to change from a stable phase to gross instability at the target site [13]. The concentration of the drugs incorporated in liposomes can be determined by various techniques such as UV–visible detection and HPLC, depending on the active compound which is inside the liposomes [14]. Thermo-sensitive liposomes release the drug when exposed to hyperthermia at 39-40°C [15]. Hyperthermia plays a very important role in cancer treatment because it increases vascular permeability, and interstitial transport and allows liposomes to release significant amounts of the drug within a very short period of being exposed to heat [15]. Anticancer constituents are usually encapsulated in liposomes. The encapsulation of the active drug into the lipid bilayer protects it from enzymatic degradation and chemical and immunologic inactivation [17]. Prostate cancer has prostate-specific membrane antigen (PSMA) which is found on all different types of prostatic tissue. PSMA increases the therapeutic chances of nanoparticles in prostate cancer treatment [18]. Chemotherapeutic drugs are limited by the fact that they are unable to reach the cancerous site in sufficient quantity to be effective. They need to be administered in high doses which ultimately lead to adverse side effects such as targeting normal cells [19]. To overcome these challenges the development of target-specific and controlled drug-release nano-delivery systems was explored.

One in fifteen men in South Africa has a high chance of developing prostate cancer in their lifetime. Globally prostate cancer rate of occurrence is different in a large number of geographical regions and races. African men have the most reported incidence rates of prostate cancer in the world [1]. Prostate cancer is projected to exponentially grow globally to 1.7 million new cases and approximately 499,000 lethalities by 2030 because of the rapidly increasing population and the large population of men who will be older than 65 years [2]. Prostate cancer ensues when cells of the prostate gland grow uncontrollably. Prostate cancer can arise from epithelial cells in the secretory glands which line the prostatic ducts [3]. The incidence of the disease has exponentially increased over the past 10 years [4]. Treatments such as chemotherapy, surgery, hormone therapy, and radiation therapy have been successful over the years for treatment of cancers, including prostate cancer. The big challenge is the side effects on prostate cancer patients, killing normal cells, and causing erectile dysfunction [5]. Nanotechnology has attracted much interest over the years in drug delivery, because of its unique properties that increase drug efficacy, selectivity, retention time, and reduction of cytotoxicity [6]. The use of nanotechnology in the treatment of cancer appears to be a promising alternative with reduced consequential side effects [7]. Immunoliposomes are phospholipid-based nanosized vehicles that have targeting molecules that help them bind to surface markers that are found on different types of tumors [8]. Liposomal nanoparticles have added advantages as drug delivery systems; they increase drug delivery, protect the drug from degradation, stabilize therapeutic compounds and increase drug performance in solid tumors [9]. Liposomes can be sensitive and responsive to stimuli such as pH, light; redox, matrixmetalloproteinase, and temperature [10]. Lipids have a certain temperature range at which their phases exchange commonly known as transition temperature (TC) [11]. The transition temperature has an impact on the encapsulation efficiency, and the stability of the liposomes. The Phosphatidylcholine (PC) is the most important phospholipid in Hydrosoy (HSPC). liposomal membranes consist of PC in a lamellar phase. The PC acyl chain degree of saturation as well as chain length largely affects the phase of the liposomal membrane. When hyperthermia is applied above the transition temperature (TC), PCs change from a solid gel to a liquid phase as the number of gauche conformations in the acyl chains increases from the trans-state of the solid gel phase. This results in a change in the membrane from gel to liquid phase allowing drugs to be released from the liposomes. When 10% of DSPE-PEG2000 is added to the liposomal formulation, thermosensitive, sterically stabilized liposomes can be obtained [12] Therefore temperature-sensitive liposomes can enhance the effectiveness of drugs and treatment outcomes, through the temperature-controlled release of the drug at the cancer site. This is achieved when the lipid is triggered to change from a stable phase to gross instability at the target site [13]. The concentration of the drugs incorporated in liposomes can be determined by various techniques such as UV–visible detection and HPLC, depending on the active compound which is inside the liposomes [14]. Thermo-sensitive liposomes release the drug when exposed to hyperthermia at 39-40°C [15]. Hyperthermia plays a very important role in cancer treatment because it increases vascular permeability, and interstitial transport and allows liposomes to release significant amounts of the drug within a very short period of being exposed to heat [15]. Anticancer constituents are usually encapsulated in liposomes. The encapsulation of the active drug into the lipid bilayer protects it from enzymatic degradation and chemical and immunologic inactivation [17]. Prostate cancer has prostate-specific membrane antigen (PSMA) which is found on all different types of prostatic tissue. PSMA increases the therapeutic chances of nanoparticles in prostate cancer treatment [18]. Chemotherapeutic drugs are limited by the fact that they are unable to reach the cancerous site in sufficient quantity to be effective. They need to be administered in high doses which ultimately lead to adverse side effects such as targeting normal cells [19]. To overcome these challenges the development of target-specific and controlled drug-release nano-delivery systems was explored.

The EM plant, commonly known as Christ of thorns is a woody, spiny succulent plant that can grow up to 1.8 m high [20]. The plant belongs to the order Malpighiales, the family Euphorbiaceae and the Genus species *Euphorbia Milii*. The family Euphorbiaceae is one of the largest Genus of medicinal plants distributed in tropical countries in Asia and Africa [21]. The EM plant has green leaves, and flowers ranging in colors like red, pink, white, and yellow. This plant is well-known for cancer therapy [22]. The plant is known for the presence of milky latex which is toxic. The stems, leaves, flowers, and roots are used in the treatment of cancer [23]. EM grows in bush and forest habitats, but usually in rocky areas (usually granite formations). The plant is native to southern and western Madagascar. The plant is also found in other countries like Brazil and Pakistan [24]. EM is widely cultivated in Africa and it is used for various medicinal uses as well as research in the field of ethnopharmacology [25]. Regardless of the number of research articles reporting the therapeutic uses of EM, data regarding its bioactivity studies related to cancer treatment is very limited. The plant is also known to have antidiabetic, and antimicrobial properties. These properties are attributed to different phytochemicals present in the plant [26]. Phytochemical studies of EM have shown the presence of flavonoids, triterpenes β-sitosterol, cycloartenol, and β-amyrin acetate [27]. This study was conducted with liposomes encapsulating EME and two prostate cancer standard drugs doxorubicin and docetaxel. Doxorubicin and docetaxel are used for the treatment of prostate cancer including the treatment of various other cancers. The combined effect of the two drugs on prostate cancer cells has been largely studied [20]. The experiments in this study were initiated with doxorubicin and continued with docetaxel because docetaxel is the first-line standard drug used for prostate cancer in South Africa. PSMA was used to address target specificity. The Liposomes used were conjugated with a specific monoclonal antibody, which binds to the extracellular surface of the extracellular domain of the PSMA to ensure that the liposomes bind only to prostate-specific cells. Bound liposomes were then prompted to release sufficient amounts of their contents when exposed to heat stimuli.

2. Materials and Methods

Plant collection and extraction

The plant was collected from Gariep nursery situated at 309 Cliffendale Dr, Faerie Glen, Pretoria, 0081, South Africa on 11 November 2020 at 11:00 (SAST) and identified by a taxonomist Dr. Pienaar, Department of Botany, University of the Free state, Bloemfontein, South Africa.

The plant was washed to remove debris, cut into small pieces, and left to dry at room temperature then ground to a fine powder. Nine grams (9 g) of the powder was suspended in 150 mL hexane, dichloromethane, and methanol sequentially. The mixtures were placed in a rotary shaker for 48 h at 25 °C at the solid: solvent ratio of 1:16. Each mixture was then filtered using filter paper (whatman® Maidstone). Filtrates were concentrated under decreased pressure at 45 °C at 150 rpm using a rotary vacuum evaporator and transferred into a pre-weighed clean vial and shade dried (without direct exposure to sunlight) at room temperature, it was thereafter stored at 4 °C until required for use.

2.1. Cell culture

Human prostate carcinoma cells LNCAP and DU145 cells were cultured in DMEM: F12 and DMEM medium respectively, supplemented with 10% fetal bovine serum (FBS), incubated at 37 °C, and 5% carbon dioxide (CO_2) until 80% confluence is reached. Following the methods by [28] [24], cell viability was determined by trypan blue staining using the automated cell counter (Cell countess TM) to obtain a cell

concentration of 1 × 10^5 cells per well, in a 96-well plate which was used in all experiments. The cells were plated and incubated for 24 h to adhere. After 24 h incubation, the media was removed and cells were treated with 100 µL of 100, 10, and 1 µg/mL of extracts in triplicates.

2.2. Cytotoxic activity of docetaxel-loaded liposomes and EM liposomes.

To evaluate the cytotoxic activity of temperature-sensitive immunoliposomes encapsulation, the EM DCM roots extract as well as the prostate cancer standard drug (docetaxel), cytotoxicity was measured using the MTT assay in the LNCap cell line. This was done with and without exposure to hyperthermia. To ensure that the drugs were becoming bioavailable intracellularly, mild hyperthermia was applied to trigger release from liposomes after cellular uptake. To study the effect of drug release beyond the transition temperature of liposomes on cell viability, a specific heating strategy was followed. Cells along with the formulations were incubated at 39–40 °C for 15 min followed by incubation at 37 °C for 48 h. The control experiment included no application of hyperthermia. The cells were then treated with MTT solution for 4 h. The formazan crystals formed were solubilized using DMSO and absorbance was measured using a multimode plate reader at 540 nm [29].

2.3. Synthesis of heat-sensitive liposomes

Liposomes were prepared and modified using the thin film method. Briefly, in a round-bottom flask, liposomes consisting of HSPC: DSPE-PEG-2000: DSPE-PEG2000-maleimide in the molar ratio of 4:1:0.2 (2mg:0.5mg:0.1mg) were dissolved in 5 ml chloroform and (2 mg) EM extract /docetaxel was dissolved in 2 ml methanol, the solutions were mixed and the organic solvents were evaporated using a rotary evaporator at 60 °C for ~20 min to form a solid film and left overnight covered with parafilm. This process encapsulated the drugs inside the liposomes. The dry heat-sensitive nanoparticles were hydrated with 2 mL of PBS and vortexed for 10 seconds at maximum speed three times to suspend the lipid materials in the solution. The solution was allowed to stand at 4 °C overnight to efficiently hydrate the lipid materials [29].

2.4. Liposome conjugation

Heat-sensitive liposomes consisting of HSPC: DSPE-PEG2000, and DSPE-PEG2000-maleimide (DSPEPEG2000-Mal) at a ratio of 4:1:0.2 were prepared. The anti-PSMA antibody and liposomes were combined at a molar ratio of 1:10 (antibody/DSPE-PEG2000-Mal liposomes) for 4 h at 4 °C with constant stirring, and the anti-PSMA antibody was then conjugated to liposomes by the reaction of sulfhydryl residues on the antibodies with the C-terminal maleimide groups of the PEG chains (29,30). The solution was ultracentrifuged at 30,000 rpm and 4 °C for 2 h to remove the unconjugated antibody. The supernatant was collected to determine the amount of residual anti-PSMA antibody using the BCA protein assay kit

2.5 Weighing of liposomes

Heat-sensitive liposomes encapsulating EM extract and liposomes encapsulating Docetaxel were measured after they were successfully synthesized and conjugated by centrifuging the PBS-hydrated liposomes for 30 min at 90, 000 g using an ultracentrifuge at 4 °C. Following centrifugation, the supernatant and pellets were separated. The pellets were weighed in milligrams.

2.6. Protein Analysis

The BCA protein assay (Pierce) was used to quantify the amount of anti-PSMA antibody conjugation onto the liposomes. The liposome solution was ultra-centrifuged for 1 h to remove the unconjugated antibody. After removing the unconjugated antibody, the supernatant was collected to determine the amount of anti-PSMA. The dilution scheme for the microplate procedure of the BCA kit was used. 1 ampule of 2 mg/mL albumin standard was used to prepare a set of diluted standards. BSA standards were diluted to a concentration of 2000, 1500, 1000, 750, 500, 250, 125, 25 µg/mL. The protein content of the samples was thereafter determined using a standard curve obtained at 562 nm [31].

2.7. Characterization of Liposomes

2.7.1. Transmission electron microscopy (TEM)

Liposomes were analyzed on negative stain electron microscopy using a JEM 1200 EXII electron microscope. 5 µmol/mL of liposome suspension was applied to carbon-coated grids and, after 2 min, the surplus was drawn off with filter paper; a saturated uranyl acetate aqueous solution was used as a staining agent. The surplus was removed with distilled water. The morphology of the sample was analyzed by TEM at 80 kV [31].

2.7.2. Scanning Electron microscopy (SEM)

The SEM was used for uniformity of particle shape and size and morphological analysis of the liposomes. The shape of the heat-sensitive immunoliposomes was analyzed by scanning electron microscopy, JEOL JEM 2010 UHR equipped with a Gatan Imaging Filter, with a 15-eV window and a 794 slow-scan CCD camera, operating at 2.00 kV [32].

2.7.3. Fourier transform infrared spectroscopy (FTIR)

The FTIR spectra of EM, doxorubicin and docetaxel-loaded thermosensitive immunoliposomes were studied to get insights into the occurrence of interaction between drugs and phospholipids [30,33].

A Perkin Elmer Spectrum Fourier-transform infrared (FTIR) spectrophotometer was used to determine the chemical composition of the samples. FTIR spectra were recorded in the range of 4000–400 cm^{-1} wavenumber at a spectral resolution of 4 cm^{-1}. Data was analyzed using the software FTIR Spectrum (Perkin Elmer)

2.8. Determination of encapsulation efficiency

The amount of drugs in temperature-sensitive liposomes was determined as follows. Liposomes were centrifuged for 30 min at 90, 000 g using an ultracentrifuge at 4 °C. Following centrifugation, the supernatant and vesicles were separated. The pellets were washed 4 times with 0.9% NaCl solution. 2.75 mL of alcohol was added to 0.25 mL liposome solution and at 42 °C incubated for 10 min to break down the heat-sensitive liposomes. When the incubation was completed, temperature sensitive liposomes were left to cool down. The free drugs were separated from heat-sensitive nanoparticles using centrifugation and the supernatant containing free drugs was collected, and adjusted with methanol for further analysis. The amount of drug released in the supernatant was determined using HPLC. For Doxorubicin, the HPLC analysis was performed using a C18 column with a mobile phase containing acetonitrile and water (32: 68, *v/v*) at a flow rate of 1.0 mL/min. The column temperature was kept at 25 °C and the Sample (10 µL) was injected. Peaks were monitored using fluorescence detection at an excitation wavelength of 480 nm and an emission wavelength of 550 nm using the fluorescence detector. For EME the HPLC analysis was performed using a C18 column with a mobile phase containing acetonitrile and water (32: 68, *v/v*) at a flow rate of 0.8 mL/min. The column temperature was kept at 25 °C and (10 µL) sample was injected. Peaks were monitored

using fluorescence detection at an excitation wavelength of 230 nm and an emission wavelength of 280 nm using the fluorescence detector HPLC run for 45 min.

2.9. Statistical Analysis

Cytotoxic activity results were analyzed with Microsoft Excel and IC50 was calculated using GraphPad Prism version 8.0 software for Windows.

3. Results

Cell growth inhibition of DU145 cells

3.1 EM roots, stems, and leaves extracts were screened for cytotoxic activity against theprostate cancer DU-145 cell line.
Extracts were tested in triplicate at concentrations of 100 µg/mL, 10 µg/mL, and 1 µg/mL.

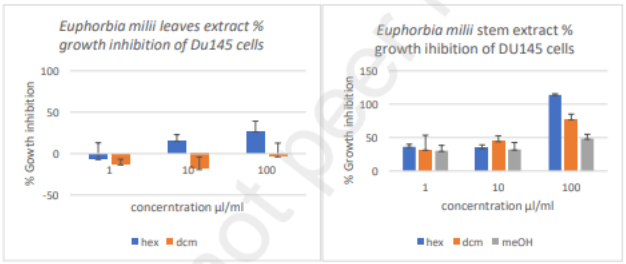

(a) (b)

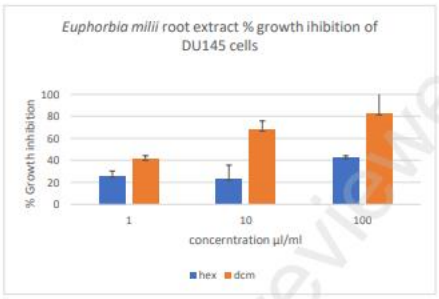

(c)

Figure 1: a) Cell growth inhibition of DU145 cells by leaves extracts of EM. Hexane leaves showed growth inhibition of less than 30% at all three concentrations. The DCM leaves showed no growth at all three concentrations **b)** Cell growth inhibition of DU145 cells by stem extracts of EM. hexane stem extract showed activity less than 50% at 1µg/ml and 10µg/ml and more than 100% activity at 100µg/ml. The DCM stem extract showed no activity at 1µg/ml and 10µg/ml and 78% activity at 100µl/ml. EM methanol extract showedno activity at all three concentrations. **C)** Cell growth inhibition of DU145 cells by root extracts of EM. EM DCM root extract showed more than 50% activity with concentrations of 10µg/ml and 100µl/ml inhibiting more than 65% of the cells (IC50). This is the only extract that showed the desirable activity when screened against the DU145 prostate cancer cells. This extract was further screened against the LNCap cell line.

3.2 *Cell anti-proliferation assay*

The EM was investigated for its cytotoxic activities against the LNCap cell line using an MTT cell viability assay. EM DCM root extract was tested in triplicateat concentrations of 100 µg/mL, 10 µg/mL, and 1 µg/mL.

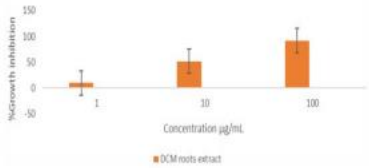

Figure 2. Cell growth inhibition of LNCap cells by root extracts of EM. The cells were treated with different concentrations (100, 10, and 1 µg/mL) of DCM root extract. EM DCM root extract showed more activity with concentrations of 10 µg/mL and 100 µg/mL inhibiting more than 51.7% of the cells (IC50). The extract's activity was further investigated in cells when encapsulated into heat-sensitive liposomes.

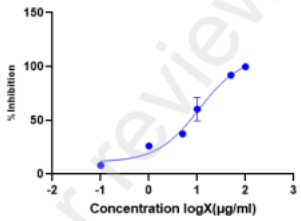

Figure 3. Cytotoxic activity of the EM DCM root extract on LNCap cells with IC50 value of 11.34 µg/mL.

3.3 Percentage inhibition of Doxorubicin, Docetaxel.

Doxorubicin and Docetaxel were added as positive controls and screened against the DU145 and LNCap prostate cancer cell lines

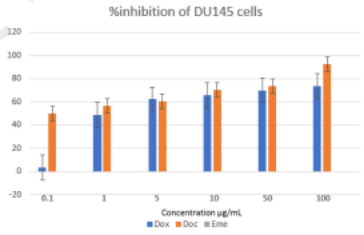

Figure 4a) The cytotoxic activity of Doxorubicin and Docetaxel was screened against the DU145 cell line. Doxorubicin showed 62%,65%,70%, and 73% inhibition at 5,10,50,100µg/ml respectively, Docetaxel was active showing above 50% activity for all concentrations.

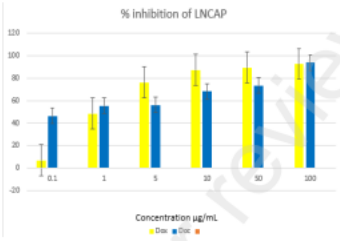

4b) The cytotoxic activity of Doxorubicin and Docetaxel. Doxorubicin showed activity of 76.25 % at 5 µg/ml and higher activity at 10,50,100 µg/ml. Docetaxel showed activity of 55.3%, 55.9 %, 68.23%, 73.43% and 93.69% at 1, 5, 10, 55, and 100 µg/ml respectively.

3.4. *Characterization of heat-sensitive liposomes*

The heat-sensitive immunoliposomes were characterized using FTIR, TEM, and SEM

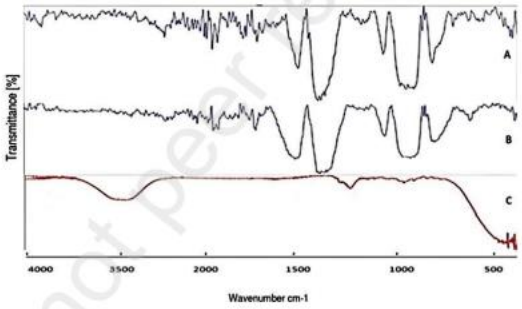

Figure 5. FTIR spectrometry was used to examine the interaction between drugs and temperature-sensitive immunoliposomes. **A** is the FTIR spectrum of EME loaded heat-sensitive immunoliposomes. **B** is the FTIR spectrum of Doxorubicin

encapsulated heat-sensitive immunoliposomes. **C** is the FTIR spectrum of Docetaxel encapsulated heat-sensitive immunoliposomes. EM loaded immunoliposomes were similar to that of doxorubicin loaded heat-sensitive immunoliposomes.

The FTIR spectra of EME loaded heat-sensitive immunoliposomes have shown a C-O peak at 179265, C-O stretching peak at 1683.56. and C-H bending peak at 1395.54 CH found in aromatic compounds of plant extracts, CN stretching. The peak at 1281.52 confirmed the presence of carboxylic acid group and aromatic amine, CO stretching peak at 1017.88. The peak between 1150–1000 is the C-F stretch showing aliphatic fluoro compounds. The peak range between 2100–2250 can be attributed to the C-C functional group which possibly indicates the presence of alkynes. Furthermore, the observed peak at 819.41 of the peak range between 1040–732 can be attributed to aromatic compounds. B is the FTIR spectrum of Doxorubicin heat-sensitive immunoliposomes showing similar peak ranges to those contained in EM loaded heat-sensitive liposomes. Doxorubicin-loaded heat-sensitive immunoliposomes have shown a C-O peak at 1792.56, C-O stretching peak at 1683.56 and C-H bending peak at 1395.54 CH found in aromatic compounds of plant extracts, CN stretching. The peak at 1281.52 confirmed the presence of carboxylic acid group and aromatic amine, CO stretching peak at 1017.88. The peak between 1150–1000 is the C-F stretch showing aliphatic fluoro compounds. The peak range between 2100–2250 can be attributed to the C-C functional group which possibly indicates the presence of alkynes. The observed peak at 819.41 of the peak range between 1040–732 can be attributed to aromatic compounds. **C.** The FTIR spectra of docetaxel loaded heat-sensitive liposomes. Docetaxel-loaded heat-sensitive liposomes have shown carboxyl acid peak at 3260.27 which are part of the (2500–3300) frequency range, the peaks in this range appear in FTIR analysis of the lipid DSPE-PEG when conjugated. In the study conducted by Marasini et al. [33] these peak ranges were attributed to the presence of methylene and methyl groups in the PEG molecules and Amide (C-O) peak at 1633.53, alkyl ketone peak at 1241.44, alkyl amine peak at 1168.89 and the peak at 1069.98 indicate the presence of polysaccharides which are part of the (1035–1149) frequency range. Ville et al. [34] found the absorption pattern between 1282 and 1020 useful for determining a phospholipid calibration curve. This peak range is seen in EME, doxorubicin, and docetaxel liposomes.

3.5. *TEM and SEM results*

Transmission electron microscopy (TEM) and scanning electron microscope (SEM) images below show the morphology of the synthesized heat-sensitive immunoliposomes observed at 50nm,100 nm, 500 nm, and 1 micrometer. For TEM analysis, the shape of the immunoliposomes appeared spherical and opaque at various parts of the grid showing stability of the nanoparticles. For SEM analysis the shape of the immunoliposomes appears to be a uniform spherical shape which correlates with the observed morphology under the transmission electron microscopy.

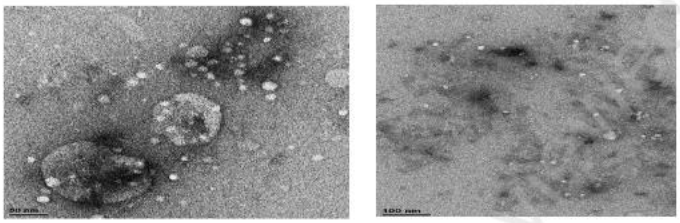

Figure 6. TEM images of empty liposomes at 50 nm and 100 nm. Transmission electron microscopy (TEM) was used to show the morphology of the immunoliposomes observed at 100 and 50 nm. TEM analysis of empty liposomes was done to confirm the formation of liposomes under experimental conditions.

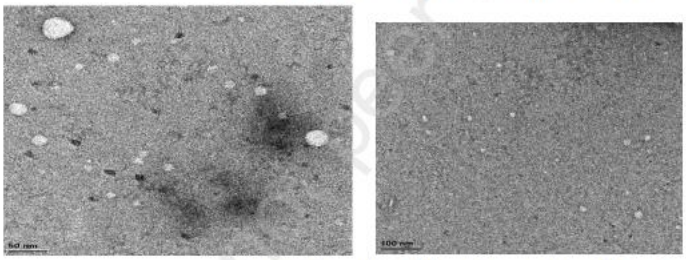

Figure 7. TEM images of EM-loaded immunoliposomes at 50 nm and 100 nm. At 50 nm the TEM images show that the EM-loaded immunoliposomes are slightly bigger than the empty immunoliposomes. In both the empty immunoliposomes and EME-loaded immunoliposomes the TEM images indicate that the shape of the immunoliposomes appeared spherical and opaque therefore this indicates that the liposomes are stable and uniform in size at 100 nm and 50 nm.

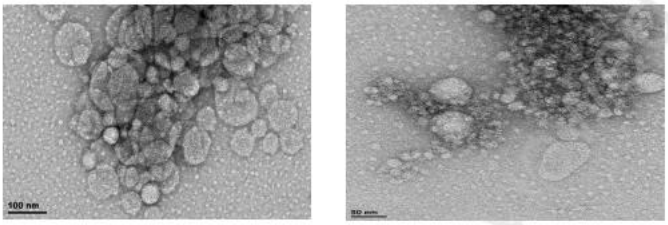

Figure 8. TEM images of doxorubicin-loaded liposomes at 100 nm and 50 nm. The larger circles that appear see through are marks caused by air-dried PBS.

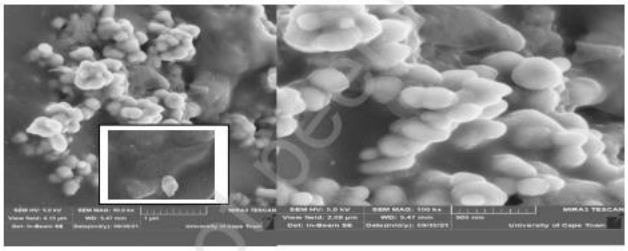

Figure 9. SEM images of empty liposomes at 1 micrometer and 500 nm. Scanning electron microscope (SEM) photographs of liposomes showing the morphology of the synthesized heat-sensitive immunoliposomes. Figure 11 below shows the SEM images of empty liposomes.

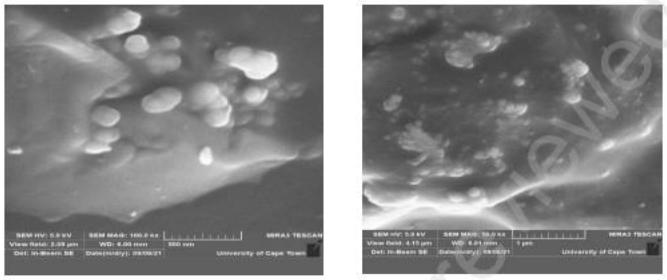

Figure 10. SEM images of EM-loaded liposomes at 500 nm and 1 µm. The morphology of the liposomes appeared to be spherical at different parts of the grid. The liposomes were air-dried therefore the cloudy substance observed is airdried PBS.

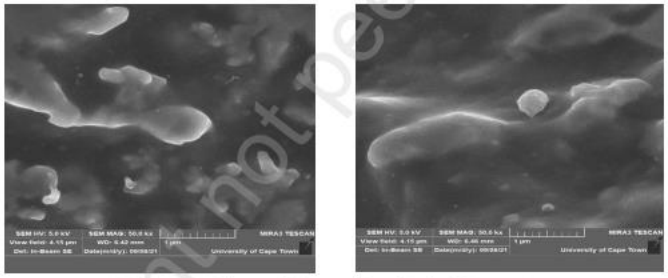

Figure 11. SEM images of doxorubicin-loaded liposomes 1 µm.

3.6. Protein Conjugation

Table 1. illustrates the total protein content of the EME and the standard drug encapsulated heat-sensitive immunoliposomes.

Samples	µg/ml	µg/ml	ug/ul	100 ug
EM 1.41	Y = 817.47(1.41) – 162.48 = 990.1527	9901.527	9.901527	10.09945
Standard drug 1.774	Y = 817.47(1.774) – 162.48 = 1287.712	12877.12	12.87712	7.765713

BCA protein assay (Pierce) was used to quantify the amount of anti-PSMA

antibody conjugation onto the liposomes. A Calibration curve was plotted to

determine the protein content of the Docetaxel-loaded immunoliposomes and EME-loaded immunoliposomes and a linear relationship were observed as (R^2 values > 0.984).
The absorbance of the EM and the standard drug at 526 nm is 1.14 and 1.774 respectively. R squared of the standard curve is 0.984.

3.7. HPLC/LCMS for drug encapsulation

Table 2. Illustrates the integrated peak area and peak height values of the chromatograms for the selected masses in the EM extract sample (sample 1) and the concentration of doxorubicin (sample 2).

Sample Name	*Analyte Peak Name*	*Analyte Peak Area (counts)*	*Analyte Peak Height (cps)*	*Calculated Concentration (ppm)*
EME	mass 271	1,98E + 07	1,23E + 06	0
EME	mass 301	1,66E + 07	6,54E + 05	0
EME	mass 318	2,62E + 07	1,44E + 06	0
EME	mass 352	4,73E + 06	2,12E + 05	0
EME	mass 637	5,39E + 05	1,57E + 04	0
EME	mass 678	1,28E + 05	2,89E + 03	0
EME	mass 754	2,17E + 06	1,74E + 05	0
EME	mass 796	9,67E + 06	6,87E + 05	0
Doxorubicin	Dox	6,78E + 06	6,66E + 05	0,607

The EME is not a pure drug therefore the concentration is seen as 0 ppm in the table above. The concentration of doxorubicin was calculated as 0.607 ppm and was therefore used as a reference to calculate the concentration of EM taking into account the area of the peak of the EME in relation to the area of the peak of the doxorubicin pure drug.

Table 3. Illustrates the integrated peak area and peak height values of the chromatograms for the masses 796 in the EM extract sample and concentration of docetaxel in the Docetaxel encapsulated liposomes when the drugs are released and not released from the liposomes

TABLSAMPLE NAME	*Analyte Peak Name*	*Analyte Peak Area(counts)*	*Analyte Peak Height (cps)*	*Calculated Concentration*
EM RELEASED	mass796	4.33E+07	2.24E+06	0
EM ENCAPSULATED	mass796	1.69E+07	1.10E+06	0
DOC RELEASED	Doc	1.75E+006	1.12E+005	9
DOC ENCAPSULATED	Doc	1.1E+006	7.70E+004	5.6

Table 3 shows the thermosensitive liposomes encapsulating drugs when run through LCMS and temperature liposomes when drugs were released by exposing the liposomes to hyperthermia at 40°c. The mass 796 of the EM plant was investigated to quantify the amount of drug detected in the liposomes. The area of the EM mass 796 peak was larger than when the EM extract was not released. The height of the EM mass 796 was higher when the EM extract was released.
The concentration of docetaxel detected when the drug was released was found to be 9 ug/ml and when liposomes were not exposed to 40°c hyperthermia the concentration was found to be 5.6 ug/ml.

The weight of liposomes was found to be
EME encapsulating liposome 4.3 mg -2.15 mg (0.5mg drug added)

Docetaxel encapsulated liposomes 4.5 mg = 2.25mg (0.5mg drug added)
Calculating Concentration of drug inside liposomes

Table 4. Shows the concentration of Docetaxel.

Sample name	Calculated concentration
Docetaxel	839 µg/ml

mg/L =1 ppm.

The concentration was found to be 839 µg/mL. in a sample of 2 mg of drug added.

3.8. Cytotoxic activity of EME and docetaxel-loaded immunoliposomes.

The cytotoxic activity of temperature-sensitive immunoliposomes encapsulating the EME and docetaxel was studied by measuring the cellular viability using the MTT assay in the LNCap cells with and without exposure to hyperthermia. To ensure that the EME and docetaxel become bioavailable intracellularly, mild hyperthermia was applied to trigger release from liposomes in one experiment and another experiment was conducted without hyperthermia. The results obtained in Figures 1 and 2 lead to further investigation of the plant extract. Figure 3 shows the IC50 value of the EME and docetaxel encapsulated immunoliposomes on LNCap cells when exposed to hyperthermia and Figure 4 shows the IC50 value of the EME and docetaxel encapsulated immunoliposomes on LNCap cells without hyperthermia.

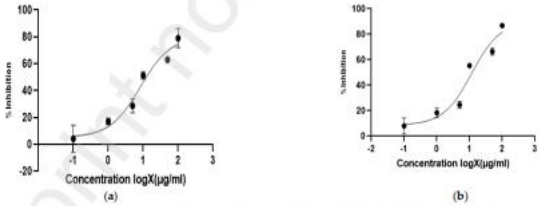

Figure 12. a) Growth inhibition of LNCap cell line by the EME encapsulated heat-sensitive immunoliposomes when exposed to heat. 51.34 % inhibition was recorded at 10 µg/mL. The IC50 was calculated to be 8.44 µg/mL. **b)** Growth inhibition of LNCap cells by Docetaxel encapsulated immunoliposomes when exposed to heat. 55.4 % inhibition was recorded at a concentration of 10 µg/mL. the IC50 was calculated to be 11.74 µg/mL.

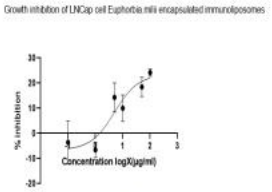

(a)

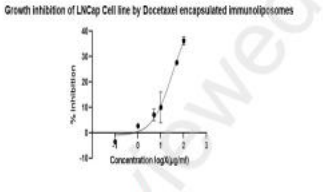

(b)

Figure 13. a) Growth inhibition of LNCap by EME encapsulated immunoliposomes without exposure to heat. No significant activity was recorded at a concentration of 10, 50, and 100 µg/mL. **b)** Growth inhibition of LNCap cells by Docetaxel encapsulated heat-sensitive immunoliposomes without exposure to heat. No significant activity was recorded at a concentration of 10, 50 and 100 µg/mL. In Figure 2, the significant cytotoxic activity of the EM DCM root extract on LNCap cells was recorded with an IC50 value of 11.34 µg/mL, when immunoliposomes were exposed to heat (figures 3a and 3b) cytotoxic activity was recorded at the concentration of 10 µg/mL with IC50 values of 8.44 µg/mL. and 11.74 µg/mL for EM and Docetaxel respectively indicating the effect of hyperthermia on heat-sensitive liposomes

4. Discussion

This research is a significant effort to reduce mortality and poor treatment outcome in prostate cancer patients, as well as toxic side effects associated with the treatment of prostate cancer.

Due to the side effects and poor therapeutic outcomes of chemotherapy, targeted and controlled drug delivery has become relevant techniques used for more effective and specific cancer treatment, with reduced toxicity. These heat-sensitive immunoliposomes encapsulated the EME together with the prostate cancer standard drugs, doxorubicin, and docetaxel

EM roots, stems, and leave extracts were screened for cytotoxic activity against the prostate cancer DU145 cell line. Extracts were tested in triplicate at concentrations of 100µg/mL, 10 µg/mL, and 1 µg/mL. The only extract that showed significant activity was the DCM root extract. The extract was further tested against the LNCap cell line.

In this study, EM root extract showed potent activity against the LNCap cells showing IC50 of 11.34. Doxorubicin and Docetaxel were used as positive controls and screened against the DU145 and LNCap prostate cancer celllines. Docetaxel was the only drug that showed activity at all concentrations for boththe LNcap and DU145 cell lines. In figure 4a Doxorubicin showedactivity from 5 µg/ml against the DU145 cell line and figure 4b shows thatDoxorubicin and Docetaxel showed activity from 5 µg/ml against the LNCap cell line. Docetaxel is used as a standard drug to treat prostate cancer [35].The cellular uptake of heat sensitive immunoliposomes by LNCap cells was studied using the EM encapsulated immunoliposomes and standard drugs (doxorubicin and docetaxel) encapsulated immunoliposomes. The Folin-Ciocalteu and aluminum chloride methods were used to confirm the total phenolic (TPC) and

total flavonoid contents (TFC) of the plant, for the phenolic and flavonoids, the highest contents were detected from methanol extracts, and the EM methanol root extract indicated the highest phenolic contents, whereas the highest contents of flavonoids were observed in aerial methanol extracts. This study showed that Flavonoids and phenolics were the most secondary metabolites present. EM DCM extracts indicated high antioxidants in relation to the methanol extracts [36].

Liposomes were prepared using HSPC: DSPE-PEG-2000: DSPE-PEG2000-maleimide in the molar ratio of 4:1:0.2 and conjugated with a PSA antibody. DSPE-PEG (2000)-amine has been used for the synthesis of solid lipid and thermosensitive liposomal nanoparticles mainly for the carriage of anticancer drugs and the synthesis of fluorescein isothiocyanate-loaded mesoporous silica nanoparticles for imaging applications. It can be used with different functional molecules such as the DSPE-2000-malmide to prepare antibody-conjugated nanoparticles for improved cellular and receptor targeting [37]. A study conducted by Alavizadeh et al. added hydrogenated soy phosphatidylcholine (HSPC) to temperature sensitive liposomes to enhance the plasma stability of liposomes, this is also supported by the study conducted by Chenj et al 2012 stating that increasing the molar ratio of HSPC can be increased to adjust the transition temperature of the liposomes from 37°C to more than 40°C. Their studies showed that adding HSPC improved the *transition temperature* resulting in improved stability of temperature-sensitive liposomes in vivo [38] DSPE-PEG2000 1,2-distearoyl-sn-glycero-3-phosphoethnolamine-N-[amino(polyethyleneglycol)-2000] (ammonium salt) chloroform is a compound lipid with a PEG chain grafted in the terminal end on the hydrophobic tail. Pegylated liposomes, also known as stealth liposomes have to extend systemic circulation via evasion of the reticuloendothelial system (RES) and this increases their accumulation in the tumor site [39,40]. In this study, hyperthermia was applied to trigger release from liposomes after cellular uptake beyond the transition temperature of 40 °C. 51.34 % inhibition was recorded at 10 µg/mL. The IC50 was calculated to be 8.437. No significant activity was recoded at concentration of 10, 50 and 100 µg/mL for LNCap cells that were not exposed to hyperthermia. The transition temperature used was 39–40 °C.

Figure 5 shows that the FTIR results of EM loaded immunoliposomes were similar to that of doxorubicin loaded heat-sensitive immunoliposomes indicating that the liposomal encapsulation of drugs did not result in the formation of new linkages, different peaks were observed for the docetaxel loaded immunoliposomes. Transmission Electron Microscopy and Scanning Electron Microscope were then used to further investigate the stability and morphology of the synthesized immunoliposomes. Both TEM and SEM indicate that the morphology of the immunoliposomes appeared spherical and opaque therefore this indicates that the liposomes are stable and uniform in size at 100 nm and 50 nm. The liposomes were air-dried therefore the cloudy substance observed is the dried PBS.

The BCA protein assay (Pierce) was used to quantify the amount of anti-PSMA antibody conjugation onto the liposomes. The BCA assay utilizes peptide bonds in proteins decreasing Cu^{2+} to Cu^{+} at a rate corresponding to the total protein. The bicinchoninic acid reagent forms a complex by binding with the Cu^{+}, this complex then absorbs light at 562 nm wavelength, this allows a link between the sample's protein concentration and absorbance [41,42] the standard curve R squared value is 0.984 (R squared value describes the best fit of the standard curve and should be above 0.96) using the $y = mx + c$ equation concentration of the EM and the standard drug was calculated to be 990.1527 and 1287.712 respectively. A dilution factor of 2µL was added in 18µL water therefore dilution factor is 10.

The entrapment efficiency was determined using HPLC and LCMS. The concentration of a plant extract within a sample cannot be quantified because extracts are not pure. LCMS was performed on EME and different masses were identified, these masses were then used as markers, masses 271, 301, 318, 352, 637, 678, 754, and 796. Table 2 indicates the integrated area and peak intensity values for the

chromatographic peaks for the selected masses in sample 1(EME) and sample 2 doxorubicin (100 x fold diluted). There are only 2 masses that are separated as clear peaks, mass 754 and 796. Other masses were badly resolved and eluted as multiple peaks. Two 0.5 mg samples were analyzed through LCMS, sample 1 which is the EME, and sample 2 which is the Doxorubicin (used as a control). A calibration curve was constructed with the Doxorubicin standard and is thus 0.6 × 100 = 60 ppm. Taking into account the area of the peak of the EME in relation to the doxorubicin pure drug. The EM mass at 796 has a peak area of 9,67E + 06 and doxorubicin has an area of 6,78E + 06 therefore the area of EME is 2.89 larger. The height of the EME peak is 6,87E + 05 and the height of the Doxorubicin peak is 6,66E + 05, the height of the EME peak is 0.21 higher than that of doxorubicin. This indicates that there is more EM extract than doxorubicin encapsulated in the liposomes. A chromatogram was constructed with the docetaxel standard drug and the concentration of docetaxel (100 × fold diluted) was determined. The concentration was found to be 839 µg/mL. in a sample of 2 mg.

5. Conclusion

Chemotherapy and other commonly used treatments have side effects, therefore recentlydeveloped drug formulations can reduce systemic toxicity and become a promising treatment alternative to achieve local control of the disease.

In summary, our study has shown that there is scientific confirmation for the traditional use of *Euphorbia Milii* as a medicinal plant for treating prostate cancer. In the study, EM DCM root extract has exhibited anticancer activity against the LNCap cells. The planthas secondary metabolites that are active against the prostate cancer cells. The EM showed significant activity when the thermosensitive liposomes are exposed to heat. The heat-sensitive anti-PSA liposomes are a great candidate with minimal side effectsthat we believe will enhance tumor-targeted drug accumulation, and therefore increase antitumor activity.

Author Contributions: M.S., supervision oversight and leadership of the research, planning, and execution, critical review and editing of the manuscript, funding acquisition; K.R., summary, introduction, abstract, methodology, results, discussion conclusion, critical review and editing of the manuscript; A.A., methodology, discussion, critical review and editing of the manuscript; S.M., review, and editing of the manuscript. All authors have read and agreed to the published version of the manuscript.

Funding: Reference: TTK160607168752, UID 107835.

Informed Consent Statement: Not applicable. This research article does not involve human subjects.

Conflicts of Interest: The authors declare that there are no conflicts of interest that could be perceived as prejudicing the impartiality of this research article.

Appendix A

The determination of the NP's entrapment efficiency of the drug was done using LCMS

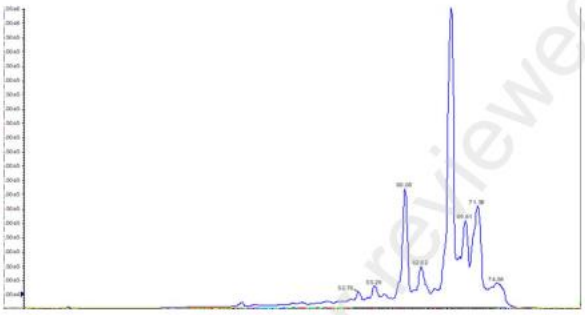

Figure 14. LCMS was run on the (EME) sample.

The most intense peak of the EM extract was observed at 67 min and this shows the spectrum of all the masses in that peak (at 67 min) between 200–1000 Da (in positive ionization mode).

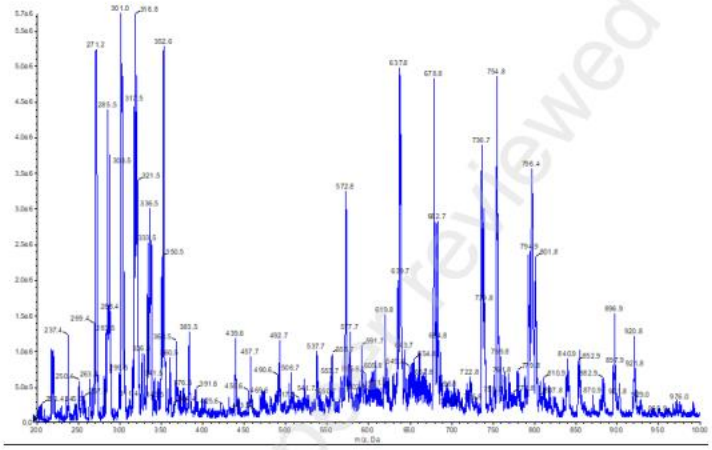

Figure 15. Indicates several masses that were identified in the EM plant extract.

The masses, the peak at 67 min were chosen as a marker for HPLC. several masses were identified in the most intense (peak at 67 min) chromatographic peaks. The masses selected were 271, 301, 318, 352, 637, 678, 754, and 796 and were used as marker masses. There are only 2 masses that are separated as—well-structured peaks, 754 and 796. The other masses were badly resolved and eluted as multiple peaks and were then integrated as one to give the values above.111

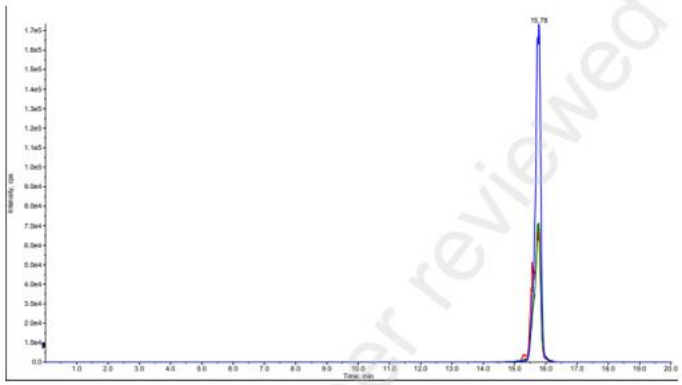

Figure 16. indicating the chromatogram of Mass 754 of the EME.

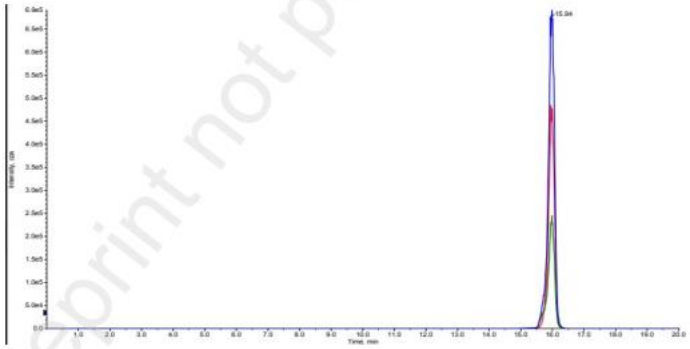

Figure 17. indicating the chromatogram of Mass 769 of the EME.

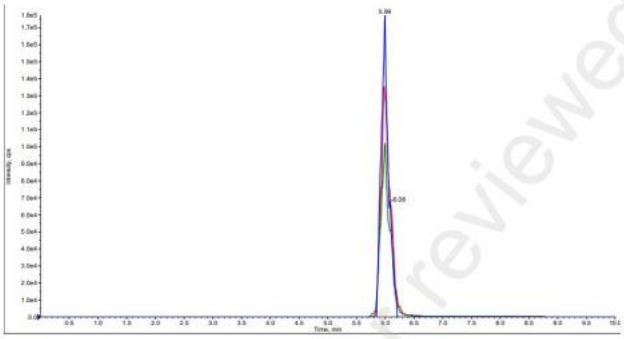

Figure 18. indicating the chromatogram of docetaxel.

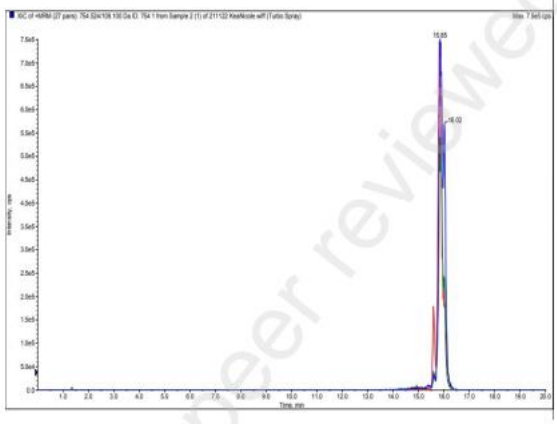

Figure 19 Indicating the Chromatogram of Mass 754 of the Euphorbia released

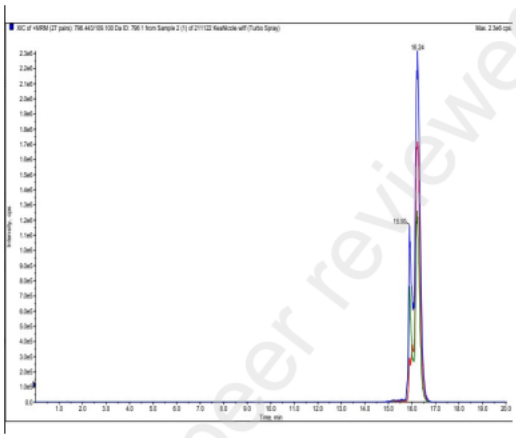

Figure 20: Indicating the Chromatogram of Mass 796 of the Euphorbia released

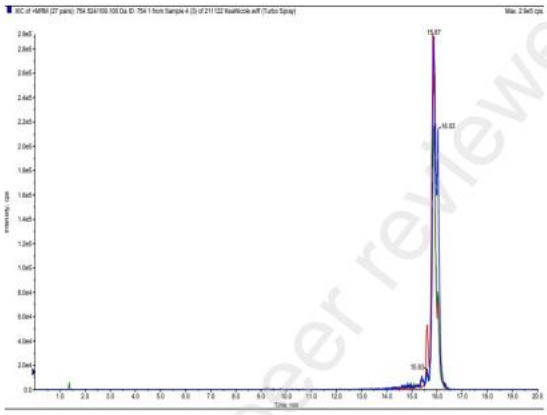

Figure 21: Indicating the Chromatogram of mass 754 of the Euphorbia unreleased

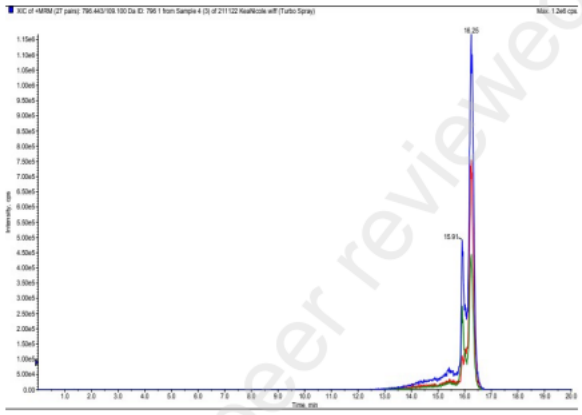

Figure 22: Indicating the Chromatogram of mass 796 of Unreleased Euphorbia

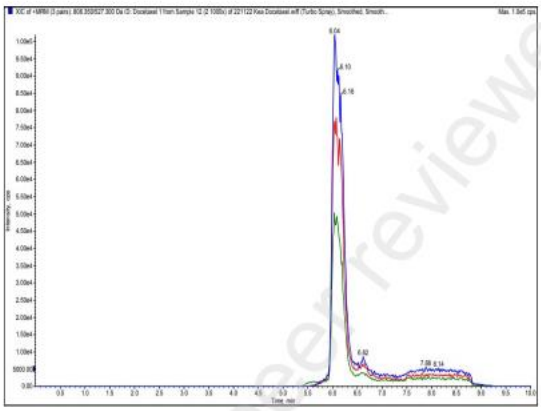

Figure 23 : Indicating the Chromatogram of released Docetaxel

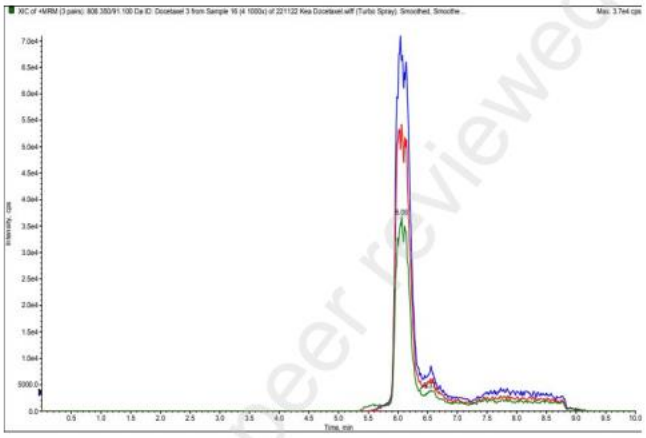

Figure 24: Indicating the Chromatogram of unreleased Docetaxel

Appendix 2

Abbreviations:

EME – *Euphorbia Milii*

extractDCM – Dichloromethane

FBS- Fetal Bovine

SynodromeEM – *Euphorbia Milii*

Tc- Transition temperature

PSMA-Prostate-Specific Membrane AntigenPC-tidylcholine

FTIR- Fourtier transform infrared SpectroscopyTEM-Transmission Electron

Microscopy

SEM-Scanning Electrone

MicroscopeDMSO-Dimethyl

sulfoxide

MTT – tetrazolium

References

1) Barbieri, C.E., Bangma, C.H., Bjartell, A., Catto, J.W., Culig, Z., Grönberg, H., Luo, J., Visakorpi, T. and Ru-bin, M.A., 2013. Themutational landscape of prostate cancer. European urology, 64(4), pp.567-576.

2) Haas, G.P., Delongchamps, N., Brawley, O.W., Wang, C.Y. and de la Roza, G., 2008. The worldwide epi-demiology of prostatecancer: perspectives from autopsy studies. The Canadian journal of urology, 15(1), p.3866.

3) Lang, S.H., Frame, F.M. and Collins, A., 2009. Prostate cancer stem cells. The Journal of Pathology: A Journal of thePathological Society of Great Britain and Ireland, 217(2), pp.299–306.

4) Alicea-Reyes, T.M., 2020. The Role of he Endocannabinoid System in Prostate Cancer Perineural Invasion (Doc-toraldissertation, University of Puerto Rico Medical Sciences (Puerto Rico).

5) Abbas, Z. and Rehman, S., 2018. An overview of cancer treatment modalities. Neoplasm, 1, pp.139–157.

6) Lakshmanan, V.K., 2016. Therapeutic efficacy of nanomedicines for prostate cancer: An update. Investiga-tive and ClinicalUrology, 57(1), pp.21–29.

7) Garcia-Pinel, B., Porras-Alcalá, C., Ortega-Rodríguez, A., Sarabia, F., Prados, J., Melguizo, C. and López-Romero, J.M., 2019. Lipid-based nanoparticles: Application and recent advances in cancer treatment. Nano-materials, 9(4), p.638.

8) Singh, A.P., Biswas, A., Shukla, A. and Maiti, P., 2019. Targeted therapy in chronic diseases using nano-material-based drugdelivery vehicles. Signal. transduction and targeted therapy, 4(1), pp.1-.

9) Jabir, N.R., Tabrez, S., Ashraf, G.M., Shakil, S., Damanhouri, G.A. and Kamal, M.A., 2012. Nanotechnology-based approachesin anticancer research. International journal of nanomedicine, 7, p.4391.

10) Mura, S., Nicolas, J. and Couvreur, P., 2013. Stimuli-responsive nanocarriers for drug delivery. Nature ma-terials, 12(11),pp.991–1003.

11) Jing, Y., Trefna, H., Persson, M., Kasemo, B. and Svedhem, S., 2014. Formation of supported lipid bi-layers on silica: relationto lipid phase transition temperature and liposome size. Soft matter, 10(1), pp.187-195.

12) Chen, J., Cheng, D., Li, J., Wang, Y., Guo, J.X., Chen, Z.P., Cai, B.C. and Yang, T., 2013. Influence of li-pid composition on thephase transition temperature of liposomes composed of both DPPC and HSPC. Drug development and industrial pharmacy, 39(2), pp.197-204.

13) Needham, D., Anyarambhatla, G., Kong, G. and Dewhirst, M.W., 2000. A new temperature-sensitive lipo-some for use withmild hyperthermia: Characterization and testing in a human tumor xenograft model. Cancer research, 60(5), pp.1197–1201.

14) Yang, D., Pornpattananangkul, D., Nakatsuji, T., Chan, M., Carson, D., Huang, C.M. and Zhang, L., 2009. The antimicrobial activity of liposomal lauric acids against Propionibacterium acnes. Biomaterials, 30(30), pp.6035–6040.

15) van Elk, M., Murphy, B.P., Eufrásio-da-Silva, T., O'Reilly, D.P., Vermonden, T., Hennink, W.E., Duffy, G.P. and

Ruiz- Hernández, E., 2016. Nanomedicines for advanced cancer treatments: Transitioning towards re-sponsive systems. Internationaljournal of pharmaceutics, 515(1–2), pp.132–164.

16) Amin, M., Huang, W., Seynhaeve, A.L. and Ten Hagen, T.L., 2020. Hyperthermia and temperature-sensitive nanomaterialsfor spatiotemporal drug delivery to solid tumors. Pharmaceutics, 12(11), p.1007.

17) Bozzuto, G. and Molinari, A., 2015. Liposomes as nanomedical devices. International journal of nanomedi-cine, 10, p.975.

18) Lakshmanan, V.K., 2016. Therapeutic efficacy of nanomedicines for prostate cancer: An update. Investi-gative and ClinicalUrology, 57(1), pp.21–29.

19) Alqosaibi, A.I., 2022. Nanocarriers for anticancer drugs: Challenges and perspectives. Saudi Journal of Biological Sciences,p.103298.

20) Li, K., Zhan, W., Chen, Y., Jha, R.K. and Chen, X., 2019. Docetaxel and doxorubicin codelivery by nanocarriers for synergistictreatment of prostate cancer. Frontiers in Pharmacology, 10, p.1436.

21) Islam, N.U., Khan, I., Rauf, A., Muhammad, N., Shahid, M. and Shah, M.R., 2015. Antinociceptive, mus-cle relaxant andsedative activities of gold nanoparticles generated by methanolic extract of Euphorbia milii. BMC complementary and alternative medicine, 15(1), pp.1-11

22) Rahman, A.H.M.M. and Akter, M., 2013. Taxonomy and medicinal uses of Euphorbiaceae (Spurge) fam-ily of Rajshahi,Bangladesh. Research in Plant. Sciences, 1(3), pp.74–80.

23) Chudasama, K., Bhatt, P., Chudasama, K. and Thaker, V., 2018. Molecular marker study in ornamental plant EM. Journal of Pharmacognosy and Phytochemistry, 7(3), pp.882–888.

24) Razanajatovo, H. (2020). "EM". IUCN Red List of Threatened Species. 2020: E.T44389A153299391. https://doi.org/10.2305/IUCN.UK.2020–1.RLTS.T44389A153299391.en. Retrieved 19 November 2021.

25) Mavundza, E.J., Street, R. and Baijnath, H., 2022. A review of the ethnomedicinal, pharmacology, cytotoxicity and phytochemistry of the genus Euphorbia in southern Africa. South African Journal of Botany, 144, pp.403-418.

26) Salehi B, Iriti M, Vitalini S, Antolak H, Pawlikowska E, Kregiel D, Sharifi-Rad J, Oyeleye SI, Ademiluyi AO, Czopek K, Staniak M, Custódio L, Coy-Barrera E, Segura-Carretero A, Cádiz-Gurrea ML, Capasso R, Cho WC, Seca AML. Euphorbia-Derived Natural Products with Potential for Use in Health Maintenance. Biomole-cules. 2019 Aug 2;9(8):337.

27) Delgado, I.F., De-Carvalho, R.R., De-Oliveira, A.C.A.X., Kuriyama, S.N., Oliveira-Filho, E.C., Souza, C.A.M. and Paumgartten, F.J.R., 2003. Absence of tumor promoting activity of EM latex on the mouse back skin. Toxicology letters, 145(2), pp.175–180.

28) Huang, H.L., Hsing, H.W., Lai, T.C., Chen, Y.W., Lee, T.R., Chan, H.T., Lyu, P.C., Wu, C.L., Lu, Y.C., Lin, S.T. and Lin, C.W., 2010. Trypsin-induced proteome alteration during cell subculture in mammalian cells. Jour-nal of biomedical science, 17(1), pp.1–10.

29) Lu, L., Ding, Y., Zhang, Y., Ho, R.J., Zhao, Y., Zhang, T. and Guo, C., 2018. Antibody-modified liposomes for tumor-targetingdelivery of timosaponin AIII. International journal of nanomedicine, 13, p.1927.

30) Chiu, G.N., Bally, M.B. and Mayer, L.D., 2003. Targeting of antibody conjugated, phosphatidylserine-containing liposomes to vascular cell adhesion molecule 1 for controlled thrombogenesis. Biochimica et Biophys-ica Acta (BBA)-Biomembranes, 1613(1–2), pp.115–121.Lu, L., Ding, Y., Zhang, Y., Ho, R. J., Zhao, Y., Zhang, T., & Guo, C. (2018). Antibody-modified liposomes for tumor- targeting delivery of timosaponin AIII. International Journal of Nanomedicine, Volume 13, 1927–1944. doi:10.2147/ijn.s153107

31) Liu, Y., Yoo, S.D., Li, L., Fang, L., Wen, Z. and Li, T., 2012. Formulation and characterization of boanmycin-loaded liposomesprepared by pH gradient experimental design. Drug delivery, 19(2), pp.90–101.

32) Mofolo, M.J., Kadhila, P., Chinsembu, K.C., Mashele, S. and Sekhoacha, M., 2020. Green synthesis of silver nanoparticles from extracts of Pechuel-loeschea leubnitziae: Their anti-proliferative activity against the U87 cell

line. Inorganic and Nano-Metal. Chemistry, 50(10), pp.949–955.

33) Marasini, R., Nguyen, T.D.T., Rayamajhi, S. and Aryal, S., 2020. Synthesis and characterization of a tumor-seeking LyP—peptide integrated lipid–polymer composite nanoparticle. Materials Advances, 1(3), pp.469–480.

34) Van Elk, M., Murphy, B.P., Eufrásio-da-Silva, T., O'Reilly, D.P., Vermonden, T., Hennink, W.E., Duffy, G.P. and Ruiz-Hernández, E., 2016. Nanomedicines for advanced cancer treatments: Transitioning towards respon-sive systems. International journal of pharmaceutics, 515(1–2), pp.132–164.

35) Markowitsch, S.D., Juetter, K.M., Schupp, P., Hauschulte, K., Vakhrusheva, O., Slade, K.S., Thomas, A., Tsaur, I., Cinatl Jr, J.,Michaelis, M. and Efferth, T., 2021. Shikonin reduces growth of docetaxel-resistant prostate cancer cells mainly through necroptosis. Cancers, 13(4), p.882.

36) Saleem, H., Zengin, G., Locatelli, M., Mollica, A., Ahmad, I., Mahomoodally, F.M., Abidin, S.A.Z. and Ahemad, N., 2019. Invitro biological propensities and chemical profiling of EM Des Moul (Euphorbiaceae): A novel source for bioactive agents. Industrial Crops and Products, 130, pp.9-15.

37) Bi, H., Xue, J., Jiang, H., Gao, S., Yang, D., Fang, Y. and Shi, K., 2019. Current developments in drug delivery with thermosensitive liposomes. Asian Journal of Pharmaceutical Sciences, 14(4), pp.365–379.

38) Alavizadeh, S.H., Gheybi, F., Nikpoor, A.R., Badiee, A., Golmohammadzadeh, S. and Jaafari, M.R., 2017. Therapeutic efficacyof cisplatin thermosensitive liposomes upon mild hyperthermia in C26 tumor bearing BALB/c mice. Molecular pharmaceutics, 14(3), pp.712–721.

39) Takayama, R., Inoue, Y., Murata, I. and Kanamoto, I., 2020. Characterization of nanoparticles using DSPE-PEG2000 andsoluplus. Colloids and Interfaces, 4(3), p.28.

40) Nie, S., 2010. Understanding and overcoming major barriers in cancer nanomedicine. Nanomedicine, 5(4), pp.523-528.

41) Hussain, M.T., Forbes, N. and Perrie, Y., 2019. Comparative analysis of protein quantification methods for the rapid determination of protein loading in liposomal formulations. Pharmaceutics, 11(1), p.39.

42) Al-Ahmady, Z.S., Chaloin, O. and Kostarelos, K., 2014. Monoclonal antibody-targeted, temperature-sensitive liposomes: Invivo tumor chemotherapeutics in combination with mild hyperthermia. Journal of Controlled Release, 196, pp.332–343.